INSTITUTE OF MATHEMATICS,
POLISH ACADEMY OF SCIENCES

DOCTORAL THESIS

Asymptotic properties of Robinson–Schensted–Knuth algorithm and jeu de taquin

Łukasz MAŚLANKA

under the supervision of
prof. dr hab. Piotr ŚNIADY

11th April, 2022

Declaration of Authorship

I, Łukasz MAŚLANKA, declare that this thesis titled "Asymptotic properties of Robinson–Schensted–Knuth algorithm and jeu de taquin" and the work presented in it are my own.

Signed:

Date:

I, Piotr ŚNIADY, declare that this thesis is ready for evaluation by reviewers.

Signed:

Date:

INSTITUTE OF MATHEMATICS, POLISH ACADEMY OF SCIENCES

Abstract

Doctor of Philosophy

Asymptotic properties of Robinson–Schensted–Knuth algorithm and jeu de taquin

by Łukasz MAŚLANKA

The Thesis is divided into three main parts, each concerning a different *limit problem for random Young tableaux*.

In the first part we show that in the Plancherel growth process of a random Young diagram *the growths which occur in the first k bottom rows of the diagram* are asymptotically independent and that asymptotically, when $n \to \infty$, for each of the first k rows the dynamics of its growth in time n can be modelled by a Poisson process with intensity $n^{-1/2}$.

In the second part, we study *the bumping routes in the surrounding of the first column* in a big random Plancherel distributed tableau. We show that in the projective coordinates the rows in which the bumping route 'jumps between' the columns can be asymptotically modelled by a Poisson process.

In the last part we investigate whether there exist some *typical shapes of the sliding path and the evacuation path* in a random rectangular tableau. We show that each of these random paths concentrates near a random curve from some particular family. We then transfer these results to the setup of *Totally Asymmetric Simple Exclusion Process* to obtain the description of the limit trajectory of the second class particle in TASEP.

INSTYTUT MATEMATYCZNY POLSKIEJ AKADEMII NAUK

Streszczenie

Rozprawa doktorska

Asymptotic properties of Robinson–Schensted–Knuth algorithm and jeu de taquin

Autor: Łukasz MAŚLANKA

Rozprawa zawiera trzy główne rozdziały. Każdy z nich opisuje inny problem graniczny dla losowych tableaux Younga.

W pierwszym rozdziale badamy *dynamikę przyrostów pierwszych k wierszy* losowego diagramu Younga w procesie wzrostu Plancherela. Pokazujemy, że przyrosty te są asymptotycznie niezależne oraz, że w granicy, gdy $n \to \infty$, dynamika przyrostu każdego z pierwszych k wierszy w czasie n może być opisana za pomocą procesu Poissona o intensywności $n^{-1/2}$.

Drugi rozdział poświęcony jest badaniu tzw. *bumping route w otoczeniu pierwszej kolumny* dla dużego losowego tableau o rozkładzie Plancherela. Pokazujemy, że stosując współrzędne projektywne, wiersze, w których bumping route „przeskakuje" między kolumnami możemy asymptotycznie opisać za pomocą procesu Poissona.

W ostatnim rozdziale pokazujemy, że istnieją typowe kształty *ścieżek jeu de taquin oraz ewakuacji* w losowym prostokątnym tableau. Dowodzimy, że te ścieżki koncentrują się blisko losowej krzywej należącej do pewnej rodziny. Powyższe rezultaty wykorzystujemy w kontekście *Totally Asymmetric Simple Exclusion Process*, otrzymując opis granicznej trajektorii cząstki drugiego rodzaju w procesie TASEP.

Acknowledgements

After 4 years of struggle and hard work, I would like to say few words from the heart.

> A reader's emotions can be sparked with few words. That's the power of dialogue.
>
> Sol Stein

I thank my advisor, Piotr Śniady, for caring for me and my development. What can be easily imagined, we spent a lot of time together doing mathematics and exchanging arguments. However, the thing for which I am mostly grateful is that he made a great work atmosphere. The mixture of professional treatment and having personal relation – like meeting to play board games (thank you, also, Agata), eating lunch together or sipping coffee in the morning – gave me a lot of place to flourish not only as a mathematician, but also as a human. :-)

> Feelings of worth can flourish only in an atmosphere where individual differences are appreciated, mistakes are tolerated, communication is open, and rules are flexible – the kind of atmosphere that is found in a nurturing family.
>
> Virginia Satir

Outside of the professional life, there are also people who should be recognized. I thank my wife, Agata, for caring for my psychical health and supporting me on all days – both good and bad. I thank also my family for being comprehensive in days in which I struggled.

> The family is an engine that allows you to conquer the world, and at the same time a bunker in which you can take refuge.
>
> Maxime Chattam

Finally, I thank myself for starting PhD studies, spending great time doing math in Toruń at the side of Piotr, and meeting new inspiring people. That was a great decision that I had made.

> Every day we should hear at least one little song, read one good poem, see one exquisite picture, and, if possible, speak a few sensible words.
>
> Johann Wolfgang von Goethe

The research within the thesis was supported by Narodowe Centrum Nauki, grant number 2017/26/A/ST1/00189.

Contents

Declaration of Authorship iii

Abstract v

Streszczenie vii

Acknowledgements ix

1 Introduction 1
- 1.1 Young diagrams and Young tableaux . . . 1
- 1.2 Robinson–Schensted–Knuth algorithm . . . 2
  - 1.2.1 Schensted row insertion . . . 3
  - 1.2.2 Robinson–Schensted–Knuth algorithm . . . 3
- 1.3 Jeu de taquin algorithm . . . 4
  - 1.3.1 Jeu de taquin and sliding path . . . 4
  - 1.3.2 Evacuation path . . . 5
- 1.4 Basics of representation theory . . . 5
- 1.5 Motivations for the results . . . 6
- 1.6 Content of the thesis . . . 8

2 Poisson limit theorems for Robinson–Schensted correspondence 9
- 2.1 Introduction . . . 9
  - 2.1.1 Notations . . . 9
  - 2.1.2 Plancherel measure, Plancherel growth process . . . 10
  - 2.1.3 The main result: Poisson limit theorem for the Plancherel growth process . . . 10
  - 2.1.4 Local spacings in the bottom rows of the recording tableau . . . 11
  - 2.1.5 The Hammersley process . . . 11
  - 2.1.6 Limit distribution of the multi-line Hammersley process . . . 12
  - 2.1.7 The idea behind the proof: the link between the Ulam's problem and the Hammersley's assumption α . . . 13
  - 2.1.8 The link with the work of Aldous and Diaconis . . . 15
  - 2.1.9 Asymptotics of the bottom rows . . . 17
  - 2.1.10 Possible generalization of Corollary 2.1.3: the bottom rows in the Schur–Weyl insertion tableau . . . 18
- 2.2 Estimates for the total variation distance . . . 21
  - 2.2.1 Total variation distance . . . 21
  - 2.2.2 Growth of rows in Plancherel growth process . . . 22
  - 2.2.3 Asymptotics of growth of a given row . . . 24
  - 2.2.4 What happens after just one step? . . . 26
  - 2.2.5 Asymptotic independence . . . 29
  - 2.2.6 Proof of Theorem 2.2.2 . . . 30
- 2.3 Proofs of the main results . . . 31

2.3.1 Proof of Theorem 2.1.1 . . . 31
2.3.2 Proof of Corollary 2.1.2 . . . 33
2.3.3 Proof of Corollary 2.1.3 . . . 35

3 Poisson limit of bumping routes **39**
3.1 Introduction . . . 39
3.1.1 Notations . . . 39
3.1.2 Plancherel measure, Plancherel growth process . . . 40
3.1.3 Bumping route . . . 40
3.1.4 Bumping routes for infinite tableaux . . . 41
3.1.5 The main problem: asymptotics of infinite bumping routes . . . 43
3.1.6 The naive hyperbola . . . 43
3.1.7 In which row a bumping route reaches a given column? . . . 45
3.1.8 Projective convention for drawing Young diagrams . . . 48
3.1.9 The main result with the right-to-left approach . . . 50
3.1.10 Asymptotics of fixed m . . . 52
3.1.11 More open problems . . . 52
3.1.12 Overview of the paper. Sketch of the proof of Theorem 3.1.2 . . . 52
3.2 Growth of the bottom rows . . . 56
3.2.1 Total variation distance . . . 56
3.2.2 Growth of rows in Plancherel growth process . . . 56
3.3 Augmented Plancherel growth process . . . 57
3.3.1 Lazy parametrization of bumping routes . . . 58
3.3.2 Trajectory of ∞ . . . 59
3.3.3 Augmented Young diagrams. Augmented shape of a tableau . . . 61
3.3.4 Augmented Young graph . . . 61
3.3.5 Lifting of paths . . . 62
3.3.6 Augmented Plancherel growth process . . . 63
3.3.7 Probability distribution of the augmented Plancherel growth process . . . 64
3.3.8 Lazy version of Proposition 3.1.9. Proof of Proposition 3.1.1 . . . 68
3.4 Transition probabilities for the augmented Plancherel growth process . . . 69
3.4.1 Approximating Bernoulli distributions by linear combinations of Poisson distributions . . . 69
3.4.2 The inclusion $\mathbb{Y}^* \subset \mathbb{N}_0 \times \mathbb{Y}$ . . . 71
3.4.3 Transition probabilities for augmented Plancherel growth processes . . . 72
3.4.4 Bumping route in the lazy parametrization converges to the Poisson process . . . 74
3.4.5 Lazy version of Remark 3.1.3 . . . 76
3.4.6 Conjectural generalization . . . 77
3.5 Removing laziness . . . 78
3.5.1 Proof of Proposition 3.1.9 . . . 78
3.5.2 Lazy parametrization versus row parametrization . . . 80
3.5.3 Proof of Theorem 3.1.2 . . . 82

4 Second class particles, typical evacuation and sliding paths **83**
4.1 Introduction . . . 83
4.1.1 TASEP system with the uniform distribution over histories . . . 83
4.1.2 Random sorting networks . . . 89
4.1.3 Sliding paths and evacuation paths in random tableaux . . . 90
4.1.4 The content of the paper . . . 93
4.2 The limit shape of sliding paths and evacuation paths . . . 94

4.2.1 Asymptotics of a single box in the evacuation trajectory 94
4.2.2 The circles of latitude g_α 94
4.2.3 The random position of the box $\lfloor \alpha N^2 \rfloor$, the limit measure ν_α 95
4.2.4 Geographic coordinates on the square 97
4.2.5 The second main result. Typical evacuation path 97
4.2.6 The third main result. Typical sliding path 99
4.2.7 Conjecture on the independence of the iterated sliding paths. 99
4.2.8 Something old, something new, something borrowed: sliding paths for random infinite tableaux 100
4.3 Preliminaries 101
4.3.1 Permutations, Young diagrams and Young tableaux, continued 101
4.3.2 Representation theory 101
4.3.3 Asymptotics of characters and the approximate factorization property 102
4.3.4 Jucys–Murphy elements 103
4.4 The longitude and surfing 103
4.4.1 The single surfer scenario 104
4.4.2 Pieri tableaux 105
4.4.3 The multisurfer scenario 106
4.4.4 Sketch of the proof of the upper bound (4.4.2) 106
4.5 Single surfer versus the multisurfer scenario 108
4.5.1 Probability that a random tableau is Pieri 109
4.5.2 Comparison of distributions of water beneath surfer(s) in both scenarios 110
4.5.3 Proof of Proposition 4.5.1 112
4.6 The distribution of the u-coordinates of the multisurfers 112
4.6.1 Counting multisurfers gives the longitude 113
4.6.2 Moments of the empirical measure G_N 114
4.6.3 Multisurfers and the representation theory 115
4.6.4 Character on a coset 118
4.6.5 Products of Jucys–Murphy elements 120
4.6.6 The mean value of M_β – the proof of (4.6.2) 123
4.6.7 The variance of M_β – the proof of (4.6.3) 126
4.6.8 Proof of Theorem 4.6.2 131
4.7 Proof of Theorem 4.4.1 132
4.7.1 Overtaking only in one direction 132
4.7.2 Relative position of the surfer 133
4.7.3 Proof of the upper bound (4.4.2) in Theorem 4.4.1 135
4.7.4 Proof of the lower bound (4.4.3) in Theorem 4.4.1 135
4.8 Proof of Theorem 4.2.3 136
4.8.1 Plan for the proof of Theorem 4.2.3 136
4.8.2 Auxiliary notation 137
4.8.3 The surfer's position can be asymptotically recovered from the theoretical longitude 137
4.8.4 A candidate for the random variable $\Psi_N(T_N)$, development of (S1) . 139
4.8.5 The proof of (S2) – the pointwise version of Theorem 4.2.3 140
4.8.6 The proof of (S3) – the full version of Theorem 4.2.3 140
4.8.7 Limit distribution of the random variable Ψ_N 142
4.9 The correspondence between evacuation and sliding paths 143
4.9.1 Dual evacuation 143
4.9.2 Proof of Theorem 4.2.4 144
4.10 Generalizations of the main results for non-square tableaux 144
4.10.1 Continuous diagrams 144

4.10.2 The asymptotic setup . . . 145
4.10.3 The limit curves . . . 145
4.10.4 The limit measures on the level curves . . . 146
4.10.5 The geographic coordinate system . . . 147
4.10.6 Extension of the main results . . . 148
4.10.7 Example: random rectangular tableaux . . . 149
4.10.8 What if the geographic coordinates system is not uniformly continuous? 152
4.11 The correspondence between Young tableaux and particle systems. Proof of Theorem 4.1.1 . . . 152
4.11.1 The correspondence between a Young diagram with a distinguished corner and a configuration of particles – Rost's mapping . . . 152
4.11.2 The correspondence between the standard tableaux and the histories of TASEP . . . 153
4.11.3 Proof of Theorem 4.1.1 . . . 154

Bibliography **155**

Chapter 1

Introduction

In this PhD thesis we investigate the asymptotics of two popular algorithms used in the study of Young diagrams and tableaux – *the Robinson–Schensted–Knuth algorithm* and *the jeu de taquin algorithm*. The results in this document (see Section 1.6 for their brief description) come from three collaborative papers [MMŚ21b; MMŚ21a; MŚ22] (all with my supervisor, Piotr Śniady, and the first two with his another PhD student, Mikołaj Marciniak). Each of the next three chapters corresponds to one of these papers.

In this chapter we will first introduce basic notations, then give some motivations for our investigations and finish with a short description of the obtained results.

We denote by $\mathbb{N}$ the set of positive integer numbers and we set $\mathbb{N}_0 := \mathbb{N} \cup \{0\}$.

1.1 Young diagrams and Young tableaux

A partition of a natural number n is a sequence $\lambda = (\lambda_0, \dots, \lambda_k)$ (for some $k \in \mathbb{N}_0$) of natural numbers such that $\lambda_0 \geqslant \lambda_1 \geqslant \cdots \geqslant \lambda_k > 0$ and $n = \sum_{n=0}^{k} \lambda_n$. Sometimes it may be more convenient to think of a partition λ as an infinite sequence $\lambda = (\lambda_p)_{p \in \mathbb{N}_0}$ in which $\lambda_p = 0$ for $p > k$.

With a partition λ of a natural number n we associate its graphical representation called *Young diagram* and denoted also by λ. The Young diagram $\lambda = (\lambda_0, \dots, \lambda_k)$ is a figure on the plane which consists of $n = \lambda_0 + \cdots + \lambda_k$ squares of side 1 placed one next to the other in $k+1$ rows in such a way that in the i-th row there are exactly λ_i squares. We use the, so called, *French convention* to draw Young diagrams, see Figure 1.1a. We enumerate the rows and columns of a Young diagram with numbers from the set $\mathbb{N}_0$ starting with 0. Each of the squares in a Young diagram will be called *a box*. The number of boxes in the Young diagram λ is called *the size of* λ and denoted by $|\lambda|$. We also define *the empty diagram*, which we denote by $\varnothing$, as the diagram which has no boxes. The set of all Young diagrams with n boxes will be denoted by $\mathbb{Y}_n$ and the set of all Young diagrams by $\mathbb{Y}$, i.e.,

$$\mathbb{Y} = \bigcup_{n=0}^{\infty} \mathbb{Y}_n.$$

The set $\mathbb{Y}$ has a structure of an oriented graph, called *Young graph*, in which an oriented edge from diagram μ to diagram λ is present if λ can be created from μ by addition of a single box (in such case we write $\mu \nearrow \lambda$).

For a Young diagram λ we consider its fillings with $|\lambda|$ real numbers with the following properties:

- in each row the numbers are increasing from left to right,
- in each column the numbers are increasing from bottom to top.

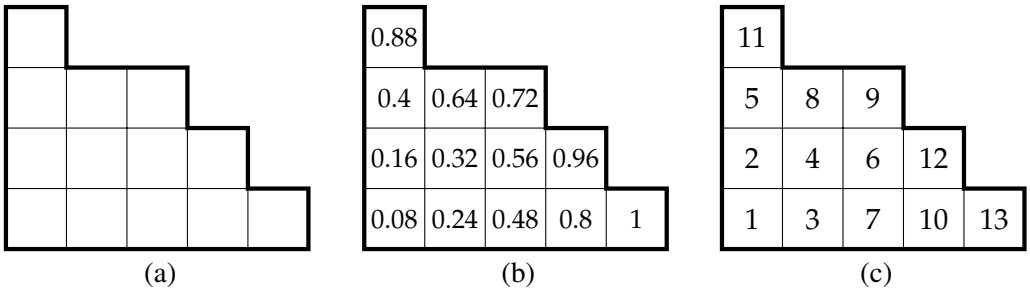

Figure 1.1: (a) The Young diagram $\lambda = (5,4,3,1)$ drawn in *the French convention*; (b) A tableau of shape λ; (c) A standard tableau of shape λ.

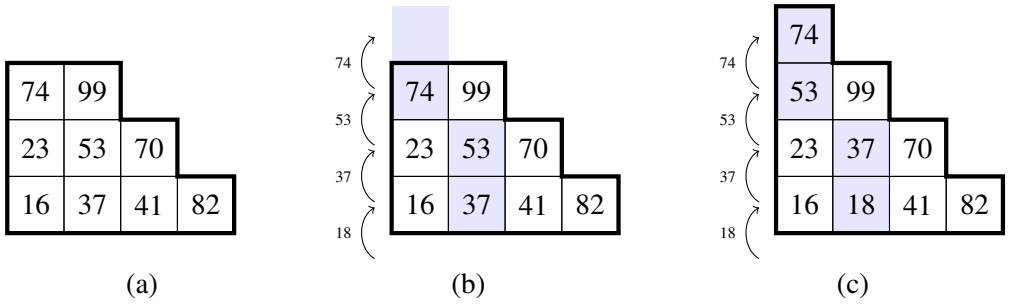

Figure 1.2: (a) The original tableau T. (b) We consider the Schensted row insertion of the number 18 to the tableau T. The highlighted boxes form the corresponding bumping route. The small numbers on the left (next to the arrows) indicate the inserted/bumped numbers. (c) The output $T \leftarrow 18$ of the Schensted insertion.

Any such filling of λ we call *a Young tableau of shape* λ (or shortly *tableau*), see Figure 1.1b. We refer to the numbers in boxes as *entries* of a tableau.

A standard Young tableau of shape λ (or shortly *standard tableau*) is a tableau with entries $1, \ldots, |\lambda|$, see Figure 1.1c. The set of standard tableaux of shape λ will be denoted by $\mathcal{T}_\lambda$.

Let T be a tableau. The shape of T we denote by $\mathrm{sh}(T)$. The number of boxes in T is called *the size of tableau* and denoted by $|T|$ or $|\mathrm{sh}(T)|$. We denote by $T_{x,y}$ the entry of tableau T which lies in the intersection of the row $y \in \mathbb{N}_0$ and the column $x \in \mathbb{N}_0$, for example, in Figure 1.2a we have $T_{0,0} = 16$, $T_{0,1} = 23$, $T_{1,0} = 37$ and so on.

We investigate asymptotics of two operations related to tableaux – the Robinson–Schensted–Knuth algorithm and jeu de taquin.

1.2 Robinson–Schensted–Knuth algorithm

The first operation on tableaux of our interest is *the Robinson–Schensted–Knuth algorithm* (shortly *RSK*). In fact, we will consider a simplified version of *the Robinson–Schensted–Knuth algorithm*; for this reason we should rather call it *the Robinson–Schensted algorithm*. Nevertheless, we use the first name because of its well-known acronym *RSK*.

RSK is an iterative algorithm during which we apply in each step *the Schensted row insertion*.

Figure 1.3: The insertion tableau $P(w)$ (on the left) and the recording tableau $Q(w)$ (on the right) obtained with the RSK algorithm applied to the sequence $w = (74, 53, 99, 23, 37, 70, 16, 18, 41, 82)$.

1.2.1 Schensted row insertion

The Schensted row insertion is an algorithm which takes as an input a tableau T and some number a. The number a is inserted into the first row (that is, the bottom row, the row with the index 0) of T to the leftmost box which contains an entry which is strictly bigger than a.

In the case when the row contains no entries which are bigger than a, we create in the first row new empty box directly to the right of $\mathrm{sh}(T)$ and we fill it with the number a, and the algorithm terminates.

If, however, the number a is inserted into a box which was not empty, the previous content a' of the box is *bumped* into the next row. This means that the algorithm is iterated but this time the number a' is inserted into the next row to the leftmost box which contains a number bigger than a' (if such box exists). We repeat these steps of row insertion and bumping until some number needs to be inserted into a new empty box.

This process is illustrated on Figures 1.2b and 1.2c. The *bumping route* consists of the boxes the entries of which were changed by the action of Schensted insertion, including the last, newly created box, see Figure 1.2c. *The outcome of the Schensted insertion* is defined as the result of the aforementioned procedure; it will be denoted by $T \leftarrow a$.

1.2.2 Robinson–Schensted–Knuth algorithm

The Robinson–Schensted–Knuth algorithm (shortly *RSK*) associates to a finite sequence $w = (w_1, \ldots, w_\ell)$ of real numbers a pair of tableaux: *the insertion tableau* $P(w)$ and *the recording tableau* $Q(w)$ of the same shape, see Figure 1.3.

The insertion tableau

$$P(w) = \Big(\big((\varnothing \leftarrow w_1) \leftarrow w_2\big) \leftarrow \cdots\Big) \leftarrow w_\ell \tag{1.2.1}$$

is defined as the result of the iterative Schensted row insertion applied to the entries of the sequence w, starting from *the empty tableau* $\varnothing$.

The recording tableau $Q(w)$ is defined as the standard Young tableau of the same shape as $P(w)$ in which each entry is equal to the number of the iteration of (1.2.1) in which the given box of $P(w)$ stopped being empty; in other words the entries of $Q(w)$ give the order in which the entries of the insertion tableau were filled.

The common shape of the insertion tableau $P(w)$ and the recording tableau $Q(w)$ will be denoted by $\mathrm{RSK}(w)$.

Theorem 1.2.1 ([Ful97, Part 1, Chapter 4]). *For any $n \in \mathbb{N}$ the Robinson–Schensted algorithm gives a bijection between the symmetric group $\mathfrak{S}_n$ and the set of pairs (P, Q) of standard tableaux with n boxes and the same shape.*

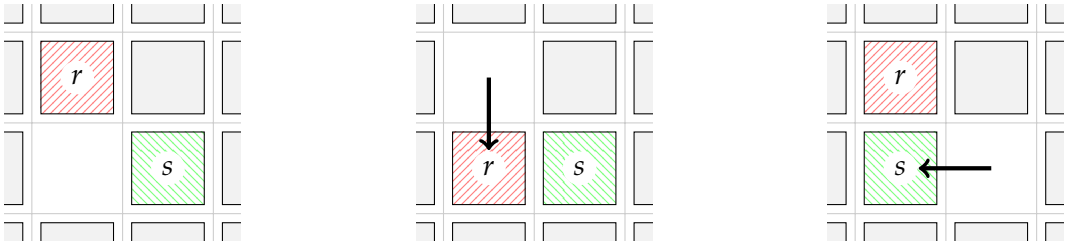

(a) (b) (c)

Figure 1.4: Elementary step of the jeu de taquin transformation: (a) the initial configuration of boxes, (b) the outcome of the slide in the case when $r < s$, (c) the outcome of the slide in the case when $s < r$. Copyright ©2014 Society for Industrial and Applied Mathematics. Reprinted from [Śni14] with permission. All rights reserved.

(a) (b)

Figure 1.5: (a) A standard Young tableau T of shape $\lambda = (5, 4, 2, 1)$. The highlighted boxes form the *sliding path*. (b) The outcome $j(T)$ of the jeu de taquin transformation. The light blue empty square indicates the box which got removed during jeu de taquin.

The RSK algorithm is of great importance in algebraic combinatorics, especially in the context of the representation theory [Ful97]. Also a fruitful area of study concerns the RSK algorithm applied to a uniformly random permutation from $\mathfrak{S}_n$, especially asymptotically in the limit $n \to \infty$, see [Rom15] and the references therein.

1.3 Jeu de taquin algorithm

The second operation on tableaux whose asymptotics we will investigate is *jeu de taquin*, [Ful97, Section 1.2]. This operation is also heavily used in the study of Young tableaux.

1.3.1 Jeu de taquin and sliding path

Jeu de taquin acts on Young tableaux in the following way (see Figures 1.5a and 1.5b): we remove the bottom-left box of the given tableau T and obtain a *hole* in its place. Then we look at the two boxes: the one to the right and the one above the hole, and choose the one which contains the smaller number. We slide this smaller box into the location of the hole, see Figure 1.4. As a result, the hole moves in the opposite direction. We continue this operation as long as there is some box to the right or above the hole. The path which was traversed by the 'traveling hole' will be called the ***sliding path***, see Figure 1.5a. The result of jeu de taquin applied to a tableau T will be denoted by $j(T)$, see Figure 1.5b. Note that the tableau $j(T)$ has one box less than T.

1.3.2 Evacuation path

For a given *standard tableau* $T \in \mathcal{T}_\lambda$ with $n = |\lambda|$ boxes the jeu de taquin transformation j can be iterated n times until we end with the empty tableau. During each iteration the box with the biggest number n either moves one node left or down, or stays put. Its trajectory will be called the ***evacuation path***.

1.4 Basics of representation theory

Young diagrams and tableaux are connected with the irreducible representations of the symmetric groups. We will now give a very short introduction to the representation theory.

Let V be a vector space over the field $\mathbb{K} = \mathbb{R}$ or $\mathbb{K} = \mathbb{C}$ and denote by $\mathrm{GL}(V)$ the set of isomorphisms of V. Let G be a finite group and let $\rho : G \to \mathrm{GL}(V)$ be a homomorphism, i.e., $\rho(gh) = \rho(g) \circ \rho(h)$ for all $g, h \in G$. Depending on the context, we call *a representation of* G the homomorphism ρ or the linear space V. We also call a homomorphism ρ *a linear group action of* G on V. We will explain this ambiguity below.

Let V and W be two vector spaces and let $\rho : G \to \mathrm{GL}(V)$ and $\pi : G \to \mathrm{GL}(W)$ be their representations. We say that the mapping $\phi : V \to W$ is a *homomorphism of representations* if

$$\forall_{g \in G} \quad \phi\big(\rho(g)(v)\big) = \pi(g)\big(\phi(v)\big)\,,$$

i.e., ϕ intertwines the representations ρ and π. Additionally, if ϕ is a bijection then we call it *isomorphism of representations*. If such isomorphism exists then we say that the *representations V and W are equivalent* (or *isomorphic*).

A subspace W of the vector space V which is invariant under the (linear) group action of G is called *a subrepresentation*. We say that a representation V is *irreducible* if it does not have nontrivial subrepresentations, i.e., other than $\{0\}$ and V.

Example 1.4.1 (Irreducible representations of the symmetric group). Each irreducible representation of the symmetric group $\mathfrak{S}_n$ corresponds to some Young diagram with n boxes, [Sag01, Theorem 2.4.4]. In particular, the trivial representation corresponds to the Young diagram (n) with 1 row and the alternating representation corresponds to the Young diagram (1^n) with n columns.

The basis of the irreducible representation of $\mathfrak{S}_n$ corresponding to the Young diagram $\lambda \in \mathbb{Y}_n$ can be encoded with the set of standard tableaux of shape λ, [Sag01, Theorem 2.6.4]. The dimension of such irreducible representation is equal to the number d_λ of standard tableaux of the shape λ.

The following two theorems lie in the foundations of the representation theory.

Lemma 1.4.2 (Schur's lemma)**.** *Let V and W be irreducible representations of the finite group G. Assume that $T : V \to W$ is a homomorphism of representations. Then $T = 0$ or T is an isomorphism. In particular, the only homomorphisms of irreducible representations of V are the multiples of identity.*

Theorem 1.4.3 (Maschke's theorem)**.** *Let G be a finite group. Any finitely dimensional representation V (over the field $K = \mathbb{R}$ or $K = \mathbb{C}$) of G is a direct sum of irreducible representations of G, i.e.,*

$$V = \bigoplus_{i=1}^{k} W_i$$

where each W_i is an irreducible representation of G. The decomposition of V into irreducible components is unique up to an isomorphism of representations.

Taking into account Schur's lemma and Maschke's theorem it becomes clear that the two notions of a representation: first as the group homomorphism and second as the vector space can be used interchangeably.

Example 1.4.4 (The left regular representation). The following example is of special interest since

- each irreducible representation of G is isomorphic to some irreducible subrepresentation of the left regular representation;
- the celebrated and intensively investigated *Plancherel measure* is a very natural probability measure on the set of irreducible components of the left regular representation.

Let G be a group and let $\mathbb{K}G$ be the group algebra of G, i.e., $\mathbb{K}G$ is the set of all formal linear combinations of the elements of G, i.e.,

$$\mathbb{K}G = \left\{ \sum_{g\in G} a_g g : \ a_g \in \mathbb{K} \right\}.$$

We consider the left action of G on the group algebra $\mathbb{K}G$, i.e., the representation $\rho : G \to \mathrm{GL}(\mathbb{K}G)$ given by

$$\forall_{h\in G} \quad \rho(h)\left(\sum_{g\in G} a_g g \right) := \sum_{g\in G} a_g hg.$$

By Maschke's theorem $\mathbb{K}G$ decomposes into the direct sum of the irreducible components. Using the theory of characters one can show that some of these irreducible components are isomorphic and $\mathbb{K}G$ can be given as the following direct sum

$$\mathbb{K}G = \bigoplus_{\nu} c_\nu V_\nu$$

where each component is indexed by different conjugation class ν of G and the coefficient $c_\nu \in \mathbb{N}$, called *multiplicity of* V_ν, is equal to the cardinality of ν. Moreover, c_ν is equal to the dimension of the vector space V_ν, i.e., $c_\nu = |\nu| = \dim V_\nu$.

The probability measure on the set of all irreducible subrepresentations of $\mathbb{K}G$ given by the formula

$$\mathrm{Plan}(\nu) := \frac{\dim V_\nu^2}{|G|}, \quad \nu - \text{irreducible component of } \mathbb{K}G,$$

is called *the Plancherel measure*.

The correspondence between irreducible representations of $\mathfrak{S}_n$ and Young diagrams, cf. Example 1.4.1, yields *the Plancherel distribution* on Young diagrams with n boxes. The probability of choosing the diagram $\lambda \in \mathbb{Y}_n$ with respect to the Plancherel measure on $\mathfrak{S}_n$ is equal to

$$\mathrm{Plan}_n(\lambda) = \frac{(d_\lambda)^2}{n!} \tag{1.4.1}$$

where d_λ denotes the number of standard tableaux of shape λ. The Plancherel measure Plan_n plays a crucial role in our research, see Chapters 2 and 3.

1.5 Motivations for the results

Many combinatorial structures can be viewed as *discrete versions of continuous geometric objects*. For example, Young diagram is a geometric shape on the Cartesian plane and a

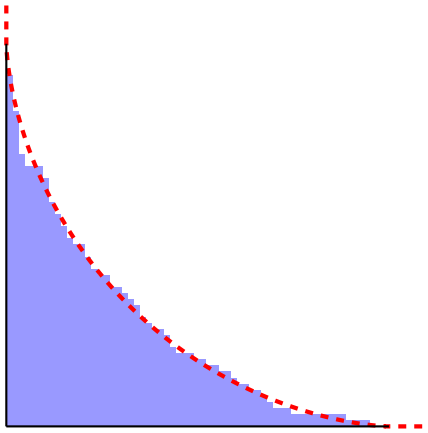

Figure 1.6: A random Young diagram with 1000 boxes (the blue angular shape consisting of small squares) sampled according to the Plancherel measure and the limit shape of its boundary – *the Vershik–Kerov–Logan–Shepp curve* (the thick red dashed curve) [LS77; VK77].

standard tableau can be viewed as a 3D block being a union of 'small' cuboids with the square base 1×1 corresponding to the size of a cell in the Young diagram (the shape of tableau) and the height equal to the entry in the corresponding cell. We can embed these structures into another space of some (continuous) geometric objects and ask whether there is some *typical asymptotic behaviour of these discrete shapes as their size parameter tends to infinity*. In many cases the randomly sampled element approaches some continuous limit. If this is a case we say that the model has *a limit shape*. Figure 1.6 shows an example of the limit shape phenomenon for the Plancherel distributed random diagram. The questions concerning the limit shapes are usually formulated *in the probabilistic setup*.

It is worth noting that the investigation of the limit shapes of random combinatorial objects is very appealing to wide range of mathematicians. Such problems were investigated, for example, by a Fields medal laureate Andrei Okounkov [Oko06], Richard Stanley [Sta07] and Anatoly Vershik [Ver95]. Also the research in this area was appreciated by the mathematical community by invitations to give lectures on International Congress of Mathematics by Philippe Biane [Bia02] or European Congress of Mathematics by my supervisor Piotr Śniady [Ś13].

There are several good reasons for studying limit shapes:

- Random combinatorial objects can be often considered as models of mathematical physics. We raise this issue in the case of *Totally Asymmetric Simple Exclusion Process* (shortly *TASEP*) in Chapter 4.

- On one hand, the representation theory is often related to some combinatorial structures (see Example 1.4.1 for an example). On the other hand, questions from group theory, harmonic analysis on groups, probability on groups or quantum information theory can be often rephrased in the language of the character theory. Therefore it is essential to understand large combinatorial objects to answer the original question.

- The *aesthetical motivation* which is twofold. Firstly, the computer simulations often gives rise to beautiful pictures. Secondly, and more importantly, the solutions of the problems related to asymptotics of random combinatorial structures often involve an appealing interface between seemingly distant disciplines of mathematics, such as combinatorics, analysis, harmonic analysis, ergodic theory, representation theory, probability theory or quantum mechanics.

In this thesis we are going to investigate *the dynamics of the growth of the first few bottom rows of a Young diagram* during the RSK insertion applied to a random input (Chapter 2), *the limit shape of the bumping route* corresponding to the Schensted insertion of 'very small' numbers (Chapter 3) and *the limit shapes of the sliding path and evacuation path* in a random tableau of rectangular shape and *the dynamics of a particular TASEP process* (Chapter 4). We will describe these specific problems and their motivations more richly in the corresponding chapters.

1.6 Content of the thesis

The proper part of this PhD thesis consists of three (almost) independent chapters.

In the first of these chapters, Chapter 2, we investigate *the way in which the first k bottom rows grow in a random Plancherel distributed diagram*. To be more precise, we consider an i.i.d. $U(0,1)$ infinite word $w = (w_1, w_2, \dots)$ and apply iteratively the RSK algorithm to its restrictions $w|_n := (w_1, \dots, w_n), n \in \mathbb{N}$, and look at the obtained Young diagrams $\mathrm{RSK}(w|_n)$. Each two results of the consecutive iteration steps differ by exactly one box (which was added in some row). Our aim is to show that the growths which happen in the first k bottom rows are asymptotically independent and that asymptotically the growth in each of them in time n can be modelled by a Poisson process with intensity $n^{-1/2}$.

In the next chapter, Chapter 3, we use the obtained result from Chapter 2 to investigate *the bumping routes in the surrounding of the first column of random Young tableau*. More precisely, to a big random Plancherel distributed standard tableau we Schensted-insert a number $m + \frac{1}{2}$ for some fixed $m \in \mathbb{N}$ and look at the corresponding bumping route. We are interested in the rows in which the bumping route 'jumps between' the columns. We show that these rows (when properly seen) can be asymptotically modelled by a Poisson process.

The last chapter, Chapter 4, is devoted to *the typical shapes of the sliding path and the evacuation path* in a random rectangular standard tableau. We show that each of the investigated random paths asymptotically focuses near a random curve belonging to some particular family. The tools used in the proofs can be applied in a more general context of C-balanced tableaux. We then transfer these results to the setup of *Totally Asymmetric Simple Exclusion Process* to obtain the description of *the limit trajectory of the second class particle* in TASEP.

Chapter 2

Poisson limit theorems for the Robinson–Schensted correspondence and for the multi-line Hammersley process

The following chapter is a modified version of the (yet nonpublished) article [MMŚ21b]:

> Marciniak, M. Marciniak, Ł. Maślanka and P. Śniady: *Poisson limit theorems for the Robinson–Schensted correspondence and for the multi-line Hammersley process*, https://arxiv.org/abs/2005.13824v2

which is available in the public repository arXiv.org.

Abstract: We consider the Robinson–Schensted–Knuth algorithm applied to a random input and study the growth of the bottom rows of the corresponding Young diagrams. We prove a multidimensional Poisson limit theorem for the resulting Plancherel growth process. In this way we extend the result of Aldous and Diaconis to more than just one row. This result can be interpreted as convergence of the multi-line Hammersley process to its stationary distribution which is given by a collection of independent Poisson point processes.

2.1 Introduction

The notions of Young diagrams and tableaux are given in Section 1.1 We will shortly recall the corresponding notation in the next subsection. The *Robinson–Schensted–Knuth algorithm* (shortly *RSK*) is defined in Section 1.2.

2.1.1 Notations

Recall from Chapter 1 that we denote the set of Young diagrams with n boxes by $\mathbb{Y}_n$ and the set of all Young diagrams by $\mathbb{Y}$. *The Young graph* is an oriented graph with vertices in $\mathbb{Y}$. The pair of diagrams μ and λ is connected by an oriented edge pointing from μ to λ if and only if λ can be created from the Young diagram μ by addition of a single box (which we denote by $\mu \nearrow \lambda$).

Recall that the rows of any Young diagram $\lambda = (\lambda_0, \lambda_1, \dots)$ are indexed by the elements of $\mathbb{N}_0$; in particular the length of the bottom row of λ is denoted by λ_0. For a tableau T we denote by $T_{x,y}$ its entry which lies in the intersection of the row $y \in \mathbb{N}_0$ and the column $x \in \mathbb{N}_0$.

Let $X\colon \Omega \to V$ be a random variable with values in some set V. When we want to phrase this statement without mentioning the sample space Ω explicitly, we will write $X \in V$.

If E is a random event, we denote by $\mathbb{1}_E$ its indicator, which is the random variable given by

$$\mathbb{1}_E(\omega) = \begin{cases} 1 & \text{if } \omega \in E, \\ 0 & \text{otherwise.} \end{cases}$$

2.1.2 Plancherel measure, Plancherel growth process

Let $\mathfrak{S}_n$ denote the symmetric group of order n. We will view each permutation $\pi \in \mathfrak{S}_n$ as a sequence $\pi = (\pi_1, \dots, \pi_n)$ which has no repeated entries, and such that $\pi_1, \dots, \pi_n \in \{1, \dots, n\}$. Recall from Theorem 1.2.1 that the restriction of RSK to the symmetric group is a bijection which to a given permutation from $\mathfrak{S}_n$ associates a pair (P, Q) of standard Young tableaux of the same shape and consisting of n boxes.

The Plancherel measure on $\mathbb{Y}_n$, denoted Plan_n, is defined as the probability distribution of the random Young diagram $\mathrm{RSK}(w)$ for a uniformly random permutation w selected from $\mathfrak{S}_n$, cf. Equation (1.4.1).

An *infinite standard Young tableau* [Ker99, Section 2.2] is a filling of the boxes in a subset of the upper-right quarterplane with positve integers, such that each row and each column is increasing, and each positive integer is used exactly once. There is a natural bijection between the set of infinite standard Young tableaux and the set of infinite sequences of Young diagrams

$$\lambda^{(0)} \nearrow \lambda^{(1)} \nearrow \cdots \qquad \text{with } \lambda^{(0)} = \varnothing; \tag{2.1.1}$$

this bijection is given by setting $\lambda^{(n)}$ to be the set of boxes of a given infinite standard Young tableau which are $\leqslant n$.

If $w = (w_1, w_2, \dots)$ is an *infinite* sequence, the recording tableau $Q(w)$ is defined as the infinite standard Young tableau in which each non-empty entry is equal to the number of the iteration in the infinite sequence of Schensted insertions

$$\big((\varnothing \leftarrow w_1) \leftarrow w_2\big) \leftarrow \cdots$$

in which the corresponding box stopped being empty, see [RŚ15, Section 1.2.4]. Under the aforementioned bijection, the recording tableau $Q(w)$ corresponds to the sequence (2.1.1) with

$$\lambda^{(n)} = \mathrm{RSK}(w_1, \dots, w_n).$$

Let $\xi = (\xi_1, \xi_2, \dots)$ be an infinite sequence of independent, identically distributed random variables with the uniform distribution $U(0,1)$ on the unit interval $[0,1]$. *The Plancherel measure on the set of infinite standard Young tableaux* is defined as the probability distribution of $Q(\xi)$. Any sequence with the same probability distribution as (2.1.1) with

$$\lambda^{(n)} = \mathrm{RSK}(\xi_1, \dots, \xi_n) \tag{2.1.2}$$

will be called *the Plancherel growth process* [Ker99]. For a more systematic introduction to this topic we recommend the monograph [Rom15, Section 1.19].

2.1.3 The main result: Poisson limit theorem for the Plancherel growth process

Theorem 2.1.1. *Let $\lambda^{(0)} \nearrow \lambda^{(1)} \nearrow \cdots$ be the Plancherel growth process. Let us fix $k \in \mathbb{N}_0$. We denote by*

$$\Lambda^{(n)} = \left(\lambda_0^{(n)}, \dots, \lambda_k^{(n)}\right) \in (\mathbb{N}_0)^{k+1}$$

the random vector formed by the lengths of the bottom $k+1$ rows of the random diagram $\lambda^{(n)}$. For each $n \in \mathbb{N}_0$ we consider the random function $\Delta_n : \mathbb{R} \to \mathbb{Z}^{k+1}$ given by

$$\Delta_n(t) = \Lambda^{(n_t)} - \Lambda^{(n)}, \tag{2.1.3}$$

where

$$n_t = \max\left(n + \lfloor t\sqrt{n} \rfloor,\ 0\right). \tag{2.1.4}$$

Then, for $n \to \infty$, the random function Δ_n converges in distribution to a tuple $(N_0, \dots, N_k)$ of $k+1$ independent copies of the standard Poisson process. This convergence is understood as convergence (with respect to the topology given by the total variation distance) of all finite-dimensional marginals $\left(\Delta_n(t_1), \dots, \Delta_n(t_\ell)\right)$ over all choices of $t_1, \dots, t_\ell \in \mathbb{R}$.

The proof is postponed to Section 2.3.1.

In Sections 2.1.4 to 2.1.7 we shall discuss the connections of this theorem with the (multi-line) Hammersley process and the *assumption* α of Hammersley, and in Section 2.1.8 the connections with the work of Aldous and Diaconis [AD95, Theorem 5(b)]. In Sections 2.1.9 and 2.1.10 we will discuss links with some other areas of mathematics.

2.1.4 Local spacings in the bottom rows of the recording tableau

Theorem 2.1.1 can be interpreted as a result about the random sets of points in which the coordinates of the function (2.1.3) have jumps; this interpretation gives the following immediate corollary. For an alternative proof see Section 2.3.2.

Corollary 2.1.2. *Let $\xi = (\xi_1, \xi_2, \dots)$ be an infinite sequence of independent, identically distributed random variables with the uniform distribution $U(0,1)$ on the unit interval $[0,1]$ and let $Q(\xi) = \left[Q_{x,y}\right]_{x,y \geqslant 0}$ be the corresponding random recording tableau with the Plancherel distribution.*

Then for any integer $k \in \mathbb{N}_0$ the collection of $k+1$ random sets

$$\left(\left\{ \frac{Q_{x,y} - n}{\sqrt{n}} \ :\ x \in \mathbb{N}_0 \right\} \ :\ y \in \{0, \dots, k\} \right) \tag{2.1.5}$$

converges in distribution, as $n \to \infty$, to a family of $k+1$ independent Poisson point processes on $\mathbb{R}$ with the unit intensity.

2.1.5 The Hammersley process

The information about the sequence $w = (w_1, \dots, w_\ell)$ can be encoded by a collection of points $(w_1, 1), \dots, (w_\ell, \ell)$ on the plane (marked as small discs on Figure 2.1a). In the insertion tableau

$$P(w) = \Big(\big((\varnothing \leftarrow w_1) \leftarrow w_2 \big) \leftarrow \cdots \Big) \leftarrow w_\ell \tag{2.1.6}$$

the time evolution of the bottom row in the process of insertions (2.1.6) can be encoded by the time evolution of a collection of particles on the real line (their trajectories are marked on Figure 2.1a as blue zig-zag lines) which is subject to the following dynamics. When we have reached one of the disks (x, t) (translation: *at time t, when a number x is inserted into the bottom row of the insertion tableau...*) one of the following happens: (i) a particle, which is first to the right of x, jumps left to x (translation: *... the newly inserted number x bumps from the bottom row the smallest number which is bigger than x*), or (ii) a new particle is created in x (translation: *the number x is appended at the end of the bottom row*), see Figure 2.1a for an illustration.

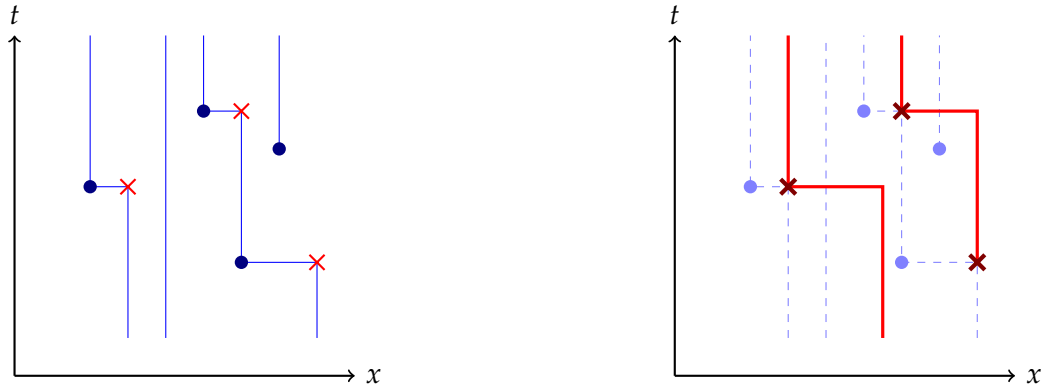

(a) (b)

Figure 2.1: (a) The dynamics of the particles in the Hammersley process with some initial configuration of the particles. The time flows from bottom to top. (b) The second line of the multi-line Hammersley process.

If the locations of the disks on the upper halfplane are random, sampled according to the Poisson point process on $I \times \mathbb{R}_+$ (for some specified set $I \subseteq \mathbb{R}$) we obtain in this way the celebrated *Hammersley process* on I [Ham72; AD95].

The information about all bumpings from the bottom row of the insertion tableau can be encoded by the dual corners [FM09] (marked on Figure 2.1a by red X crosses). These crosses are used as an input for the dynamics of the second row of the insertion tableau in an analogous way as the disks were used for the dynamics of the bottom row, see Figure 2.1b. In other words, the output of the Hammersley process (which will be the first line of the *multi-line Hammersley process* which we will construct) is used as the input for the second line of the *multi-line Hammersley process*.

This procedure can be iterated; in this way the dynamics of all rows of the insertion tableau is fully encoded by *the multi-line Hammersley process* [FM09]. The name is motivated by the analogy with the tandem queues where the happy customers who exit one waiting line are the input for the second line.

2.1.6 Limit distribution of the multi-line Hammersley process

As we already mentioned, the entries of the bottom row of the insertion tableau can be interpreted as positions of the particles in (the de-Poissonized version of) the Hammersley interacting particle process on the unit interval $[0,1]$. Therefore the following result (Corollary 2.1.3 below) is a generalization of the result of Aldous and Diaconis [AD95, Theorem 5(b)] which concerned only the special case $k = 0$ of the single-line Hammersley process (in the Poissonized setup). For a more detailed discussion of the link between these results see Section 2.1.8.

The general case $k \geqslant 0$ can be interpreted as a statement about the convergence of the multi-line version of the Hammersley process *on the the unit interval* $[0,1]$ to its stationary distribution *on the whole real line* $\mathbb{R}$ which was calculated by Fan and Seppäläinen [FS20, Theorem 5.1].

Note that in his original paper [Ham72, Section 9] Hammersley considered the particle process with a discrete time parameter indexed by non-negative integers. Slightly confusingly, this process with the modern terminology would be referred to as *the de-Poissonized version of the Hammersley process* (as opposed to *the Hammersley process* in which the time is continuous and the input is given by the Poisson point process on the quarterplane). It follows

that the setup which we consider in Corollary 2.1.3 coincides with the one from the original paper of Hammersley. The special case $k = 0$ of Corollary 2.1.3 was conjectured already by Hammersley [Ham72, *"assumption α"* on page 371] who did not predict the exact value of the intensity of the Poisson process.

Corollary 2.1.3. *Let $\xi = (\xi_1, \dots \xi_n)$ be a sequence of independent, identically distributed random variables with the uniform distribution $U(0,1)$ on the unit interval $[0,1]$ and let*

$$\left[P^{(n)}_{x,y}\right]_{y\in\mathbb{N}_0,\, 0\leqslant x<\lambda^{(n)}_y} = P(\xi_1, \dots, \xi_n)$$

be the corresponding insertion tableau; we denote by $\lambda^{(n)}$ its shape.

For any integer $k \in \mathbb{N}_0$ and any real number $0 < w < 1$ the collection of $k+1$ random sets $\mathcal{P}^{(n)}_0, \dots, \mathcal{P}^{(n)}_k$ with

$$\mathcal{P}^{(n)}_y := \left\{ \sqrt{n}\left(P^{(n)}_{x,y} - w\right) \,:\, 0 \leqslant x < \lambda^{(n)}_y \right\} \tag{2.1.7}$$

converges in distribution, as $n \to \infty$, to a family of $k+1$ independent Poisson point processes on $\mathbb{R}$ with the intensity $\frac{1}{\sqrt{w}}$.

The above statement remains true for $w = 1$ but the limit in this case is a family of $k+1$ independent Poisson point processes on the negative halfline $\mathbb{R}_-$ with the unit intensity.

The key ingredient of the proof is to use some symmetries of the RSK algorithm which allow to interchange the roles of the insertion tableau and the recording tableau, see Section 2.3.3 for the details.

We were inspired to state Corollaries 2.1.2 and 2.1.3 by the work of Azangulov [Aza20] who studied fluctuations of the last entry in the bottom row of $P^{(n)}$ around $w = 1$; more specifically he proved that the (shifted and rescaled) last entry in the bottom row

$$\sqrt{n}\left(1 - P^{(n)}_{0,\lambda^{(n)}_0 - 1}\right)$$

converges in law to the exponential distribution $\mathrm{Exp}(1)$.

2.1.7 The idea behind the proof: the link between the Ulam's problem and the Hammersley's assumption α

The key idea behind the proof of Theorem 2.1.1 lies in the intimate interplay between *the Ulam's problem* and *the Hammersley's assumption α* which was already subject to investigation by several researchers in this field.

2.1.7.1 Ulam's problem

Recall that Ulam [Ula61] asked about the value of the limit

$$c = \lim_{n\to\infty} \frac{\mathbb{E}\lambda^{(n)}_0}{\sqrt{n}}.$$

The first solution to this problem consisted of two components: proving the lower bound $c \geqslant 2$ and the upper bound $c \leqslant 2$; interestingly these two components have quite different proofs.

The lower bound $c \geqslant 2$ was proved independently by Logan and Shepp [LS77] as well as by Vershik and Kerov [VK77] by finding explicitly the limit shape of typical random

Young diagrams distributed according to the Plancherel measure. Both proofs were based on the hook-length formula for the number of standard Young tableaux of prescribed shape and finding the minimizer of the corresponding functional. An alternative approach which avoids the variational calculus is to use the results of Biane [Bia01] in order to show that the (scaled down) *transition measure* of a Plancherel-distributed random diagram $\lambda^{(n)}$ converges in probability to *the semicircle distribution* and to deduce that the probability of the event $\lambda_0^{(n)} < (2-\epsilon)\sqrt{n}$ converges to zero for each $\epsilon > 0$.

This lower bound $c \geqslant 2$ will play an important role in our paper and we will use it in order to show Proposition 2.2.7 (more specifically, we use it in Lemma 2.2.5).

The upper bound $c \leqslant 2$ is due to Vershik and Kerov [VK85a]. This upper bound plays an even more important role in our paper. We will come back to this topic in Section 2.1.7.3 below.

2.1.7.2 Hammersley's assumption α

Hammersley formulated his *assumption* α [Ham72, page 371] as a rather vague statement (*"It is reasonable to assume that the distribution of the discontinuities y_i is locally homogenous and random"*) which we interpret as a conjecture that the local behavior of the numbers in the bottom row of the insertion tableau $P^{(n)}$ after appropriate rescaling converges to some Poisson point process with unspecified intensity, cf. Corollary 2.1.3. Hammersley also gave an informal argument which explained how *the assumption* α would give solution to the Ulam's problem and he correctly predicted the value of the constant $c = 2$.

The first proof of a result of the flavor of *the assumption* α is the aforementioned work of Aldous and Diaconis [AD95, Theorem 5(b)]. Interestingly, the proof starts with two separate parts: one which happens to give an alternative proof for the upper bound $c \leqslant 2$ for the constant in the Ulam's problem, and one which happens to give an alternative proof for the lower bound $c \geqslant 2$. Finally, the combination of these two results gives the desired proof of *the assumption* α.

The arguments in the aforementioned papers [Ham72; AD95] were based on a probabilistic analysis of the Hammersley process viewed as an interacting particle system (see Section 2.1.5) and thus were quite different from those mentioned in Section 2.1.7.1.

2.1.7.3 The idea of the proof

As we can see from the aforementioned papers [Ham72; AD95], the Ulam's problem and the assumption α are intimately related one with another and a solution to one of them gives (at least heuristically) the solution to the other one. From this perspective it is somewhat surprising that the original solution to the Ulam's problem contained in the papers [LS77; VK77; VK85a] did not result with a corresponding proof of the assumption α in the language of the Plancherel growth process and random Young diagrams. The current paper fills this gap.

Our strategy is to revisit the proof of the upper bound $c \leqslant 2$ which is due to Vershik and Kerov [VK85a, Section 3, Lemma 6] (see also [VK85b, Section 3, Lemma 6] for the English translation; be advised that there are *two* lemmas having number 6 in this paper). With the notations used in our paper (see the proof of Lemma 2.2.8), this proof can be rephrased as an application of the Cauchy–Schwarz inequality for a clever choice of a pair of vectors X and Y of (approximately) unit length. It is somewhat surprising that such a coarse bound as Cauchy–Schwarz inequality gives the optimal upper bound $c \leqslant 2$ for the Ulam's constant. This phenomenon is an indication that the Cauchy–Schwarz inequality is applied here in a setting in which it becomes (asymptotically) saturated, which implies that the vectors X and Y

are (approximately) multiples of one another and therefore $X \approx Y$. It follows in particular that

$$\langle X - Y,\ \ Y \rangle \approx 0. \tag{2.1.8}$$

Let $\lambda^{(0)} \nearrow \lambda^{(1)} \nearrow \cdots$ be the Plancherel growth process. It turns out that a slight modification of the left-hand side of (2.1.8) has a natural probabilistic interpretation as the total variation distance between:

- the probability distribution of the Young diagram $\lambda^{(n)}$, and
- the *conditional* probability distribution of the Young diagram $\lambda^{(n)}$ *under the condition* that the growth between the diagrams $\lambda^{(n-1)}$ and $\lambda^{(n)}$ occurred in a specified row.

In particular, (2.1.8) implies that this total variation distance converges to zero as $n \to \infty$, see Lemma 2.2.8 for a precise statement.

Heuristically, this means that the information about the number of the row $r^{(n)}$ in which the growth occurred between $\lambda^{(n-1)}$ and $\lambda^{(n)}$ does not influence too much the distribution of the resulting random Young diagram $\lambda^{(n)}$. Since the Plancherel growth process is a Markov process, this argument can be iterated to show that the numbers of the rows

$$r^{(n+1)}, \ldots, r^{(n+\ell)} \tag{2.1.9}$$

in which the growths occur in the part of the Plancherel growth process $\lambda^{(n)} \nearrow \cdots \nearrow \lambda^{(n+\ell)}$ are approximately independent random variables, see Theorem 2.2.2 for a precise statement. Various variants of the assumption α are now simple corollaries.

This approach gives some additional information — which does not seem to be available by the hydrodynamic approach [AD95; CG05] — about the asymptotic independence of the rows (2.1.9) *and* the shape of the final Young diagram $\lambda^{(n+\ell)}$, see Theorem 2.2.2 for more detail. This additional information will be essential in Chapter 3 ([MMŚ21a]) devoted to the refined asymptotics of the bumping routes.

The aforementioned Lemma 2.2.8 can be seen as an additional step in the reasoning which was overlooked by the authors of [VK85a]. The monograph of Romik [Rom15, Section 1.19] contains a more pedagogical presentation of these ideas of Vershik and Kerov; in the following we will use Romik's notations with some minor adjustments.

Note that, analogously as the proof of Aldous and Diaconis [AD95, Theorem 5(b)], our proof of the assumption α is based on combining two components: the one which is related to the lower bound $c \geqslant 2$ in the Ulam's problem (see Lemma 2.2.5) and the one related to the upper bound $c \leqslant 2$ (see the proof of Lemma 2.2.8) and only combination of these two components completes the proof.

2.1.8 The link with the work of Aldous and Diaconis

Following the notations from [AD95] we consider the Hammersley process on $\mathbb{R}_+$ (starting from the empty configuration of the particles) and denote by $\mathbf{N}^+(x,t)$ the number of particles at time t which have their spacial coordinate $\leqslant x$. Aldous and Diaconis [AD95, Theorem 5(b)] proved that for each fixed $w > 0$ the counting process

$$\Big(\mathbf{N}^+(ws + y, s) - \mathbf{N}^+(ws, s),\ y \in \mathbb{R}\Big) \tag{2.1.10}$$

converges in distribution, as $s \to \infty$, to the Poisson counting process with intensity $w^{-1/2}$.

2.1.8.1 The link of Corollary 2.1.3

In the following we sketch very briefly the proof that the special case of Corollary 2.1.3 which corresponds to $k = 0$ is equivalent to the aforementioned result of Aldous and Diaconis.

Due to the *space-time scale invariance* [AD95, Lemma 4], the stochastic process (2.1.10) has the same distribution as

$$\left(\mathbf{N}^+\left(w + \frac{y}{s}, s^2\right) - \mathbf{N}^+\left(w, s^2\right),\ y \in \mathbb{R} \right). \tag{2.1.11}$$

Let $\eta_1(s^2) < \eta_2(s^2) < \cdots$ denote the positions of the particles at time s^2. The result of Aldous and Diaconis can be therefore rephrased as convergence in distribution of the set of jumps of the function (2.1.11) which is equal to

$$\left\{ s \cdot \left[\eta_i\left(s^2\right) - w \right] : i \in \mathbb{N} \right\} \tag{2.1.12}$$

towards the Poisson point process with the intensity $w^{-1/2}$.

For simplicity we restrict our attention to $0 < w < 1$ (the general case $w > 0$ can be obtained by an application of a slightly more involved space-time scale invariance). The above result does not change if we modify our setup and consider the Hammersley process on the unit interval $[0, 1]$. The number of disks (which are the input for the Hammersley process) in the rectangle $[0, 1] \times [0, t]$ is equal to the value $N(t)$ of the Poisson process at time t. With the notations of Corollary 2.1.3, the entries $\left(P^{(n)}_{x,0} : 0 \leqslant x < \lambda^{(n)}_0\right)$ of the bottom row in the insertion tableau $P^{(n)}$ can be interpreted as the coordinates of the particles in the Hammersley process at the time when n disks appeared; it follows that the set (2.1.12) is equal to

$$\left\{ s \cdot \left[P^{(N(s^2))}_{x,0} - w \right] \ :\ 0 \leqslant x < \lambda^{(n)}_0 \right\}. \tag{2.1.13}$$

In this way we proved that the distribution of the random set (2.1.13) (which appears in a reformulation of the result of Aldous and Diaconis) is the mixture of the probability distribution of the random set $\mathcal{P}^{(n)}_0$ given by (2.1.7) which corresponds to the bottom row, rescaled by the factor $\frac{s}{\sqrt{n}}$. The mixture is taken over $n := N(s^2)$ which has the Poisson distribution $\mathrm{Pois}(s^2)$. Since the scaling factor $\frac{s}{\sqrt{n}}$ converges in probability to 1 as $s \to \infty$, the scaling is asymptotically irrelevant.

We proved in this way that the result of Aldous and Diaconis [AD95, Theorem 5(b)] is a consequence of the special case of Corollary 2.1.3 for $k = 0$, obtained by a straightforward Poissonization procedure.

The implication in the opposite direction is more challenging, but general de-Poissonization techniques [JS98] can be used to show that the result of Aldous and Diaconis implies the special case $k = 0$ of our Corollary 2.1.3.

2.1.8.2 The link of Theorem 2.1.1

In the following we sketch the proof that the special case of Theorem 2.1.1 which corresponds to $k = 0$ is equivalent to the result of Aldous and Diaconis (2.1.10). For simplicity we will consider only the special case $w = 1$; the general case $w > 0$ would follow from a slightly more complex scaling of the space-time.

Due to the *space-time scale invariance* [AD95, Lemma 4], the stochastic process (2.1.10) in the special case $w = 1$ has the same distribution as

$$\left(\mathbf{N}^+\left(s^2 + ys,\, 1\right) - \mathbf{N}^+\left(s^2,\, 1\right),\; y \in \mathbb{R}\right)$$

and, due to the *space-time interchange property* [AD95, Lemma 3], the same distribution as

$$\left(\mathbf{N}^+\left(1,\, s^2 + ts\right) - \mathbf{N}^+\left(1,\, s^2\right),\; t \in \mathbb{R}\right). \tag{2.1.14}$$

By [AD95, Theorem 5(b)] the process (2.1.10) for $w = 1$ or, equivalently, the process (2.1.14) converges for $s \to \infty$ to the Poisson process with the unit intensity. This result does not change if we modify our setup and consider the Hammersley process on the unit interval $[0, 1]$.

For each $t \geqslant 0$ the number of disks (which are the input for the Hammersley process) in the rectangle $[0, 1] \times [0, t]$ is equal to the value $N(t)$ of the Poisson process at time t. Thus the number of all particles at time t, given by $\mathbf{N}^+(1, t) = \lambda_0^{(N(t))}$, is equal to the length of the bottom row of the insertion tableau after $N(t)$ disks appeared. In this way we proved that the probability distribution of the process (2.1.14) coincides with the probability distribution of the process

$$\left(\lambda_0^{\left(N(s^2+ts)\right)} - \lambda_0^{\left(N(s^2)\right)},\; t \in \mathbb{R}\right). \tag{2.1.15}$$

We set $n := N(s^2)$ and

$$\tau(t) = \frac{N(s^2 + ts) - N(s^2)}{\sqrt{N(s^2)}} \tag{2.1.16}$$

so that $N(s^2 + ts) = n_{\tau(t)}$ with the notations from (2.1.4). In the case when $N(s^2) = 0$ and (2.1.16) is not well-defined, we declare that $n_{\tau(t)} = N(s^2 + ts)$ by definition. Since the probability of the event that $N(s^2) = 0$ converges to zero as $s \to \infty$, this will not create problems in the following.

The random function τ converges in probability, as $s \to \infty$, to the identity map $t \mapsto t$ uniformly over compact subsets. With these notations the probability distribution of the process (2.1.14) coincides with the probability distribution of the process

$$\left(\lambda_0^{\left(n_{\tau(t)}\right)} - \lambda_0^{(n)},\; t \in \mathbb{R}\right). \tag{2.1.17}$$

By taking the average over the random values of n and τ it follows that the special case of Theorem 2.1.1 for $k = 0$ implies that (2.1.17) indeed converges to the Poisson process. We proved in this way that the result of Aldous and Diaconis [AD95, Theorem 5(b)] (at least in the special case $w = 1$) is a consequence of the special case of Theorem 2.1.1 for $k = 0$, obtained by a rather straightforward Poissonization procedure.

The implication in the opposite direction is more challenging, but again general de-Poissonization techniques [JS98] can be applied.

2.1.9 Asymptotics of the bottom rows

The research related to the Ulam's problem culminated in the works of Baik, Deift and Johansson [BDJ99; BDJ00] as well as its extensions [BOO00; Oko00; Joh01]. Roughly speaking, these results say that the suitably normalized lengths of the bottom rows of a Plancherel distributed random Young diagram converge to an explicit non-Gaussian limit

which is related to the eigenvalues of a large GUE random matrix, see the monograph [Rom15] for a more pedagogical introduction.

Such a non-Gaussian limit behavior for the lengths of the bottom rows is at a sharp contrast with our Theorem 2.1.1 which states that the growths of the bottom rows $\Delta_n(t)$ are given by the Poisson process which with the right scaling converges to the Brownian motion. This discrepancy is an indication that the process $\Delta_n(t)$ considered in that theorem *cannot* be approximated by the Poisson process in the scaling as $t = t(n) \gg 1$. It would be interesting to find the scaling in which this passage from the regime of independent growths to the non-Gaussian regime related to the random matrices occurs. See also Problem 2.3.2.

2.1.10 Possible generalization of Corollary 2.1.3: the bottom rows in the Schur–Weyl insertion tableau

We suspect that Corollary 2.1.3 is a special case of a conjectural result which would hold in a much wider generality. In the current section we will present the details.

2.1.10.1 Schur–Weyl insertion tableau

For given positive integers d and n let $w = (w_1, \dots, w_n)$ be a sequence of independent, identically distributed random variables with the uniform distribution on the discrete set $\{1, \dots, d\}$ with d elements; we denote by $P = P(w_1, \dots, w_n)$ the corresponding insertion tableau. This random tableau appears naturally in the context of *the Schur–Weyl duality* which we review in the following. The tensor product $\left(\mathbb{C}^d\right)^{\otimes n}$ has a natural structure of a $\mathfrak{S}_n \times \mathrm{GL}_d(\mathbb{C})$-module; the irreducible components are naturally indexed by Young diagrams. *The Schur–Weyl measure* is defined as the probability distribution on Young diagrams which corresponds to sampling a random irreducible component of $\left(\mathbb{C}^d\right)^{\otimes n}$ with the probability proportional to the dimension of the component, see [Mél11] for the details. The probability distribution of the shape of P coincides with the Schur–Weyl measure; for this reason we will call the random tableau P itself *the Schur–Weyl insertion tableau*.

In the scaling when $d, n \to \infty$ tend to infinity in such a way that $d \simeq c\sqrt{n}$ for some $c > 0$, there is a law of large numbers for *the global form* of the scaled down insertion tableau P, see [MŚ20b, Remark 1.6 and Section 1.7.3].

In the following we will concentrate on another aspect of the Schur–Weyl insertion tableau P, namely in the entries which are located in the bottom row, near its end. For an integer $i \in \{1, \dots, d\}$ we denote by $M_i = M_i(P)$ the number of occurrences of i in the bottom row of P; our problem is to understand the joint distribution of the family of random variables M_i indexed by $i \in I$ in some interval of the form

$$I = \{d + 1 - \ell, d + 2 - \ell, \dots, d\} \tag{2.1.18}$$

for some choice of an integer $\ell \geqslant 1$.

There are two interesting limits which one can consider in this setup, namely the one when the size of the alphabet $d \to \infty$ tends to infinity, and the one when the length of the sequence $n \to \infty$ tends to infinity. In the following we will review these two limits and discuss what happens when these two limits are iterated.

2.1.10.2 The limit $d \to \infty$

When $d \to \infty$ and the length n of the sequence is fixed, the probability that $w_1, \dots, w_n$ are all distinct converges to 1. In the following we consider the conditional probability space for which $w_1, \dots, w_n$ are all distinct; it is easy to check that such a conditional joint distribution of the ratios $\frac{w_1}{d}, \dots, \frac{w_n}{d}$ converges to that of a tuple $\xi_1, \dots, \xi_n$ of independent random variables

with the uniform distribution $U(0,1)$. It follows that the (conditional, and hence unconditional as well) probability distribution of the tableau $\frac{1}{d}P$ (which is obtained from P by dividing each entry by d) converges to the probability distribution of the insertion tableau $P(\xi_1, \ldots, \xi_n)$.

We see that the iterated limit in which we *first* take the limit as the size of the alphabet $d \to \infty$ tends to infinity and *then* the limit $n \to \infty$ as the length of the sequence tends to infinity, is the one in which we recover Corollary 2.1.3. Heuristically, we can expect that if $n \to \infty$ and $d = d(n) \gg n^2$ tends to infinity fast enough, each integer from the interval I given by (2.1.18) of moderate length $\ell = O\left(\frac{d}{\sqrt{n}}\right)$ will not appear more than once (except for asymptotically negligible probability); and that the probability that a given integer $i \in I$ will appear in the bottom row is of order

$$q = \frac{n}{d} \cdot \frac{1}{\sqrt{n}} = \frac{\sqrt{n}}{d} \approx \frac{\sqrt{n}}{d + \sqrt{n}} \ll 1$$

which is approximately the product of the probability that i belongs to the sequence w (which is roughly $\frac{n}{d}$) and the probability that a given large entry of the sequence w will be in the bottom row (which is roughly $\frac{1}{\sqrt{n}}$ by Corollary 2.1.3).

Such a Bernoulli probability distribution on the set $\{0,1\}$ with the success probability q can be approximated by the geometric distribution on the set of non-negative integers with the parameter $p = 1 - q$. We formalize this informal discussion as the following conjecture.

Conjecture 2.1.4. *Let $d = d(n)$ and $\ell = \ell(n)$ be as above.*
Then the total variation distance between:

- *the random vector of the multiplicities*

$$(M_i : i \in I)\,,$$

and

- *the collection of ℓ independent random variables, each with the geometric distribution* $\mathrm{Geo}(p)$ *with the parameter*

$$p = 1 - \frac{\sqrt{n}}{d + \sqrt{n}} = \frac{d}{d + \sqrt{n}}$$

converges to zero, as $n \to \infty$.

In the following we will discuss whether this conjecture is plausible also in some other choices of the scaling for the parameters d and n.

2.1.10.3 The limit $n \to \infty$

For the purposes of the current section by *the $d \times d$ GUE random matrix* we understand the random matrix with the Gaussian distribution supported on Hermitian $d \times d$ matrices, which is invariant under conjugation by unitary matrices, and normalized in such a way that the variance of each diagonal entry is equal to d. The *traceless GUE random matrix* is obtained from the above random matrix by subtracting a multiple of the identity matrix in such a way that the trace of the outcome is equal to zero.

For $m \in \{0, 1, \ldots, d\}$ we denote by

$$\lambda^{(\downarrow m)} = \left(\lambda_0^{(\downarrow m)}, \ldots, \lambda_{m-1}^{(\downarrow m)}\right) = \mathrm{sh}\, P^{\leqslant m}$$

the shape of the tableau $P^{\leqslant m}$ which is obtained from the Schur–Weyl random insertion tableau P by keeping only the boxes which are at most m; in particular $\lambda^{(\downarrow d)}$ is the shape of P. Recall that P and, as a consequence, $\lambda^{(\downarrow m)}$ as well, depend implicitly on the choice of the positive integers d and n. In the following we fix the value of the integer $d \geqslant 1$ and let n vary. Johansson [Joh01, Theorem 1.6] proved that the distribution of the random vector

$$\frac{d\lambda^{(\downarrow d)} - n}{\sqrt{n}}$$

converges, as $n \to \infty$, to the joint distribution of the eigenvalues $\operatorname{spec} X$ of the *traceless* $d \times d$ *GUE random matrix* $(X_{ij})_{1 \leqslant i,j \leqslant d}$. This result can be further extended using the ideas of Kuperberg [Kup02]; one can show that the joint distribution of the random vectors

$$\frac{d\lambda^{(\downarrow d)} - n}{\sqrt{n}}, \quad \frac{d\lambda^{(\downarrow d-1)} - n}{\sqrt{n}}, \quad \ldots, \quad \frac{d\lambda^{(\downarrow 1)} - n}{\sqrt{n}}$$

converges in distribution to the joint distribution of the eigenvalues of X, together with the eigenvalues of the minors of X obtained by iterative removal of the last row and the last column:

$$\operatorname{spec}(X_{ij})_{1 \leqslant i,j \leqslant d}, \quad \operatorname{spec}(X_{ij})_{1 \leqslant i,j \leqslant d-1}, \quad \ldots, \quad \operatorname{spec}(X_{ij})_{1 \leqslant i,j \leqslant 1}. \tag{2.1.19}$$

Since the content of the current section is mostly heuristic, we skip the details of the proof; the key point is to use [CŚ09, Corollary 5.2].

With the above notations, for $m \in \{2, \ldots, d\}$ we have that $M_m = \lambda_0^{(\downarrow m)} - \lambda_0^{(\downarrow m-1)}$ is the number of entries in the bottom row of the tableau P which are equal to m. Also, for $m \in \{1, \ldots, d\}$ let $\mu^{(m)} = \max\big(\operatorname{spec}(X_{ij})_{1 \leqslant i,j \leqslant m}\big)$ be the largest eigenvalue of the minor $(X_{ij})_{1 \leqslant i,j \leqslant m}$. The aforementioned result implies, in particular, that the probability distribution of the random vector

$$\frac{d}{\sqrt{n}} \left(M_d,\ M_{d-1},\ \ldots,\ M_2\right) \tag{2.1.20}$$

which describes the content of the bottom row of P (after disregarding all entries equal to 1) converges, as $n \to \infty$, to the joint distribution of the entries of the random vector

$$\left(\mu^{(d)} - \mu^{(d-1)},\ \mu^{(d-1)} - \mu^{(d-2)},\ \ldots,\ \mu^{(2)} - \mu^{(1)}\right). \tag{2.1.21}$$

Gorin and Shkolnikov [GS17, Corollary 1.3] studied the asymptotics $d \to \infty$ of the probability distribution of any prefix of a fixed length ℓ of the random vector (2.1.21). In this scaling the difference between *the GUE random matric* and *the traceless GUE random matrix* turns out to be irrelevant. More specifically, they proved that for each fixed value of an integer $\ell \geqslant 1$ the joint distribution of the random variables

$$\left(\mu^{(d)} - \mu^{(d-1)},\ \mu^{(d-1)} - \mu^{(d-2)},\ \ldots,\ \mu^{(d+1-\ell)} - \mu^{(d-\ell)}\right)$$

converges to the distribution of ℓ independent random variables, each with the exponential distribution $\operatorname{Exp}(1)$.

By combining these results it follows that for each fixed integer $\ell \geqslant 1$ the probability distribution of the random vector

$$\frac{d}{\sqrt{n}} \left(M_d,\ M_{d-1},\ \ldots,\ M_{d+1-\ell}\right)$$

converges to that of independent exponential random variables in the iterated limit in which

we *first* take the limit $n \to \infty$ as the length of the sequence tends to infinity, and *then* the limit as the size of the alphabet $d \to \infty$ tends to infinity. Since the exponential distribution arises naturally as a limit of the geometric distribution $\mathrm{Geo}(p)$ in the scaling as $p \to 0$, we suspect that the following stronger result is true.

Conjecture 2.1.5. *Conjecture 2.1.4 remains true if $d = d(n)$ is a sequence of positive integers with tends to infinity in a sufficiently slow way and $\ell \geqslant 1$ is a fixed integer.*

2.1.10.4 The joint limit $d, n \to \infty$

Heuristically, each of the iterated limits considered at the very end of the Sections 2.1.10.2 and 2.1.10.3 can be seen as a limit in which both variables $d, n \to \infty$ tend to infinity in such a way that one of these variables grows much faster than the other one. With these two extreme cases covered one can wonder whether Conjecture 2.1.4 holds true in general.

Conjecture 2.1.6. *Conjecture 2.1.4 remains true if $d = d(n)$ is an arbitrary sequence of positive integers which tends to infinity and $\ell = \ell(n)$ is a sequence of positive integers which is either constant or tends to infinity in such a way that $\ell = O\left(\frac{d}{\sqrt{n}}\right)$.*

Particularly interesting is the *balanced scaling* in which n and d tend to infinity in such a way that $\frac{d}{\sqrt{n}}$ converges to some limit so that the law of large numbers applies to the shape of P [Bia01, Section 3] as well as to the tableau P itself [MŚ20b, Remark 1.6 and Section 1.7.3]. Conjecture 2.1.6 concerns the entries in the bottom row; we conjecture that an analogous result for any fixed number of bottom rows remains true.

2.2 Estimates for the total variation distance

Our main tool for proving the main results of the paper is Theorem 2.2.2. It gives an insight into the way in which the first rows of a Young diagram develop in the Plancherel growth process (thanks to this part we will have Theorem 2.1.1 as a straightforward corollary), together with the information about the global shape of the Young diagram. This latter additional information will be key for the developments in Chapter 3.

2.2.1 Total variation distance

Suppose that μ and ν are probability measures on the same discrete set S. Such measures can be identified with real-valued functions on S. We define the *total variation distance* between the measures μ and ν

$$\delta(\mu, \nu) := \frac{1}{2} \left\| \mu - \nu \right\|_{\ell^1} = \max_{X \subset S} \left| \mu(X) - \nu(X) \right| \tag{2.2.1}$$

as half of their ℓ^1 distance as functions. If X and Y are two random variables with values in the same discrete set S, we define their total variation distance $\delta(X, Y)$ as the total variation distance between their probability distributions.

Several times we will use the following simple lemma.

Lemma 2.2.1.

(a) Let $X = (X_1, X_2)$ and $Y = (Y_1, Y_2)$ be random vectors with independent coordinates and such that their first coordinates have equal distribution: $X_1 \stackrel{d}{=} Y_1$. Then the total

variation distance between the vectors is equal to the total variation distance between their second coordinates:

$$\delta(X, Y) = \delta(X_2, Y_2).$$

(b) Let $X = (X_1, \ldots, X_\ell)$ and $Y = (Y_1, \ldots, Y_\ell)$ be random vectors with independent coordinates. Then the total variation distance between the random vectors is bounded by the sum of the coordinate-wise total variation distances:

$$\delta(X, Y) \leqslant \sum_{1 \leqslant i \leqslant \ell} \delta(X_i, Y_i).$$

(c) If $\mu_1, \ldots, \mu_\ell$ and $\nu_1, \ldots, \nu_l$ are discrete measures on some vector space then the total variation distance between their convolutions is bounded by the sum of the summand-wise total variation distances:

$$\delta\left(\mu_1 * \cdots * \mu_\ell,\ \nu_1 * \cdots * \nu_\ell\right) \leqslant \sum_{1 \leqslant i \leqslant \ell} \delta(\mu_i, \nu_i).$$

This result seems to be folklore wisdom [pik15], nevertheless we failed to find a conventional reference and we provide a proof below.

Proof. For part (a) we view the total variation distance $\delta(X, Y)$ as half of the appropriate ℓ^1 norm. This double sum factorizes thanks to independence.

For the part (b) we consider a collection of random vectors given by

$$Z^i = (Y_1, \ldots, Y_i, X_{i+1}, \ldots, X_\ell) \qquad \text{for } i \in \{0, \ldots, \ell\}.$$

In this way $Z^0 = X$ and $Z^\ell = Y$; the neighboring random vectors Z^{i-1} and Z^i differ only on the i-th coordinate. By the triangle inequality

$$\delta(X, Y) \leqslant \sum_{1 \leqslant i \leqslant \ell} \delta(Z^{i-1}, Z^i) = \sum_{1 \leqslant i \leqslant \ell} \delta(X_i, Y_i),$$

where the last equality is a consequence of part (a).

In order to prove part (c) we shall use (b) with the special choice that X_i is a random variable with the distribution μ_i and Y_i is a random variable with the distribution ν_i. An application of the same measurable map to both arguments $X = (X_1, \ldots, X_\ell)$ and $Y = (Y_1, \ldots, Y_\ell)$ cannot increase the total variation distance between them, so

$$\delta\left(\mu_1 * \cdots * \mu_\ell,\ \nu_1 * \cdots * \nu_\ell\right) = \delta(X_1 + \cdots + X_\ell, Y_1 + \cdots + Y_\ell) \leqslant \delta(X, Y).$$

The application of part (b) to the right-hand side completes the proof. □

2.2.2 Growth of rows in Plancherel growth process

Let us fix an integer $k \in \mathbb{N}_0$. We define the finite set $\mathcal{N} = \{0, 1, \ldots, k, \infty\}$ which can be interpreted as the set of the natural numbers from the perspective of a person who cannot count on numbers bigger than k (for example, for $k = 3$ we would have *"zero, one, two, three, many"*).

Let $\lambda^{(0)} \nearrow \lambda^{(1)} \nearrow \cdots$ be the Plancherel growth process. For integers $n \geqslant 1$ and $r \in \mathbb{N}_0$ we denote by $E_r^{(n)}$ the random event which occurs if the unique box of the skew diagram $\lambda^{(n)}/\lambda^{(n-1)}$ is located in the row with the index r. For $n \geqslant 1$ we define the random variable

$R^{(n)}$ which takes values in $\mathcal{N}$ and which is given by

$$R^{(n)} = \begin{cases} r & \text{if the event } E_r^{(n)} \text{ occurs for } 0 \leqslant r \leqslant k, \\ \infty & \text{if the event } E_r^{(n)} \text{ occurs for some } r > k, \end{cases}$$

and which — from the perspective of the aforementioned person with limited counting skills — gives the number of the row in which the growth occurred.

Let $\ell = \ell(m)$ be a sequence of non-negative integers such that

$$\ell = O\left(\sqrt{m}\right).$$

For a given integer $m \geqslant (k+1)^2$ we focus on the specific part of the Plancherel growth process

$$\lambda^{(m)} \nearrow \cdots \nearrow \lambda^{(m+\ell)}. \tag{2.2.2}$$

We will encode some partial information about the growths of the rows as well as about the final Young diagram in (2.2.2) by the random vector

$$V^{(m)} = \left(R^{(m+1)}, \ldots, R^{(m+\ell)}, \lambda^{(m+\ell)}\right) \in \mathcal{N}^\ell \times \mathbb{Y}. \tag{2.2.3}$$

We also consider the random vector

$$\overline{V}^{(m)} = \left(\overline{R}^{(m+1)}, \ldots, \overline{R}^{(m+\ell)}, \overline{\lambda}^{(m+\ell)}\right) \in \mathcal{N}^\ell \times \mathbb{Y} \tag{2.2.4}$$

which is defined as a sequence of independent random variables; the random variables $\overline{R}^{(m+1)}, \ldots, \overline{R}^{(m+\ell)}$ have the same distribution given by

$$\mathbb{P}\left\{\overline{R}^{(m+i)} = r\right\} = \frac{1}{\sqrt{m}} \qquad \text{for } r \in \{0, \ldots, k\}, \tag{2.2.5}$$

$$\mathbb{P}\left\{\overline{R}^{(m+i)} = \infty\right\} = 1 - \frac{k+1}{\sqrt{m}} \tag{2.2.6}$$

and $\overline{\lambda}^{(m+\ell)}$ is distributed according to Plancherel measure $\mathrm{Plan}_{m+\ell}$; in particular the random variables $\lambda^{(m+\ell)}$ and $\overline{\lambda}^{(m+\ell)}$ have the same distribution.

Heuristically, the following result states that when Plancherel growth process is in an advanced stage and we observe a relatively small number of its additional steps, the growths of the bottom rows occur approximately like independent random variables. Additionally, these growths do not affect too much the final shape of the Young diagram.

Theorem 2.2.2. *With the above notations, for each fixed $k \in \mathbb{N}_0$ the total variation distance between $V^{(m)}$ and $\overline{V}^{(m)}$ converges to zero, as $m \to \infty$; more specifically*

$$\delta\left(V^{(m)}, \overline{V}^{(m)}\right) = o\left(\frac{\ell}{\sqrt{m}}\right).$$

The proof is postponed to Section 2.2.6; in the forthcoming Sections 2.2.3 to 2.2.5 we will gather the tools which are necessary for this goal.

2.2.3 Asymptotics of growth of a given row

Our main result in this subsection is Proposition 2.2.7 which gives asymptotics of the probability of a growth of a given row in the Plancherel growth process. This result is not new; it was proved by Okounkov [Oko00, Proposition 2]. Nevertheless we provide an alternative (hopefully simpler) proof below. As a preparation, we start with some auxiliary lemmas.

In the following we keep the notations from the beginning of Section 2.2.2; in particular $\lambda^{(0)} \nearrow \lambda^{(1)} \nearrow \cdots$ is the Plancherel growth process. Let $K \in \mathbb{N}_0$ be fixed. For $n \geqslant 1$ we define

$$s_K^{(n)} = \sum_{0 \leqslant r \leqslant K} \mathbb{P}\left(E_r^{(n)}\right). \tag{2.2.7}$$

Lemma 2.2.3. *For each $K \in \mathbb{N}_0$ the sequence $s_K^{(1)}, s_K^{(2)}, \ldots$ is weakly decreasing.*

Proof. For $n \geqslant 1$ let $\mathbf{d}_n$ denote the unique box of the skew diagram $\lambda^{(n)}/\lambda^{(n-1)}$. In this way $s_K^{(n)}$ is equal to the probability that the box $\mathbf{d}_n$ is located in one of the rows $0, 1, \ldots, K$.

Romik and Śniady [RŚ15, Section 3.3] constructed a random sequence of boxes $\mathbf{q}_1, \mathbf{q}_2, \ldots$ (which is "*the jeu de taquin trajectory in the lazy parametrization*") such that for each $n \geqslant 1$ we have equality of distributions [RŚ15, Lemma 3.4]

$$\mathbf{d}_n \stackrel{d}{=} \mathbf{q}_n$$

and, furthermore, each box $\mathbf{q}_{n+1}$ is obtained from the previous one $\mathbf{q}_n$ by moving one node to the right, or node up, or by staying put. In this way

$$\big(\text{the number of the row of } \mathbf{q}_n\big)_{n \geqslant 1}$$

is a weakly increasing sequence of random variables. It follows that the corresponding cumulative distribution functions evaluated in point K

$$s_K^{(n)} = \mathbb{P}\big\{(\text{the number of the row of } \mathbf{d}_n) \leqslant K\big\} = \mathbb{P}\big\{(\text{the number of the row of } \mathbf{q}_n) \leqslant K\big\}$$

form a weakly decreasing sequence, which completes the proof. □

Lemma 2.2.4. *For each $K \in \mathbb{N}_0$ and $n \geqslant 1$*

$$s_K^{(n)} \leqslant \frac{K+1}{\sqrt{n}}.$$

Proof. The monograph of Romik [Rom15, Section 1.19] contains the proof (which is based on the work of Vershik and Kerov [VK85a; VK85b, Section 3, Lemma 6]) of the inequality

$$\mathbb{P}\left(E_r^{(n)}\right) \leqslant \frac{1}{\sqrt{n}} \tag{2.2.8}$$

in the special case of the bottom row $r = 0$. After some minor adjustments this proof is applicable to the general case of $r \in \mathbb{N}_0$ (in fact, these adjustments are explicitly explained in the proof of Eq. (2.2.13) later on). The summation over $r \in \{0, \ldots, K\}$ concludes the proof. □

Lemma 2.2.5. *For each $K \in \mathbb{N}_0$*

$$\liminf_{n \to \infty} \frac{s_K^{(1)} + \cdots + s_K^{(n)}}{\sqrt{n}} \geqslant 2(K+1).$$

Proof. We write $\lambda^{(n)} = (\lambda_0^{(n)}, \lambda_1^{(n)}, \dots)$ so that $\lambda_r^{(n)}$ is the length of the appropriate row of the Young diagram $\lambda^{(n)}$. The work of Logan and Shepp [LS77] as well as the work of Vershik and Kerov [VK77] contains the proof that for each $\epsilon > 0$

$$\lim_{n\to\infty} \mathbb{P}\left\{ \frac{\lambda_r^{(n)}}{\sqrt{n}} < 2 - \epsilon \right\} = 0 \tag{2.2.9}$$

in the special case of the bottom row $r = 0$. We will revisit this proof and explain how to adjust it for the general case $r \in \mathbb{N}_0$.

With the notations of Romik [Rom15, the proof of Theorem 1.23], if (2.2.9) were not true for some $\epsilon > 0$ and $r \in \mathbb{N}_0$, then for infinitely many values of n the corresponding function ψ_n (which encodes the Young diagram $\lambda^{(n)}$ in *the Russian coordinate system* [Rom15, Section 1.17]) would be bounded from above by the shifted absolute value function $|u| + r\sqrt{\frac{2}{n}}$ on the interval $\left[\sqrt{2} - \frac{\epsilon}{\sqrt{2}}, \sqrt{2}\right]$. Clearly this would prevent ψ_n from converging uniformly to the limit shape in contradiction to Logan–Shepp–Vershik–Kerov limit theorem [Rom15, Theorem 1.22].

Equation (2.2.9) implies that for each $r \in \mathbb{N}_0$

$$\liminf_{n\to\infty} \frac{\mathbb{E}\lambda_r^{(n)}}{\sqrt{n}} \geqslant 2. \tag{2.2.10}$$

We revisit the ideas of Vershik and Kerov [VK85a; VK85b, Section 3, Lemma 6], see also [Rom15, Section 1.19]. Since the indicator of the event $E^{(m)}$ fulfills

$$\mathbb{1}_{E_r^{(m)}} = \lambda_r^{(m)} - \lambda_r^{(m-1)}$$

it follows that

$$\mathbb{P}\left(E_r^{(m)}\right) = \mathbb{E}\mathbb{1}_{E_r^{(m)}} = \mathbb{E}\lambda_r^{(m)} - \mathbb{E}\lambda_r^{(m-1)}.$$

By summing over $1 \leqslant m \leqslant n$ and over $0 \leqslant r \leqslant K$ it follows that

$$s_K^{(1)} + \dots + s_K^{(n)} = \mathbb{E}\lambda_0^{(n)} + \dots + \mathbb{E}\lambda_K^{(n)}.$$

Application of (2.2.10) completes the proof. □

Lemma 2.2.6. *For each* $K \in \mathbb{N}_0$

$$\lim_{n\to\infty} \sqrt{n}\, s_K^{(n)} = K + 1. \tag{2.2.11}$$

Proof. We will use a simplified notation and write $s^{(i)} = s_K^{(i)}$.

The upper bound for the left-hand side is a consequence of Lemma 2.2.4.

For the lower bound, suppose *a contrario* that for some $\epsilon > 0$ there exist infinitely many values of an integer $n \geqslant 1$ for which

$$\sqrt{n}\, s^{(n)} < (1 - \epsilon)(K + 1). \tag{2.2.12}$$

Let $C > 0$ be a number which will be fixed later in the proof and set $m = n + \lfloor Cn \rfloor$.

Lemmas 2.2.3 and 2.2.4 imply that

$$\frac{s^{(1)} + \cdots + s^{(m)}}{(K+1)\sqrt{n}} \leqslant \frac{\left(s^{(1)} + \cdots + s^{(n)}\right) + (m-n)s^{(n)}}{(K+1)\sqrt{n}} < \frac{1}{\sqrt{n}}\left(\frac{1}{\sqrt{1}} + \cdots + \frac{1}{\sqrt{n}}\right) + (1-\epsilon)\frac{m-n}{n}.$$

On the right-hand side we may bound the sum $\frac{1}{\sqrt{1}} + \cdots + \frac{1}{\sqrt{n}}$ by the corresponding integral, thus

$$\sqrt{\frac{m}{n}} \cdot \frac{s^{(1)} + \cdots + s^{(m)}}{(K+1)\sqrt{m}} = \frac{s^{(1)} + \cdots + s^{(m)}}{(K+1)\sqrt{n}} < \frac{1}{\sqrt{n}} \int_0^n \frac{1}{\sqrt{x}}\,\mathrm{d}x + (1-\epsilon)\frac{m-n}{n} = 2 + (1-\epsilon)\frac{m-n}{n}.$$

Passing to the limit $n \to \infty$ for the values of n for which (2.2.12) holds true, Lemma 2.2.5 and the above inequality imply that

$$2\sqrt{1+C} \leqslant 2 + (1-\epsilon)C.$$

However, the above inequality is *not* fulfilled for any

$$0 < C < \frac{4\epsilon}{(1-\epsilon)^2}$$

which completes the proof *a contrario*. □

The following result is due to Okounkov [Oko00, Proposition 2]. We provide an alternative, hopefully simpler proof below.

Proposition 2.2.7. *For each* $i \in \mathbb{N}_0$

$$\lim_{n\to\infty} \sqrt{n}\,\mathbb{P}\left(E_i^{(n)}\right) = 1.$$

Proof. From (2.2.7) it follows that

$$\sqrt{n}\,\mathbb{P}\left(E_i^{(n)}\right) = \sqrt{n}\left(s_i^{(n)} - s_{i-1}^{(n)}\right) = \sqrt{n}\,s_i^{(n)} - \sqrt{n}\,s_{i-1}^{(n)}.$$

To each of the two summands on the right-hand side we apply Lemma 2.2.6 which completes the proof. □

2.2.4 What happens after just one step?

We will prove Lemma 2.2.8 and Lemma 2.2.9 which show that the (rough) information about the number of the row in which the growth of a Young diagram occurred does not influence too much the probability distribution of the resulting Young diagram.

Lemma 2.2.8. *For each* $r \in \mathbb{N}_0$ *the total variation distance between:*

- *the probability distribution of* $\lambda^{(n)}$ *(i.e., the Plancherel measure on the set* $\mathbb{Y}_n$*), and*
- *the* conditional *probability distribution of* $\lambda^{(n)}$ under the condition *that the event* $E_r^{(n)}$ *occurred,*

converges to zero, as $n \to \infty$.

Proof. For a Young diagram $\mu = (\mu_0, \mu_1, \dots)$ and $r \in \mathbb{N}_0$ we denote by

$$\operatorname{del}_r \mu = (\mu_0, \dots, \mu_{r-1}, \mu_r - 1, \mu_{r+1}, \dots)$$

the Young diagram obtained from μ by removing a single box from the row with the index r. The Young diagram $\operatorname{del}_r \mu$ is well-defined only if $\mu_r > \mu_{r+1}$.

We consider the finite-dimensional vector space of real-valued functions on the set $\mathbb{Y}_n$ of Young diagrams with n boxes. For any subset $A \subseteq \mathbb{Y}_n$ we consider the non-negative bilinear form on this space

$$\langle f, g \rangle_A = \sum_{\mu \in A} f_\mu \, g_\mu$$

and the corresponding seminorm

$$\|f\|_A := \sqrt{\langle f, f \rangle_A}.$$

An important special case is $A = \mathbb{Y}_n$ with the corresponding norm $\|\cdot\|_{\mathbb{Y}_n}$.

We consider two special vectors X, Y in this space:

$$X_\mu := \begin{cases} \frac{1}{\sqrt{(n-1)!}} \, d_{\operatorname{del}_r \mu}, & \text{if } \operatorname{del}_r \mu \text{ is well-defined,} \\ 0 & \text{otherwise,} \end{cases}$$

$$Y_\mu := \frac{d_\mu}{\sqrt{n!}}$$

where d_μ denotes the number of standard Young tableaux of shape μ. An important feature of these vectors is that for any set $A \subseteq \mathbb{Y}_n$

$$\begin{aligned} \|Y\|_A^2 &= \mathbb{P}\left\{\lambda^{(n)} \in A\right\}, \\ \langle X, Y \rangle_A &= \sqrt{n}\, \mathbb{P}\left\{\lambda^{(n)} \in A \text{ and } E_r^{(n)}\right\}, \\ \|X\|_A^2 &= \mathbb{P}\left\{\lambda^{(n-1)} \in \operatorname{del}_r A\right\}, \end{aligned}$$

see [Rom15, Section 1.19].

In particular, for the special case $A = \mathbb{Y}_n$

$$c_n := \sqrt{n}\, \mathbb{P}\left(E_r^{(n)}\right) = \langle X, Y \rangle_{\mathbb{Y}_n} \leqslant \|X\|_{\mathbb{Y}_n} \cdot \|Y\|_{\mathbb{Y}_n} \leqslant 1. \tag{2.2.13}$$

By Proposition 2.2.7 the left-hand side converges to 1 as $n \to \infty$. Since $\|X\|_{\mathbb{Y}_n} \leqslant 1$ and $\|Y\|_{\mathbb{Y}_n} = 1$, it follows that

$$\lim_{n\to\infty} c_n = \lim_{n\to\infty} \langle X, Y \rangle_{\mathbb{Y}_n} = \lim_{n\to\infty} \|X\|_{\mathbb{Y}_n} = 1.$$

As a consequence, a simple calculation using bilinearity of the scalar product shows that

$$\lim_{n\to\infty} \left\| c_n^{-1} X - Y \right\|_{\mathbb{Y}_n} = 0.$$

For any $A \subseteq \mathbb{Y}_n$ it follows therefore that

$$\left|\mathbb{P}\left\{\lambda^{(n)} \in A \;\middle|\; E_r^{(n)}\right\} - \mathbb{P}\left\{\lambda^{(n)} \in A\right\}\right| = \\ = \left|\frac{\langle X, Y\rangle_A}{\sqrt{n}\,\mathbb{P}\left(E_r^{(n)}\right)} - \langle Y, Y\rangle_A\right| = \left|\left\langle c_n^{-1}X - Y, Y\right\rangle_A\right| \leqslant \\ \left\|c_n^{-1}X - Y\right\|_{\mathbb{Y}_n} \cdot \|Y\|_{\mathbb{Y}_n}.$$

The right-hand side does not depend on the choice of A and converges to zero which concludes the proof. □

Lemma 2.2.9. *For each $k \in \mathbb{N}_0$ the total variation distance between:*

- *the probability distribution of $\lambda^{(n)}$ (i.e., the Plancherel measure on the set $\mathbb{Y}_n$), and*
- *the* conditional *probability distribution of $\lambda^{(n)}$* under the condition *that the event $\left(E_0^{(n)} \cup \cdots \cup E_k^{(n)}\right)^c$ occurred,*

is of order $o\left(\frac{1}{\sqrt{n}}\right)$, as $n \to \infty$.

Proof. For real numbers x and $c > 0$ we will denote by $x \pm c$ some unspecified real number in the interval $[x - c, x + c]$. In the following we will use the quantity $s_k^{(n)}$ defined in (2.2.7). We denote

$$F^{(n)} = \left(E_0^{(n)} \cup \cdots \cup E_k^{(n)}\right)^c.$$

Let C_n be the maximum (over $r \in \{0, \ldots, k\}$) of the total variation distance considered in Lemma 2.2.8. The law of total probability implies that for any set $A \subseteq \mathbb{Y}_n$

$$\mathbb{P}\left\{\lambda^{(n)} \in A\right\} = \\ \sum_{0 \leqslant r \leqslant k} \mathbb{P}\left\{\lambda^{(n)} \in A \;\middle|\; E_r^{(n)}\right\} \mathbb{P}\left(E_r^{(n)}\right) + \mathbb{P}\left\{\lambda^{(n)} \in A \;\middle|\; F^{(n)}\right\} \mathbb{P}\left(F^{(n)}\right) = \\ \sum_{0 \leqslant r \leqslant k} \left[\mathbb{P}\left\{\lambda^{(n)} \in A\right\} \pm C_n\right] \mathbb{P}\left(E_r^{(n)}\right) + \mathbb{P}\left\{\lambda^{(n)} \in A \;\middle|\; F^{(n)}\right\} \mathbb{P}(F^{(n)}) = \\ \mathbb{P}\left\{\lambda^{(n)} \in A\right\} s_k^{(n)} \pm C_n s_k^{(n)} + \mathbb{P}\left\{\lambda^{(n)} \in A \;\middle|\; F^{(n)}\right\} \left(1 - s_k^{(n)}\right).$$

By solving the above equation for the conditional probability we get

$$\mathbb{P}\left\{\lambda^{(n)} \in A \;\middle|\; F^{(n)}\right\} = \frac{\mathbb{P}\left\{\lambda^{(n)} \in A\right\}\left(1 - s_k^{(n)}\right) \pm C_n s_k^{(n)}}{1 - s_k^{(n)}}.$$

In this way we proved that the total variation distance considered in the statement of the lemma is bounded from above by

$$\frac{C_n s_k^{(n)}}{1 - s_k^{(n)}}. \tag{2.2.14}$$

The asymptotics of the individual factors in (2.2.14) is provided by Lemma 2.2.8 (which gives $C_n = o(1)$) and by Lemma 2.2.6 or, equivalently, by Okounkov's result Proposition 2.2.7 $\left(\text{which gives } s_k^{(n)} = O\left(\frac{1}{\sqrt{n}}\right)\right)$; this completes the proof. □

2.2.5 Asymptotic independence

As an intermediate step towards the proof of Theorem 2.2.2 we consider a sequence of independent random variables

$$\widetilde{V}^{(m)} = \left(\widetilde{R}^{(m+1)}, \dots, \widetilde{R}^{(m+\ell)}, \widetilde{\lambda}^{(m+\ell)}\right) \in \mathcal{N}^{\ell} \times \mathbb{Y} \tag{2.2.15}$$

which is independent with the vectors $V^{(m)}$ and $\overline{V}^{(m)}$ (recall the definitions in (2.2.3) and (2.2.4)), and such that the marginal distributions of $V^{(m)}$ and (2.2.15) coincide:

$$\begin{aligned} \widetilde{R}^{(m+i)} &\stackrel{d}{=} R^{(m+i)}, \qquad \text{for all } 1 \leqslant i \leqslant \ell \\ \widetilde{\lambda}^{(m+\ell)} &\stackrel{d}{=} \lambda^{(m+\ell)}. \end{aligned}$$

In particular, the probability distribution of $\widetilde{V}^{(m)}$ depends implicitly on k which is the number of the rows of Young diagrams which we observe.

Lemma 2.2.10. *For each $k \in \mathbb{N}_0$ there exists a sequence $b_n = o\left(\frac{1}{\sqrt{n}}\right)$ with the property that for all $m \geqslant (k+1)^2$ and $\ell \geqslant 1$ and $i \in \{1, \dots, \ell\}$*

$$\delta\Big(\left(\widetilde{R}^{(m+1)}, \dots, \widetilde{R}^{(m+i-1)}, R^{(m+i)}, R^{(m+i+1)}, \dots, R^{(m+\ell)}, \lambda^{(m+\ell)}\right), \left(\widetilde{R}^{(m+1)}, \dots, \widetilde{R}^{(m+i-1)}, \widetilde{R}^{(m+i)}, R^{(m+i+1)}, \dots, R^{(m+\ell)}, \lambda^{(m+\ell)}\right)\Big) \leqslant b_{m+i}. \tag{2.2.16}$$

The only difference between the two random vectors considered in (2.2.16) lies in the i-th coordinate: in the first vector this coordinate is equal to $R^{(m+i)}$ while in the second to $\widetilde{R}^{(m+i)}$.

Proof. For an integer $n \geqslant 1$ we define

$$b_n := \sum_{r \in \mathcal{N}} \mathbb{P}\left(R^{(n)} = r\right) \times \sum_{\lambda \in \mathbb{Y}_n} \left| \mathbb{P}\left(\lambda^{(n)} = \lambda \;\middle|\; R^{(n)} = r\right) - \mathbb{P}\left(\lambda^{(n)} = \lambda\right) \right|.$$

For the summands corresponding to $r \in \{0, \dots, k\}$ we note that the random events $\left\{R^{(n)} = r\right\}$ and $E_r^{(n)}$ are equal and we apply Proposition 2.2.7 and Lemma 2.2.8. For the summand $r = \infty$ we apply Lemma 2.2.9. This gives the desired asymptotics $b_n = o\left(\frac{1}{\sqrt{n}}\right)$. In the following we will show that this sequence indeed fulfills (2.2.16).

An iterative application of Lemma 2.2.1(a) shows that the left-hand side of (2.2.16) is equal to the total variation distance of the suffixes

$$\delta\Big(\left(R^{(m+i)}, R^{(m+i+1)}, \dots, R^{(m+\ell)}, \lambda^{(m+\ell)}\right), \left(\widetilde{R}^{(m+i)}, R^{(m+i+1)}, \dots, R^{(m+\ell)}, \lambda^{(m+\ell)}\right)\Big).$$

In order to evaluate the latter we consider an arbitrary set $X \subseteq \mathcal{N}^{\ell+1-i} \times \mathbb{Y}$. We can write

$$X = \bigcup_{r \in \mathcal{N}} \{r\} \times X_r$$

for some family of sets $X_r \subseteq \mathcal{N}^{\ell-i} \times \mathbb{Y}$ indexed by $r \in \mathcal{N}$. Since the Plancherel growth process (2.2.2) is a Markov process [Ker99, Sections 2.2 and 2.4],

$$\begin{aligned}
&\mathbb{P}\left(\left(R^{(m+i)}, R^{(m+i+1)}, \ldots, R^{(m+\ell)}, \lambda^{(m+\ell)}\right) \in X\right) = \\
&\sum_{r\in\mathcal{N}} \sum_{\lambda\in\mathbb{Y}_{m+i}} \mathbb{P}\left(R^{(m+i)} = r \text{ and } \lambda^{(m+i)} = \lambda\right) \times \\
&\qquad\qquad \mathbb{P}\left(\left(R^{(m+i+1)}, \ldots, R^{(m+\ell)}, \lambda^{(m+\ell)}\right) \in X_r \,\middle|\, \lambda^{(m+i)} = \lambda\right) = \\
&\sum_{r\in\mathcal{N}} \sum_{\lambda\in\mathbb{Y}_{m+i}} \mathbb{P}\left(R^{(m+i)} = r\right) \mathbb{P}\left(\lambda^{(m+i)} = \lambda \,\middle|\, R^{(m+i)} = r\right) \times \\
&\qquad\qquad \mathbb{P}\left(\left(R^{(m+i+1)}, \ldots, R^{(m+\ell)}, \lambda^{(m+\ell)}\right) \in X_r \,\middle|\, \lambda^{(m+i)} = \lambda\right). \qquad (2.2.17)
\end{aligned}$$

An analogous, but simpler calculation shows that

$$\begin{aligned}
&\mathbb{P}\left(\left(\widetilde{R}^{(m+i)}, R^{(m+i+1)}, \ldots, R^{(m+\ell)}, \lambda^{(m+\ell)}\right) \in X\right) = \\
&\sum_{r\in\mathcal{N}} \sum_{\lambda\in\mathbb{Y}_{m+i}} \mathbb{P}\left(R^{(m+i)} = r\right) \mathbb{P}\left(\lambda^{(m+i)} = \lambda\right) \times \\
&\qquad\qquad \mathbb{P}\left(\left(R^{(m+i+1)}, \ldots, R^{(m+\ell)}, \lambda^{(m+\ell)}\right) \in X_r \,\middle|\, \lambda^{(m+i)} = \lambda\right). \qquad (2.2.18)
\end{aligned}$$

The first and the third factor on the right-hand side of (2.2.17) coincide with their counterparts on the right-hand side of (2.2.18), and the third factor is bounded from above by 1. It follows that the absolute value of the difference between (2.2.17) and (2.2.18) is bounded from above by b_{m+i}, as required. □

2.2.6 Proof of Theorem 2.2.2

Proof. An iterative application of the triangle inequality combined with Lemma 2.2.10 implies that

$$\begin{aligned}
&\delta\Big(\left(R^{(m+1)}, \ldots, R^{(m+\ell)}, \lambda^{(m+\ell)}\right), \\
&\qquad\qquad \left(\widetilde{R}^{(m+1)}, \ldots, \widetilde{R}^{(m+\ell)}, \widetilde{\lambda}^{(m+\ell)}\right)\Big) = o\left(\frac{\ell}{\sqrt{m}}\right). \qquad (2.2.19)
\end{aligned}$$

On the other hand, thanks to the independence of the coordinates, Lemma 2.2.1(b) gives

$$\begin{aligned}
&\delta\Big(\left(\widetilde{R}^{(m+1)}, \ldots, \widetilde{R}^{(m+\ell)}, \widetilde{\lambda}^{(m+\ell)}\right), \left(\overline{R}^{(m+1)}, \ldots, \overline{R}^{(m+\ell)}, \overline{\lambda}^{(m+\ell)}\right)\Big) \\
&\qquad\qquad \leqslant \sum_{1\leqslant i\leqslant \ell} \delta\left(\widetilde{R}^{(m+i)}, \overline{R}^{(m+i)}\right). \qquad (2.2.20)
\end{aligned}$$

In the remaining part of the proof we will investigate the individual summand which

corresponds to $n := m + i$. We have

$$\delta\left(\widetilde{R}^{(n)}, \overline{R}^{(n)}\right) = \frac{1}{2}\sum_{0\leqslant r\leqslant k}\left|\mathbb{P}\left(\widetilde{R}^{(n)} = r\right) - \mathbb{P}\left(\overline{R}^{(n)} = r\right)\right| + \frac{1}{2}\left|\mathbb{P}\left(\widetilde{R}^{(n)} = \infty\right) - \mathbb{P}\left(\overline{R}^{(n)} = \infty\right)\right|. \quad (2.2.21)$$

The equality

$$\mathbb{P}\left(\widetilde{R}^{(n)} = \infty\right) = 1 - \sum_{0\leqslant r\leqslant k}\mathbb{P}\left(\widetilde{R}^{(n)} = r\right)$$

and the analogous equality for $\overline{R}^{(n)}$ imply that the right-hand side of (2.2.21) can be bounded as follows:

$$\delta\left(\widetilde{R}^{(n)}, \overline{R}^{(n)}\right) \leqslant \sum_{0\leqslant r\leqslant k}\left|\mathbb{P}\left(\widetilde{R}^{(n)} = r\right) - \mathbb{P}\left(\overline{R}^{(n)} = r\right)\right|. \quad (2.2.22)$$

Below we will find the asymptotics of the individual summands on the right-hand side.

For any $0 \leqslant r \leqslant k$, by the definitions

$$\mathbb{P}\left(\widetilde{R}^{(n)} = r\right) = \mathbb{P}\left(R^{(n)} = r\right) = \mathbb{P}\left(E_r^{(n)}\right)$$

and by Proposition 2.2.7 we get the asymptotics of the probability $\mathbb{P}\left(\widetilde{R}^{(n)} = r\right)$. The asymptotics of the probability $\mathbb{P}\left(\overline{R}^{(n)} = r\right)$ is given by its definition (2.2.5). It follows that the total variation distance in (2.2.22) is of order $o\left(\frac{1}{\sqrt{n}}\right)$.

In this way we proved that

$$\delta\Big(\left(\widetilde{R}^{(m+1)}, \dots, \widetilde{R}^{(m+\ell)}, \widetilde{\lambda}^{(m+\ell)}\right), \left(\overline{R}^{(m+1)}, \dots, \overline{R}^{(m+\ell)}, \overline{\lambda}^{(m+\ell)}\right)\Big) \leqslant o\left(\frac{\ell}{\sqrt{m}}\right). \quad (2.2.23)$$

The triangle inequality combined with (2.2.19) and (2.2.23) completes the proof. □

The following problem was asked by Maciej Dołęga.

Question 2.2.11. Plancherel growth process may be defined in terms of Schur polynomials and the corresponding Pieri rule. Is it possible to apply the ideas presented in the current section in the context of some other growth processes on $\mathbb{Y}$ (such as *Jack–Plancherel growth process* [Ker00]) which are related to other classical families of symmetric polynomials (such as *Jack polynomials*)?

2.3 Proofs of the main results

2.3.1 Proof of Theorem 2.1.1

Let $\mathbf{N}(t) = \big(N_0(t), \dots, N_k(t)\big), t \in \mathbb{R}$, be a collection of $k+1$ independent copies of the standard Poisson process. Let us fix some real number $c > 0$; in the following we assume that n is big enough so that $n - c\sqrt{n} \geqslant (k+1)^2$. It follows in particular that

$$n_t = n + \lfloor t\sqrt{n}\rfloor \qquad \text{for } t \in [-c, c].$$

We denote

$$L = L(n) = n_c - n_{-c} = \lfloor c\sqrt{n} \rfloor - \lfloor -c\sqrt{n} \rfloor.$$

Lemma 2.3.1. *For each $c > 0$ the total variation distance between the random vector*

$$\left(\Lambda^{(n+i)} - \Lambda^{(n)} : \lfloor -c\sqrt{n} \rfloor \leqslant i \leqslant \lfloor c\sqrt{n} \rfloor \right) \in \left(\mathbb{Z}^{k+1} \right)^{L+1} \tag{2.3.1}$$

and the corresponding random vector

$$\left(\mathbf{N}\left(\frac{i}{\sqrt{n}} \right) : \lfloor -c\sqrt{n} \rfloor \leqslant i \leqslant \lfloor c\sqrt{n} \rfloor \right) \in \left(\mathbb{Z}^{k+1} \right)^{L+1} \tag{2.3.2}$$

converges to zero, as $n \to \infty$ tends to infinity.

Proof. We consider the bijection

$$\mathbb{Z}^L \ni \left(a_i : \lfloor -c\sqrt{n} \rfloor \leqslant i \leqslant \lfloor c\sqrt{n} \rfloor \quad \text{with} \quad a_0 = 0 \right) \mapsto \left(a_i - a_{i-1} : \lfloor -c\sqrt{n} \rfloor < i \leqslant \lfloor c\sqrt{n} \rfloor \right) \in \mathbb{Z}^L.$$

Since an application of a bijection does not change the total variation distance, the aforementioned total variation distance between (2.3.1) and (2.3.2) is equal to the total variation distance $\delta(A, B)$ between the corresponding sequences of the increments, i.e.,

$$\begin{aligned} A &:= \left(\Lambda^{(n+i)} - \Lambda^{(n+i-1)} : \lfloor -c\sqrt{n} \rfloor < i \leqslant \lfloor c\sqrt{n} \rfloor \right) \\ &= \left(\left(\mathbb{1}_{R^{(n+i)}=0}, \ldots, \mathbb{1}_{R^{(n+i)}=k} \right) : \lfloor -c\sqrt{n} \rfloor < i \leqslant \lfloor c\sqrt{n} \rfloor \right) \end{aligned}$$

and the sequence of independent random vectors

$$B := \left(\mathbf{N}\left(\frac{i}{\sqrt{n}} \right) - \mathbf{N}\left(\frac{i-1}{\sqrt{n}} \right) : \lfloor -c\sqrt{n} \rfloor < i \leqslant \lfloor c\sqrt{n} \rfloor \right).$$

In the following we use the notations from Section 2.2.2 with $m := \left\lfloor n - c\sqrt{n} \right\rfloor$ and $\ell := L$. In particular we consider the collection of random variables $\overline{R}^{(m)}$ with the probability distribution given by (2.2.5) and (2.2.6) for this specific value of m. We define

$$\overline{A} := \left(\left(\mathbb{1}_{\overline{R}^{(n+i)}=0}, \ldots, \mathbb{1}_{\overline{R}^{(n+i)}=k} \right) : \lfloor -c\sqrt{n} \rfloor < i \leqslant \lfloor c\sqrt{n} \rfloor \right);$$

our strategy will be to apply the triangle inequality

$$\delta(A, B) \leqslant \delta(A, \overline{A}) + \delta(\overline{A}, B). \tag{2.3.3}$$

In order to bound the first summand on the right-hand side of (2.3.3) we apply Theorem 2.2.2 for the aforementioned values of m and ℓ; it follows that

$$\delta(A, \overline{A}) \leqslant \delta\left(V^{(m)}, \overline{V}^{(m)} \right) = o(1).$$

For the second summand on the right-hand side of (2.3.3) we apply Lemma 2.2.1(b)

$$\delta(\overline{A}, B) = \sum_{\lfloor -c\sqrt{n}\rfloor < i \leqslant \lfloor c\sqrt{n}\rfloor} \delta\Bigg(\left(\mathbb{1}_{\overline{R}^{(n+i)}=0}, \ldots, \mathbb{1}_{\overline{R}^{(n+i)}=k} \right), \underbrace{\mathrm{Pois}\left(\frac{1}{\sqrt{n}}\right) \times \cdots \times \mathrm{Pois}\left(\frac{1}{\sqrt{n}}\right)}_{k+1 \text{ factors}} \Bigg) = O\left(\frac{1}{\sqrt{n}}\right),$$

where the last bound follows from a direct calculation of the total variation distance of specific probability distributions on $\mathbb{N}_0^{k+1}$. □

Proof of Theorem 2.1.1. For given $t_1, \ldots, t_\ell \in \mathbb{R}$ we select arbitrary $c > \max(|t_1|, \ldots, |t_\ell|)$. Let n be big enough so that $n - c\sqrt{n} \geqslant (k+1)^2$. We apply Lemma 2.3.1; from the two random vectors which appear in this lemma we select the coordinates which correspond to $i \in \left\{\lfloor t_1\sqrt{n}\rfloor, \ldots, \lfloor t_\ell\sqrt{n}\rfloor\right\}$. It follows that the total variation distance between the law of the finite-dimensional marginal

$$\left(\Lambda^{(n_{t_1})} - \Lambda^{(n)}, \ldots, \Lambda^{(n_{t_\ell})} - \Lambda^{(n)}\right)$$

and the law of the appropriate marginal of $\mathbf{N}$, that is

$$\left(\mathbf{N}\left(\frac{\lfloor t_1\sqrt{n}\rfloor}{\sqrt{n}}\right), \ldots, \mathbf{N}\left(\frac{\lfloor t_\ell\sqrt{n}\rfloor}{\sqrt{n}}\right) \right) \tag{2.3.4}$$

converges to zero as $n \to \infty$.

On the other hand, by the maximal coupling lemma [Tho00, Section 8.3, Eq. (8.19)] (the definition of the total variance distance therein differs from ours by the factor 2), the total variation distance between (2.3.4) and

$$\left(\mathbf{N}(t_1), \ldots, \mathbf{N}(t_\ell)\right)$$

is bounded from above by

$$\mathbb{P}\left\{ \mathbf{N}\left(\frac{\lfloor t_i\sqrt{n}\rfloor}{\sqrt{n}}\right) \neq \mathbf{N}(t_i) \text{ for some } i \in \{1, \ldots, \ell\} \right\} = O\left(\frac{1}{\sqrt{n}}\right).$$

An application of the triangle inequality for the total variation distance completes the proof. □

Problem 2.3.2. Find the precise rate of convergence in Lemma 2.2.8 and Theorem 2.2.2. This convergence probably cannot be too fast because this would imply that an analogue of Theorem 2.1.1 holds true also in the scaling when in (2.1.3) we study $t \gg 1$, and the latter would potentially contradict the non-Gaussianity results for the lengths of the rows of Plancherel-distributed Young diagrams [BDJ99; BDJ00; BOO00; Joh01].

2.3.2 Proof of Corollary 2.1.2

Proof. Let $c > 0$ be arbitrary. We consider $n \in \mathbb{N}_0$ which is big enough so that $n - c\sqrt{n} - 1 \geqslant (k+1)^2$. We denote

$$I_n = \left\{ \left\lceil n - c\sqrt{n} \right\rceil, \ldots, \left\lfloor n + c\sqrt{n} \right\rfloor \right\}.$$

Our strategy is to apply Theorem 2.2.2 for $m := \lceil n - c\sqrt{n} \rceil - 1$ and $\ell := |I_n|$; in particular in the following we will use the collection of random variables $\overline{R}^{(i)}$ over $i \in I_n$ with the probability distribution given by (2.2.5) and (2.2.6) for this specific value of m.

We consider the following three collections of $k+1$ random subsets of I_n:

- the sequence $A = (A_0, \ldots, A_k)$ with

$$\begin{aligned} A_y &= \left\{ Q_{x,y} : x \in \mathbb{N}_0 \right\} \cap I_n \\ &= \left\{ i \in I_n : R^{(i)} = y \right\} \end{aligned}$$

  obtained by selecting the entries of the bottom $k+1$ rows of the recording tableau which belong to the specified interval,

- the sequence $\overline{A} = \left(\overline{A}_0, \ldots, \overline{A}_k\right)$ with

$$\overline{A}_y = \left\{ i \in I_n : \overline{R}^{(i)} = y \right\},$$

- the sequence $B = (B_0, \ldots, B_k)$ obtained by independent sampling, i.e., such that the family of random events $\left\{ i \in B_y \right\}$ indexed by $i \in I$ and $y \in \{0, \ldots, k\}$ is a family of independent events, each having equal probability $\frac{1}{\sqrt{n}}$.

Theorem 2.2.2 implies that the total variation distance $\delta\left(A, \overline{A}\right)$ converges to zero, as $n \to \infty$.

The information about the sequence $\overline{A}$ can be alternatively encoded by the sequence of independent random variables $(v_i : i \in I_n)$ given by

$$v_i = \left(\mathbb{1}_{i \in \overline{A}_0}, \ldots, \mathbb{1}_{i \in \overline{A}_k}\right) = \left(\mathbb{1}_{\overline{R}^{(i)}=0}, \ldots, \mathbb{1}_{\overline{R}^{(i)}=k}\right) \qquad \text{for } i \in I_n$$

Analogously the information about B can be encoded by the sequence of independent random variables $(w_i : i \in I_n)$, where

$$w_i = \left(\mathbb{1}_{i \in B_0}, \ldots, \mathbb{1}_{i \in B_k}\right) \qquad \text{for } i \in I_n.$$

By Lemma 2.2.1(b) it follows that the total variation distance for the vectors

$$\delta(\overline{A}, B) = \delta(v, w) \leqslant \sum_{i \in I_n} \delta(v_i, w_i)$$

is bounded by the sum of the coordinatewise total variation distances. The asymptotics of the individual summand

$$\delta(v_i, w_i) = o\left(\frac{1}{\sqrt{n}}\right)$$

is a consequence of a direct calculation based on the explicit form of the two probability distributions involved here. In this way we proved that the total variation distance $\delta(\overline{A}, B)$ converges to 0 as $n \to \infty$.

We apply a shift and a scaling to the random sets which form the collection A and the collection B; it follows that the total variation distance between

- the collection of random subsets of $\mathbb{R}$

$$\left(\left\{ \frac{Q_{x,y} - n}{\sqrt{n}} \ : \ x \in \mathbb{N}_0 \right\} \cap [-c, c] : \ y \in \{0, \dots, k\} \right)$$

obtained by truncating (2.1.5), and

- the collection of random subsets of $\mathbb{R}$

$$\left(\left\{ \frac{j - n}{\sqrt{n}} \ : \ j \in B_y \right\} : \ y \in \{0, \dots, k\} \right) \tag{2.3.5}$$

converges to zero as $n \to \infty$.

Each random set from the collection (2.3.5) converges in distribution to the Poisson point process on the interval $[-c, c]$, see [DVJ08, Proposition 11.3.I], which concludes the proof. □

2.3.3 Proof of Corollary 2.1.3

We start with an auxiliary result.

Lemma 2.3.3. *For real numbers $p, \lambda \geqslant 0$ and for integers $k \geqslant 0$ and n such that $p(k+1) \leqslant 1$ let $\xi_1, \dots, \xi_n$ be independent, identically distributed random variables with the uniform distribution $U(0,1)$ and let $\overline{R}^{(1)}, \dots, \overline{R}^{(n)}$ be independent, identically distributed random variables with the distribution*

$$\begin{cases} \mathbb{P}\left\{ \overline{R}^{(i)} = r \right\} = p & \text{for } r \in \{0, \dots, k\}, \\ \mathbb{P}\left\{ \overline{R}^{(i)} = \infty \right\} = 1 - (k+1)p, \end{cases} \tag{2.3.6}$$

cf. (2.2.5) *and* (2.2.6) *for an analogous distribution in a similar context.*

Then for any real numbers a, b such that $0 \leqslant a \leqslant b \leqslant 1$ the total variation distance between:

(a) the collection of $k+1$ random sets

$$\left([a, b] \cap \left\{ \xi_i : \overline{R}^{(i)} = y \right\} \ : \ y \in \{0, \dots, k\} \right), \tag{2.3.7}$$

and

(b) the collection of $k+1$ independent Poisson point processes $N_0, \dots, N_k$ on the interval $[a, b]$ with the intensity λ,

is bounded from above by

$$(k+1)^2 np^2 l^2 + (k+1) \cdot \left| \lambda l - npl \right|,$$

where $l = b - a$ is the length of the interval.

Proof. For each $i \in \{0, \dots, k\}$ the corresponding Poisson point process N_i can be generated by the following two-step procedure. Firstly, we sample the number of points $\mathfrak{n}_i$; it is a random variable with the Poisson distribution with the parameter λl, where $l := b - a$ is the length of

the interval. Secondly, we take $\mathfrak{n}_i$ independent random elements of the unit interval $[a, b]$ with the uniform distribution. The random variables $\mathfrak{n}_0, \ldots, \mathfrak{n}_k$ which correspond to independent Poisson processes are independent.

A similar construction can be performed for the collection (2.3.7) of random sets: we first sample the vector $(\mathfrak{m}_0, \ldots, \mathfrak{m}_k)$ of the cardinalities of the sets from (2.3.7) and then for each index $i \in \{0, \ldots, k\}$ we sample $\mathfrak{m}_i$ elements of the interval $[a, b]$. In this case, however, the random variables $\mathfrak{m}_0, \ldots, \mathfrak{m}_k$ are not independent.

From the above discussion it follows that the total variation distance considered in the statement of this lemma between (a) and (b) is equal to the total variation distance between the random vectors $\mathfrak{m} = (\mathfrak{m}_0, \ldots, \mathfrak{m}_k)$ and $\mathfrak{n} = (\mathfrak{n}_0, \ldots, \mathfrak{n}_k)$. In the following we will bound the latter distance.

The distribution of the random vector

$$\mathfrak{m} = \sum_{1 \leqslant j \leqslant n} \left(\mathbb{1}_{\overline{R}^{(j)}=0}, \ldots, \mathbb{1}_{\overline{R}^{(j)}=k} \right)$$

is the n-fold additive convolution of the discrete probability measure $\mathcal{M}$ on $\mathbb{Z}^{k+1}$ which to each basis vector $e_i = [0, \ldots, 0, 1, 0, \ldots, 0] \in \mathbb{Z}^{k+1}$ associates the probability pl and to the zero vector associates the remaining probability $1 - (k+1)pl$.

On the other hand, the distribution of the random vector $\mathfrak{n}$ can be alternatively seen as the n-fold additive convolution of the product measure $\mathcal{N} = \mathrm{Pois}\left(\frac{\lambda l}{n}\right) \times \cdots \times \mathrm{Pois}\left(\frac{\lambda l}{n}\right)$ on $\mathbb{Z}^{k+1}$. We also consider an auxiliary product measure $\mathcal{N}' = \mathrm{Pois}\left(pl\right) \times \cdots \times \mathrm{Pois}\left(pl\right)$ on $\mathbb{Z}^{k+1}$.

By Lemma 2.2.1(c) and the triangle inequality it follows that

$$\delta(\mathfrak{m}, \mathfrak{n}) \leqslant n\, \delta\left(\mathcal{M}, \mathcal{N}\right) \leqslant n\, \delta\left(\mathcal{M}, \mathcal{N}'\right) + n\, \delta\left(\mathcal{N}', \mathcal{N}\right). \tag{2.3.8}$$

For the first summand on the right-hand side, by a direct calculation of the positive part of the difference of the two measures and its ℓ^1 norm, we have

$$n\, \delta\left(\mathcal{M}, \mathcal{N}'\right) = n(k+1)\left[pl - ple^{-pl(k+1)}\right] \leqslant n(k+1)^2 p^2 l^2,$$

where the inequality follows from an elementary bound on the exponential function. For the second summand on the right-hand side of (2.3.8) we apply Lemma 2.2.1(c) in order to bound the total variation distance between two Poisson distributions; it follows that

$$n\, \delta\left(\mathcal{N}', \mathcal{N}\right) \leqslant (k+1) \cdot \left|\lambda l - npl\right|$$

which completes the proof. □

Proof of Corollary 2.1.3. We start with the case when $0 < w < 1$. We will show a stronger result that for each $A > 0$ the total variation distance between:

(i) the collection of $k+1$ sets

$$\left(\mathcal{P}_y^{(n)} \cap [-A, A] \;:\; y \in \{0, \ldots, k\} \right), \tag{2.3.9}$$

(cf. (2.1.7)), and

(ii) the collection of $k+1$ independent Poisson point processes on the interval $[-A, A]$ with the intensity $\frac{1}{\sqrt{w}}$

converges to zero, as $n \to \infty$.

As the first step, let us fix $\epsilon > 0$. Let Z_1 be the number of the entries of the sequence $\xi_1, \ldots, \xi_n$ which are weakly smaller than $w - \frac{A}{\sqrt{n}}$ and let Z_2 be the number of the entries of this sequence which are strictly smaller than $w + \frac{A}{\sqrt{n}}$; clearly the probability distribution of Z_1 and Z_2 is a binomial distribution. By Bienaymé–Chebyshev inequality it follows that the constant

$$B := A + \frac{1}{\sqrt{\epsilon}}$$

has the property that for each positive integer n

$$\mathbb{P}\left(Z_1 < n_{\min}\right) \leqslant \epsilon, \qquad \mathbb{P}\left(Z_2 \geqslant n_{\max}\right) \leqslant \epsilon \tag{2.3.10}$$

with

$$n_{\min} := \left\lfloor nw - B\sqrt{n} \right\rfloor, \qquad n_{\max} := \left\lceil nw + B\sqrt{n} \right\rceil.$$

In the following we assume that n is big enough so that

$$1 \leqslant n_{\min} \leqslant n_{\max} \leqslant n.$$

Without loss of generality we may assume that the entries of the sequence $\xi_1, \ldots, \xi_n$ are not repeated. It follows that this sequence can be encoded by two pieces of information:

- the sequence of order statistics $0 < \xi_{(1)} < \cdots < \xi_{(n)} < 1$, and
- the permutation $\pi = (\pi_1, \ldots, \pi_n)$ which encodes the order of the entries, i.e. $\pi_i < \pi_j$ if and only if $\xi_i < \xi_j$;

these two pieces of information are clearly independent and the permutation π is a uniformly random element of the symmetric group.

Since RSK algorithm is sensitive only to the relative order of the entries and not to their exact values, the insertion tableaux $P(\xi_1, \ldots, \xi_n)$ can be obtained from the insertion tableau $P(\pi_1, \ldots, \pi_n)$ by replacing each entry by the corresponding order statistic. It follows that the entries of a given row $y \in \mathbb{N}_0$ of the insertion tableau can be alternatively described as follows:

$$\left\{ P^{(n)}_{x,y} \ : \ 0 \leqslant x < \lambda^{(n)}_y \right\} = \left\{ \xi_{(i)} : i \text{ is in the row } y \text{ of the tableau } P(\pi_1, \ldots, \pi_n) \right\}.$$

It follows in particular that the intersection $\mathcal{P}^{(n)}_y \cap [-A, A]$ is defined in terms of (a certain subset of) the set of these order statistics $\xi_{(i)}$ which belong to the interval

$$I := [a, b]$$

with

$$a := w - \frac{A}{\sqrt{n}}, \qquad b := w + \frac{A}{\sqrt{n}}.$$

If neither of the two random events appearing in (2.3.10) holds true then this set of order statistics fulfills

$$I \cap \left\{ \xi_{(1)}, \ldots, \xi_{(n)} \right\} \subseteq \left\{ \xi_{(n_{\min})}, \ldots, \xi_{(n_{\max})} \right\};$$

under this condition it follows that in order to find the number of the row of $P^{(n)}$ which contains a given order statistic $\xi_{(i)} \in I$ it is enough to know the number of the row of the tableau $P(\pi_1, \ldots, \pi_n)$ which contains a given number j, over all choices of $j \in \{n_{\min}, \ldots, n_{\max}\}$. Here and in the following by *the number of the row* we will understand the element of the

fixed finite set $\mathcal{N} = \{0, \dots, k, \infty\}$ with the convention that the element ∞ corresponds to all rows above the bottom $k+1$ rows.

The insertion tableau $P(\pi) = Q\left(\pi^{-1}\right)$ is equal to the recording tableau of the inverse permutation; as a consequence the probability distribution of $P(\pi)$ is given by the Plancherel measure, can be interpreted as (a part of) the Plancherel growth process and thus Theorem 2.2.2 is applicable to this tableau. It follows that the probability distribution of the vector formed by the so understood *numbers of the rows* of the boxes $n_{\min}, \dots, n_{\max}$ can be approximated (up to an error $o(1)$ with respect to the total variation distance) by a sequence of independent random variables with the probability distribution given by (2.3.6) for $p = \frac{1}{\sqrt{n_{\min}}}$. Here and in the following we assume that n is big enough so that $(k+1)p \leqslant 1$.

The above two paragraphs show that the total variation distance between the collection

$$\left([a,b] \cap \left\{ P^{(n)}_{x,y} : x \geqslant 0 \right\} : y \in \{0, \dots, k\} \right), \tag{2.3.11}$$

of truncated entries of the bottom rows and the collection (2.3.7) is bounded from above by $2\epsilon + o(1)$. On the other hand, Lemma 2.3.3 applied to $\lambda = \sqrt{\frac{n}{w}}$ shows that the total variation distance between (2.3.7) and the collection of $k+1$ independent Poisson point processes (b) with the intensity λ on the interval I converges to zero. We combine these two bounds by the triangle inequality; as a result the total variation distance between (2.3.11) and (b) is bounded from above by $2\epsilon + o(1)$.

We consider the affine transformation $x \mapsto \sqrt{n}\,(x - w)$ which maps the interval $[a,b]$ to $[-A, A]$. This affine transformation also maps the random collection (2.3.11) to (2.3.9) from (i); it also maps the collection of Poisson processes (b) from Lemma 2.3.3 with the intensity λ to the collection (ii) of Poisson processes with the intensity $\lambda \frac{1}{\sqrt{n}} = \frac{1}{\sqrt{w}}$. The application of this affine transformation preserves the total variation distance between the random variables, so the inequality from the previous paragraph completes the proof.

In the case when $w = 1$ the above proof can be easily adjusted by changing the definitions of $n_{\max} := n$ and $b := 1$. □

Chapter 3

Poisson limit of bumping routes in the Robinson–Schensted correspondence

The following chapter is a modified version of the article [MMŚ21a]:

> M. Marciniak, Ł. Maślanka and P. Śniady: *Poisson limit of bumping routes in the Robinson–Schensted correspondence*, Probab. Theory Related Fields, vol. 181, Art. no. 4, 2021, doi: 10.1007/s00440-021-01084-y

which is available also in the public repository arXiv.org, https://arxiv.org/abs/2005.14397v2.

Abstract: We consider the Robinson–Schensted–Knuth algorithm applied to a random input and investigate the shape of the bumping route (in the vicinity of the y-axis) when a specified number is inserted into a large Plancherel-distributed random tableau. We show that after a projective change of the coordinate system the bumping route converges in distribution to the Poisson process.

3.1 Introduction

The notions of Young diagrams and tableaux are given in Section 1.1 We will shortly recall the corresponding notation in the next subsection. The *Robinson–Schensted–Knuth algorithm* (shortly *RSK*) is defined in Section 1.2.

3.1.1 Notations

Recall from Chapter 1 that we denote the set of all Young diagrams with n boxes by $\mathbb{Y}_n$ and the set of all Young diagrams by $\mathbb{Y}$. *The Young graph* is an oriented graph with vertices in $\mathbb{Y}$. The pair of diagrams μ and λ is connected by an oriented edge pointing from μ to λ if and only if λ can be created from the Young diagram μ by addition of a single box (which we denote by $\mu \nearrow \lambda$).

Recall that the rows of any Young diagram $\lambda = (\lambda_0, \lambda_1, \dots)$ are indexed by the elements of $\mathbb{N}_0$; in particular the length of the bottom row of λ is denoted by λ_0. For a tableau T we denote by $T_{x,y}$ its entry which lies in the intersection of the row $y \in \mathbb{N}_0$ and the column $x \in \mathbb{N}_0$. If p is a number which appears exactly once in a tableau T, we define the *position of the box with the number* p as the Cartesian coordinates of the bottom-left corner of the unique square which contains p; we denote this position by $\mathrm{pos}_p(T)$. For example, for T from Figure 3.1a, $\mathrm{pos}_{53}(T) = (1,1)$.

3.1.2 Plancherel measure, Plancherel growth process

Let $\mathfrak{S}_n$ denote the symmetric group of order n. We will view each permutation $\pi \in \mathfrak{S}_n$ as a sequence $\pi = (\pi_1, \dots, \pi_n)$ which has no repeated entries, and such that $\pi_1, \dots, \pi_n \in \{1, \dots, n\}$. Recall from Theorem 1.2.1 that the restriction of RSK to the symmetric group is a bijection which to a given permutation from $\mathfrak{S}_n$ associates a pair (P, Q) of standard Young tableaux of the same shape, consisting of n boxes. A fruitful area of study concerns the RSK algorithm applied to a uniformly random permutation from $\mathfrak{S}_n$, especially asymptotically in the limit $n \to \infty$, see [Rom15] and the references therein.

The Plancherel measure on $\mathbb{Y}_n$, denoted Plan_n, is defined as the probability distribution of the random Young diagram $\mathrm{RSK}(w)$ for a uniformly random permutation $w \in \mathfrak{S}_n$.

An *infinite standard Young tableau* [Ker99, Section 2.2] is a filling of the boxes in a subset of the upper-right quarterplane with positive integers, such that each row and each column is increasing, and each positive integer is used exactly once. There is a natural bijection between the set of infinite standard Young tableaux and the set of infinite paths in the Young graph

$$\lambda^{(0)} \nearrow \lambda^{(1)} \nearrow \cdots \qquad \text{with } \lambda^{(0)} = \varnothing; \tag{3.1.1}$$

this bijection is given by setting $\lambda^{(n)}$ to be the set of boxes of a given infinite standard Young tableau which are $\leqslant n$.

If $w = (w_1, w_2, \dots)$ is an *infinite* sequence, the recording tableau $Q(w)$ is defined as the infinite standard Young tableau in which each non-empty entry is equal to the number of the iteration in the infinite sequence of Schensted row insertions

$$\big((\varnothing \leftarrow w_1) \leftarrow w_2\big) \leftarrow \cdots$$

in which the corresponding box stopped being empty, see [RŚ15, Section 1.2.4]. Under the aforementioned bijection, the recording tableau $Q(w)$ corresponds to the sequence (3.1.1) with

$$\lambda^{(n)} = \mathrm{RSK}(w_1, \dots, w_n).$$

Let $\xi = (\xi_1, \xi_2, \dots)$ be an infinite sequence of independent, identically distributed random variables with the uniform distribution $U(0, 1)$ on the unit interval $[0, 1]$. *The Plancherel measure on the set of infinite standard Young tableaux* is defined as the probability distribution of $Q(\xi)$. Any sequence with the same probability distribution as (3.1.1) with

$$\lambda^{(n)} = \mathrm{RSK}(\xi_1, \dots, \xi_n) \tag{3.1.2}$$

will be called *the Plancherel growth process* [Ker99]. It turns out that the Plancherel growth process is a Markov chain [Ker99, Sections 2.2 and 2.4]. For a more systematic introduction to this topic we recommend the monograph [Rom15, Section 1.19].

3.1.3 Bumping route

The *bumping route* consists of the boxes the entries of which were changed by the action of Schensted insertion, including the last, newly created box, see Figures 3.1b and 3.1c. The bumping route will be denoted by $T \leftsquigarrow a$ or by $T_{\leftsquigarrow a}$ depending on current typographic needs. In any row $y \in \mathbb{N}_0$ there is at most one box from the bumping route $T \leftsquigarrow a$; we denote by $T_{\leftsquigarrow a}(y)$ its x-coordinate. We leave $T_{\leftsquigarrow a}(y)$ undefined if such a box does not exist. In this way

$$T \leftsquigarrow a \;= \Big\{ \big(T_{\leftsquigarrow a}(y), y\big) : y \in \mathbb{N}_0 \Big\}. \tag{3.1.3}$$

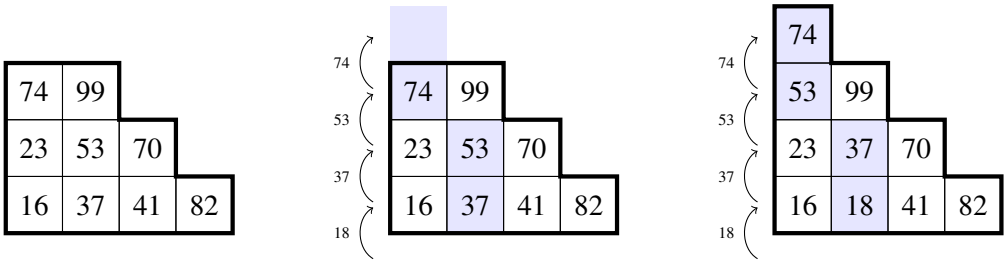

(a) (b) (c)

Figure 3.1: (a) The original tableau T. (b) We consider the Schensted row insertion of the number 18 to the tableau T. The highlighted boxes form the corresponding bumping route. The small numbers on the left (next to the arrows) indicate the inserted/bumped numbers. (c) The output $T \leftarrow 18$ of the Schensted insertion.

For example, for the tableau T from Figure 3.1a and $a = 18$ we have

$$T_{\leftsquigarrow a}(y) = \begin{cases} 1 & \text{for } y \in \{0,1\}, \\ 0 & \text{for } y \in \{2,3\}. \end{cases}$$

The bumping route $T \leftsquigarrow a$ can be visualized either as a collection of its boxes or as a plot of the function

$$x(y) = T_{\leftsquigarrow a}(\lfloor y \rfloor), \qquad y \in \mathbb{R}_+,$$

cf. the thick red line on Figure 3.2a.

3.1.4 Bumping routes for infinite tableaux

Any bumping route which corresponds to an insertion to a *finite* tableau is, well, also finite. This is disadvantageous when one aims at the asymptotics of such a bumping route in a row of index y in the limit $y \to \infty$. For such problems it would be preferable to work in a setup in which the bumping routes are infinite; we present the details in the following.

Let us fix the value of an integer $m \in \mathbb{N}_0$. Now, for an integer $n \geqslant m$ we consider a real number $0 < \alpha_n < 1$ and a finite sequence $\xi = (\xi_1, \dots, \xi_n)$ of independent, identically distributed random variables with the uniform distribution $U(0,1)$ on the unit interval $[0,1]$. In order to remove some randomness from this picture we will condition the choice of ξ in such a way that there are exactly m entries of ξ which are smaller than α_n; heuristically this situation is similar to a scenario without conditioning, for the choice of

$$\alpha_n = \frac{m}{n}. \tag{3.1.4}$$

We will study the bumping route

$$P(\xi_1, \dots, \xi_n) \leftsquigarrow \alpha_n \tag{3.1.5}$$

in the limit as $n \to \infty$ and m is fixed.

Without loss of generality we may assume that the entries of the sequence ξ are all different. Let $\pi \in \mathfrak{S}_n$ be the unique permutation which encodes the relative order of the entries in the sequence ξ, that is

$$\Big(\pi_i < \pi_j\Big) \iff \Big(X_i < X_j\Big)$$

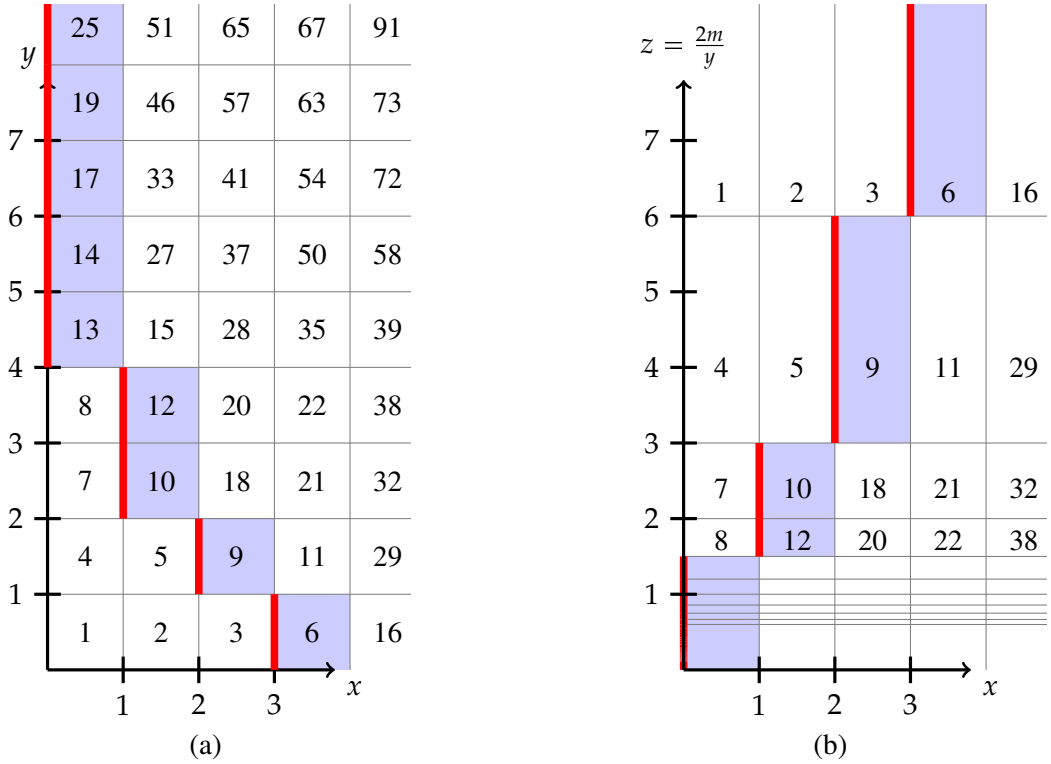

Figure 3.2: (a) The French convention for drawing tableaux. An example of an infinite standard Young tableau T sampled with the Plancherel distribution. The highlighted boxes form a bumping route obtained by adding the entry $m + 1/2$ for $m = 3$. The thick red line is the corresponding plot of the function $x(y) = T_{\leftsquigarrow m+1/2}(\lfloor y \rfloor)$. (b) The same tableau shown in the projective coordinates Oxz with $z = \frac{2m}{y}$. The thick red line is the plot of the function $x(z) = T_{\leftsquigarrow m+1/2}(\lfloor \frac{2m}{z} \rfloor)$.

for any $1 \leqslant i, j \leqslant n$. Since the algorithm behind the Robinson–Schensted–Knuth correspondence depends only on the relative order of the involved numbers and not their exact values, it follows that the bumping route (3.1.5) coincides with the bumping route

$$P(\pi_1, \dots, \pi_n) \leftsquigarrow m + 1/2. \tag{3.1.6}$$

The probability distribution of π is the uniform measure on $\mathfrak{S}_n$; it follows that the probability distribution of the tableau $P(\pi_1, \dots, \pi_n)$ which appears in (3.1.6) is the Plancherel measure Plan_n on the set of standard Young tableaux with n boxes. Since such a Plancherel-distributed random tableau with n boxes can be viewed as a truncation of an infinite standard Young tableau T with the Plancherel distribution, the bumping routes (3.1.5) and (3.1.6) can be viewed as truncations of the infinite bumping route

$$T \leftsquigarrow m + 1/2, \tag{3.1.7}$$

see Figure 3.2a for an example.

3.1.5 The main problem: asymptotics of infinite bumping routes

The aim of the current paper is to investigate the asymptotics of the *infinite* bumping route (3.1.7) in the limit $m \to \infty$.

Heuristically, this corresponds to investigation of the asymptotics of the *finite* bumping routes (3.1.5) in the simplified setting when we do not condition over some additional properties of ξ, in the scaling in which α_n does not tend to zero too fast (so that $\lim_{n\to\infty} \alpha_n n = \infty$, cf. (3.1.4)), but on the other hand α_n should tend to zero fast enough so that the bumping route is long enough that our asymptotic questions are well defined. We will not pursue in this direction and we will stick to the investigation of the *infinite* bumping route (3.1.7).

Even though Romik and Śniady [RŚ16] considered the asymptotics of *finite* bumping routes, their discussion is nevertheless applicable in our context. It shows that in the *balanced scaling* when we focus on the part of the bumping route with the Cartesian coordinates (x, y) of magnitude $x, y = O(\sqrt{m})$, the shape of the bumping route (scaled down by the factor $\frac{1}{\sqrt{m}}$) converges in probability towards an explicit curve, which we refer to as *the limit bumping curve*, see Figure 3.3 for an illustration.

In the current paper we go beyond the scaling used by Romik and Śniady and investigate the part of the bumping route with the Cartesian coordinates of order $x = O(1)$ and $y \gg \sqrt{m}$. This part of the bumping curves was not visible on Figure 3.3; in order to reveal it one can use the semi-logarithmic plot, cf. Figures 3.4 and 3.5.

3.1.6 The naive hyperbola

The first step in this direction would be to stretch the validity of the results of Romik and Śniady [RŚ16] beyond their limitations and to expect that the limit bumping curve describes the asymptotics of the bumping routes also in this new scaling. This would correspond to the investigation of the asymptotics of the (non-rescaled) limit bumping curve $\big(x(y), y\big)$ in the regime $y \to \infty$. The latter analysis was performed by Marciniak [Mar21]; one of his results is that

$$\lim_{y\to\infty} x(y)y = 2;$$

in other words, for $y \to \infty$ the *non-rescaled* limit bumping curve can be approximated by the hyperbola $xy = 2$ while its *rescaled* counterpart which we consider in the current paper by the hyperbola

$$xy = 2m \tag{3.1.8}$$

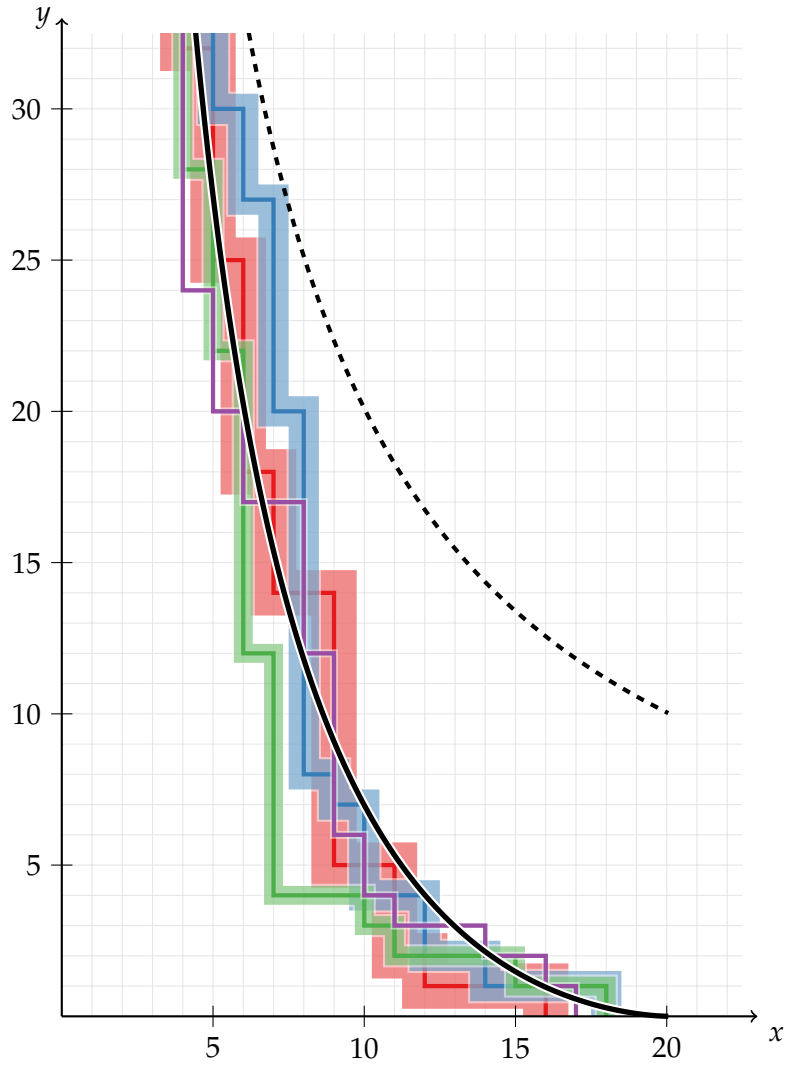

Figure 3.3: Four sample bumping routes corresponding to an insertion $T \leftarrow m + 1/2$ for $m = 100$ and a random infinite standard Young tableau T which was sampled according to the Plancherel measure. In order to improve visibility, each bumping route is visualized as the plot of the corresponding function $y \mapsto T_{\rightsquigarrow m+1/2}(\lfloor y \rfloor)$, cf. Figure 3.2a, and not as a collection of boxes. Colour and thickness were added in order to help identify the routes. The solid line is the (rescaled) *limit bumping curve*. The dashed line is the hyperbola $xy = 2m$, cf. Equation (3.1.8).

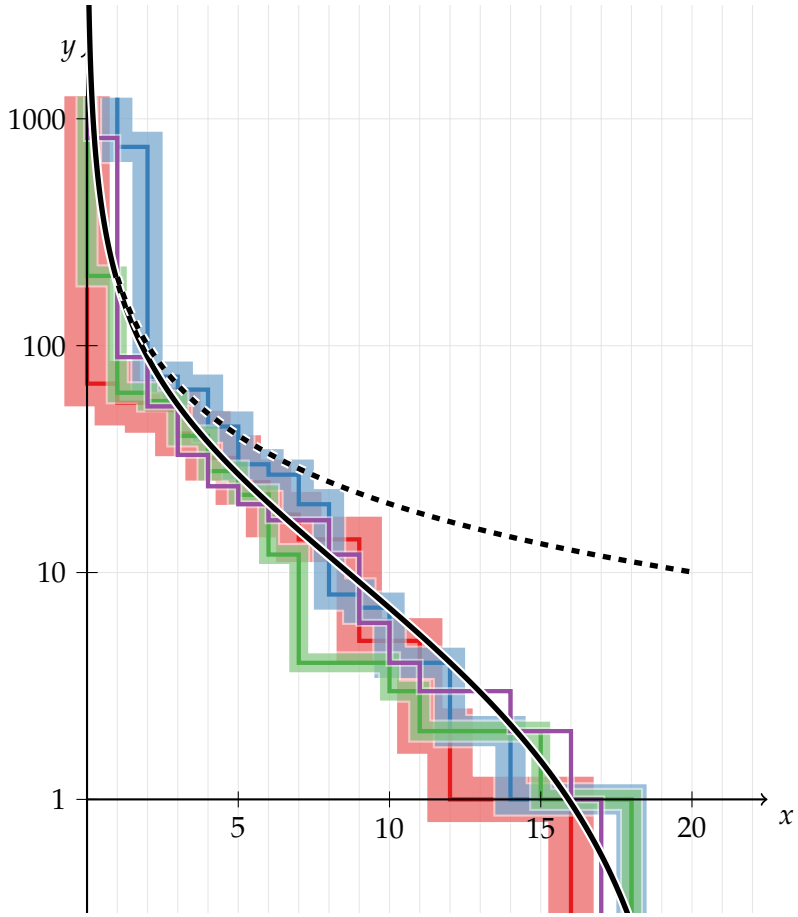

Figure 3.4: The content of Figure 3.3 shown with the axis y in the logarithmic scale.

which is shown on Figure 3.3 as the dashed line. At the very end of Section 3.1.8 we will discuss the extent to which this naive approach manages to confront the reality.

3.1.7 In which row a bumping route reaches a given column?

Let us fix some (preferably infinite) standard Young tableau T. The bumping route in each step jumps to the next row, directly up or to the left to the original column; in other words

$$T_{\leftsquigarrow m+1/2}(0) \geqslant T_{\leftsquigarrow m+1/2}(1) \geqslant \cdots$$

is a weakly decreasing sequence of non-negative integers.

For $x, m \in \mathbb{N}_0$ we denote by

$$Y_x^{[m]} = Y_x = \min\left\{y \in \mathbb{N}_0 : T_{\leftsquigarrow m+1/2}(y) \leqslant x\right\} \tag{3.1.9}$$

the index of the first row in which the bumping route $T\leftsquigarrow m + 1/2$ reaches the column with the index x (or less, if the bumping route skips the column x completely). For example, for the tableau T from Figure 3.2a we have

$$Y_0^{[3]} = 4, \quad Y_1^{[3]} = 2, \quad Y_2^{[3]} = 1, \quad Y_3^{[3]} = Y_4^{[3]} = \cdots = 0.$$

If such a row does not exist we set $Y_x = \infty$; the following result shows that we do not have to worry about such a scenario.

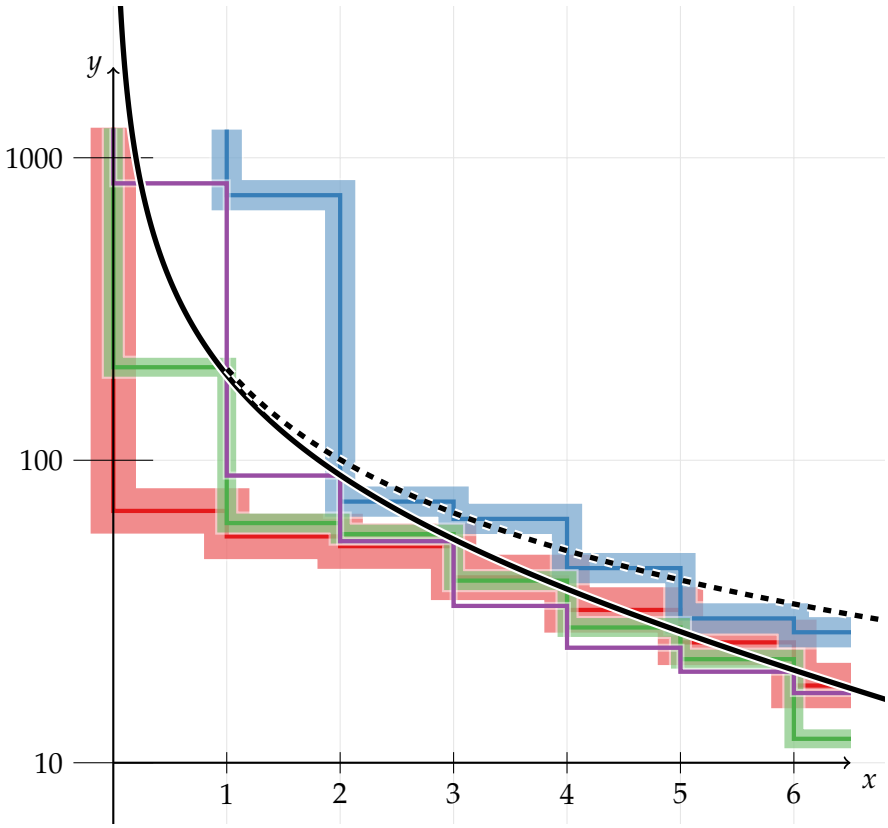

Figure 3.5: Zoom on a part of Figure 3.4. In this kind of scaling when $x = O(1)$ and $y \gg \sqrt{m}$ the results of Romik and Śniady [RŚ16] are *not* applicable and the rescaled limit bumping curve (the solid line) is shown for illustration purposes only.

Proposition 3.1.1. *For a random infinite standard Young tableau T with the Plancherel distribution*

$$Y_x^{[m]} < \infty \qquad \text{for all } x, m \in \mathbb{N}_0$$

holds true almost surely.

The proof is postponed to Section 3.3.8. For a sketch of the proof of an equivalent result see the work of Vershik [Ver20, Proposition 4] who uses different methods.

Theorem 3.1.2 (The main result)**.** *Assume that T is an infinite standard Young tableau with the Plancherel distribution. With the above notations, the random set*

$$\left(\frac{2m}{Y_0^{[m]}}, \frac{2m}{Y_1^{[m]}}, \dots \right)$$

converges in distribution, as $m \to \infty$, to the Poisson point process on $\mathbb{R}_+$ with the unit intensity.

The proof is postponed to Section 3.5.3.

Remark 3.1.3. The Poisson point process [Kin93, Section 4]

$$(0 < \xi_0 < \xi_1 < \cdots) \tag{3.1.10}$$

on $\mathbb{R}_+$ can be viewed concretely as the sequence of partial sums

$$\begin{aligned} \xi_0 &= \psi_0, \\ \xi_1 &= \psi_0 + \psi_1, \\ \xi_2 &= \psi_0 + \psi_1 + \psi_2, \\ &\vdots \end{aligned}$$

for a sequence (ψ_i) of independent, identically distributed random variables with the exponential distribution $\mathrm{Exp}(1)$. Thus a concrete way to express the convergence in Theorem 3.1.2 is to say that for each $l \in \mathbb{N}_0$ the joint distribution of the *finite* tuple of random variables

$$\left(\frac{2m}{Y_0^{[m]}}, \dots, \frac{2m}{Y_l^{[m]}} \right)$$

converges, as $m \to \infty$, to the joint distribution of the sequence of partial sums

$$\left(\psi_0, \quad \psi_0 + \psi_1, \quad \dots, \quad \psi_0 + \psi_1 + \cdots + \psi_l \right).$$

Corollary 3.1.4. *For each $x \in \mathbb{N}_0$ the random variable $\frac{Y_x^{[m]}}{2m}$ converges in distribution, as $m \to \infty$, to the reciprocal of the Erlang distribution* $\mathrm{Erlang}(x+1, 1)$.

In particular, for $x = 0$ it follows that the random variable $\frac{Y_0^{[m]}}{2m}$ which measures the (rescaled) number of steps of the bumping route to reach the leftmost column converges in distribution, as $m \to \infty$, to the Fréchet distribution of shape parameter $\alpha = 1$:

$$\lim_{m \to \infty} \mathbb{P} \left(\frac{Y_0^{[m]}}{2m} \leqslant u \right) = e^{-\frac{1}{u}} \qquad \text{for any } u \in \mathbb{R}_+. \tag{3.1.11}$$

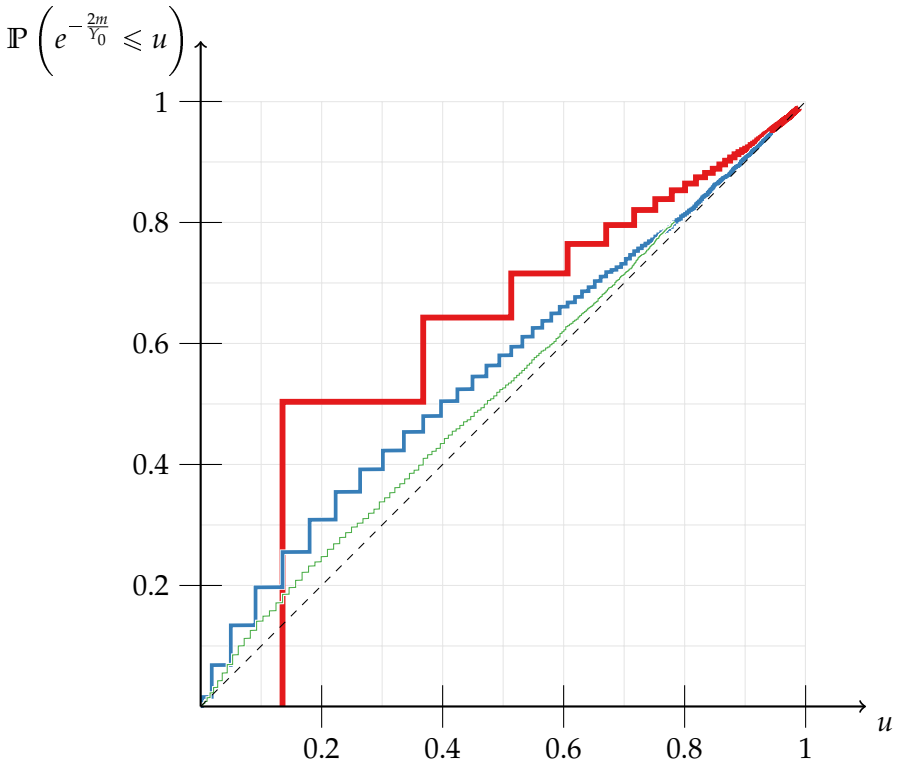

Figure 3.6: Monte Carlo simulations of the cumulative probability distribution function for the random variable $e^{-\frac{2m}{Y_0}}$. The thick red line corresponds to $m = 1$ (sample size is equal to 10 000); the blue line corresponds to $m = 6$ (sample size 3 000); the thin green line corresponds to $m = 25$ (sample size 2 500). The dashed line corresponds to the cumulative probability distribution function of the uniform distribution $U(0,1)$ on the unit interval. Due to constraints on computation time it was not possible to get Monte Carlo data for all values of u. The staircase feature of the plots is due to the discrete nature of the probability distribution of Y_0.

The Fréchet distribution has a heavy tail; in particular its first moment is infinite which provides a theoretical explanation for a bad time complexity of some of our Monte Carlo simulations.

Equivalently, the random variable $e^{-\frac{2m}{Y_0}}$ converges in distribution, as $m \to \infty$, to the uniform distribution $U(0,1)$ on the unit interval. Figure 3.6 presents the results of Monte Carlo simulations which illustrate this result.

3.1.8 Projective convention for drawing Young diagrams

Usually in order to draw a Young diagram we use the French convention and the Oxy coordinate system, cf. Figure 3.2a. For our purposes it will be more convenient to change the parametrization of the coordinate y by setting

$$z = z(y) = \frac{2m}{y}.$$

This convention allows us to show an infinite number of rows of a given tableau on a finite piece of paper, cf. Figure 3.2b. We will refer to this way of drawing Young tableaux as *the projective convention*; it is somewhat reminiscent of the *English convention* in the sense that the numbers in the tableau increase along the columns *from top to bottom*.

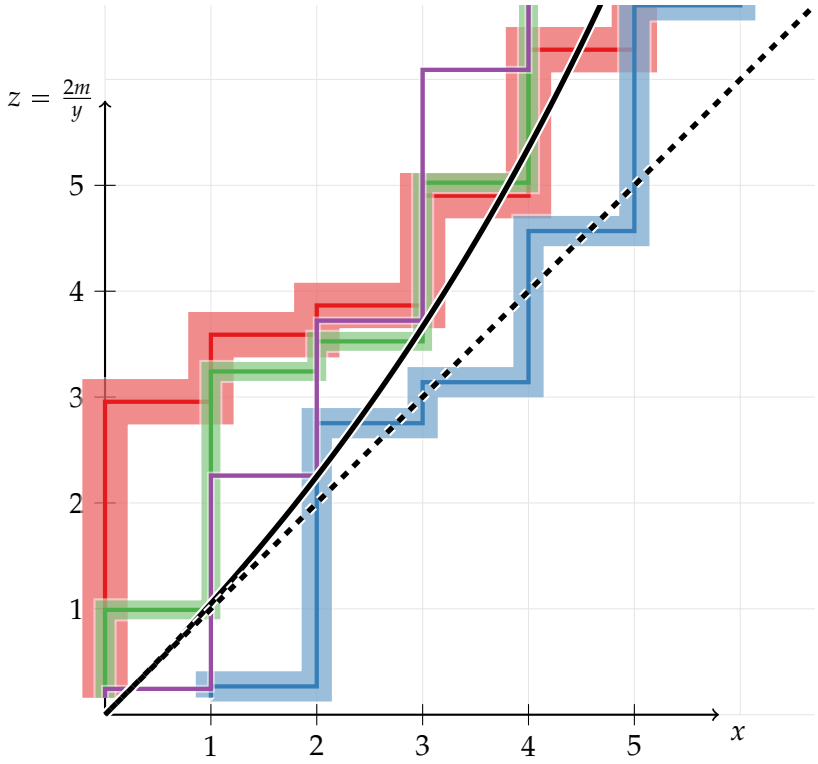

Figure 3.7: The bumping routes from Figure 3.3 shown in the projective convention (see also Figure 3.2b). The dashed line $x = z$ corresponds to the hyperbola (3.1.8); it is tangent in 0 to the rescaled limit bumping curve (the solid line); it is also the plot of the mean value of the Poisson process $z \mapsto \mathbb{E}N(z)$.

In the projective convention the bumping route can be seen as the plot of the function

$$x^{\mathrm{proj}}_{T,m}(z) = T_{\rightsquigarrow m+1/2}\left(\left\lfloor \frac{2m}{z} \right\rfloor\right) \qquad \text{for } z \in \mathbb{R}_+ \tag{3.1.12}$$

shown on Figure 3.2b as the thick red line.

With these notations Theorem 3.1.2 allows the following convenient reformulation.

Theorem 3.1.5 (The main result, reformulated)**.** *Let T be a random infinite standard Young tableau with the Plancherel distribution. For $m \to \infty$ the stochastic process*

$$\left\{x^{\mathrm{proj}}_{T,m}(z),\ z > 0\right\} \tag{3.1.13}$$

converges in distribution to the standard Poisson counting process $\{N(z),\ z > 0\}$ with the unit intensity.

For an illustration see Figure 3.7.

Remark 3.1.6. In Theorem 3.1.5 above, the convergence in distribution for stochastic processes is understood as follows: for any *finite* collection $z_1, \dots, z_l > 0$ we claim that the joint distribution of the tuple of random variables

$$\left(x^{\mathrm{proj}}_{T,m}(z_1), \dots, x^{\mathrm{proj}}_{T,m}(z_l)\right)$$

converges in the weak topology of probability measures, as $m \to \infty$, to the joint distribution of the tuple of random variables

$$\big(N(z_1), \dots, N(z_l)\big).$$

Proof of Theorem 3.1.5. The process (3.1.13) is a counting process. By the definition (3.1.12), the time of its k-th jump (for an integer $k \geqslant 1$)

$$\inf\Big\{z > 0 : \ x^{\mathrm{proj}}_{T,m}(z) = k\Big\} = \frac{2m}{Y^{[m]}_{k-1}}$$

is directly related to the number of the row in which the bumping route reaches the column with the index $k-1$. By Theorem 3.1.2 the joint distribution of the times of the jumps converges to the Poisson point process; it follows therefore that (3.1.13) converges to the Poisson counting process, as required. □

The plot of the mean value of the standard Poisson process $z \mapsto \mathbb{E}N(z)$ is the straight line $x = z$ which is shown on Figure 3.7 as the dashed line. Somewhat surprisingly it coincides with the hyperbola (3.1.8) shown in the projective coordinate system; a posteriori this gives some justification to the naive discussion from Section 3.1.6.

3.1.9 The main result with the right-to-left approach

Theorem 3.1.2 was formulated in a compact way which may obscure the true nature of this result. Our criticism is focused on the *left-to-right approach* from Remark 3.1.3 which might give a false impression that the underlying mechanism for generating the random variable $\frac{2m}{Y^{[m]}_{x+1}}$ describing the 'time of arrival' of the bumping route to the column number $x+1$ is based on generating first the random variable $\frac{2m}{Y^{[m]}_{x}}$ related to the previous column (that is the column directly to the left), and adding some 'waiting time' for the transition. In fact, such a mechanism is not possible without the time travel because the chronological order of the events is opposite: the bumping route first visits the column $x+1$ and *then* lands in the column x. In the following we shall present an alternative, *right-to-left* viewpoint which explains better the true nature of Theorem 3.1.2.

For the Poisson point process (3.1.10) and an integer $l \geqslant 1$ we consider the collection of random variables

$$\xi_l, R_0, R_1, \dots, R_{l-1} \tag{3.1.14}$$

which consists of ξ_l and the ratios

$$R_i := \frac{\xi_{i+1}}{\xi_i}$$

of consecutive entries of (ξ_i). Then (3.1.14) are independent random variables with the distributions that can be found easily. This observation can be used to *define* $\xi_0, \dots, \xi_l$ from the Poisson point process by setting

$$\xi_i = \xi_l \, \frac{1}{R_{l-1}} \frac{1}{R_{l-2}} \cdots \frac{1}{R_i} \qquad \text{for } 0 \leqslant i \leqslant l.$$

With this in mind we may reformulate Theorem 3.1.2 as follows.

Theorem 3.1.7 (The main result, reformulated). *For any integer $l \geqslant 0$ the joint distribution of the tuple of random variables*

$$\left(\frac{Y_l^{[m]}}{2m}, \quad \frac{Y_{l-1}^{[m]}}{2m}, \quad \frac{Y_{l-2}^{[m]}}{2m}, \quad \dots, \quad \frac{Y_0^{[m]}}{2m} \right) \tag{3.1.15}$$

converges, as $m \to \infty$, to the joint distribution of the random variables

$$\left(\frac{1}{\xi_l}, \quad \frac{1}{\xi_l} R_{l-1}, \quad \frac{1}{\xi_l} R_{l-1} R_{l-2}, \quad \dots, \quad \frac{1}{\xi_l} R_{l-1} \cdots R_0 \right), \tag{3.1.16}$$

where $\xi_l, R_{l-1}, \dots, R_0$ are independent random variables, the distribution of ξ_l is equal to $\mathrm{Erlang}(l+1, 1)$, *and for each $i \geqslant 0$ the distribution of the ratio R_i is supported on $[1, \infty)$ with the power law*

$$\mathbb{P}(R_i > u) = \frac{1}{u^{i+1}} \qquad \text{for } u \geqslant 1. \tag{3.1.17}$$

The order of the random variables in (3.1.15) reflects the chronological order of the events, from left to right. Heuristically, (3.1.16) states that the transition of the bumping route from the column $x+1$ to the column x gives a *multiplicative* factor R_x to the total waiting time, with the factors $R_0, R_1, \dots$ independent.

It is more common in mathematical and physical models that the total waiting time for some event arises as a *sum* of some independent summands, so the *multiplicative* structure in Theorem 3.1.7 comes as a small surprise. We believe that this phenomenon can be explained heuristically as follows: when we study the transition of the bumping route from row y to the next row $y+1$, the probability of the transition from column $x+1$ to column x seems asymptotically to be equal to

$$\frac{x+1}{y} + o\left(\frac{1}{y}\right) \qquad \text{for fixed value of } x, \text{ and for } y \to \infty.$$

This kind of decay would explain both the multiplicative structure ('if a bumping route arrives to a given column very late, it will stay in this column even longer') as well as the power law (3.1.17). We are tempted therefore to state the following conjecture which might explain the aforementioned transition probabilities of the bumping routes.

Conjecture 3.1.8. *For a Plancherel-distributed random infinite standard Young tableau T*

$$\mathbb{P}\left\{ T_{x-1,y+1} < T_{x,y} \right\} = \frac{x}{y} + o\left(\frac{1}{y}\right) \qquad \text{for fixed } x \geqslant 1 \text{ and } y \to \infty,$$

$$\mathbb{P}\left\{ T_{x-2,y+1} < T_{x,y} \right\} = o\left(\frac{1}{y}\right) \qquad \text{for fixed } x \geqslant 2 \text{ and } y \to \infty.$$

Furthermore, for each $x \in \{1, 2, \dots\}$ the set of points

$$\left\{ \log \frac{y}{c} : y \in \{c, c+1, \dots\} \text{ and } T_{x-1,y+1} < T_{x,y} \right\} \tag{3.1.18}$$

converges, as $c \to \infty$, to Poisson point process on $\mathbb{R}_+$ with the constant intensity equal to x.

Numerical experiments are not conclusive and indicate interesting clustering phenomena for the random set (3.1.18).

3.1.10 Asymptotics of fixed m

The previous results concerned the bumping routes $T \rightsquigarrow m + \frac{1}{2}$ in the limit $m \to \infty$ as the inserted number tends to infinity. In the following we concentrate on another class of asymptotic problems which concern the fixed value of m.

The following result shows that (3.1.11) gives asymptotically a very good approximation for the distribution tail of $Y_0^{[m]}$ in the scaling when m is fixed and the number of the row $y \to \infty$ tends to infinity.

Proposition 3.1.9. *For each integer $m \geqslant 1$*

$$\lim_{y\to\infty} y\, \mathbb{P}\left\{Y_0^{[m]} \geqslant y\right\} = 2m.$$

This result is illustrated on Figure 3.6 in the behavior of each of the cumulative distribution functions in the neighborhood of $u = 1$. The proof is postponed to Section 3.5.1.

Question 3.1.10. What can we say about the other columns, that is the tail asymptotics of $\mathbb{P}\left\{Y_x^{[m]} \geqslant y\right\}$ for fixed values of $x \in \mathbb{N}_0$ and $m \geqslant 1$, in the limit $y \to \infty$?

3.1.11 More open problems

Let T be a random Plancherel-distributed infinite standard Young tableau. We consider the *bumping tree* [Duz19] which is defined as the collection of all possible bumping routes for this tableau

$$\left(T \rightsquigarrow m + 1/2 \,:\, m \in \mathbb{N}_0\right),$$

which can be visualized, for example, as on Figure 3.8. Computer simulations suggest that the set of boxes which can be reached by *some* bumping route for a given tableau T is relatively 'small'. It would be interesting to state this vague observation in a meaningful way. We conjecture that the pictures such as Figure 3.8 which use the logarithmic scale for the y coordinate converge (in the scaling when $x = O(1)$ is bounded and $y \to \infty$) to some meaningful particle jump-and-coalescence process.

3.1.12 Overview of the paper. Sketch of the proof of Theorem 3.1.2

As we already mentioned, the detailed proof of Theorem 3.1.2 is postponed to Section 3.5.3. In the following we present an overview of the paper and a rough sketch of the proof.

3.1.12.1 Trajectory of infinity. Lazy parametrization of the bumping route

Without loss of generality we may assume that the Plancherel-distributed infinite tableau T from the statement of Theorem 3.1.2 is of the form $T = Q(\xi_1, \xi_2, \dots)$ for a sequence $\xi_1, \xi_2, \dots$ of independent, identically distributed random variables with the uniform distribution $U(0, 1)$.

We will iteratively apply Schensted row insertion to the entries of the infinite sequence

$$\xi_1, \dots, \xi_m, \infty, \xi_{m+1}, \xi_{m+2}, \dots \tag{3.1.19}$$

which is the initial sequence ξ with our favorite symbol ∞ inserted at the position $m + 1$. At step $m + 1$ the symbol ∞ is inserted at the end of the bottom row; as further elements of the sequence (3.1.19) are inserted, the symbol ∞ stays put or is being bumped to the next row, higher and higher.

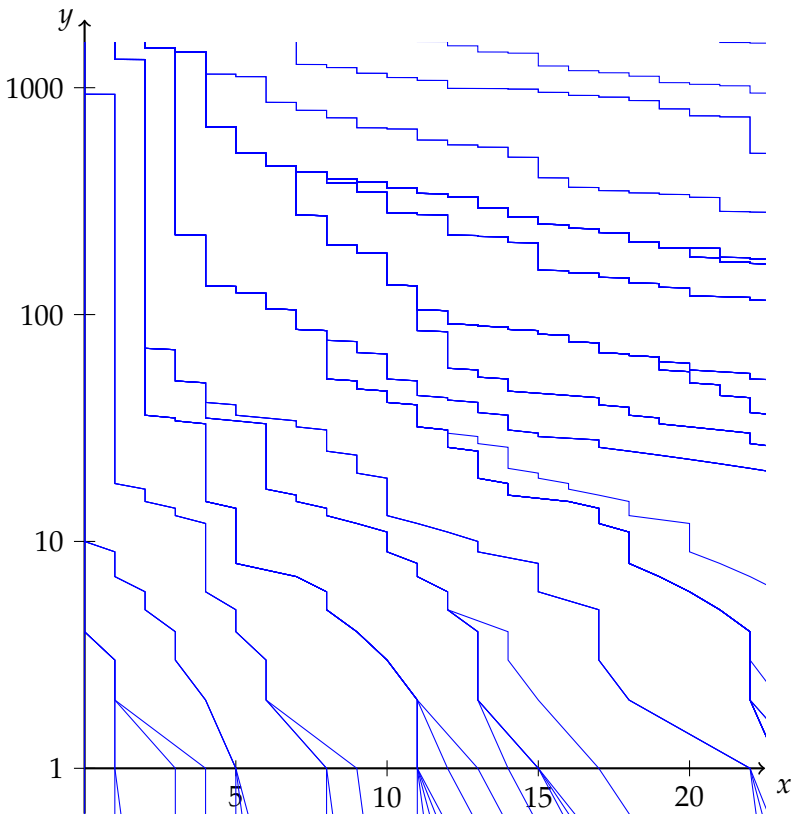

Figure 3.8: All possible bumping routes (*"the bumping tree"*) for a given Plancherel-distributed random infinite standard Young tableau. The y axis is shown using the logarithmic scale. In order to improve visibility, each bumping route was drawn as a piecewise-affine function connecting the points (3.1.3) and *not* as a jump function as in Figure 3.2a.

In Proposition 3.3.1 we will show that the trajectory of ∞ in this infinite sequence of Schensted row insertions

$$\Big(\big(P(\xi_1,\dots,\xi_m,\infty)\leftarrow\xi_{m+1}\big)\leftarrow\xi_{m+2}\Big)\leftarrow\cdots \tag{3.1.20}$$

coincides with the bumping route $T \leftsquigarrow m+1/2$. Thus our main problem is equivalent to studying the time evolution of the position of ∞ in the infinite sequence of row insertions (3.1.20). This time evolution also provides a convenient alternative parametrization of the bumping route, called *lazy parametrization*.

3.1.12.2 Augmented Young diagrams

For $t \geqslant m$ we consider the insertion tableau

$$\mathcal{T}^{(t)} = P(\xi_1,\dots,\xi_m,\infty,\xi_{m+1},\dots,\xi_t) \tag{3.1.21}$$

which appears at an intermediate step in (3.1.20) after some finite number of row insertions was performed. By removing the information about the entries of the tableau $\mathcal{T}^{(t)}$ we obtain the *shape* of $\mathcal{T}^{(t)}$, denoted by $\mathrm{sh}\,\mathcal{T}^{(t)}$, which is a Young diagram with $t+1$ boxes. In the following we will explain how to modify the notion of *the shape of a tableau* so that it better fits our needs.

Let us remove from the tableau $\mathcal{T}^{(t)}$ the numbers $\xi_1,\dots,\xi_t$ and let us keep only the information about the position of the box which contains the symbol ∞. The resulting object, called *augmented Young diagram* (see Figure 3.9 for an illustration), can be regarded as a pair $\Lambda^{(t)} = (\lambda, \square)$ which consists of:

- the Young diagram λ with t boxes which keeps track of the positions of the boxes with the entries $\xi_i, i \in \{1,\dots,t\}$, in $\mathcal{T}^{(t)}$;
- the outer corner $\square$ of λ which is the position of the box with ∞ in $\mathcal{T}^{(t)}$.

We will say that $\mathrm{sh}^*\,\mathcal{T}^{(t)} = \Lambda^{(t)}$ is the *augmented shape* of $\mathcal{T}^{(t)}$.

The set of augmented Young diagrams, denoted $\mathbb{Y}^*$, has a structure of an oriented graph which is directly related to Schensted row insertion, as follows. For a pair of augmented Young diagrams $\Lambda, \widetilde{\Lambda} \in \mathbb{Y}^*$ we say that $\Lambda \nearrow \widetilde{\Lambda}$ if there exists a tableau T (which contains exactly one entry equal to ∞) such that $\Lambda = \mathrm{sh}^*\,T$ and there exists some number x such that $\widetilde{\Lambda} = \mathrm{sh}^*(T \leftarrow x)$, see Figure 3.10 and Section 3.3.4 for more details.

With these notations the time evolution of the position of ∞ in the sequence of row insertions (3.1.20) can be extracted from the sequence of the corresponding augmented shapes

$$\Lambda^{(m)} \nearrow \Lambda^{(m+1)} \nearrow \cdots . \tag{3.1.22}$$

3.1.12.3 Augmented Plancherel growth processes

The random sequence (3.1.22) is called *the augmented Plancherel growth process initiated at time m*; in Section 3.3.6 we will show that it is a Markov chain with dynamics closely related to the usual (i.e., non-augmented) Plancherel growth process. Since we have a freedom of choosing the value of the integer $m \in \mathbb{N}_0$, we get a whole family of augmented Plancherel growth processes. It turns out that the transition probabilities for these Markov chains do not depend on the value of m.

Our strategy is to use the Markov property of augmented Plancherel growth processes combined with the following two pieces of information.

- *Probability distribution at a given time t.* In Proposition 3.3.9 we give an asymptotic description of the probability distribution of $\Lambda^{(t)}$ in the scaling when $m, t \to \infty$ in such a way that $t = \Theta(m^2)$.

- *Averaged transition probabilities.* In Proposition 3.4.2 we give an asymptotic description of the transition probabilities for the augmented Plancherel growth processes between two moments of time n and n' (with $n < n'$) in the scaling when $n, n' \to \infty$.

Thanks to these results we will prove Theorem 3.4.3 which gives an asymptotic description of the probability distribution of the trajectory of the symbol ∞ or, equivalently, the bumping route in the lazy parametrization.

Finally, in Section 3.5 we explain how to translate this result to the non-lazy parametrization of the bumping route in which the boxes of the bumping route are parametrized by the index of the row; this completes the proof of Theorem 3.1.2.

The main difficulty lies in the proofs of the aforementioned Proposition 3.3.9 and Proposition 3.4.2; in the following we sketch their proofs.

3.1.12.4 Probability distribution of the augmented Plancherel growth process at a given time.

In order to prove the aforementioned Proposition 3.3.9 we need to understand the probability distribution of the augmented shape of the insertion tableau $\mathcal{T}^{(t)}$ given by (3.1.21) in the scaling when $m = O(\sqrt{t})$. Thanks to some symmetries of the RSK algorithm, the tableau $\mathcal{T}^{(t)}$ is equal to the transpose of the insertion tableau

$$P(\underbrace{\xi_t, \xi_{t-1}, \dots, \xi_{m+1}}_{t-m \text{ entries}}, \infty, \xi_m, \dots, \xi_1) \tag{3.1.23}$$

which corresponds to the original sequence read backwards. Since the probability distribution of the sequence ξ is invariant under permutations, the augmented shape of the tableau (3.1.23) can be viewed as the value at time t of the augmented Plancherel growth process initiated at time $m' := t - m$.

The remaining difficulty is therefore to understand the probability distribution of the augmented Plancherel growth process initiated at time m', after additional m steps of Schensted row insertion were performed. We are interested in the asymptotic setting when $m' \to \infty$ and the number of additional steps $m = O(\sqrt{m'})$ is relatively small. This is precisely the setting which was considered in Chapter 2 ([MMŚ21b]) about the Poisson limit theorem for the Plancherel growth process. We summarize these results in Section 3.2; based on them we prove in Proposition 3.3.6 that the index of the row of the symbol ∞ in the tableau (3.1.23) is asymptotically given by the Poisson distribution.

By taking the transpose of the augmented Young diagrams we recover Proposition 3.3.9, as desired.

3.1.12.5 Averaged transition probabilities

We will sketch the proof of the aforementioned Proposition 3.4.2 which concerns an augmented Plancherel growth process

$$\Lambda^{(n)} \nearrow \Lambda^{(n+1)} \nearrow \cdots \tag{3.1.24}$$

for which the initial probability distribution at time n is given by $\Lambda^{(n)} = \left(\lambda^{(n)}, \square^{(n)}\right)$, where $\lambda^{(n)}$ is a random Young diagram with n boxes distributed (approximately) according to the Plancherel measure and $\square^{(n)}$ is its outer corner located in the column with the fixed index k.

Our goal is to describe the probability distribution of this augmented Plancherel growth process at some later time n', asymptotically as $n, n' \to \infty$.

Our first step in this direction is to approximate the probability distribution of the Markov process (3.1.24) by a certain linear combination (with real, positive and negative, coefficients) of the probability distributions of augmented Plancherel growth processes initiated at time m. This linear combination is taken over the values of m which are of order $O\left(\sqrt{n}\right)$. Finding such a linear combination required the results which we discussed above in Section 3.1.12.4, namely a good understanding of the probability distribution at time n of the augmented Plancherel growth process initiated at some specified time $m = O\left(\sqrt{n}\right)$.

The probability distribution of $\Lambda^{(n')}$ is then approximately equal to the aforementioned linear combination of the laws (this time evaluated at time n') of the augmented Plancherel growth processes initiated at some specific times m. This linear combination is straightforward to analyze because for each individual summand the results from Section 3.1.12.4 are applicable. This completes the sketch of the proof of Proposition 3.4.2.

3.2 Growth of the bottom rows

In the current section we will gather some results and some notations from Chapter 2 which will be necessary for the purposes of the current work.

3.2.1 Total variation distance

Suppose that μ and ν are (signed) measures on the same discrete set S. Such measures can be identified with real-valued functions on S. We define the *total variation distance* between the measures μ and ν

$$\delta(\mu, \nu) := \frac{1}{2} \left\| \mu - \nu \right\|_{\ell^1} \tag{3.2.1}$$

as half of their ℓ^1 distance as functions. If X and Y are two random variables with values in the same discrete set S, we define their total variation distance $\delta(X, Y)$ as the total variation distance between their probability distributions (which are probability measures on S).

Usually in the literature the total variation distance is defined only for probability measures. In such a setup the total variation distance can be expressed as

$$\delta(\mu, \nu) = \max_{X \subset S} \left| \mu(X) - \nu(X) \right| = \left\| (\mu - \nu)^+ \right\|_{\ell^1}. \tag{3.2.2}$$

In the current paper we will occasionally use the notion of the total variation distance also for signed measures for which (3.2.1) and (3.2.2) are *not* equivalent.

3.2.2 Growth of rows in Plancherel growth process

Let $\lambda^{(0)} \nearrow \lambda^{(1)} \nearrow \cdots$ be the Plancherel growth process. For integers $n \geqslant 1$ and $r \in \mathbb{N}_0$ we denote by $E_r^{(n)}$ the random event which occurs if the unique box of the skew diagram $\lambda^{(n)}/\lambda^{(n-1)}$ is located in the row with the index r.

The following result was proved by Okounkov [Oko00, Proposition 2], see also Proposition 2.2.7 for an alternative proof.

Proposition 3.2.1. *For each* $r \in \mathbb{N}_0$

$$\lim_{n \to \infty} \sqrt{n}\, \mathbb{P}\left(E_r^{(n)} \right) = 1.$$

Let us fix an integer $k \in \mathbb{N}_0$. We define $\mathcal{N} = \{0, 1, \dots, k, \infty\}$. For $n \geqslant 1$ we define the random variable $R^{(n)} \in \mathcal{N}$ which is given by

$$R^{(n)} = \begin{cases} r & \text{if the event } E_r^{(n)} \text{ occurs for } 0 \leqslant r \leqslant k, \\ \infty & \text{if the event } E_r^{(n)} \text{ occurs for some } r > k. \end{cases}$$

Let $\ell = \ell(n)$ be a sequence of non-negative integers such that

$$\ell = O\left(\sqrt{n}\right).$$

For a given integer $n \geqslant (k+1)^2$ we focus on the specific part of the Plancherel growth process

$$\lambda^{(n)} \nearrow \cdots \nearrow \lambda^{(n+\ell)}. \tag{3.2.3}$$

We will encode some partial information about the growths of the rows as well as about the final Young diagram in (3.2.3) by the random vector

$$V^{(n)} = \left(R^{(n+1)}, \dots, R^{(n+\ell)}, \lambda^{(n+\ell)}\right) \in \mathcal{N}^\ell \times \mathbb{Y}. \tag{3.2.4}$$

We also consider the random vector

$$\overline{V}^{(n)} = \left(\overline{R}^{(n+1)}, \dots, \overline{R}^{(n+\ell)}, \overline{\lambda}^{(n+\ell)}\right) \in \mathcal{N}^\ell \times \mathbb{Y} \tag{3.2.5}$$

which is defined as a sequence of independent random variables; the random variables $\overline{R}^{(n+1)}, \dots, \overline{R}^{(n+\ell)}$ have the same distribution given by

$$\begin{aligned} \mathbb{P}\left\{\overline{R}^{(n+i)} = r\right\} &= \frac{1}{\sqrt{n}} && \text{for } r \in \{0, \dots, k\},\ 1 \leqslant i \leqslant \ell, \\ \mathbb{P}\left\{\overline{R}^{(n+i)} = \infty\right\} &= 1 - \frac{k+1}{\sqrt{n}} \end{aligned}$$

and $\overline{\lambda}^{(n+\ell)}$ is distributed according to the Plancherel measure $\mathrm{Plan}_{n+\ell}$; in particular the random variables $\lambda^{(n+\ell)}$ and $\overline{\lambda}^{(n+\ell)}$ have the same distribution.

Heuristically, the following result states that when the Plancherel growth process is in an advanced stage and we observe a relatively small number of its additional steps, the growths of the bottom rows occur approximately like independent random variables. Additionally, these growths do not affect too much the final shape of the Young diagram.

Theorem 3.2.2 ([MMŚ21b, Theorem 2.2]). *With the above notations, for each fixed $k \in \mathbb{N}_0$ the total variation distance between $V^{(n)}$ and $\overline{V}^{(n)}$ converges to zero, as $n \to \infty$; more specifically*

$$\delta\left(V^{(n)}, \overline{V}^{(n)}\right) = o\left(\frac{\ell}{\sqrt{n}}\right).$$

3.3 Augmented Plancherel growth process

In this section we will introduce our main tool: *the augmented Plancherel growth process* which keeps track of the position of a very large number in the insertion tableau when new random numbers are inserted.

3.3.1 Lazy parametrization of bumping routes

Our first step towards the proof of Theorem 3.1.2 is to introduce a more convenient parametrization of the bumping routes. In (3.1.3) we used y, the number of the row, as the variable which parametrizes the bumping route. In the current section we will introduce the *lazy parametrization*.

Let us fix a (finite or infinite) standard Young tableau T and an integer $m \in \mathbb{N}_0$. For a given integer $t \geqslant m$ we denote by

$$\square^{\mathrm{lazy}}_{T,m}(t) = \left(x^{\mathrm{lazy}}_{T,m}(t), y^{\mathrm{lazy}}_{T,m}(t)\right)$$

the coordinates of the first box in the bumping route $T \leftsquigarrow m + 1/2$ which contains an entry of T which is bigger than t. If such a box does not exists, this means that the bumping route is finite, and all boxes of the tableau T which belong to the bumping route are $\leqslant t$. If this is the case we define $\square^{\mathrm{lazy}}_{T,m}(t)$ to be the last box of the bumping route, i.e. the box of the bumping route which lies outside of T. We will refer to

$$t \mapsto \left(x^{\mathrm{lazy}}_{T,m}(t), y^{\mathrm{lazy}}_{T,m}(t)\right) \tag{3.3.1}$$

as the *lazy parametrization of the bumping route*.

For example, for the infinite tableau T from Figure 3.2a and $m = 3$ the usual parametrization of the bumping route is given by

$$T_{\leftsquigarrow m+1/2}(y) = \begin{cases} 3 & \text{for } y = 0, \\ 2 & \text{for } y = 1, \\ 1 & \text{for } y = 2, \\ 1 & \text{for } y = 3, \\ 0 & \text{for } y \geqslant 4, \end{cases}$$

while its lazy counterpart is given by

$$\square^{\mathrm{lazy}}_{T,m}(t) = \left(x^{\mathrm{lazy}}_{T,m}(t), y^{\mathrm{lazy}}_{T,m}(t)\right) = \begin{cases} (3,0) & \text{for } t \in \{3,4,5\}, \\ (2,1) & \text{for } t \in \{6,7,8\}, \\ (1,2) & \text{for } t = 9, \\ (1,3) & \text{for } t \in \{10,11\}, \\ (0,4) & \text{for } t = 12, \\ (0,5) & \text{for } t = 13, \\ (0,6) & \text{for } t \in \{14,15,16\}, \\ \vdots & \end{cases}$$

Clearly, the set of values of the function (3.3.1) coincides with the bumping route understood in the traditional way (3.1.3).

We denote by $T|_{\leqslant t}$ the outcome of keeping only these boxes of T which are at most t. Note that the element of the bumping route

$$\square^{\mathrm{lazy}}_{T,m}(t) = \mathrm{sh}\left(T|_{\leqslant t} \leftarrow m + 1/2\right) \,/\, \mathrm{sh}\left(T|_{\leqslant t}\right) \tag{3.3.2}$$

is the unique box of the difference of two Young diagrams on the right-hand side.

3.3.2 Trajectory of ∞

Let $\xi = (\xi_1, \xi_2, \dots)$ be a sequence of independent, identically distributed random variables with the uniform distribution $U(0,1)$ on the unit interval $[0,1]$ and let $m \geqslant 0$ be a fixed integer. We will iteratively apply Schensted row insertion to the entries of the infinite sequence

$$\xi_1, \dots, \xi_m, \infty, \xi_{m+1}, \xi_{m+2}, \dots$$

which is the initial sequence ξ with our favorite symbol ∞ inserted at position $m+1$. (The Readers who are afraid of infinity may replace it by any number which is strictly bigger than all of the entries of the sequence ξ.) Our goal is to investigate the position of the box containing ∞ as a function of the number of iterations. More specifically, for an integer $t \geqslant m$ we define

$$\square_m^{\mathrm{traj}}(t) = \mathrm{Pos}_\infty\big(P(\xi_1, \dots, \xi_m, \infty, \xi_{m+1}, \dots, \xi_t)\big) \tag{3.3.3}$$

to be the position of the box containing ∞ in the appropriate insertion tableau. This problem was formulated by Duzhin [Duz19]; the first asymptotic results in the scaling in which $m \to \infty$ and $t = O(m)$ were found by Marciniak [Mar21]. In the current paper we go beyond this scaling and consider $m \to \infty$ and $t = O\Big(m^2\Big)$; the answer for this problem is essentially contained in Theorem 3.4.3.

The following result shows a direct link between the above problem and the asymptotics of bumping routes. This result also shows an interesting link between the papers [RŚ16] and [Mar21].

Proposition 3.3.1. *Let $\xi_1, \xi_2, \dots$ be a (non-random or random) sequence and $T = Q(\xi_1, \xi_2, \dots)$ be the corresponding recording tableau. Then for each $m \in \mathbb{N}$ the bumping route in the lazy parametrization coincides with the trajectory of ∞ as defined in (3.3.3):*

$$\square_{T,m}^{\mathrm{lazy}}(t) = \square_m^{\mathrm{traj}}(t) \qquad \text{for each integer } t \geqslant m. \tag{3.3.4}$$

We will provide two proofs of Proposition 3.3.1. The first one is based on the following classic result of Schützengerger.

Fact 3.3.2 ([Sch63])**.** *For any permutation σ the insertion tableau $P(\sigma)$ and the recording tableau $Q(\sigma^{-1})$, which corresponds to the inverse of σ, are equal.*

The first proof of Proposition 3.3.1. Let $\pi = (\pi_1, \dots, \pi_t) \in \mathfrak{S}_t$ be the *permutation generated by the sequence* $(\xi_1, \dots, \xi_t)$, that is the unique permutation such that for any choice of indices $i < j$ the condition $\pi_i < \pi_j$ holds true if and only if $\xi_i \leqslant \xi_j$. Let $\pi^{-1} = (\pi_1^{-1}, \dots, \pi_t^{-1})$ be the inverse of π. Since RSK depends only on the relative order of entries, the restricted tableau $T|_{\leqslant t}$ is equal to

$$T|_{\leqslant t} = Q(\xi_1, \dots, \xi_t) = Q(\pi) = P(\pi^{-1}). \tag{3.3.5}$$

By (3.3.2), (3.3.5) and Fact 3.3.2 it follows that

$$\begin{aligned}
\square^{\mathrm{lazy}}_{T,m}(t) &= \mathrm{sh}\left(P(\pi^{-1}) \leftarrow m+1/2\right) \;/\; \mathrm{sh}\, P(\pi^{-1}) \\
&= \mathrm{sh}\, P\left(\pi_1^{-1},\ldots,\pi_t^{-1}, m+1/2\right) \;/\; \mathrm{sh}\, P\left(\pi_1^{-1},\ldots,\pi_t^{-1}\right) \\
&= \mathrm{Pos}_{t+1}\left(Q\left(\pi_1^{-1},\ldots,\pi_t^{-1}, m+1/2\right)\right) \\
&\overset{\text{Fact 3.3.2}}{=} \mathrm{Pos}_{t+1}\left(P(\pi_1,\ldots,\pi_m,t+1,\pi_{m+1},\ldots,\pi_t)\right) \\
&= \mathrm{Pos}_{\infty}\left(P(\xi_1,\ldots,\xi_m,\infty,\xi_{m+1},\ldots,\xi_t)\right) \\
&= \square^{\mathrm{traj}}_{m}(t)
\end{aligned}$$

since the permutation $(\pi_1,\ldots,\pi_m,t+1,\pi_{m+1},\ldots,\pi_t)$ is the inverse of the permutation generated by the sequence $(\pi_1^{-1},\ldots,\pi_t^{-1},m+1/2)$. □

The above proof has an advantage of being short and abstract. The following alternative proof highlights the 'dynamic' aspects of the bumping routes and the trajectory of infinity.

The second proof of Proposition 3.3.1. We use induction over the variable t.

The induction base $t = m$ is quite easy: $\square^{\mathrm{lazy}}_{T,m}(m)$ is the leftmost box in the bottom row of T which contains a number which is bigger than m. This box is the first to the right of the last box in the bottom row in the tableau $Q(\xi_1,\ldots,\xi_m)$. On the other hand, since this recording tableau has the same shape as the insertion tableau $P(\xi_1,\ldots,\xi_m)$, it follows that $\square^{\mathrm{traj}}_{m}(m) = \square^{\mathrm{lazy}}_{T,m}(m)$ and the proof of the induction base is completed.

We start with an observation that ∞ is bumped in the process of calculating the row insertion

$$P(\xi_1,\ldots,\xi_m,\infty,\xi_{m+1},\ldots,\xi_t) \leftarrow \xi_{t+1} \tag{3.3.6}$$

if and only if the position of ∞ at time t, that is $\square^{\mathrm{traj}}_{m}(t)$, is the unique box which belongs to the skew diagram

$$\mathrm{RSK}(\xi_1,\ldots,\xi_{t+1}) / \mathrm{RSK}(\xi_1,\ldots,\xi_t).$$

The latter condition holds true if and only if the entry of T located in the box $\square^{\mathrm{traj}}_{m}(t)$ fulfills

$$T_{\square^{\mathrm{traj}}_{m}(t)} = t+1.$$

In order to make the induction step we assume that the equality (3.3.4) holds true for some $t \geqslant m$. There are the following two cases.

Case 1. Assume that the entry of T located in the box $\square^{\mathrm{lazy}}_{T,m}(t)$ is strictly bigger than $t+1$. In this case the lazy bumping route stays put and

$$\square^{\mathrm{lazy}}_{T,m}(t+1) = \square^{\mathrm{lazy}}_{T,m}(t).$$

By the induction hypothesis, the entry of T located in the box $\square^{\mathrm{traj}}_{m}(t) = \square^{\mathrm{lazy}}_{T,m}(t)$ is bigger than $t+1$. By the previous discussion, ∞ is not bumped in the process of calculating the row insertion (3.3.6) hence

$$\square^{\mathrm{traj}}_{m}(t+1) = \square^{\mathrm{traj}}_{m}(t)$$

and the inductive step holds true.

Case 2. Assume that the entry of T located in the box $\square^{\mathrm{lazy}}_{T,m}(t)$ is equal to $t+1$. In this case the lazy bumping route moves to the next row. It follows that $\square^{\mathrm{lazy}}_{T,m}(t+1)$ is the leftmost box

of T in the row above $\square^{\mathrm{lazy}}_{T,m}(t)$ which contains a number which is bigger than $T_{\square^{\mathrm{lazy}}_{T,m}(t)} = t+1$.

By the induction hypothesis, $T_{\square^{\mathrm{traj}}_{m}(t)} = T_{\square^{\mathrm{lazy}}_{T,m}(t)} = t+1$, so ∞ is bumped in the process of calculating the row insertion (3.3.6) to the next row r. The box $\square^{\mathrm{traj}}_{m}(t+1)$ is the first to the right of the last box in the row r in $\mathrm{RSK}(\xi_1, \ldots, \xi_t, \xi_{t+1})$. Clearly, this is the box in the row r of T which has the least entry among those which are bigger than $t+1$, so it is the same as $\square^{\mathrm{lazy}}_{T,m}(t+1)$. □

3.3.3 Augmented Young diagrams. Augmented shape of a tableau

For the motivations and heuristics behind the notion of augmented Young diagrams see Section 3.1.12.2.

A pair $\Lambda = (\lambda, \square)$ will be called an *augmented Young diagram* if λ is a Young diagram and $\square$ is one of its outer corners, see Figure 3.9b. We will say that λ is *the regular part of* Λ and that $\square$ is *the special box of* Λ.

The set of augmented Young diagrams will be denoted by $\mathbb{Y}^*$ and for $n \in \mathbb{N}_0$ we will denote by $\mathbb{Y}^*_n$ the set of augmented Young diagrams $(\lambda, \square)$ with the additional property that λ has n boxes (which we will shortly denote by $|\lambda| = n$).

Suppose T is a tableau with the property that exactly one of its entries is equal to ∞. We define the *augmented shape of* T

$$\mathrm{sh}^* T = \left(\mathrm{sh}\left(T \backslash \{\infty\}\right), \mathrm{Pos}_\infty T\right) \in \mathbb{Y}^*,$$

as the pair which consists of (a) the shape of T after removal of the box with ∞, and (b) the location of the box with ∞ in T, see Figure 3.9.

3.3.4 Augmented Young graph

The set $\mathbb{Y}^*$ can be equipped with a structure of an oriented graph, called *augmented Young graph*. We declare that a pair $\Lambda \nearrow \widetilde{\Lambda}$ forms an oriented edge (with $\Lambda = (\lambda, \square) \in \mathbb{Y}^*$ and $\widetilde{\Lambda} = (\widetilde{\lambda}, \widetilde{\square}) \in \mathbb{Y}^*$) if the following two conditions hold true:

$$\lambda \nearrow \widetilde{\lambda} \text{ and } \widetilde{\square} = \begin{cases} \text{the outer corner of } \widetilde{\lambda} \\ \quad \text{which is in the row above } \square & \text{if } \widetilde{\lambda}/\lambda = \{\square\}, \\ \square & \text{otherwise,} \end{cases} \tag{3.3.7}$$

see Figure 3.9 for an illustration. If $\Lambda \nearrow \widetilde{\Lambda}$ (with $\Lambda = (\lambda, \square) \in \mathbb{Y}^*$ and $\widetilde{\Lambda} = (\widetilde{\lambda}, \widetilde{\square}) \in \mathbb{Y}^*$) are such that $\square \neq \widetilde{\square}$ (which corresponds to the first case on the right-hand side of (3.3.7)), we will say that *the edge* $\Lambda \nearrow \widetilde{\Lambda}$ *is a bump*.

The above definition was specifically tailored so that the following simple lemma holds true.

Lemma 3.3.3. *Assume that T is a tableau which has exactly one entry equal to ∞ and let x be some finite number. Then*

$$\left(\mathrm{sh}^* T\right) \nearrow \left(\mathrm{sh}^*\left(T \leftarrow x\right)\right).$$

(a) (b)

Figure 3.9: (a) Example of a tableau T which has exactly one entry equal to ∞. (b) The augmented shape $\mathrm{sh}^* T = (\lambda, \square)$ of the tableau T. The regular part $\lambda = (4,2,1)$ is shown as the Young diagram drawn with solid lines, the position of the special box $\square = (x_\square, y_\square) = (2,1)$ is marked as the decorated box drawn with the dotted lines. With the notations of Section 3.4.2 this augmented Young diagram corresponds to $(x_\square, \lambda) = (2, \lambda) \in \mathbb{N}_0 \times \mathbb{Y}$.

Proof. Let $T' := T/\{\infty\}$ be the tableau T with the box containing ∞ removed. Denote $(\lambda, \square) = \mathrm{sh}^* T$ and $(\widetilde{\lambda}, \widetilde{\square}) = \mathrm{sh}^*(T \leftarrow x)$; their regular parts

$$\lambda = \mathrm{sh}\, T',$$
$$\widetilde{\lambda} = \mathrm{sh}\left(T' \leftarrow x\right)$$

clearly fulfill $\lambda \nearrow \widetilde{\lambda}$.

The position $\widetilde{\square}$ of ∞ in $T \leftarrow x$ is either:

- in the row immediately above the position $\square$ of ∞ in T (this happens exactly if ∞ was bumped in the insertion $T \leftarrow x$; equivalently if $\widetilde{\lambda}/\lambda = \{\square\}$), or
- the same as the position $\square$ of ∞ in T (this happens exactly when ∞ was not bumped; equivalently if $\widetilde{\lambda}/\lambda \neq \{\square\}$).

Clearly these two cases correspond to the second condition in (3.3.7) which completes the proof. □

3.3.5 Lifting of paths

We consider the *'covering map'* $p : \mathbb{Y}^* \to \mathbb{Y}$ given by taking the regular part

$$\mathbb{Y}^* \ni (\lambda, \square) \overset{p}{\mapsto} \lambda \in \mathbb{Y}.$$

Lemma 3.3.4. *For any $\Lambda^{(m)} \in \mathbb{Y}^*$ and any path in the Young graph*

$$\lambda^{(m)} \nearrow \lambda^{(m+1)} \nearrow \cdots \in \mathbb{Y} \tag{3.3.8}$$

with a specified initial element $\lambda^{(m)} = p\left(\Lambda^{(m)}\right)$ there exists the unique lifted path

$$\Lambda^{(m)} \nearrow \Lambda^{(m+1)} \nearrow \cdots \in \mathbb{Y}^*$$

in the augmented Young graph with the specified initial element $\Lambda^{(m)}$, and such that $\lambda^{(t)} = p\left(\Lambda^{(t)}\right)$ holds true for each $t \in \{m, m+1, \dots\}$.

Proof. From (3.3.7) it follows that for each $(\lambda, \square) \in \mathbb{Y}^*$ and each $\widetilde{\lambda}$ such that $\lambda \nearrow \widetilde{\lambda}$ there exists a unique $\widetilde{\square}$ such that $(\lambda, \square) \nearrow (\widetilde{\lambda}, \widetilde{\square})$. This shows that, given $\Lambda^{(i)}$, the value of

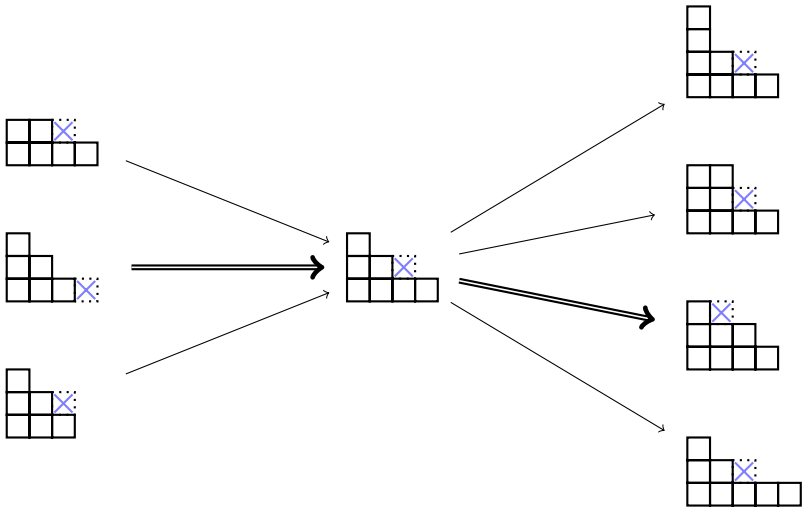

Figure 3.10: A part of the augmented Young graph. For each vertex $(\lambda, \square) \in \mathbb{Y}^*$ the regular part λ is drawn with the solid line and the special box $\square$ is indicated as a decorated dotted square. For clarity this figure shows only the direct neighborhood of the augmented Young diagram $(\lambda, \square)$ with $\lambda = (4,2,1)$ and $\square = (2,1)$. The double thick arrows indicate the edges which are *bumps*.

$\Lambda^{(i+1)}$ is determined uniquely. This observation implies that the lemma can be proved by a straightforward induction. $\square$

3.3.6 Augmented Plancherel growth process

We keep the notations from the beginning of Section 3.3.2, i.e., we assume that $\xi = (\xi_1, \xi_2, \dots)$ is a sequence of independent, identically distributed random variables with the uniform distribution $U(0,1)$ on the unit interval $[0,1]$ and $m \geqslant 0$ is a fixed integer. We consider a path in the augmented Young graph

$$\Lambda_m^{(m)} \nearrow \Lambda_m^{(m+1)} \nearrow \cdots \tag{3.3.9}$$

given by

$$\Lambda_m^{(t)} = \mathrm{sh}^* P(\xi_1, \dots, \xi_m, \infty, \xi_{m+1}, \dots, \xi_t) \qquad \text{for any integer } t \geqslant m$$

(Lemma 3.3.3 shows that (3.3.9) is indeed a path in $\mathbb{Y}^*$). We will call (3.3.9) *the augmented Plancherel growth process initiated at time m*. The coordinates of the special box of $\Lambda_m^{(t)} = \left(\lambda^{(t)}, \square_m^{(t)}\right)$ will be denoted by

$$\square_m^{(t)} = \left(x_m^{(t)}, y_m^{(t)}\right).$$

Theorem 3.3.5. *The augmented Plancherel growth process initiated at time m is a Markov chain with the transition probabilities given for any $t \geqslant m$ by*

$$\mathbb{P}\left(\Lambda_m^{(t+1)} = \widetilde{\Lambda} \,\middle|\, \Lambda_m^{(t)} = \Lambda\right) = \begin{cases} \mathbb{P}\left(\lambda^{(t+1)} = \widetilde{\lambda} \,\middle|\, \lambda^{(t)} = \lambda\right) & \text{if } \Lambda \nearrow \widetilde{\Lambda}, \\ 0 & \text{otherwise} \end{cases} \tag{3.3.10}$$

for any $\Lambda, \widetilde{\Lambda} \in \mathbb{Y}^*$, where λ is the regular part of Λ and $\widetilde{\lambda}$ is the regular part of $\widetilde{\Lambda}$. These transition probabilities do not depend on the choice of m. The conditional probability on the right-

hand side is the transition probability for the Plancherel growth process $\lambda^{(0)} \nearrow \lambda^{(1)} \nearrow \cdots$.

Proof. The path (3.3.9) is the unique lifting (cf. Lemma 3.3.4) of the sequence of the regular parts

$$\lambda^{(m)} \nearrow \lambda^{(m+1)} \nearrow \cdots \tag{3.3.11}$$

with the initial condition that the special box $\square_m^{(m)}$ is the outer corner of $\lambda^{(m)}$ which is located in the bottom row. It follows that for any augmented Young diagrams $\Sigma_m, \ldots, \Sigma_{t+1} \in \mathbb{Y}^*$ with the regular parts $\sigma_m, \ldots, \sigma_{t+1} \in \mathbb{Y}$

$$\mathbb{P}\left(\Lambda_m^{(m)} = \Sigma_m, \ \ldots, \ \Lambda_m^{(t+1)} = \Sigma_{t+1}\right) = \\ = \begin{cases} \mathbb{P}\left(\lambda^{(m)} = \sigma_m, \ \ldots, \ \lambda^{(t+1)} = \sigma_{t+1}\right) & \text{if } \Sigma_m \nearrow \cdots \nearrow \Sigma_{t+1} \text{ and} \\ & \text{the special box of } \Sigma_m \\ & \text{is in the bottom row,} \\ 0 & \text{otherwise.} \end{cases} \tag{3.3.12}$$

The sequence of the regular parts (3.3.11) forms the usual Plancherel growth process (with the first m entries truncated) hence it is a Markov chain (the proof that the usual Plancherel growth process is a Markov chain can be found in [Ker99, Sections 2.2 and 2.4]). It follows that the probability on the top of the right-hand side of (3.3.12) can be written in the product form in terms of the probability distribution of $\lambda^{(m)}$ and the transition probabilities for the Plancherel growth process.

We compare (3.3.12) with its counterpart for $t := t - 1$; this shows that the conditional probability

$$\mathbb{P}\left(\Lambda_m^{(t+1)} = \Sigma_{t+1} \;\middle|\; \Lambda_m^{(m)} = \Sigma_m, \ \ldots, \ \Lambda_m^{(t)} = \Sigma_t\right)$$

is equal to the right-hand side of (3.3.10) for $\widetilde{\Lambda} := \Sigma_{t+1}$ and $\Lambda := \Sigma_t$. In particular, this conditional probability does not depend on the values of $\Sigma_m, \ldots, \Sigma_{t-1}$ and the Markov property follows. □

The special box in the augmented Plancherel growth process can be thought of as a *test particle* which provides some information about the local behavior of the usual Plancherel growth process. From this point of view it is reminiscent of the *second class particle* in the theory of interacting particle systems or *jeu de taquin trajectory* for infinite tableaux [RŚ15].

3.3.7 Probability distribution of the augmented Plancherel growth process

Proposition 3.3.6 and Proposition 3.3.9 below provide information about the probability distribution of the augmented Plancherel growth process at time t for $t \to \infty$ in two distinct asymptotic regimes: very soon after the augmented Plancherel process was initiated (that is when $t = m + O(\sqrt{m})$, cf. Proposition 3.3.6) and after a very long time after the augmented Plancherel process was initiated (that is when $t = \Theta(m^2) \gg m$, cf. Proposition 3.3.9).

Proposition 3.3.6. *Let $z > 0$ be a fixed positive number and let $t = t(m)$ be a sequence of positive integers such that $t(m) \geqslant m$ and with the property that*

$$\lim_{m\to\infty} \frac{t - m}{\sqrt{t}} = z.$$

Let $\Lambda_m^{(m)} \nearrow \Lambda_m^{(m+1)} \nearrow \cdots$ be the augmented Plancherel growth process initiated at time m. We denote $\Lambda_m^{(t)} = \left(\lambda^{(t)}, \square_m^{(t)}\right)$; let $\square_m^{(t)} = \left(x_m^{(t)}, y_m^{(t)}\right)$ be the coordinates of the special box

of $\Lambda_m^{(t)}$.

a) *The probability distribution of* $y_m^{(t)}$ *converges, as* $m \to \infty$, *to the Poisson distribution* $\mathrm{Pois}(z)$ *with parameter* z.

b) *For each* $k \in \mathbb{N}_0$ *the total variation distance between*

- *the conditional probability distribution of* $\lambda^{(t)}$ *under the condition that* $y_m^{(t)} = k$, *and*
- *the Plancherel measure* Plan_t

converges to 0, *as* $m \to \infty$.

c) *The total variation distance between*

- *the probability distribution of the random vector*

$$\left(\lambda^{(t)}, y_m^{(t)}\right) \in \mathbb{Y} \times \mathbb{N}_0 \tag{3.3.13}$$

and

- *the product measure*

$$\mathrm{Plan}_t \times \mathrm{Pois}(z)$$

converges to 0, *as* $m \to \infty$.

Let us fix an integer $k \geqslant 0$. We use the notations from Section 3.2.2 for $n := m$ and $\ell = t - m$ so that $n + \ell = t$; we assume that m is big enough so that $m \geqslant (k+1)^2$. Our general strategy is to read the required information from the vector $V^{(n)}$ given by (3.2.4) and to apply Theorem 3.2.2. Before the proof of Proposition 3.3.6 we start with the following auxiliary result.

For $s \geqslant m$ we define the random variable $y_m^{(s)}\downarrow_{\mathcal{N}} \in \mathcal{N}$ by

$$y_m^{(s)}\downarrow_{\mathcal{N}} = \begin{cases} y_m^{(s)} & \text{if } y_m^{(s)} \in \{0, 1, \ldots, k\}, \\ \infty & \text{otherwise.} \end{cases}$$

We also define the random variable $F_s \in \{0, \ldots, k\}$ by

$$F_s = \begin{cases} y_m^{(s)}\downarrow_{\mathcal{N}} & \text{if } y_m^{(s)}\downarrow_{\mathcal{N}} \neq \infty, \\ \text{arbitrary element of } \{0, \ldots, k\} & \text{otherwise.} \end{cases}$$

Lemma 3.3.7. *For each* $s \geqslant m$ *the value of* F_s *can be expressed as an explicit function of the entries of the sequence* R *related to the past, that is*

$$R^{(m+1)}, \ldots, R^{(s)}.$$

For any integer $p \in \{0, \ldots, k\}$ *the equality* $y_m^{(s)} = p$ *holds true if and only if there are exactly* p *values of the index* $u \in \{m+1, \ldots, s\}$ *with the property that*

$$R^{(u)} = F_{u-1}. \tag{3.3.14}$$

The inequality $y_m^{(s)} > k$ *holds if and only if there are at least* $k+1$ *values of the index* $u \in \{m+1, \ldots, s\}$ *with this property.*

Proof. There are *exactly* $y_m^{(s)}$ edges which are bumps in the path

$$\Lambda^{(m)} \nearrow \cdots \nearrow \Lambda^{(s)} \tag{3.3.15}$$

because each bump increases the y-coordinate of the special box by 1. Note that an edge $\Lambda^{(u-1)} \nearrow \Lambda^{(u)}$ in this path is a bump if and only if

$$\text{the event } E_r^{(u)} \text{ occurs for the row } r = y_m^{(u-1)}. \tag{3.3.16}$$

If $y_m^{(s)} \leqslant k$ then for any $u \in \{m+1, \ldots, s\}$ the equality $F_u = y_m^{(u)}$ holds true; furthermore the event (3.3.16) occurs if and only if $R^{(u)} = y_m^{(u-1)}$. It follows that there are *exactly* $y_m^{(s)}$ values of the index $u \in \{m+1, \ldots, s\}$ such that (3.3.14) holds true.

On the other hand, if $y_m^{(s)} > k$ we can apply the above reasoning to the truncation of the path (3.3.15) until after the $(k+1)$-st bump occurs. It follows that in this case there are *at least* $k+1$ values of the index $u \in \{m+1, \ldots, s\}$ with the property (3.3.14). In this way we proved the second part of the lemma.

By the second part of the lemma, the value of $y_m^{(s)}\downarrow_{\mathcal{N}}$ can be expressed as an explicit function of both (i) the previous values

$$y_m^{(m)}\downarrow_{\mathcal{N}}, \ \ldots, \ y_m^{(s-1)}\downarrow_{\mathcal{N}}, \tag{3.3.17}$$

and (ii) the entries of the sequence R related to the past, that is

$$R^{(m+1)}, \ \ldots, \ R^{(s)}. \tag{3.3.18}$$

By iteratively applying this observation to the previous values (3.3.17) it is possible to express the value of $y_m^{(s)}\downarrow_{\mathcal{N}}$ *purely* in terms of (3.3.18). Also the value of

$$F_s = F_s\left(R^{(m+1)}, \ \ldots, \ R^{(s)}\right)$$

can be expressed as a function of the entries of the sequence R related to the past, as required. □

Proof of Proposition 3.3.6. Lemma 3.3.7 shows that the event $y_m^{(t)} = k$ can be expressed in terms of the vector $V^{(n)}$ given by (3.2.4). We apply Theorem 3.2.2; it follows that the probability $\mathbb{P}\left\{y_m^{(t)} = k\right\}$ is equal, up to an additive error term $o(1)$, to the probability that there are exactly k values of the index $u \in \{m+1, \ldots, t\}$ with the property that

$$\overline{R}^{(u)} = F_{u-1}\left(\overline{R}^{(m+1)}, \ldots, \overline{R}^{(u-1)}\right). \tag{3.3.19}$$

We denote by A_u the random event that the equality (3.3.19) holds true.

Let $i_1 < \cdots < i_l$ be an increasing sequence of integers from the set $\{m+1, \ldots, t\}$ for $l \geqslant 1$. We will show that

$$\mathbb{P}\left(A_{i_1} \cap \cdots \cap A_{i_l}\right) = \frac{1}{\sqrt{m}}\,\mathbb{P}\left(A_{i_1} \cap \cdots \cap A_{i_{l-1}}\right). \tag{3.3.20}$$

Indeed, by Lemma 3.3.7, the event $A_{i_1} \cap \cdots \cap A_{i_{l-1}}$ is a disjoint finite union of some random events of the form

$$B_{r_{m+1},\ldots,r_j} = \left\{\overline{R}^{(m+1)} = r_{m+1}, \ \overline{R}^{(m+2)} = r_{m+2}, \ \ldots, \ \overline{R}^{(j)} = r_j\right\}$$

over some choices of $r_{m+1}, r_{m+2}, \ldots, r_j \in \mathcal{N}$, where $j := i_l - 1$. Since the random variables $\left(\overline{R}^{(i)}\right)$ are independent, it follows that

$$\mathbb{P}\left(B_{r_{m+1},\ldots,r_j} \cap A_{i_l}\right) = \frac{1}{\sqrt{m}}\,\mathbb{P}\left(B_{r_{m+1},\ldots,r_j}\right). \tag{3.3.21}$$

By summing over the appropriate values of $r_{m+1}, \ldots, r_j \in \mathcal{N}$ the equality (3.3.20) follows.

By iterating (3.3.20) it follows that the events $A_{m+1}, \ldots, A_t$ are independent and each has equal probability $\frac{1}{\sqrt{m}}$.

By the Poisson limit theorem [Dur10, Theorem 3.6.1] the probability of k successes in ℓ Bernoulli trials as above converges to the probability of the atom k in the Poisson distribution with the intensity parameter equal to

$$\lim_{m\to\infty} \frac{\ell}{\sqrt{m}} = \lim_{m\to\infty} \frac{t-m}{\sqrt{t}} = z$$

which concludes the proof of part *a)*.

The above discussion also shows that the conditional probability distribution considered in point *b)* is equal to the conditional probability distribution of the last coordinate $\lambda^{(t)}$ of the vector $V^{(n)}$ under certain condition which is expressed in terms of the coordinates $R^{(m+1)}, \ldots, R^{(t)}$. By Theorem 3.2.2 this conditional probability distribution is in the distance $o(1)$ (with respect to the total variation distance) to its counterpart for the random vector $\overline{V}^{(n)}$. The latter conditional probability distribution, due to the independence of the coordinates of $\overline{V}^{(n)}$, is equal to the Plancherel measure Plan_t, which concludes the proof of *b)*.

Part *c)* is a direct consequence of parts *a)* and *b)*. □

For an augmented Young diagram $\Lambda = \left(\lambda, (x, y)\right)$ we define its *transpose* $\Lambda^T = \left(\lambda^T, (y, x)\right)$.

Lemma 3.3.8. *For any integers $m, m' \geqslant 0$ the probability distributions at time $t = m + m'$ of the augmented Plancherel growth processes initiated at times m and m' respectively are related by*

$$\Lambda_m^{(t)} \overset{d}{=} \left[\Lambda_{m'}^{(t)}\right]^T.$$

Proof. Without loss of generality we may assume that the random variables $\xi_1, \ldots, \xi_t$ are *distinct* real numbers. An application of Greene's theorem [Gre74, Theorem 3.1] shows that the insertion tableaux which correspond to a given sequence of distinct numbers and this sequence read backwards

$$P(\xi_1, \ldots, \xi_m, \infty, \xi_{m+1}, \ldots, \xi_t) = \left[P(\xi_t, \xi_{t-1}, \ldots, \xi_{m+1}, \infty, \xi_m, \xi_{m-1}, \ldots, \xi_1)\right]^T$$

are transposes of one another. It follows that also the augmented shapes are transposes of one another:

$$\Lambda_m^{(t)} = \mathrm{sh}^*\, P(\xi_1, \ldots, \xi_m, \infty, \xi_{m+1}, \ldots, \xi_t) = \left[\mathrm{sh}^*\, P(\underbrace{\xi_t, \xi_{t-1}, \ldots, \xi_{m+1}}_{m' \text{ entries}}, \infty, \xi_m, \xi_{m-1}, \ldots, \xi_1)\right]^T.$$

Since the sequence (ξ_i) and its any permutation $\left(\xi_{\sigma(i)}\right)$ have the same distributions, the right-hand side has the same probability distribution as $\left[\Lambda^{(t)}_{m'}\right]^T$, as required. □

Proposition 3.3.9. *Let $z > 0$ be a fixed real number. Let $t = t(m)$ be a sequence of positive integers such that $t(m) \geqslant m$ and with the property that*

$$\lim_{m\to\infty} \frac{m}{\sqrt{t}} = z.$$

Let $\Lambda^{(m)}_m \nearrow \Lambda^{(m+1)}_m \nearrow \cdots$ be the augmented Plancherel growth process initiated at time m. We denote $\Lambda^{(t)}_m = \left(\lambda^{(t)}, \square^{(t)}_m\right)$; let $\square^{(t)}_m = \left(x^{(t)}_m, y^{(t)}_m\right)$ be the coordinates of the special box at time t.

The total variation distance between

- *the probability distribution of the random vector*

$$\left(x^{(t)}_m, \lambda^{(t)}\right) \in \mathbb{N}_0 \times \mathbb{Y} \tag{3.3.22}$$

and

- *the product measure*

$$\mathrm{Pois}(z) \times \mathrm{Plan}_t$$

converges to 0, as $m \to \infty$.

Proof. By Lemma 3.3.8 the probability distribution of (3.3.22) coincides with the probability distribution of

$$\left(y^{(t)}_{m'}, \left[\lambda^{(t)}\right]^T\right) \tag{3.3.23}$$

for $m' := t - m$. The random vector (3.3.23) can be viewed as the image of the vector $\left(y^{(t)}_{m'}, \lambda^{(t)}\right)$ under the bijection

$$\mathrm{id} \times T : (y, \lambda) \mapsto (y, \lambda^T).$$

By Proposition 3.3.6 it follows that the total variation distance between (3.3.23) and the push-forward measure

$$(\mathrm{id} \times T)\left(\mathrm{Pois}(z) \times \mathrm{Plan}_t\right) = \mathrm{Pois}(z) \times \mathrm{Plan}_t$$

converges to zero as $m \to \infty$; the last equality holds since the Plancherel measure is invariant under transposition. □

3.3.8 Lazy version of Proposition 3.1.9. Proof of Proposition 3.1.1

In Section 3.1.7 we parametrized the shape of the bumping route by the sequence $Y_0, Y_1, \ldots$ which gives *the number of the row* in which the bumping route reaches a specified column, cf. (3.1.9). With the help of Proposition 3.3.1 we can define the lazy counterpart of these quantities: for $x, m \in \mathbb{N}_0$ we denote by

$$T^{[m]}_x = T_x = \min\left\{t : x^{(t)}_m \leqslant x\right\}$$

the *time* it takes for the bumping route (in the lazy parametrization) to reach the specified column.

The following result is the lazy version of Proposition 3.1.9.

Lemma 3.3.10. *For each integer $m \geqslant 1$*

$$\lim_{u\to\infty} \sqrt{u}\, \mathbb{P}\left\{T_0^{[m]} > u\right\} = m.$$

Proof. By Lemma 3.3.8, for any $u \in \mathbb{N}_0$

$$\mathbb{P}\left\{T_0^{[m]} > u\right\} = \mathbb{P}\left\{x_m^{(u)} \geqslant 1\right\} = \mathbb{P}\left\{y_{u-m}^{(u)} \geqslant 1\right\}.$$

In the special case $m = 1$ the proof is particularly easy: the right-hand side is equal to $\mathbb{P}\left(E_0^{(u)}\right)$ and Proposition 3.2.1 provides the necessary asymptotics.

For the general case $m \geqslant 1$ we use the notations from Section 3.2.2 for $k = 0$, and $n = u - m$, and $\ell = m$. The event $y_{u-m}^{(u)} \geqslant 1$ occurs if and only if at least one of the numbers $R^{(n+1)}, \dots, R^{(n+\ell)}$ is equal to 0. We apply Theorem 3.2.2; it follows that the probability of the latter event is equal, up to an additive error term of the order $o\left(\frac{m}{\sqrt{u-m}}\right) = o\left(\frac{1}{\sqrt{u}}\right)$, to the probability that in m Bernoulli trials with success probability $\frac{1}{\sqrt{n}}$ there is at least one success. In this way we proved that

$$\mathbb{P}\left\{y_{u-m}^{(u)} \geqslant 1\right\} = \frac{m}{\sqrt{u}} + o\left(\frac{1}{\sqrt{u}}\right),$$

as desired. □

Proof of Proposition 3.1.1. Since $Y_0^{[m]} \geqslant Y_1^{[m]} \geqslant \cdots$ is a weakly decreasing sequence, it is enough to consider the case $x = 0$. We apply Lemma 3.3.10 in the limit $u \to \infty$. It follows that the probability that the bumping route $T \leftsquigarrow m + 1/2$ does not reach the column with the index 0 is equal to

$$\lim_{u\to\infty} \mathbb{P}\left\{T_0^{[m]} \geqslant u\right\} = 0,$$

as required. □

3.4 Transition probabilities for the augmented Plancherel growth process

Our main result in this section is Theorem 3.4.3. It will be the key tool for proving the main results of the current paper.

3.4.1 Approximating Bernoulli distributions by linear combinations of Poisson distributions

The following Lemma 3.4.1 is a technical result which will be necessary later in the proof of Proposition 3.4.2. Roughly speaking, it gives a positive answer to the following question: *for a given value of $k \in \mathbb{N}_0$, can the point measure δ_k be approximated by a linear combination of the Poisson distributions in some explicit, constructive way?* A naive approach to this problem would be to consider a scalar multiple of the Poisson distribution $e^z \operatorname{Pois}(z)$ which corresponds to the sequence of weights

$$\mathbb{N}_0 \ni m \mapsto \frac{1}{m!} z^m$$

and then to consider its k-th derivative with respect to the parameter z for $z = 0$. This is not exactly a solution to the original question (the derivative is not a linear combination), but since

the derivative can be approximated by the forward difference operator, this naive approach gives a hint that an expression such as (3.4.1) in the special case $p = 1$ might be, in fact, a good answer.

Lemma 3.4.1. *Let us fix an integer $k \geqslant 0$ and a real number $0 \leqslant p \leqslant 1$. For each $h > 0$ the linear combination of the Poisson distributions*

$$\nu_{k,p,h} := \frac{1}{\left(e^h - 1\right)^k} \sum_{0 \leqslant j \leqslant k} (-1)^{k-j} \binom{k}{j} e^{jh} \operatorname{Pois}(pjh) \tag{3.4.1}$$

is a probability measure on $\mathbb{N}_0$.

As $h \to 0$, the measure $\nu_{k,p,h}$ converges (in the sense of total variation distance) to the binomial distribution $\operatorname{Binom}(k, p)$.

Proof. The special case $p = 1$. For a function f on the real line we consider its *forward difference* function $\Delta[f]$ given by

$$\Delta[f](x) = f(x+1) - f(x).$$

It follows that the iterated forward difference is given by

$$\Delta^k[f](x) = \sum_{0 \leqslant j \leqslant k} (-1)^j \binom{k}{j} f(x + k - j).$$

A priori, $\nu_{k,1,h}$ is a signed measure with the total mass equal to

$$\frac{1}{\left(e^h - 1\right)^k} \sum_{0 \leqslant j \leqslant k} (-1)^{k-j} \binom{k}{j} e^{jh} = \frac{1}{\left(e^h - 1\right)^k} \Delta^k \left[e^{hx}\right](0). \tag{3.4.2}$$

The right-hand side of (3.4.2) is equal to 1, since the forward difference of an exponential function is again an exponential:

$$\Delta \left[e^{hx}\right] = \left(e^h - 1\right) e^{hx}.$$

The atom of $\nu_{k,1,h}$ at an integer $m \geqslant 0$ is equal to

$$\nu_{k,1,h}(m) = \frac{1}{\left(e^h - 1\right)^k m!} \sum_{0 \leqslant j \leqslant k} (-1)^{k-j} \binom{k}{j} (jh)^m = \frac{h^m}{\left(e^h - 1\right)^k m!} \Delta^k \left[x^m\right](0).$$

Note that the monomial x^m can be expressed in terms of the falling factorials $x^{\underline{p}}$ with the coefficients given by the Stirling numbers of the second kind:

$$x^m = \sum_{0 \leqslant p \leqslant m} \left\{ {m \atop p} \right\} x^{\underline{p}},$$

hence

$$\Delta^k \left[x^m\right] = \sum_p \left\{ {m \atop p} \right\} \Delta^k \left[x^{\underline{p}}\right] = \sum_{p \geqslant k} \left\{ {m \atop p} \right\} p^{\underline{k}} \, x^{\underline{p-k}}.$$

When we evaluate the above expression at $x = 0$, there is only one non-zero summand

$$\Delta^k \left[x^m\right](0) = \left\{ {m \atop k} \right\} k!.$$

Thus

$$\nu_{k,1,h}(m) = \frac{h^m k!}{\left(e^h-1\right)^k m!} \left\{ {m \atop k} \right\} \geqslant 0,$$

and the above expression is non-zero only for $m \geqslant k$. All in all, $\nu_{k,1,h}$ is a probability measure on $\mathbb{N}_0$, as required.

It follows that the total variation distance between $\mathrm{Binom}(k,1) = \delta_k$ and $\nu_{k,1,h}$ is equal to

$$\sum_{i=0}^{\infty} \left[\delta_k(i) - \nu_{k,1,h}(i)\right]^+ = 1 - \nu_{k,1,h}(k) = 1 - \frac{h^k}{\left(e^h-1\right)^k} \xrightarrow{h\to 0} 0,$$

as required.

The general case. For a signed measure μ which is supported on $\mathbb{N}_0$ and $0 \leqslant p \leqslant 1$ we define the signed measure $C_p[\mu]$ on $\mathbb{N}_0$ by

$$C_p[\mu](k) = \sum_{j \geqslant k} \mu(j) \binom{j}{k} p^k (1-p)^{j-k}.$$

In the case when μ is a probability measure, $C_p[\mu]$ has a natural interpretation as the probability distribution of a compound binomial random variable $\mathrm{Binom}(M,p)$, where M is a random variable with the probability distribution given by μ.

It is easy to check that for any $0 \leqslant q \leqslant 1$ the image of a binomial distribution

$$C_p[\mathrm{Binom}(n,q)] = \mathrm{Binom}(n,pq)$$

is again a binomial distribution, and for any $\lambda \geqslant 0$ the image of a Poisson distribution

$$C_p[\mathrm{Pois}(\lambda)] = \mathrm{Pois}(p\lambda)$$

is again a Poisson distribution. Since C_p is a linear map, by the very definition (3.4.1) it follows that

$$C_p[\nu_{k,1,h}] = \nu_{k,p,h}; \tag{3.4.3}$$

in particular the latter is a probability measure, as required. By considering the limit $h \to 0$ of (3.4.3) we get

$$\lim_{h\to 0} \nu_{k,p,h} = C_p\left[\mathrm{Binom}(k,1)\right] = \mathrm{Binom}(k,p)$$

in the sense of total variation distance, as required. □

3.4.2 The inclusion $\mathbb{Y}^* \subset \mathbb{N}_0 \times \mathbb{Y}$

We will extend the meaning of the notations from Section 3.3.3 to a larger set. The map

$$\mathbb{Y}^* \ni (\lambda, \square) \mapsto (x_\square, \lambda\,) \in \mathbb{N}_0 \times \mathbb{Y}, \tag{3.4.4}$$

where $\square = (x_\square, y_\square)$, allows us to identify $\mathbb{Y}^*$ with a subset of $\mathbb{N}_0 \times \mathbb{Y}$. For a pair $(x,\lambda) \in \mathbb{N}_0 \times \mathbb{Y}$ we will say that λ is its *regular part*.

We define the edges in this larger set $\mathbb{N}_0 \times \mathbb{Y} \supset \mathbb{Y}^*$ as follows: we declare that $(x,\lambda) \nearrow (\widetilde{x},\widetilde{\lambda})$ if the following two conditions hold true:

$$\lambda \nearrow \widetilde{\lambda} \quad \text{and} \quad \widetilde{x} = \begin{cases} \max\left\{\widetilde{\lambda}_i : \widetilde{\lambda}_i \leqslant x\right\} & \text{if the unique box of } \widetilde{\lambda}/\lambda \\ & \quad \text{is located in the column } x, \\ x & \text{otherwise.} \end{cases} \tag{3.4.5}$$

In this way the oriented graph $\mathbb{Y}^*$ is a subgraph of $\mathbb{N}_0 \times \mathbb{Y}$.

An analogous lifting property as in Lemma 3.3.4 remains valid if we assume that the initial element $\Lambda^{(m)} \in \mathbb{N}_0 \times \mathbb{Y}$ and the elements of the lifted path

$$\Lambda^{(m)} \nearrow \Lambda^{(m+1)} \nearrow \cdots \in \mathbb{N}_0 \times \mathbb{Y}$$

are allowed to be taken from this larger oriented graph.

With these definitions the transition probabilities (3.3.10) also make sense if $\Lambda, \widetilde{\Lambda} \in \mathbb{N}_0 \times \mathbb{Y}$ are taken from this larger oriented graph and can be used to define Markov chains valued in $\mathbb{N}_0 \times \mathbb{Y}$.

3.4.3 Transition probabilities for augmented Plancherel growth processes

For the purposes of the current section we will view $\mathbb{Y}^*$ as a subset of $\mathbb{N}_0 \times \mathbb{Y}$, cf. (3.4.4). In this way the augmented Plancherel growth process initiated at time m, cf. (3.3.9), can be viewed as the aforementioned Markov chain

$$\left(\left(x_m^{(t)}, \lambda^{(t)} \right) \right)_{t \geqslant m} \tag{3.4.6}$$

valued in $\mathbb{N}_0 \times \mathbb{Y}$.

Let us fix some integer $n \in \mathbb{N}_0$. For each integer $m \in \{0, \ldots, n\}$ we may remove some initial entries of the sequence (3.4.6) and consider the Markov chain

$$\left(\left(x_m^{(t)}, \lambda^{(t)} \right) \right)_{t \geqslant n} \tag{3.4.7}$$

which is indexed by the time parameter $t \geqslant n$. In this way we obtain a whole family of Markov chains (3.4.7) indexed by an integer $m \in \{0, \ldots, n\}$ which have the same transition probabilities (3.3.10).

The latter encourages us to consider a general class of Markov chains

$$\left(\left(x^{(t)}, \lambda^{(t)} \right) \right)_{t \geqslant n} \tag{3.4.8}$$

valued in $\mathbb{N}_0 \times \mathbb{Y} \supset \mathbb{Y}^*$, for which the transition probabilities are given by (3.3.10) and for which the initial probability distribution of $\left(x^{(n)}, \lambda^{(n)} \right)$ can be arbitrary. We will refer to each such a Markov chain as *augmented Plancherel growth process*.

Proposition 3.4.2. *Let an integer $k \in \mathbb{N}_0$ and a real number $0 < p < 1$ be fixed, and let $n' = n'(n)$ be a sequence of integers such that $n' \geqslant n$ and*

$$\lim_{n \to \infty} \sqrt{\frac{n}{n'}} = p.$$

For a given integer $n \geqslant 0$ let (3.4.8) be an augmented Plancherel growth process with the initial probability distribution at time n given by

$$\delta_k \times \mathrm{Plan}_n .$$

Then the total variation distance

$$\delta \left\{ \left(x^{(n')}, \lambda^{(n')} \right), \ \mathrm{Binom}\left(k, p\right) \times \mathrm{Plan}_{n'} \right\} \tag{3.4.9}$$

converges to 0*, as* $n \to \infty$.

Proof. Let $\epsilon > 0$ be given. By Lemma 3.4.1 there exists some $h > 0$ with the property that for each $q \in \{1, p\}$ the total variation distance between the measure $\nu_{k,q,h}$ defined in (3.4.1) and the binomial distribution $\mathrm{Binom}(k, q)$ is bounded from above by ϵ.

Let T be a map defined on the set of probability measures on $\mathbb{N}_0 \times \mathbb{Y}_n$ in the following way. For a probability measure μ on $\mathbb{N}_0 \times \mathbb{Y}_n$ consider the augmented Plancherel growth process (3.4.8) with the initial probability distribution at time n given by μ and define $T\mu$ to be the probability measure on $\mathbb{N}_0 \times \mathbb{Y}_{n'}$ which gives the probability distribution of $\left(x^{(n')}, \lambda^{(n')}\right)$ at time n'.

It is easy to extend the map T so that it becomes a linear map between the vector space of *signed* measures on $\mathbb{N}_0 \times \mathbb{Y}_n$ and the vector space of *signed* measures on $\mathbb{N}_0 \times \mathbb{Y}_{n'}$. We equip both vector spaces with a metric which corresponds to the total variation distance. Then T is a contraction because of Markovianity of the augmented Plancherel growth process.

For $m \in \{0, \ldots, n\}$ and $t \geqslant n$ we denote by $\mu_m(t)$ the probability measure on $\mathbb{N}_0 \times \mathbb{Y}$, defined by the probability distribution at time t of the augmented Plancherel growth process $\left(x_m^{(t)}, \lambda^{(t)}\right)$ initiated at time m. For the aforementioned value of $h > 0$ we consider the signed measure on $\mathbb{N}_0 \times \mathbb{Y}_t$ given by the linear combination

$$\mathbb{P}(t) := \frac{1}{\left(e^h - 1\right)^k} \sum_{0 \leqslant j \leqslant k} (-1)^{k-j} \binom{k}{j} e^{jh} \mu_{\lfloor jh\sqrt{n} \rfloor}(t)$$

(which is well-defined for sufficiently big values of n which assure that $kh\sqrt{n} < n \leqslant t$).

We apply Proposition 3.3.9; it follows that for any $j \in \{0, \ldots, k\}$ the total variation distance between $\mu_{\lfloor jh\sqrt{n} \rfloor}(n)$ and the product measure

$$\mathrm{Pois}(jh) \times \mathrm{Plan}_n$$

converges to 0, as $n \to \infty$; it follows that the total variation distance between $\mathbb{P}(n)$ and the product measure

$$\nu_{k,1,h} \times \mathrm{Plan}_n \tag{3.4.10}$$

converges to 0, as $n \to \infty$. On the other hand, the value of $h > 0$ was selected in such a way that the total variation distance between the probability measure (3.4.10) and the product measure

$$\delta_k \times \mathrm{Plan}_n \tag{3.4.11}$$

is smaller than ϵ. In this way we proved that

$$\limsup_{n \to \infty} \delta\Big\{ \mathbb{P}(n),\ \delta_k \times \mathrm{Plan}_n \Big\} \leqslant \epsilon.$$

An analogous reasoning shows that

$$\limsup_{n \to \infty} \delta\Big\{ \mathbb{P}(n'),\ \mathrm{Binom}(k, p) \times \mathrm{Plan}_{n'} \Big\} \leqslant \epsilon.$$

The image of $\mathbb{P}(n)$ under the map T can be calculated by linearity of T:

$$\mathbb{P}(n') = T\mathbb{P}(n).$$

By the triangle inequality and the observation that the map T is a contraction,

$$(3.4.9) \leqslant \delta\left\{ \left(x^{(n')}, \lambda^{(n')}\right),\ \mathbb{P}(n') \right\} + \epsilon \leqslant \delta\left\{ \left(x^{(n)}, \lambda^{(n)}\right),\ \mathbb{P}(n) \right\} + \epsilon \leqslant 2\epsilon$$

holds true for sufficiently big values of n, as required. □

3.4.4 Bumping route in the lazy parametrization converges to the Poisson process

Let $\big(N(t) : t \geqslant 0\big)$ denote the Poisson counting process which is independent from the Plancherel growth process $\lambda^{(0)} \nearrow \lambda^{(1)} \nearrow \cdots$. The following result is the lazy version of Theorem 3.1.5.

Theorem 3.4.3. *Let $l \geqslant 1$ be a fixed integer, and $z_1 > \cdots > z_l$ be a fixed sequence of positive real numbers.*

Let $\Lambda_m^{(m)} \nearrow \Lambda_m^{(m+1)} \nearrow \cdots$ be the augmented Plancherel growth process initiated at time m. We denote $\Lambda_m^{(t)} = \big(\lambda^{(t)}, \square_m^{(t)}\big)$; let $\square_m^{(t)} = \big(x_m^{(t)}, y_m^{(t)}\big)$ be the coordinates of the special box at time t.

For each $1 \leqslant i \leqslant l$ let $t_i = t_i(m)$ be a sequence of positive integers such that

$$\lim_{m\to\infty} \frac{m}{\sqrt{t_i}} = z_i.$$

We assume that $t_1 \leqslant \cdots \leqslant t_l$. Then the total variation distance between

- *the probability distribution of the vector*

$$\Big(x_m^{(t_1)}, \ldots, x_m^{(t_l)}, \lambda^{(t_l)}\Big), \tag{3.4.12}$$

  and

- *the probability distribution of the vector*

$$\Big(N(z_1), \ldots, N(z_l), \lambda^{(t_l)}\Big) \tag{3.4.13}$$

converges to 0, as $m \to \infty$.

Proof. We will perform the proof by induction over l. Its main idea is that the collection of the random vectors (3.4.12) over $l \in \{1, 2, \ldots\}$ forms a Markov chain; the same holds true for the analogous collection of the random vectors (3.4.13). We will compare their initial probability distributions (thanks to Proposition 3.3.9) and — in a very specific sense — we will compare the kernels of these Markov chains (with Proposition 3.4.2). We present the details below.

The induction base $l = 1$ coincides with Proposition 3.3.9.

We will prove now the induction step. We start with the probability distribution of the vector (3.4.12) (with the substitution $l := l + 1$). Markovianity of the augmented Plancherel growth process implies that this probability distribution is given by

$$\begin{aligned}
&\mathbb{P}\left\{\Big(x_m^{(t_1)}, \ldots, x_m^{(t_{l+1})}, \lambda^{(t_{l+1})}\Big) = (x_1, \ldots, x_{l+1}, \lambda)\right\} = \\
&\sum_{\mu\in\mathbb{Y}_{t_l}} \mathbb{P}\left\{\Big(x_m^{(t_1)}, \ldots, x_m^{(t_l)}, \lambda^{(t_l)}\Big) = (x_1, \ldots, x_l, \mu)\right\} \times \\
&\qquad \times \mathbb{P}\left\{\Big(x_m^{(t_{l+1})}, \lambda^{(t_{l+1})}\Big) = (x_{l+1}, \lambda) \;\middle|\; \Big(x_m^{(t_l)}, \lambda^{(t_l)}\Big) = (x_l, \mu)\right\}
\end{aligned} \tag{3.4.14}$$

for any $x_1, \dots, x_{l+1} \in \mathbb{N}_0$ and $\lambda \in \mathbb{Y}$. We define the probability measure $\mathbb{Q}$ on $\mathbb{N}_0^{l+1} \times \mathbb{Y}$ which to a tuple $\left(x_1, \dots, x_{l+1}, \lambda\right)$ assigns the probability

$$\mathbb{Q}\left(x_1, \dots, x_{l+1}, \lambda\right) := \sum_{\mu \in \mathbb{Y}_{t_l}} \mathbb{P}\left\{\left(N(z_1), \dots, N(z_l)\right) = (x_1, \dots, x_l)\right\} \times \mathrm{Plan}_{t_l}(\mu) \times \\ \times \mathbb{P}\left\{\left(x_m^{(t_{l+1})}, \lambda^{(t_{l+1})}\right) = \left(x_{l+1}, \lambda\right) \,\middle|\, \left(x_m^{(t_l)}, \lambda^{(t_l)}\right) = \left(x_l, \mu\right)\right\}. \quad (3.4.15)$$

In the light of the general definition (3.4.8) of the augmented Plancherel growth process, the measures (3.4.14) and (3.4.15) on $\mathbb{N}_0^{l+1} \times \mathbb{Y}$ can be viewed as applications of the same Markov kernel (which correspond to the last factors on the right-hand side of (3.4.14) and (3.4.15))

$$\mathbb{P}\left\{\left(x_m^{(t_{l+1})}, \lambda^{(t_{l+1})}\right) = \left(x_{l+1}, \lambda\right) \,\middle|\, \left(x_m^{(t_l)}, \lambda^{(t_l)}\right) = \left(x_l, \mu\right)\right\}, \quad \mu \in \mathbb{Y}_{t_l},$$

to two specific initial probability distributions. Since such an application of a Markov kernel is a contraction (with respect to the total variation distance), we proved in this way that the total variation distance between (3.4.14) and (3.4.15) is bounded from above by the total variation distance between the initial distributions, that is the random vectors (3.4.12) and (3.4.13). By the inductive hypothesis the total variation distance between the measures $\mathbb{P}$ and $\mathbb{Q}$ converges to zero as $m \to \infty$. The remaining difficulty is to understand the asymptotic behavior of the measure $\mathbb{Q}$.

Observe that the sum on the right hand side of (3.4.15)

$$\sum_{\mu \in \mathbb{Y}_{t_l}} \mathrm{Plan}_{t_l}(\mu) \times \mathbb{P}\left\{\left(x_m^{(t_{l+1})}, \lambda^{(t_{l+1})}\right) = \left(x_{l+1}, \lambda\right) \,\middle|\, \left(x_m^{(t_l)}, \lambda^{(t_l)}\right) = \left(x_l, \mu\right)\right\} = \\ = \mathbb{P}\left\{\left(x^{(n')}, \lambda^{(n')}\right) = \left(x_{l+1}, \lambda\right) \,\middle|\, \left(x^{(n)}, \lambda^{(n)}\right) \stackrel{d}{=} \delta_k \times \mathrm{Plan}_n\right\} \quad (3.4.16)$$

is the probability distribution of the random vector $\left(x^{(n')}, \lambda^{(n')}\right)$ which appears in Proposition 3.4.2 with $n' = t_{l+1}$, and $n = t_l$, and $p = \frac{z_{l+1}}{z_l}$, and $k = x_l$. Therefore we proved that the measure $\mathbb{Q}$ is in an $o(1)$-neighborhood of the following probability measure

$$\mathbb{Q}'\left(x_1, \dots, x_{l+1}, \lambda\right) := \mathbb{P}\left\{\left(N(z_1), \dots, N(z_l)\right) = (x_1, \dots, x_l)\right\} \times \\ \times \mathrm{Plan}_{n'}(\lambda)\, \mathrm{Binom}\left(x_l, \frac{z_{l+1}}{z_l}\right)(x_{l+1}). \quad (3.4.17)$$

It is easy to check that

$$\mathbb{P}\left(N(z_{l+1}) = x_{l+1} \,\middle|\, N(z_l) = x_l\right) = \mathrm{Binom}\left(x_l, \frac{z_{l+1}}{z_l}\right)(x_{l+1}).$$

Hence the probability of the binomial distribution which appears as the last factor on the right-hand side of (3.4.17) can be interpreted as the conditional probability distribution of the Poisson process in the past, given its value in the future.

We show that the Poisson counting process with the reversed time is also a Markov process.

Since the Poisson counting process has independent increments, the probability of the event

$$\big(N(z_1),\dots,N(z_l)\big) = (x_1,\dots,x_l)$$

can be written as a product; an analogous observation is valid for $l := l+1$. Due to cancellations of the factors which contribute to the numerator and the denominator, the following conditional probability can be simplified:

$$\begin{aligned}\mathbb{P}\left(N(z_{l+1}) = x_{l+1} \,\middle|\, \big(N(z_1),\dots,N(z_l)\big) = (x_1,\dots,x_l)\right) = \\ = \frac{\mathbb{P}\left\{\big(N(z_1),\dots,N(z_{l+1})\big) = (x_1,\dots,x_{l+1})\right\}}{\mathbb{P}\left\{\big(N(z_1),\dots,N(z_l)\big) = (x_1,\dots,x_l)\right\}} = \\ = \frac{\mathbb{P}\big(N(z_l) = x_l \,\wedge\, N(z_{l+1}) = x_{l+1}\big)}{\mathbb{P}\big(N(z_l) = x_l\big)} = \\ = \mathbb{P}\left(N(z_{l+1}) = x_{l+1} \,\middle|\, N(z_l) = x_l\right).\end{aligned}$$

By combining the above observations with (3.4.17) it follows that

$$\mathbb{Q}'\left(x_1,\dots,x_{l+1},\lambda\right) = \mathbb{P}\left\{\big(N(z_1),\dots,N(z_{l+1})\big) = (x_1,\dots,x_{l+1})\right\}\ \mathrm{Plan}_{t_{l+1}}(\lambda)$$

is the probability distribution of (3.4.13) (with the obvious substitution $l := l+1$) which completes the inductive step. □

3.4.5 Lazy version of Remark 3.1.3

The special case $l = 0$ of the following result seems to be closely related to a very recent work of Azangulov and Ovechkin [AO20] who used different methods.

Proposition 3.4.4. *Let (ψ_i) be a sequence of independent, identically distributed random variables with the exponential distribution* $\mathrm{Exp}(1)$.

For each $l \in \mathbb{N}_0$ the joint distribution of the finite tuple of random variables

$$\left(\frac{m}{\sqrt{T_0^{[m]}}},\dots,\frac{m}{\sqrt{T_l^{[m]}}}\right) \tag{3.4.18}$$

converges, as $m \to \infty$, to the joint distribution of the sequence of partial sums

$$\big(\psi_0,\quad \psi_0+\psi_1,\quad \dots,\quad \psi_0+\psi_1+\dots+\psi_l\big).$$

Proof. For any $s_0,\dots,s_l > 0$ the cumulative distribution function of the random vector (3.4.18)

$$\begin{aligned}\mathbb{P}\left(\frac{m}{\sqrt{T_0^{[m]}}} < s_0,\quad \dots,\quad \frac{m}{\sqrt{T_l^{[m]}}} < s_l\right) = \\ \mathbb{P}\left(x_m^{(t_0)} > 0,\quad x_m^{(t_1)} > 1,\quad \dots,\quad x_m^{(t_l)} > l\right)\end{aligned} \tag{3.4.19}$$

can be expressed directly in terms of the cumulative distribution of the random vector $\left(x_m^{(t_0)}, \dots, x_m^{(t_l)}\right)$ with

$$t_i = t_i(m) = \left\lfloor \left(\frac{m}{s_i}\right)^2 \right\rfloor.$$

Theorem 3.4.3 shows that the right-hand side of (3.4.19) converges to

$$\mathbb{P}\Big(N(s_0) > 0, \quad N(s_1) > 1, \quad \dots, \quad N(s_l) > l\Big) = \mathbb{P}\Big(\psi_0 \leqslant s_0, \quad \psi_0 + \psi_1 \leqslant s_1, \quad \dots, \quad \psi_0 + \dots + \psi_l \leqslant s_l\Big),$$

where

$$\psi_i = \inf\Big\{t : N(t) \geqslant i+1\Big\} - \inf\Big\{t : N(t) \geqslant i\Big\}, \quad i \in \mathbb{N}_0,$$

denote the time between the jumps of the Poisson process. Since $(\psi_0, \psi_1, \dots)$ form a sequence of independent random variables with the exponential distribution, this concludes the proof. □

3.4.6 Conjectural generalization

We revisit Section 3.3.2 with some changes. This time let

$$\xi = (\dots, \xi_{-2}, \xi_{-1}, \xi_0, \xi_1, \dots)$$

be a *doubly* infinite sequence of independent, identically distributed random variables with the uniform distribution $U(0,1)$ on the unit interval $[0,1]$. Let us fix $m \in \mathbb{R}_+$. For $s, t \in \mathbb{R}_+$ we define

$$\big(x_m(s,t), y_m(s,t)\big) = \mathrm{Pos}_\infty\left(P\left(\xi_{-\lfloor ms \rfloor}, \dots, \xi_{-2}, \xi_{-1}, \infty, \xi_1, \xi_2, \dots, \xi_{\left\lfloor \frac{m^2}{t^2} \right\rfloor}\right)\right).$$

Let $\mathcal{N}$ denote the Poisson point process with the uniform unit intensity on $\mathbb{R}_+^2$. For $s, t \in \mathbb{R}_+$ we denote by

$$\mathcal{N}_{s,t} = \mathcal{N}\left([0,s] \times [0,t]\right)$$

the number of sampled points in the specified rectangle.

Conjecture 3.4.5. *The random function*

$$\mathbb{R}_+^2 \ni (s,t) \mapsto x_m(s,t) \tag{3.4.20}$$

converges in distribution to Poisson point process

$$\mathbb{R}_+^2 \ni (s,t) \mapsto \mathcal{N}_{s,t} \tag{3.4.21}$$

in the limit as $m \to \infty$.

Note that the results of the current paper show the convergence of the marginals which correspond to (a) fixed value of s and all values of $t > 0$ (cf. Theorem 3.4.3), or (b) fixed value of t and all values of $s > 0$ (this is a corollary from the proof of Proposition 3.3.9).

It is a bit discouraging that the contour curves obtained in computer experiments (see Figure 3.11) *do not seem* to be counting the number of points from some set which belong to a specified rectangle, see Figure 3.12 for comparison. On the other hand, maybe the value

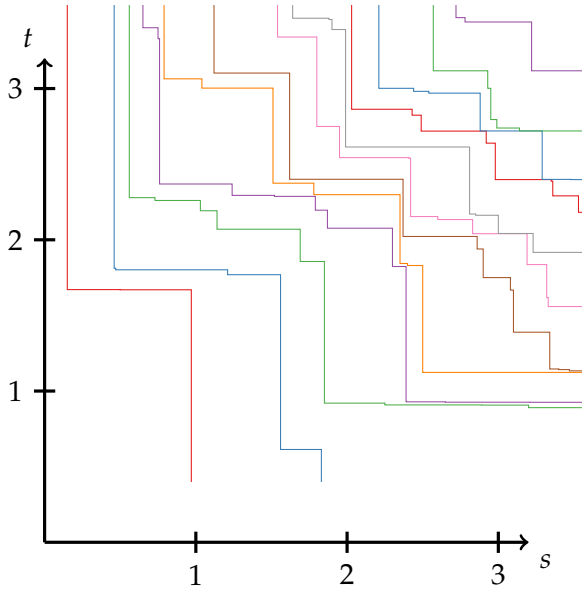

Figure 3.11: Computer simulation of the level curves of the function (3.4.20) for $m = 100$. A part of the plot which corresponds to small values of t was not shown due to restrictions on the computation time.

of m used in our experiments was not big enough to reveal the asymptotic behavior of these curves.

3.5 Removing laziness

Most of the considerations above concerned the lazy parametrization of the bumping routes. In this section we will show how to pass to the parametrization by the row number and, in this way, to prove the remaining claims from Section 3.1 (that is Theorem 3.1.2 and Proposition 3.1.9).

3.5.1 Proof of Proposition 3.1.9

Our general strategy in this proof is to use Lemma 3.3.10 and to use the observation that a Plancherel-distributed random Young diagram with n boxes has approximately $2\sqrt{n}$ columns in the scaling when $n \to \infty$.

Proof of Proposition 3.1.9. We denote by $c^{(n)}$ the number of rows (or, equivalently, the length of the leftmost column) of the Young diagram $\lambda^{(n)}$. Our proof will be based on an observation (recall Proposition 3.3.1) that

$$\Upsilon_0^{[m]} = c^{\left(T_0^{[m]}\right)}.$$

Let $\epsilon > 0$ be fixed. Since $c^{(n)}$ has the same distribution as the length of the bottom row of a Plancherel-distributed random Young diagram with n boxes, the large deviation results [DZ99; Sep98] show that there exists a constant $C_\epsilon > 0$ such that

$$\mathbb{P}\left(\sup_{n \geqslant n_0} \left|\frac{c^{(n)}}{\sqrt{n}} - 2\right| > \epsilon\right) \leqslant \sum_{n \geqslant n_0} \mathbb{P}\left(\left|\frac{c^{(n)}}{\sqrt{n}} - 2\right| > \epsilon\right) \leqslant$$

$$\sum_{n \geqslant n_0} e^{-C_\epsilon \sqrt{n}} = O\left(e^{-C_\epsilon \sqrt{n_0}}\right) \leqslant o\left(\frac{1}{n_0}\right) \quad (3.5.1)$$

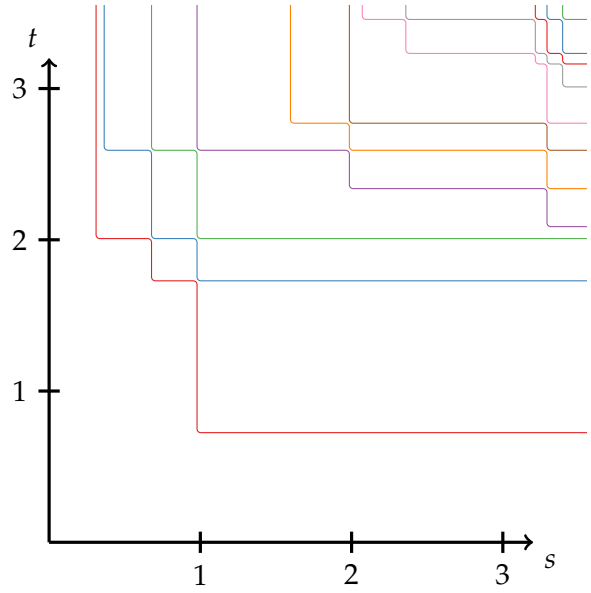

Figure 3.12: Computer simulation of the level curves of the function (3.4.21) for Poisson point process.

in the limit as $n_0 \to \infty$.

Consider an arbitrary integer $y \geqslant 1$. Assume that (i) the event on the left-hand side of (3.5.1) *does not* hold true for $n_0 := y$, *and* (ii) $Y_0^{[m]} \geqslant y$. Since $T_0^{[m]} \geqslant Y_0^{[m]} \geqslant y$ it follows that

$$\left| \frac{Y_0^{[m]}}{\sqrt{T_0^{[m]}}} - 2 \right| = \left| \frac{c\left(T_0^{[m]}\right)}{\sqrt{T_0^{[m]}}} - 2 \right| \leqslant \epsilon$$

hence

$$T_0^{[m]} \geqslant \left(\frac{y}{2+\epsilon} \right)^2 . \tag{3.5.2}$$

By considering two possibilities: either the event on the left-hand side of (3.5.1) holds true for $n_0 := y$ or not, it follows that

$$\mathbb{P}\left\{ Y_0^{[m]} \geqslant y \right\} \leqslant o\left(\frac{1}{y}\right) + \mathbb{P}\left\{ T_0^{[m]} \geqslant \left(\frac{y}{2+\epsilon} \right)^2 \right\} .$$

Lemma 3.3.10 implies therefore that

$$\mathbb{P}\left\{ Y_0^{[m]} \geqslant y \right\} \leqslant \frac{(2+\epsilon)m}{y} + o\left(\frac{1}{y}\right)$$

which completes the proof of the upper bound.

For the lower bound, assume that (i) the event on the left-hand side of (3.5.1) *does not* hold true for

$$n_0 := \left\lceil \left(\frac{y}{2-\epsilon} \right)^2 \right\rceil$$

and (ii) $T_0^{[m]} \geqslant n_0$. In an analogous way as in the proof of (3.5.2) it follows that

$$Y_0^{[m]} \geqslant (2-\epsilon)\sqrt{T_0^{[m]}} \geqslant (2-\epsilon)\sqrt{n_0} \geqslant y.$$

By considering two possibilities: either the event on the left-hand side of (3.5.1) holds true or not, it follows that that

$$\mathbb{P}\left\{T_0^{[m]} \geqslant n_0\right\} \leqslant o\left(\frac{1}{y}\right) + \mathbb{P}\left\{Y_0^{[m]} \geqslant y\right\}.$$

Lemma 3.3.10 implies therefore that

$$\mathbb{P}\left\{Y_0^{[m]} \geqslant y\right\} \geqslant \frac{(2-\epsilon)m}{y} + o\left(\frac{1}{y}\right)$$

which completes the proof of the lower bound. □

3.5.2 Lazy parametrization versus row parametrization

Proposition 3.5.1. *For each* $x \in \mathbb{N}_0$

$$\lim_{m\to\infty} \frac{Y_x^{[m]}}{\sqrt{T_x^{[m]}}} = 2$$

holds true in probability.

Regretfully, the ideas used in the proof of Proposition 3.1.9 (cf. Section 3.5.1 above) are not directly applicable for the proof of Proposition 3.5.1 when $x \geqslant 1$ because we are not aware of suitable large deviation results for the lower tail of the distribution of a specific row a Plancherel-distributed Young diagram, other than the bottom row.

Our general strategy in this proof is to study the length $\mu_x^{(t)}$ of the column with the fixed index x in the Plancherel growth process $\lambda^{(t)}$, as $t \to \infty$. Since we are unable to get asymptotic *uniform* bounds for

$$\left|\frac{\mu_x^{(t)}}{\sqrt{t}} - 2\right| \tag{3.5.3}$$

over *all* integers t such that $\frac{t}{m^2}$ belongs to some compact subset of $(0,\infty)$ in the limit $m \to \infty$, as a substitute we consider a *finite* subset of $(0,\infty)$ of the form

$$\left\{c(1+\epsilon),\ \ldots,\ c(1+\epsilon)^l\right\}$$

for arbitrarily small values of $c, \epsilon > 0$ and arbitrarily large integer $l \geqslant 0$ and prove the appropriate bounds for the integers $t_i(m)$ for which $\frac{t_i}{m^2}$ are approximately elements of this finite set. We will use monotonicity in order to get some information about (3.5.3) also for the integers t which are between the numbers $\{t_i(m)\}$.

Proof. Let $\epsilon > 0$ be fixed. Let $\delta > 0$ be arbitrary. By Proposition 3.4.4 the law of the random variable $\frac{m}{\sqrt{T_x^{[m]}}}$ converges to the Erlang distribution which is supported on $\mathbb{R}_+$ and has no atom in 0. Let W be a random variable with the latter probability distribution; in this way the

law of $\frac{T_x^{[m]}}{m^2}$ converges to the law of W^{-2}. Let $c > 0$ be a sufficiently small number such that

$$\mathbb{P}\left(W^{-2} < c\right) < \delta.$$

Now, let $l \in \mathbb{N}_0$ be a sufficiently big integer so that

$$\mathbb{P}\left(c(1+\epsilon)^l < W^{-2}\right) < \delta.$$

We define

$$t_i = t_i(m) = \left\lfloor m^2 c(1+\epsilon)^i \right\rfloor \qquad \text{for } i \in \{0, \dots, l\}.$$

With these notations there exists some m_1 with the property that for each $m \geqslant m_1$

$$\mathbb{P}\left(t_0 < T_x^{[m]} \leqslant t_l\right) > 1 - 2\delta. \tag{3.5.4}$$

Let $\mu^{(n)} = \left[\lambda^{(n)}\right]^T$ be the transpose of $\lambda^{(n)}$; in this way $\mu_x^{(n)}$ is the number of the boxes of T which are in the column x and contain an entry $\leqslant n$. The probability distribution of $\mu^{(n)}$ is also given by the Plancherel measure. The monograph of Romik [Rom15, Theorem 1.22] contains that proof that

$$\frac{\mu_x^{(t_i(m))}}{\sqrt{t_i(m)}} \xrightarrow{\mathbb{P}} 2$$

holds true in the special case of the bottom row $i = 0$; it is quite straightforward to check that this proof is also valid for each $i \in \{0, \dots, l\}$, for the details see the proof of Lemma 2.2.5. Hence there exists some m_2 with the property that for each $m \geqslant m_2$ the probability of the event

$$\left| \frac{\mu_x^{(t_i(m))}}{\sqrt{t_i(m)}} - 2 \right| < \epsilon \quad \text{holds } \textit{for each } i \in \{0, \dots, l\} \tag{3.5.5}$$

is at least $1 - \delta$.

Let us consider an elementary event T with the property that the event considered in (3.5.4) occurred, that is $t_0 < T_x^{[m]} \leqslant t_l$, *and* the event (3.5.5) occurred. Since $t_0 \leqslant \cdots \leqslant t_l$ form a weakly increasing sequence, there exists an index $j = j(T) \in \{0, \dots, l-1\}$ such that

$$t_j < T_x^{[m]} \leqslant t_{j+1}.$$

It follows that

$$\mu_x^{(t_j)} < Y_x^{[m]} \leqslant \mu_x^{(t_{j+1})}$$

hence

$$(2-\epsilon)\frac{1}{\sqrt{1+\epsilon}+o(1)} < \frac{\mu_x^{(t_j)}}{\sqrt{t_{j+1}}} \leqslant \frac{Y_x^{[m]}}{\sqrt{T_x^{[m]}}} \leqslant \frac{\mu_x^{(t_{j+1})}}{\sqrt{t_j}} < (2+\epsilon)\left(\sqrt{1+\epsilon}+o(1)\right). \tag{3.5.6}$$

In this way we proved that for each $m \geqslant \max(m_1, m_2)$ the probability of the event (3.5.6) is at least $1 - 3\delta$, as required. □

3.5.3 Proof of Theorem 3.1.2

Proof. For each integer $l \geqslant 0$ Proposition 3.4.4 gives the asymptotics of the joint probability distribution of the random variables $T_0^{[m]}, \ldots, T_l^{[m]}$ which concern the shape of the bumping route in the lazy parametrization. On the other hand, Proposition 3.5.1 allows us to express asymptotically these random variables by their non-lazy counterparts $Y_0^{[m]}, \ldots, Y_l^{[m]}$. The discussion from Remark 3.1.3 completes the proof. □

Chapter 4

Second class particles and limit shapes of evacuation and sliding paths for random tableaux

The following chapter is a modified version of the (yet nonpublished) article [MŚ22]:

> Ł. Maślanka and P. Śniady: *Second class particles and limit shapes of evacuation and sliding paths for random tableaux*, https://arxiv.org/abs/1911.08143v3

which is available in the public repository arXiv.org. The 12-page extended abstract [MŚ20a] of this article was published in the proceedings of the *32nd International Conference on Formal Power Series and Algebraic Combinatorics, FPSAC 2020*.

Abstract: We investigate two closely related setups. In the first one we consider a TASEP-style system of particles with specified initial and final configurations. The probability of each history of the system is assumed to be equal. We show that the rescaled trajectory of the *second class particle* converges (as the size of the system tends to infinity) to a random arc of an ellipse.

In the second setup we consider a uniformly random Young tableau of square shape and look for typical (in the sense of probability) *sliding paths* and *evacuation paths* in the asymptotic setting as the size of the square tends to infinity. We show that the probability distribution of such paths converges to a random *meridian* connecting the opposite corners of the square. We also discuss analogous results for non-square Young tableaux.

4.1 Introduction

The results of the current chapter concern two distinct setups which are closely connected. The first one, presented in Section 4.1.1, involves a certain interacting particle system. The second one, presented in Section 4.1.3, involves random Young tableaux. Basic informations concerning Young tableaux are given in Section 1.1.

4.1.1 TASEP system with the uniform distribution over histories

4.1.1.1 The setup

For given integers $N, M \geqslant 1$ we consider the particle system depicted on Figure 4.1. There are $N+M-1$ nodes, labeled by the integers from the set

$$\{-N+1, \dots, 0, 1, \dots, M-1\}. \tag{4.1.1}$$

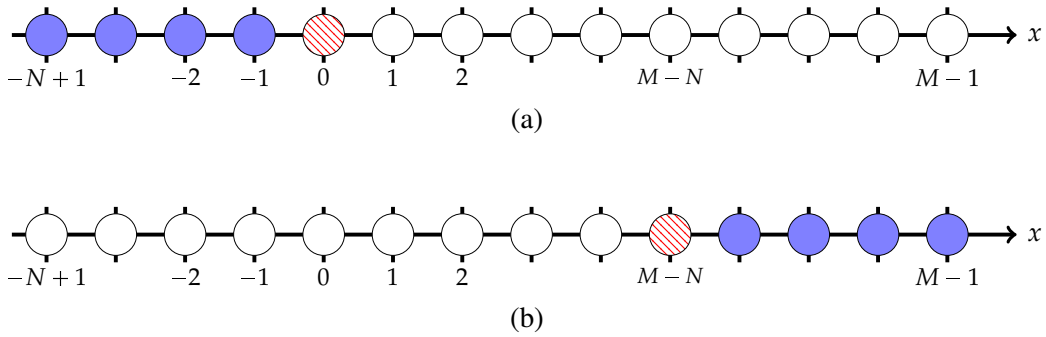

Figure 4.1: (a) The initial configuration of the particle system. The first class particles are depicted as filled blue circles, the holes are depicted as empty circles. The striped red circle denotes the second class particle. (b) The final configuration of the particle system.

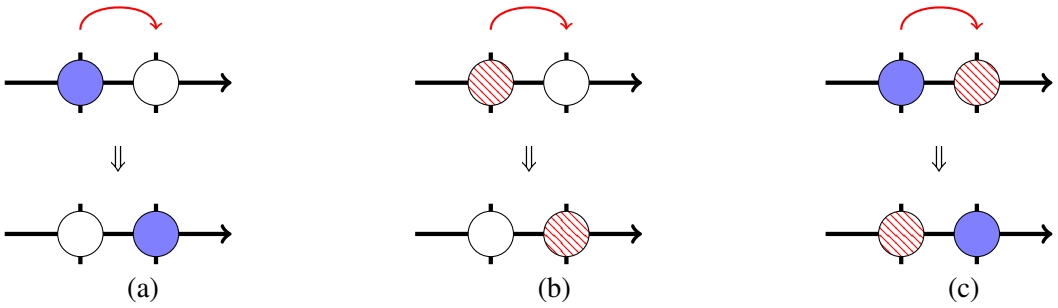

Figure 4.2: Three allowed types of transitions: (a) a first class particle can jump to the right if the next node is free, (b) the second class particle can jump to the right if the next node is free, (c) the first class particle can jump to the right if the next node is occupied by the second class particle; in this case the second class particle has to yield and the particles exchange their places.

In the initial configuration (which corresponds to the time $t = 1$) the $N - 1$ nodes which correspond to the negative integers are occupied by *the first class particles*, the $M - 1$ nodes which correspond to the positive integers are empty (or, equivalently, are occupied by *holes*), and the node which corresponds to zero is occupied by ***the second class particle***, see Figure 4.1a.

In each step exactly one of the following transitions occurs:

- any particle (first or second class) may jump right to the next node provided that this node is empty, see Figures 4.2a and 4.2b, or
- a first class particle may jump right to the next node provided that this node is occupied by the second class particle. In this case the second class particle has to yield and jumps one node to the left, see Figure 4.2c.

The *second class particle* is an analogue of a passenger with a cheap second class ticket who has to yield the seat to any passenger with a more expensive first class ticket.

It is not very difficult to show that no matter which transitions occur, the system terminates at time $t_{\max} = MN$ (that is after $MN - 1$ transitions) in the configuration shown on Figure 4.1b in which no additional transition is allowed.

By the *history* we will understand the information about the state of the particle system over all values of the time $t \in \{1, \ldots, t_{\max}\}$, see Figure 4.3 for an example. We consider the finite set of all possible histories of the particle system and associate to each such a history equal probability. In other words, we consider a version of the TASEP (which is an acronym

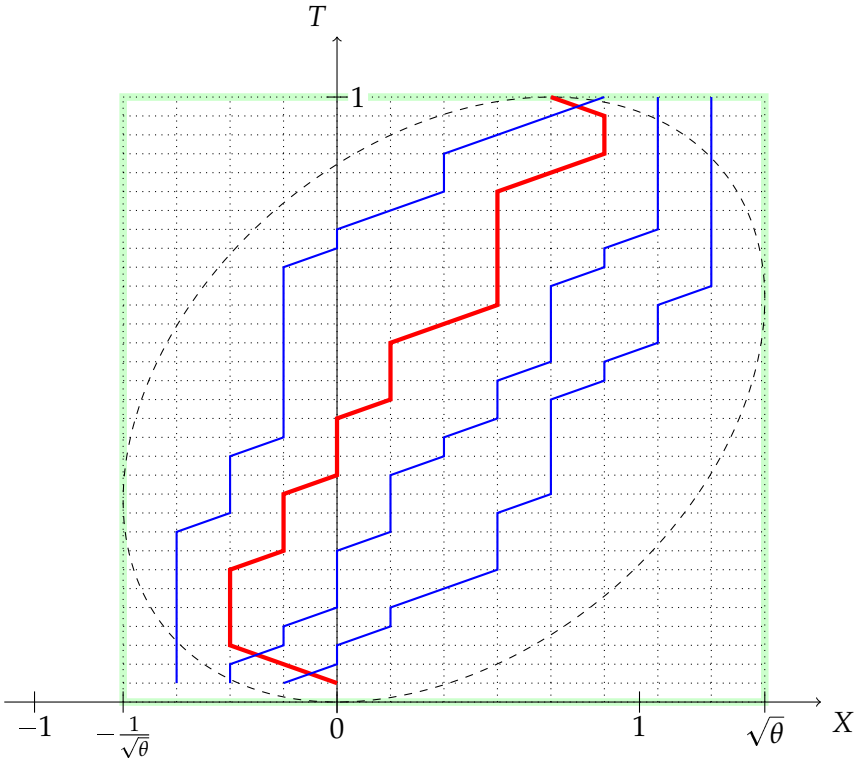

Figure 4.3: Sample history of the particle system for $N = 4$ and $M = 8$. The trajectories of the first class particles are shown as solid blue lines, the trajectory of the second class particle is shown as the thick red line. The thick green rectangle indicates the *bounding box*. The dashed line indicates *the arctic ellipse* which corresponds to the shape parameter $\theta = \frac{M}{N} = 2$.

for Totally Asymmetric Simple Exclusion Process) system [Spi70] with modified transition probabilities.

4.1.1.2 Why second class particles?

Macroscopic quantities describing an interacting particle system (such as particle density) are usually described by nonlinear partial differential equations (PDEs for short). For example, the famous Burgers equation [Bur48] describes the density profile in the hydrodynamical limit for the asymmetric simple exclusion process [BF87]. Weak solutions of nonlinear PDEs can develop singularities, often referred to as *shocks*. The shocks can be found by looking for the crossings of the characteristic lines of the PDE.

Ferrari [Fer92] discovered that a second class particle, depending on the place in which it begins its journey, can identify microscopically the location of the shock or describe the behavior of the characteristic lines of the limiting hydrodynamic equation. Ferrari and Fontes showed in [FF94] that this hydrodynamical limit converges to the traveling wave solution of the inviscid Burgers equation. This connection was later transferred to more general settings by Rezakhanlou [Rez95], Ferrari and Kipnis [FK95], Seppäläinen [Sep01] and others. Furthermore, the second class particle enters naturally in the study of the fluctuations of the current of particles [FF94].

A pictorial interpretation of TASEP as a traffic model is given in [MG05]. The particles are interpreted as cars on a single-line highway with no possibility of passing (which corresponds to the exclusion rule) and the shock corresponds to the front of the traffic jam. The motion of the shock is referred to as the *propagation of the shock* or the *rarefaction wave* (or *rarefaction*

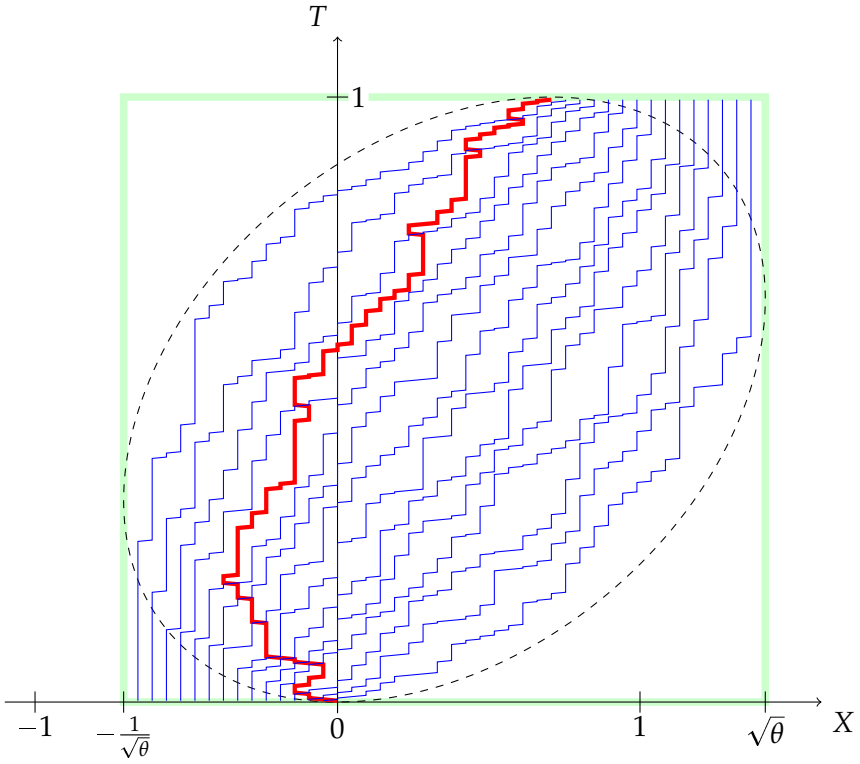

Figure 4.4: An analogue of Figure 4.3 for $N = 15$ and $M = 30$.

fan) depending whether the shock moves to the left or is being resorpted. The second class particle identifies the shock and allows to qualitatively describe its motion.

Mountford and Guiol [MG05] studied in fact a more advanced physical interpretation of the TASEP model as a moving interface on the plane (space-time). This gave them a powerful tool to analyze the shocks in the TASEP process in terms of the last passage percolation.

A nice heuristic (as well as rigorous) explanation of the shocks behavior and the importance of the second class particles in this context can be found in the book of Liggett [Lig99, Part III].

4.1.1.3 The asymptotic setup

We assume that (M_i) and (N_i) are two sequences of positive integers which tend to infinity and such that their ratio

$$\lim_{i\to\infty} \frac{M_i}{N_i} = \theta > 0$$

converges to some positive limit which we call *the shape parameter*. For $t \in \{1, \dots, M_i N_i\}$ we denote by $u_i(t) \in \{-N_i + 1, \dots, M_i - 1\}$ the position of the second class particle at time t. In order to keep the notation lightweight we will sometimes omit the index i and instead of $M_i, N_i, u_i(t)$ we will write shortly $M, N, u(t)$.

Until now we parameterized the space using the integer parameter $x \in \{-N + 1, \dots, M - 1\}$ and the time using the integer parameter $t \in \{1, \dots, MN\}$, however for asymptotic questions it is more convenient to pass to the rescaled coordinates

$$X = \frac{x}{\sqrt{MN}} \in \left[-\frac{1}{\sqrt{M/N}}, \sqrt{M/N}\right],$$
$$T = \frac{t}{t_{\max}} \in [0, 1],$$

see Figures 4.3 and 4.4. The rectangle

$$B_\theta = \left\{ (X,T) : X \in \left[-\frac{1}{\sqrt{\theta}}, \sqrt{\theta} \right], \quad T \in [0,1] \right\} \tag{4.1.2}$$

which shows the range in which the coordinates X and T vary asymptotically will be called *the bounding box*; on Figures 4.3 to 4.5 it is shown as the green rectangle.

For each value of the parameter $s \in [-1,1]$ we define a function

$$\Xi_s \colon [0,1] \to \left[-\frac{1}{\sqrt{\theta}}, \sqrt{\theta} \right]$$

given by

$$\Xi_s(T) = 2\sqrt{T(1-T)}\, s + \frac{\theta - 1}{\sqrt{\theta}}\, T,$$

see Figure 4.5.

4.1.1.4 The main result 1: the trajectory of the second class particle

Theorem 4.1.1. *We keep the assumptions and notations from Section 4.1.1.3.*

Then there exists a sequence (S_i) of random variables with the property that the supremum distance

$$\sup_{T \in [0,1]} \left| \frac{1}{\sqrt{M_i N_i}}\, u_i\big(\lceil T M_i N_i \rceil \big) - \Xi_{S_i}(T) \right|$$

converges in probability to zero, as $i \to \infty$.

The probability distribution of S_i is supported on the interval $[-1,1]$ and for $i \to \infty$ it converges to the standard semicircular distribution with the density

$$f_{\mathrm{SC}}(x) = \frac{2}{\pi}\sqrt{1-x^2} \qquad \text{for } x \in [-1,1]. \tag{4.1.3}$$

This theorem is illustrated on Figure 4.5. Its proof is postponed to Section 4.11. This result is analogous to the results of Ferrari and Kipnis [FK95], as well as Mountford and Guiol [MG05] for the usual TASEP system starting from a decreasing shock profile.

4.1.1.5 The limit trajectories

Each curve Ξ_s for the parameter $s \in [-1,1]\backslash\{0\}$ is an arc of an ellipse which fits into the bounding box B_θ, passes through the points

$$(0,0), \qquad \left(\frac{\theta - 1}{\sqrt{\theta}}, 1 \right), \tag{4.1.4}$$

and is tangent there to the bottom and the top edge of the bounding box B_θ. In the degenerate case $s = 0$ the curve Ξ_0 is a straight line connecting the aforementioned two points (4.1.4). The union of the two extreme curves Ξ_{-1} and Ξ_1 is the unique ellipse (which we call *the arctic ellipse*) which is inscribed into the bounding box B_θ and is tangent to its bottom and its top side in the aforementioned two points (4.1.4), see Figure 4.5. In the special case $\theta = 1$ the scaling of the axes can be chosen in such a way that the arctic ellipse becomes a circle which we call the *"the arctic circle"*. Our use of this name is not a coincidence since it turns out to be indeed related to the celebrated *arctic circle theorem* [Rom12].

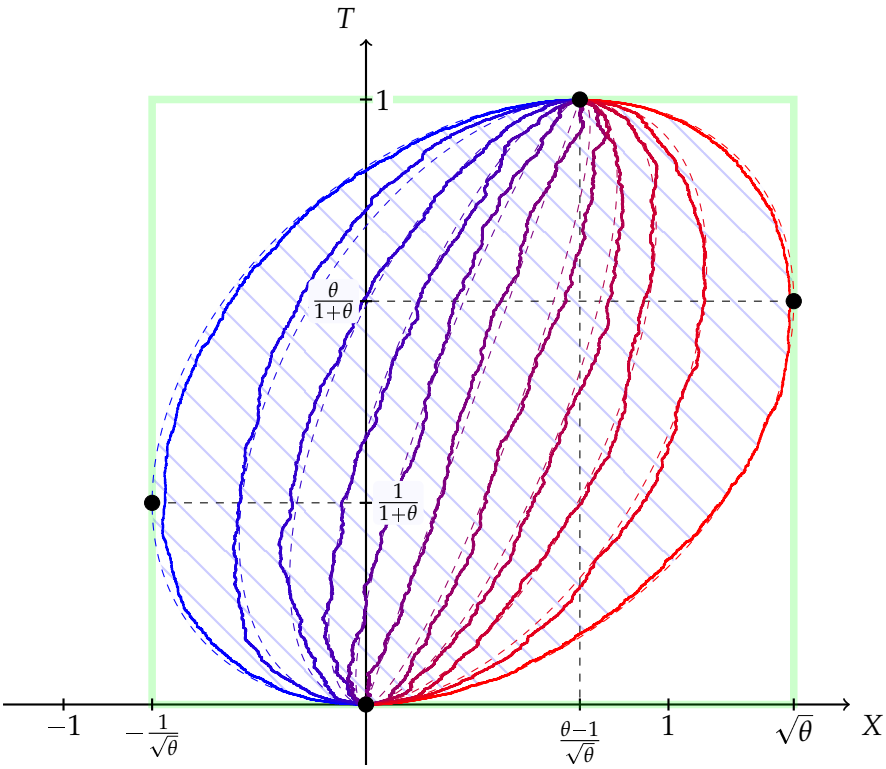

Figure 4.5: The dashed lines are arcs of ellipses Ξ_s for the shape parameter $\theta = 2$. The shown values of the parameter $s \in F_{\mathrm{SC}}^{-1}\left\{0/10, 1/10, \ldots, 10/10\right\}$ are the deciles of the semicircle distribution (above $F_{\mathrm{SC}}\colon [-1,1] \to [0,1]$ denotes the cumulative distribution function of the semicircle distribution (4.1.3)). The shaded region forms *the arctic ellipse*. The four black dots are the points where the arctic ellipse is tangent to the bounding box. The solid zigzag lines are trajectories of the second class particle for $N = 500$ and $M = 1000$. These trajectories were selected from a sample of 1000 simulations; each of them corresponds to an appropriate empirical decile of the distribution of the second class particle at time $T = \frac{1}{2}$.

4.1.2 Random sorting networks

Theorem 4.1.1 can be regarded as the solution to a toy version of the problem of *random sorting networks* considered by Angel, Holroyd, Romik, and Virág [Ang+07]. More specifically, we consider the symmetric group $\mathfrak{S}_N + M - 1$ viewed as the set of permutations of the set of nodes (4.1.1) and the permutation $\rho_{N,M} \in \mathfrak{S}_N + M - 1$ defined as

$$\rho_{N,M}(i) = \begin{cases} i + M & \text{if } i \in \{-N+1, \dots, -1\}, \\ M - N & \text{if } i = 0, \\ i - N & \text{if } i \in \{1, \dots, M-1\} \end{cases}$$

which describes the change of the positions of the particles and holes during the passage from the initial configuration shown on Figure 4.1a to the final configuration shown on Figure 4.1b. For an integer $s \in \{-N+1, \dots, M-2\}$ denote the adjacent transposition at location s by $\tau_s = (s, s+1) \in \mathfrak{S}_N + M - 1$.

Any history of the particle system considered in Section 4.1.1.1 can be encoded by the sequence $s_1, \dots, s_{t_{\max}-1} \in \{-N+1, \dots, M-2\}$, where s_t and $s_t + 1$ are the nodes which are interchanged in t-th transition. It is easy to check that

$$\rho_{N,M} = \tau_{s_{t_{\max}-1}} \tau_{s_{t_{\max}-2}} \cdots \tau_{s_2} \, \tau_{s_1} \tag{4.1.5}$$

and the corresponding sequence of partial products

$$\mathrm{id}, \quad \tau_{s_1}, \quad \tau_{s_2}\tau_{s_1}, \quad \dots, \quad \tau_{s_{t_{\max}-1}} \tau_{s_{t_{\max}-2}} \cdots \tau_{s_2} \, \tau_{s_1} \tag{4.1.6}$$

is a shortest path from the identity permutation id to $\rho_{N,M}$ in the Cayley graph of the symmetric group $\mathfrak{S}_N + M - 1$ generated by adjacent transpositions.

Conversely, each shortest path (4.1.6) in the Cayley graph gives a valid history of the particle system. Any such a shortest path will be called *a sorting network*. The trajectory of the second class particle

$$\big(u(t) : t \in \{1, \dots, t_{\max}\}\big) = \\ \big(0, \quad \tau_{s_1}(0), \quad \tau_{s_2}\tau_{s_1}(0), \quad \dots, \quad \tau_{s_{t_{\max}-1}} \cdots \tau_{s_2}\tau_{s_1}(0)\big) \tag{4.1.7}$$

corresponds in this language to the sequence of images of 0 under the action of the entries of the sequence (4.1.6).

Angel, Holroyd, Romik, and Virág [Ang+07] considered a more difficult version of this setup in which the permutation $\rho_{N,M}$ is replaced by the *reverse permutation* $\rho \in \mathfrak{S}_N + M - 1$ given by

$$\rho(i) = M - N - i$$

and—among several other results—stated some conjectures concerning the asymptotic behavior of the right-hand side of (4.1.7) for a *random sorting network*, i.e., a random shortest path from the identity permutation id to the reverse permutation ρ, sampled with the uniform distribution. We focus today on [Ang+07, Conjecture 1] which is a direct analogue of our Theorem 4.1.1. A minor difference is that the limit curves which appear in Theorem 4.1.1 form a one-parameter family of arcs of ellipses while the limit curves which appear in [Ang+07, Conjecture 1] form a one-parameter family of *sine curves*. (At first sight it might appear that the family of curves in [Ang+07] has two parameters, but one of these parameters can be eliminated by the requirement about the positions of the endpoints.)

The aforementioned conjecture [Ang+07, Conjecture 1] was proved only very recently by Dauvergne and Virág [DV20] who used methods quite different from those which we use in

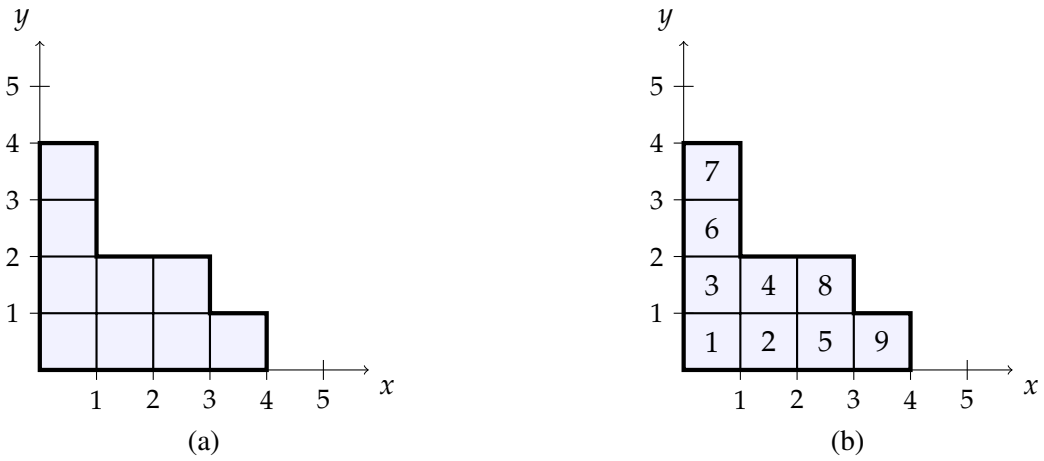

Figure 4.6: (a) The Young diagram $\lambda = (4,3,1,1)$ shown in the Cartesian coordinate system. (b) Example of a standard Young tableau of shape λ.

the current paper.

4.1.3 Sliding paths and evacuation paths in random tableaux

As promised, we turn now to the second interest area of the current paper, namely to random Young tableaux.

4.1.3.1 Notations related to Young diagrams and tableaux

We assume the reader's basic knowledge of tableaux theory, including partitions, (skew) Young diagrams, standard (skew) Young tableaux, RSK algorithm, jeu de taquin, rectification, Littlewood–Richardson coefficients and basics of the representation theory of the symmetric groups (you may recall some of these definitions in Chapter 1).

We denote the set of all partitions of n by $\mathbb{Y}_n$. We draw Young diagrams on the Cartesian plane using the French convention, that is, we draw them from the bottom to the top, see Figure 4.6a.

For any Young diagram λ we denote the set of standard Young tableaux of shape λ by $\mathcal{T}_\lambda$. *The shape* of a tableau T will be denoted by $\mathrm{sh}(T)$ and its size by $|\mathrm{sh}(T)|$, or shortly $|T|$.

Let T be a tableau. If p is a number which appears exactly once in T (which will always be the case in our considerations), we define the *position of the box with the number* p as the Cartesian coordinates of the bottom-left corner of the unique square which contains p; we denote this position by $\mathrm{pos}_p(T)$. For example, for T from Figure 4.6b, $\mathrm{pos}_5(T) = (2,0)$.

We will have a particular interest in Young diagrams and tableaux of square shape. By $\square_N \in \mathbb{Y}_{N^2}$ we denote the square diagram with side of length N.

4.1.3.2 Sliding paths and evacuation paths

Jeu de taquin acts on Young tableaux in the following way (see Figures 4.8a and 4.8b): we remove the bottom-left box of the given tableau T and obtain a *hole* in its place. Then we look at the two boxes: the one to the right and the one above the hole, and choose the one which contains the smaller number. We slide this smaller box into the location of the hole, see Figure 4.7. As a result, the hole moves in the opposite direction. We continue this operation as long as there is some box to the right or above the hole. The path which was traversed by

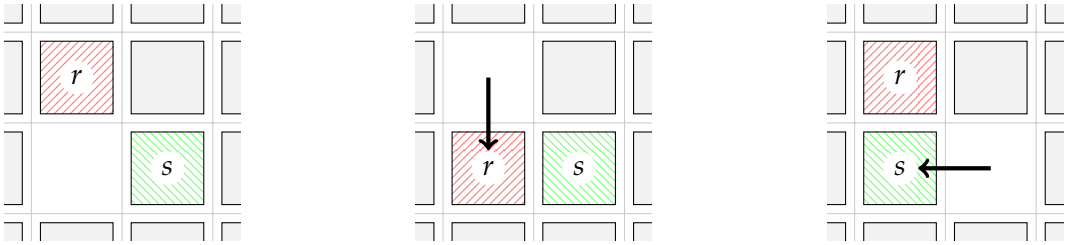

(a) (b) (c)

Figure 4.7: Elementary step of the jeu de taquin transformation: (a) the initial configuration of boxes, (b) the outcome of the slide in the case when $r < s$, (c) the outcome of the slide in the case when $s < r$. Copyright ©2014 Society for Industrial and Applied Mathematics. Reprinted from [Śni14] with permission. All rights reserved.

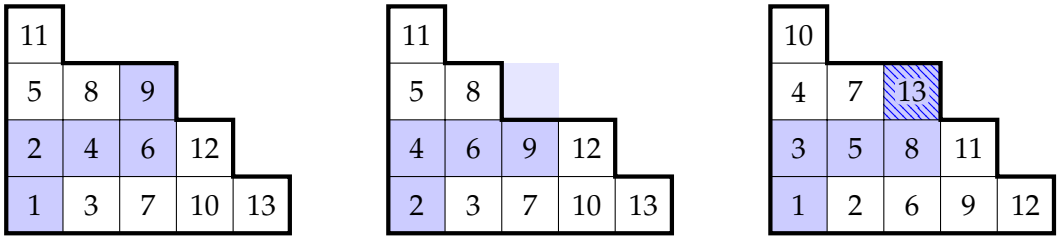

(a) (b) (c)

Figure 4.8: (a) A standard Young tableau T of shape $\lambda = (5,4,2,1)$. The highlighted boxes form the *sliding path*. (b) The outcome $j(T)$ of the jeu de taquin transformation. (c) The result $\partial^*(T)$ of the *dual promotion* applied to T.

the 'traveling hole' will be called the ***sliding path***, see Figure 4.8a. The result of jeu de taquin applied to a tableau T will be denoted by $j(T)$, see Figure 4.8b.

If T is a standard tableau then $j(T)$ is no longer standard because the numbering of its boxes starts with 2; however, if we decrease each entry of $j(T)$ by 1 then it becomes standard. This observation allows us to define the *dual promotion* $\partial^* : \mathcal{T}_\lambda \to \mathcal{T}_\lambda$ which is a bijection on the set of standard Young tableaux of any fixed shape λ. The idea is to put once again the box with the number $|T|$ to the aforementioned standardized version of the tableau $j(T)$ in the place where we removed a box during jeu de taquin, see Figure 4.8c.

For a given tableau $T \in \mathcal{T}_\lambda$ with $n = |\lambda|$ boxes the jeu de taquin transformation j can be iterated n times until we end with the empty tableau. During each iteration the box with the biggest number n either moves one node left or down, or stays put. Its trajectory

$$\operatorname{evac}(T) = \Big(\operatorname{pos}_n(T),\ \operatorname{pos}_n\big(j(T)\big),\ \ldots,\ \operatorname{pos}_n\big(j^{n-1}(T)\big) \Big) \tag{4.1.8}$$

will be called the ***evacuation path***.

4.1.3.3 The main results 2 and 3: asymptotics of sliding paths and evacuation paths

Observe that if we draw the boxes of a given square tableau $T \in \mathcal{T}_{\square_N}$ as little squares of size $\frac{1}{N}$ then the corresponding sliding path is a zigzag line connecting the opposite corners of the unit square $[0,1]^2$. *Let $T \in \mathcal{T}_{\square_N}$ be a random standard Young tableau of square shape (sampled with the uniform probability distribution on $\mathcal{T}_{\square_N}$ which will be denoted $\mathbb{P}_N$). Our goal is to find asymptotics of such random zigzag lines in the limit as $N \to \infty$, see Figure 4.9.*

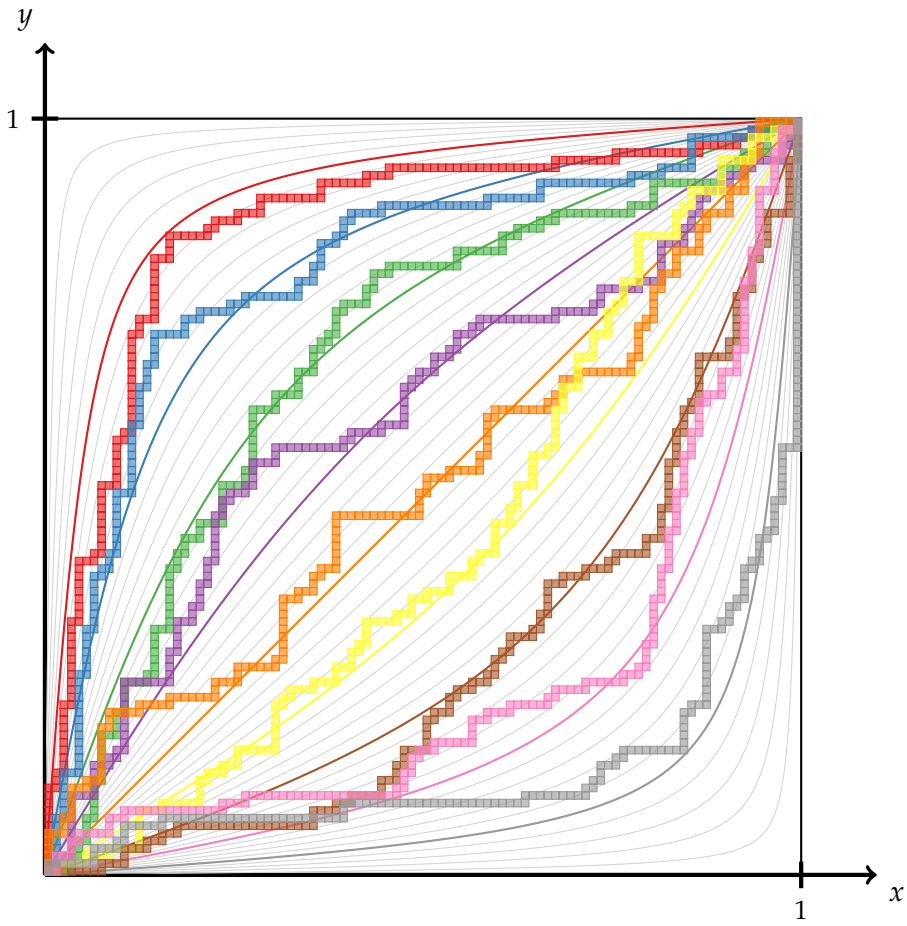

Figure 4.9: The nine zigzag lines are sample sliding paths for random square tableaux of size $N = 100$, selected so that they cross the anti-diagonal near the corresponding meridians (smooth thick curves) with the longitudes $\psi \in \{1/10, 2/10, \ldots, 9/10\}$. The gray lines are the meridians with the longitudes $\psi \in \{2/100, 4/100, \ldots, 98/100\}$. See also the blue-to-red family of curves on Figure 4.13.

We will show that there exists a family of smooth lines, called *meridians*, which connect the opposite corners of the unit square, with the property that the probability distribution of *the scaled sliding path for a random tableau converges, as* $N \to \infty$, *to a random meridian*.

An analogous result holds true for the scaled evacuation path for a random square tableau: during iteratively applied jeu de taquin operations j, the biggest box of the tableau asymptotically moves along a random meridian.

A version of this result applies also to the other boxes of the tableau; it follows that the time evolution of the tableau in the iterated applications of jeu de taquin

$$T,\ j(T),\ j^2(T),\ \ldots, j^{N^2}(T) \tag{4.1.9}$$

converges in probability, as $N \to \infty$, to dynamics of an incompressible liquid which flows along the meridians.

For the details of our results, see Theorems 4.2.3 and 4.2.4 in Section 4.2.

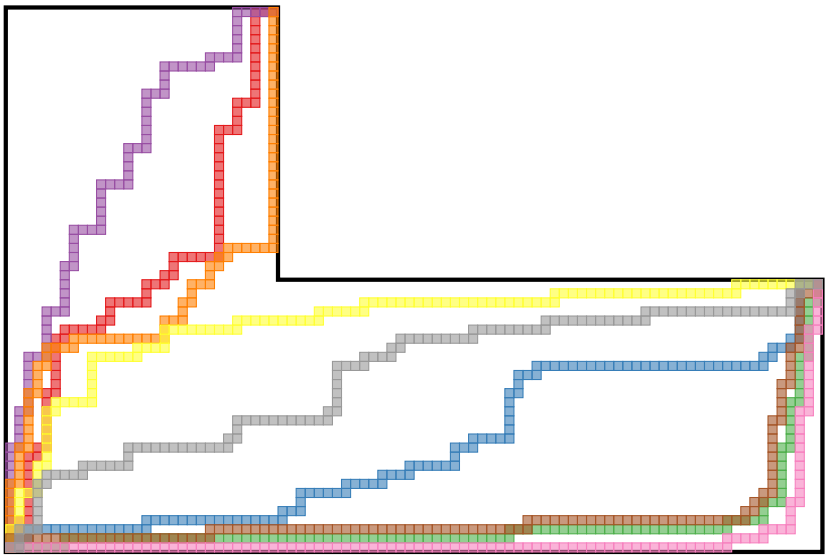

Figure 4.10: Sample sliding paths in random Young tableaux of an L-shape with 3600 boxes.

4.1.3.4 Not only squares

For simplicity and concreteness we stated our main results concerning random Young tableaux only for large random Young tableaux of *square shape*. However, analogous results hold true also for random tableaux of shape which is a *balanced Young diagram* (see Section 4.3 for the definition and Figure 4.10 for a teaser). In Section 4.10 we present a way in which the results obtained in this paper can be used (or generalized) in order to cover the class of balanced Young diagrams.

4.1.4 The content of the paper

The paper is organized as follows.

In Section 4.2 we state the main results (Theorems 4.2.3 and 4.2.4) about the typical shapes of the evacuation paths and sliding paths in square Young tableaux.

In Section 4.3 we give basic definitions on permutations and representation theory.

In Section 4.4 we introduce a 'surfers' language which we will use to describe dynamics of the box with the biggest entry (which we will call 'the surfer') and the smaller boxes ('the water'). In this spirit we also introduce the story of the *multisurfers* which will play a crucial role in our proofs and considerations. We will use this new multisurfer story later as a point of reference for the original problem of the (single) surfer in order to prove Theorem 4.4.1 concerning the position of the surfer along its journey. We sketch the proof in Section 4.4.4.

In Section 4.5 we show the way in which we will embed simultaneously both the story of the single surfer and the story of the multisurfers into a common universe.

In Section 4.6 we provide Theorem 4.6.2 concerning the distribution of the multisurfers on the water. We use here the Jucys–Murphy elements to give a direct link between the statistical properties of the multisurfers and the symmetric group characters evaluated on certain polynomials in the Jucys–Murphy elements.

In Section 4.7 we use the aforementioned results from Sections 4.5 and 4.6 to prove Theorem 4.4.1.

In Section 4.8 we prove Theorem 4.2.3 concerning typical evacuation paths.

Section 4.9 is devoted to the proof of Proposition 4.9.1 which shows the equivalence between the problems of finding the sliding paths and the evacuation paths in random Young

tableaux of given shape.

In Section 4.10 we extend our main results (Theorem 4.10.5) concerning typical evacuation and sliding paths to some subset of C-balanced Young tableaux.

In Section 4.11 we provide the link between the trajectory of the second class particle in an interacting particle system and the sliding path for a random Young tableau and prove Theorem 4.1.1.

4.2 The limit shape of sliding paths and evacuation paths

4.2.1 Asymptotics of a single box in the evacuation trajectory

As we mentioned in Section 4.1.3, we will focus on random standard Young tableaux of square shape $\square_N$ sampled according to the uniform measure $\mathbb{P}_N$. The symbol T_N will be reserved for such a uniformly random square Young tableau of shape $\square_N$.

The position of each of the boxes in the evacuation path (4.1.8) coincides with the position of a specific box in the standard Young tableau obtained by iterating the dual promotion ∂^*:

$$\mathrm{pos}_{N^2}\left(j^i(T_N)\right) = \mathrm{pos}_{N^2-i}\left(\partial^{*i}(T_N)\right). \tag{4.2.1}$$

Since $\partial^*\colon \mathcal{T}_{\square_N} \to \mathcal{T}_{\square_N}$ is a bijection, for each $i \geqslant 0$ the latter standard tableaux $\partial^{*i}(T_N)$ is also a uniformly random square Young tableau. It follows that the solution to the (much simpler) problem of understanding the asymptotics of a *single* element of the evacuation trajectory (4.1.8) follows from the work of Pittel and Romik [PR07], see also Section 4.2.3 below. In the current section we will recall the details of their work and we will use it to state our second main result, Theorem 4.2.3 (which addresses the more complex problem of understanding the *whole* evacuation trajectory (4.1.8)) and the third main result, Theorem 4.2.4.

4.2.2 The circles of latitude g_α

The *Russian coordinate system* is given by the following transformation of the Cartesian plane (warning: our notations differ from those of Pittel and Romik [PR07] who scale the coordinates below by an additional factor $1/\sqrt{2}$):

$$u := x - y, \qquad v := x + y,$$

see Figure 4.11.

For each $0 \leqslant \alpha \leqslant 1$ and $u \in \left[-2\sqrt{\alpha(1-\alpha)}, 2\sqrt{\alpha(1-\alpha)}\right]$ define

$$k_{\alpha,u} := \sqrt{4\alpha(1-\alpha) - u^2}$$

and for any $0 < \alpha < 1$ the function

$$h_\alpha\colon \left[-2\sqrt{\alpha(1-\alpha)}, 2\sqrt{\alpha(1-\alpha)}\right] \to \mathbb{R}$$

given by

$$h_\alpha(u) := \begin{cases} \frac{2u}{\pi}\arctan\left(\frac{1-2\alpha}{k_{\alpha,u}}\cdot u\right) + \frac{2}{\pi}\arctan\left(\frac{k_{\alpha,u}}{1-2\alpha}\right) & \text{if } 0 < \alpha < \frac{1}{2}, \\ 2 - \frac{2u}{\pi}\arctan\left(\frac{2\alpha-1}{k_{\alpha,u}}\cdot u\right) - \frac{2}{\pi}\arctan\left(\frac{k_{\alpha,u}}{2\alpha-1}\right) & \text{if } \frac{1}{2} < \alpha < 1, \\ 1 & \text{if } \alpha = \frac{1}{2}. \end{cases} \tag{4.2.2}$$

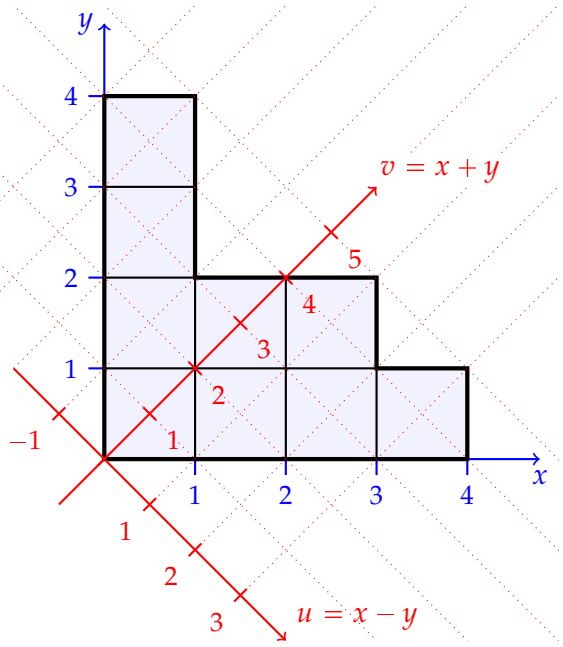

Figure 4.11: The Cartesian and the Russian coordinate systems on the plane.

In the expression above there may occur $k_{\alpha,u} = 0$ in the denominator; in such case (for fixed $\alpha \in (0,1)$) we consider the appropriate limit: if $u_0 = \pm 2\sqrt{\alpha(1-\alpha)}$ then

$$h_\alpha(u_0) := \lim_{u \to u_0} h_\alpha(u) = \begin{cases} u_0 & \text{for } 0 < \alpha < \frac{1}{2}, \\ 2 - u_0 & \text{for } \frac{1}{2} < \alpha < 1. \end{cases}$$

Additionally we define the one-point functions $h_0(0) := 0$ and $h_1(0) := 2$.

For any $\alpha \in [0,1]$ we consider the curve which in the Russian coordinate system is defined as

$$g_\alpha^{\mathrm{Rus}} := \left\{ \big(u, h_\alpha(u)\big) : |u| \leqslant 2\sqrt{\alpha(1-\alpha)} \right\} \subset \mathbb{R}^2 \tag{4.2.3}$$

and, equivalently, in the Cartesian coordinates is given by (see Figures 4.12 and 4.13)

$$g_\alpha := \left\{ \left(\frac{u + h_\alpha(u)}{2}, \frac{h_\alpha(u) - u}{2} \right) : |u| \leqslant 2\sqrt{\alpha(1-\alpha)} \right\} \subset [0,1]^2.$$

We call g_α ***the circle of latitude*** with the latitude α.

Roughly speaking, for each $\alpha \in [0,1]$ the (scaled down) *α-level curve* (which separates the boxes with entries $\leqslant \alpha N^2$ from the boxes bigger than this threshold, see Figure 4.12) in a uniformly random square tableau T_N converges in probability, as $N \to \infty$, to the circle of latitude g_α, see [PR07, Theorem 1] for a precise statement.

4.2.3 The random position of the box $\lfloor \alpha N^2 \rfloor$, the limit measure ν_α

Pittel and Romik [PR07, Theorem 2] also found the explicit formula for the limit distribution of the scaled down location

$$\frac{1}{N} \operatorname{pos}_{\lfloor \alpha N^2 \rfloor}(T_N)$$

of the entry $\lfloor \alpha N^2 \rfloor$ in a uniformly random square Young tableau T_N, as $N \to \infty$. This limit distribution turns out to be supported on the circle of latitude g_α and thus it is uniquely

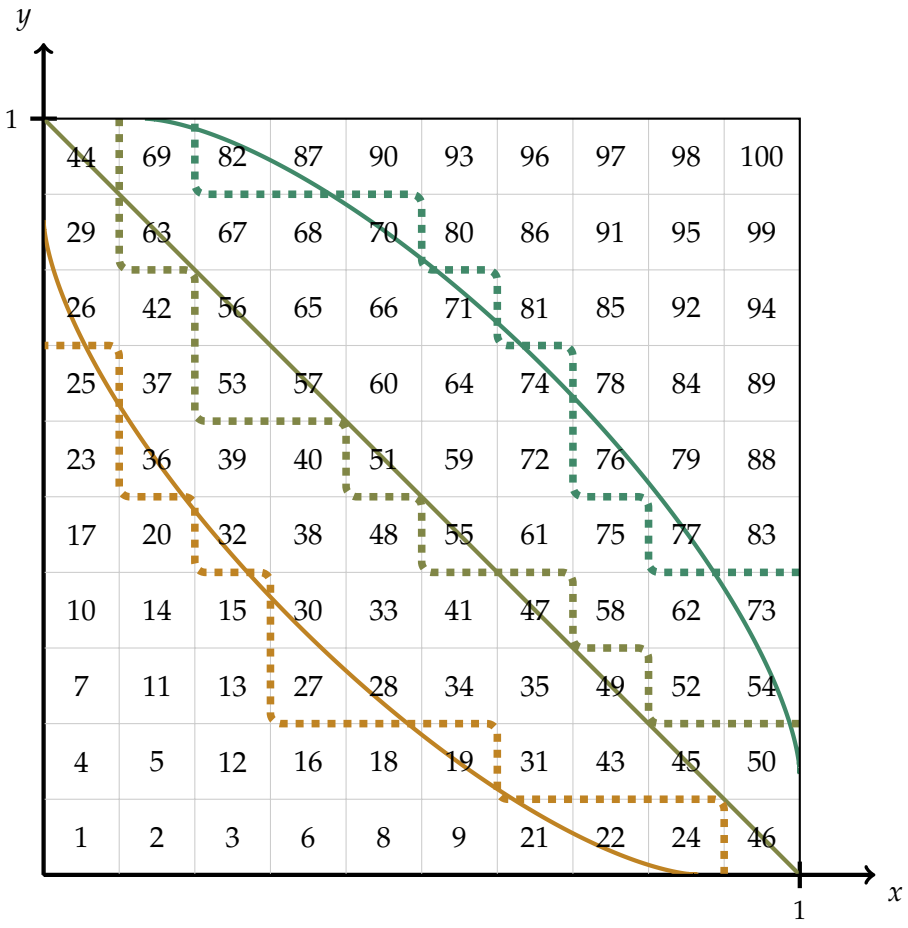

Figure 4.12: A scaled down sample random square tableau of size $N = 10$. The zigzag lines are the level curves for $\alpha \in \{1/4, 2/4, 3/4\}$. The smooth lines are the corresponding circles of latitude g_α, see also the orange-to-green family of curves on Figure 4.13.

determined by the probability distribution of the u-coordinate. The latter, denoted by ν_α, turns out to be the semicircular distribution on the interval $\left[-2\sqrt{\alpha(1-\alpha)}, 2\sqrt{\alpha(1-\alpha)}\right]$ with the density

$$f_{\nu_\alpha}(u) := \frac{k_{\alpha,u}}{2\pi\alpha(1-\alpha)}. \tag{4.2.4}$$

4.2.4 Geographic coordinates on the square

For any point $p = (x, y) \in [0,1]^2$ of the unit square there is exactly one $\alpha = \alpha(p) \in [0,1]$ such that p lies on the curve g_α. We say that *the latitude of* p is equal to α. With the notations of Pittel and Romik [PR07] the latitude $\alpha(x, y) = L(x, y)$ is just the limit height function of random square standard Young tableaux.

The *longitude of* p, which we denote by

$$\psi(p) = \nu_\alpha\Big(\big(-\infty, x-y\big]\Big) = F_{\nu_\alpha}(x-y),$$

is defined as the mass of the points on the curve g_α which have their u-coordinate not greater than the u-coordinate of the point p or, equivalently, in terms of the cumulative distribution function F_{ν_α} of the measure ν_α. Notice that $\psi((0,0)) = \psi((1,1)) = 1$. The set of points of the unit square $[0,1]^2$ with equal longitude ψ is a curve called the *meridian* ψ, see Figures 4.9 and 4.13.

For given $\alpha \in (0,1)$ and $\psi \in [0,1]$ we denote by

$$P_{\alpha,\psi} = \left(x_\alpha^\psi, y_\alpha^\psi\right) \in [0,1]^2$$

the unique point of the unit square $[0,1]^2$ with the latitude α and the longitude ψ. We set additionally $P_{0,\psi} = (0,0)$ and $P_{1,\psi} = (1,1)$ for any $\psi \in [0,1]$. We denote by

$$u_\alpha^\psi := x_\alpha^\psi - y_\alpha^\psi \quad \text{and} \quad v_\alpha^\psi := x_\alpha^\psi + y_\alpha^\psi$$

the u- and v-coordinate of the point $\left(x_\alpha^\psi, y_\alpha^\psi\right) = P_{\alpha,\psi}$.

Remark 4.2.1. We will not use the following observation, but fans of cartography may find it interesting: for reasons which will hopefully become obvious later on, the map

$$[0,1]^2 \ni (\alpha, \psi) \mapsto P_{\alpha,\psi} \in [0,1]^2$$

is *equiareal* which manifests by equality of the areas of the curvilinear rectangles on Figure 4.13.

Remark 4.2.2. The result of Pittel and Romik [PR07, Theorem 2] is a special case of a general phenomenon of existence of the level curves (circles of latitudes) for random Young tableaux of specified shape. Biane [Bia98] proved that such level curves exist for any balanced sequence of Young diagrams, see Section 4.10 for more information.

4.2.5 The second main result. Typical evacuation path

For a given tableau $T_N \in \mathcal{T}_{\square_N}$ and $t \in [0,1)$ we denote by

$$X_t = X_t(T_N) = \frac{1}{N}\operatorname{pos}_{N^2}\left(j^{\lfloor tN^2 \rfloor}(T_N)\right) \in [0,1]^2 \tag{4.2.5}$$

the scaled down position of the point from the evacuation path $\operatorname{evac}(T_N)$, cf. (4.1.8). Clearly, the parameter t indicates how many boxes were removed so far and therefore we can relate to

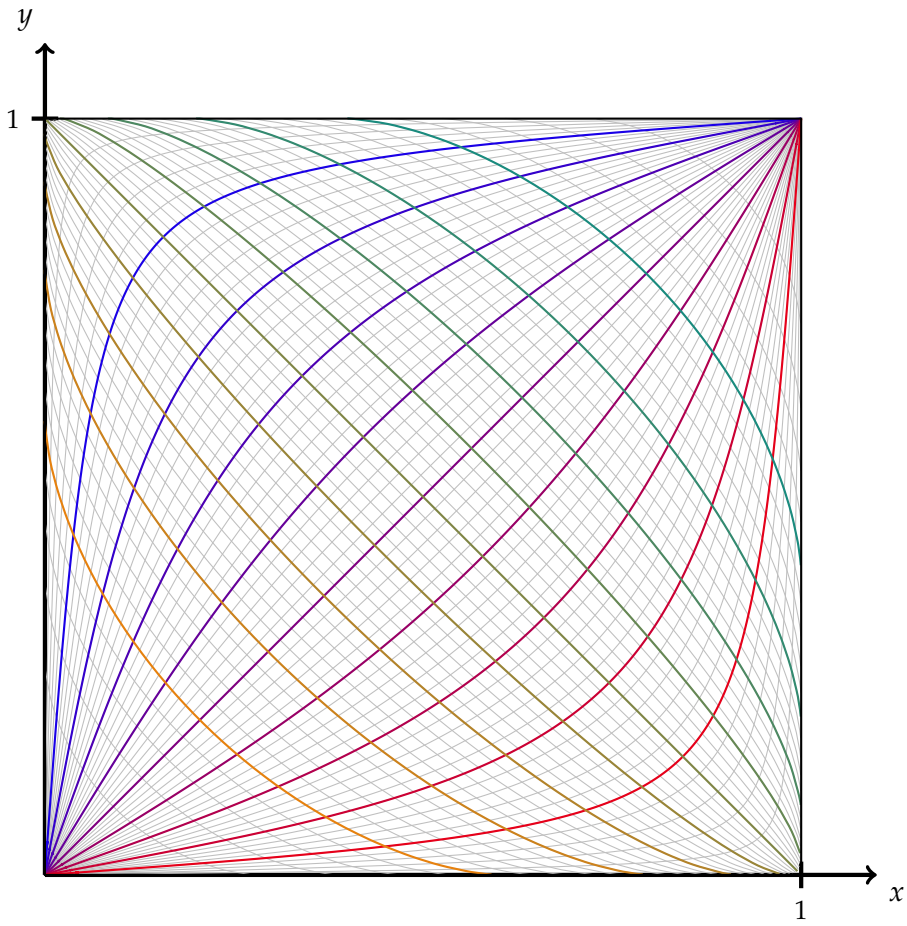

Figure 4.13: The geographic coordinate system on the unit square $[0,1]^2$. The blue-to-red family of thick colored curves connecting the bottom left and the upper right corner are the meridians with the longitudes $\psi \in \{1/10, 2/10, \dots, 9/10\}$. The gray lines are the meridians with the longitudes $\psi \in \{2/100, 4/100, \dots, 98/100\}$, cf. Figure 4.9. The orange-to-green family of thick colored curves are the circles of latitudes g_α with the latitudes $\alpha \in \{1/10, 2/10, \dots, 9/10\}$. The thin, gray lines are the circles of latitude g_α with the latitudes $\alpha \in \{2/100, 4/100, \dots, 98/100\}$, see Figure 4.12. The shown meridians and circles of latitude split the square into a 50×50 grid of curvilinear rectangles with equal areas.

it as the *time*.

Our second main result states that, asymptotically, *the scaled evacuation path in a random square tableau is a random meridian*, see Figure 4.9.

Theorem 4.2.3. *For each $N \in \mathbb{N}$ there exists a random variable $\Psi_N \colon \mathcal{T}_{\square_N} \to [0,1]$ such that the supremum distance*

$$\sup_{t \in [0,1]} \left| X_t(T_N) - P_{1-t, \Psi_N(T_N)} \right| \tag{4.2.6}$$

converges in probability to zero, as $N \to \infty$. More explicitly: for each $\varepsilon > 0$

$$\lim_{N \to \infty} \mathbb{P}_N \Big\{ T_N \in \mathcal{T}_{\square_N} : \sup_{t \in [0,1]} \left| X_t(T_N) - P_{1-t, \Psi_N(T_N)} \right| > \varepsilon \Big\} = 0.$$

The probability distribution of the random variable Ψ_N converges, as $N \to \infty$, to the uniform distribution on the unit interval $[0,1]$.

In other words (with a small abuse of notation), the random trajectory $\big(X_t(T_N)\big)_{t\in[0,1]}$ with respect to the supremum norm converges in distribution to a random meridian $\Big(P_{1-t,\psi}\Big)_{t\in[0,1]}$ when $N \to \infty$, that is shortly,

$$\big(X_t(T_N)\big)_{t\in[0,1]} \xrightarrow[N\to\infty]{\mathrm{d}} \Big(P_{1-t,\psi}\Big)_{t\in[0,1]},$$

where ψ is a random variable with the uniform $U(0,1)$ distribution.

The proof is postponed to Section 4.8 and the preparations to it will take the majority of time.

4.2.6 The third main result. Typical sliding path

Let T be a standard Young tableau with n boxes. Sometimes when investigating the sliding path, we are concerned not only about its shape, but also we would like to be able to tell which entries were placed in the rearranged boxes. This motivates the notion of *the sliding path in the lazy parametrization* (or shortly *the lazy sliding path*) which is a sequence of boxes $\mathbf{q}(T) := (\mathbf{q}_1, \dots, \mathbf{q}_n) \subset \mathbb{N}^2$ where $\mathbf{q}_i$ is the last box along the sliding path corresponding to T (cf. Figure 4.8a) which contains a number $\leqslant i$, cf. [Rom15, Section 3.3].

Our third main result is stated in the language of lazy sliding path and says that, asymptotically, *the scaled sliding path in a random square tableau is, just like in Theorem 4.2.3, a random meridian*, see Figure 4.9.

Theorem 4.2.4. *For each $N \in \mathbb{N}$ there exists a random variable $\widetilde{\Psi}_N \colon \mathcal{T}_{\square_N} \to [0,1]$ such that the supremum distance*

$$\sup_{t\in[0,1]} \left| \frac{1}{N}\mathbf{q}_{\lceil tN^2\rceil}(T_N) - P_{t,\widetilde{\Psi}_N(T_N)} \right|$$

converges in probability to zero, as $N \to \infty$.

The probability distribution of the random variable $\widetilde{\Psi}_N$ converges, as $N \to \infty$, to the uniform distribution on the unit interval $[0,1]$.

In other words (with a small abuse of notation), the lazy sliding path $\Big(\mathbf{q}_{\lceil tN^2\rceil}(T_N)\Big)_{t\in[0,1]}$ with respect to the supremum norm converges in distribution to a random meridian $\Big(P_{t,\psi}\Big)_{t\in[0,1]}$ when $N \to \infty$, that is shortly,

$$\frac{1}{N}\mathbf{q}_{\lceil tN^2\rceil}(T_N) \xrightarrow[N\to\infty]{\mathrm{d}} P_{t,\psi}$$

where ψ is a random variable with the uniform $U(0,1)$ distribution.

The proof is postponed to Section 4.9.2 and is based on showing that the random lazy sliding path and the (reversed) random evacuation path have the same distribution, cf. Proposition 4.9.1. In other words, we show that the problem of finding typical sliding paths is equivalent to the problem of finding typical evacuation paths from Theorem 4.2.3.

4.2.7 Conjecture on the independence of the iterated sliding paths.

Recall from Section 4.1.3.2 that the dual promotion ∂^* is a bijection defined by a two-step procedure in which first we apply the jeu de taquin and then we add the box which was

removed from the initial tableau T. We can iterate ∂^* on the random tableau T_N and get *the sequence of iterated sliding paths*

$$\mathbf{q}(T_N), \quad \mathbf{q}\big(\partial^*(T_N)\big), \quad \mathbf{q}\Big((\partial^*)^2(T_N)\Big), \quad \dots. \tag{4.2.7}$$

Since ∂^* is a bijection, Theorem 4.2.4 provides asymptotics of the distribution of each element of the sequence (4.2.7) separately. The following conjecture aims to provide asymptotic information about their *joint* distribution.

Conjecture 4.2.5. *For each integer $k \geqslant 1$ the probability distribution of the random vector*

$$\Big(\widetilde{\Psi}_N(T_N), \quad \widetilde{\Psi}_N\big(\partial^*(T_N)\big), \quad \dots, \quad \widetilde{\Psi}_N\big((\partial^*)^{k-1}(T_N)\big)\Big)$$

converges, as $N \to \infty$, to the uniform distribution on the unit cube $[0,1]^k$.

Romik and the second named author proved an analogue of this conjecture in the case of the Plancherel-distributed random infinite tableaux, see [Rom15, the comment below Theorem 1.5] and Section 4.2.8 for more details.

4.2.8 Something old, something new, something borrowed: sliding paths for random infinite tableaux

The problem of the asymptotic shape of a sliding path (analogous to the one from Theorem 4.2.4) was studied before by Romik and the second named author [Rom15, Section 1.3] for a certain *infinite* random Young tableau, more specifically for the recording tableau $Q(x_1, x_2, \dots)$ obtained by applying the Robinson–Schensted correspondence to an infinite sequence $(x_1, x_2, \dots)$ of independent, identically distributed random variables with the uniform distribution on the unit interval $[0,1]$. Such a choice corresponds to sampling the random Young tableau according to, so called, *the Plancherel measure*.

In such a setting the sliding path happens to converge almost surely to a straight line with a random direction [Rom15, Theorem 1.1], in other words the analogue of our meridians in the context of the Plancherel measure is given by the straight lines emanating from the origin of the coordinate system.

One of the main difficulties in the proof of Theorem 4.2.4 will be the construction of the random variables $\widetilde{\Psi}_N$ which provide the longitude of the meridian along which the sliding path travels. This difficulty is absent in [Rom15] because in that context the analogue of the longitude turns out to be simply equal to x_1, the first entry of the random sequence to which the Robinson–Schensted correspondence is applied.

It would be tempting to repeat the approach from [Rom15] in our context, for example one could proceed as follows. Let

$$\pi^{(N)} = \Big(\pi_1^{(N)}, \dots, \pi_{N^2}^{(N)}\Big)$$

be a uniformly random element of the set of *extremal Erdős–Szekeres permutations*, i.e., permutations with the property that the corresponding tableaux associated via the Robinson–Schensted correspondence have the square shape $\square_N$. Then the corresponding recording tableau $T_N = Q(\pi^{(N)})$ is, as required, a uniformly random standard Young tableau of square shape $\square_N$. A naive guess would be that one possible choice for the random variable $\widetilde{\Psi}_N$ is again (a rescaled version of) the first entry of the permutation, i.e., $\pi_1^{(N)}$.

Uniformly random extremal Erdős–Szekeres permutations were investigated by Romik [Rom06] who proved, among other results, that the probability distribution of $\frac{1}{N^2}\pi_1^{(N)}$ converges to the point measure concentrated in $\frac{1}{2}$. For this reason it seems that the random

variables $\pi_1^{(N)}$ do not carry any information which would be useful for our purposes, hence the approach from [Rom15] is not applicable here directly, and the construction of the random variables $\widetilde{\Psi}_N$ must follow different ideas.

Despite this fundamental difference, an astute reader may notice that our proof of Theorem 4.2.3 follows a path parallel to the one of [Rom15, Theorem 5.1]. For example, the counterpart of our Proposition 4.6.5 (which can be viewed as a result about a certain random process of *removal* of boxes from a Young diagram) is [Rom15, Theorem 4.4] (which concerns a certain random process of *addition* of boxes to a Young diagram).

4.3 Preliminaries

4.3.1 Permutations, Young diagrams and Young tableaux, continued

We continue Section 4.1.3.1 where some basic definitions were introduced.

For any natural number n, we define the set $[n] := \{1, \dots, n\}$. From the following on (unlike in Section 4.1.2) we will view the symmetric group $\mathfrak{S}_n$ as the group of permutations of the set $[n]$. We define *the length of a permutation* π to be the minimal number of factors necessary to write π as a product of (arbitrary, not necessarily adjacent!) transpositions, and denote it by $|\pi|$.

For any Young diagram λ, we denote *the number of standard Young tableaux* of shape λ by $d_\lambda = |\mathcal{T}_\lambda|$. If $T \in \mathcal{T}_\lambda$ and $0 \leqslant p \leqslant |\lambda|$ we consider the *restriction of T to its p least boxes* by removing the entries which are bigger than p, and denote the obtained tableau by $T|_{\leqslant p}$ (clearly, it is also a standard Young tableau).

For $C \geqslant 1$ we say that a Young diagram λ is *C-balanced* if λ has at most $C\sqrt{|\lambda|}$ rows and at most $C\sqrt{|\lambda|}$ columns.

For a tableau T and an integer p which appears exactly once in T (which will always be the case in our considerations) we define *the u-coordinate of the box with the entry p* as

$$u_p^T := x - y \qquad \text{for } (x, y) = \operatorname{pos}_p(T).$$

Note that in the literature, for instance in [CSST10], such a u-coordinate is called the *content*.

We will also consider skew tableaux obtained by removing some boxes from Young tableaux. Let $T \in \mathcal{T}_\lambda$ be a standard Young tableau. If T with the boxes with entries $a_1, \dots, a_i$ removed is a skew tableau, we denote it by $T\backslash\{a_1, \dots, a_i\}$. Clearly, $T\backslash\{p+1, \dots, |\lambda|\} = T|_{\leqslant p}$ is also a standard Young tableau.

4.3.2 Representation theory

Reader may recall the basics of the representation theory in Section 1.4.

If G is a finite group and $\rho\colon G \to \operatorname{End} V$ is its representation on a finite-dimensional complex linear space V, then by

$$\xi_V(g) := \operatorname{Tr} \rho(g), \qquad g \in G,$$

we denote its *character* (we write just ξ if it is clear which representation we consider). We also consider the *normalized character* $\chi_V\colon G \to \mathbb{C}$ given by

$$\chi_V := \frac{1}{\dim V} \cdot \xi_V = \frac{1}{\xi_V(\mathrm{id})} \cdot \xi_V.$$

Additionally, for any element of the group algebra

$$f = \sum_{g \in G} f_g g \in \mathbb{C}G$$

we denote by $\chi_V(f)$ the *extension of the character by linearity* given by

$$\chi_V(f) := \sum_{g \in G} f_g \chi_V(g) \in \mathbb{C}.$$

On the vector space of functions $\mathcal{G} := \{f \colon G \to \mathbb{C}\}$ we consider the *standard scalar product* given by

$$\langle f, g \rangle := \frac{1}{|G|} \sum_{h \in G} f(h) \overline{g(h)}, \qquad \text{for } f, g \in \mathcal{G},$$

where $\bar{c}$ denotes the complex conjugation.

We will denote by $\hat{G}$ the family of irreducible representations (*irreps* for short) of G. It is known that the system of irreducible characters $\{\xi_{V_x}\}_{x \in \hat{G}}$ is orthonormal. Therefore for the normalized irreducible characters the following holds:

$$\left\langle \chi_{V_1}, \chi_{V_2} \right\rangle = \begin{cases} \frac{1}{\dim V_1} & \text{if } \chi_{V_1} = \chi_{V_2}, \\ 0 & \text{otherwise.} \end{cases}$$

Let V be a finite-dimensional representation and let

$$V = \bigoplus_{x \in \hat{G}} m_x V_x$$

be its decomposition into irreducible components, where $m_x \in \mathbb{N}$ denotes the multiplicity of x. By *a random irreducible component* of V we will understand a random element of $\hat{G}$ sampled according to the probability measure $\mathcal{P}_V$ which is proportional to the total dimension of all copies of a given irrep in V:

$$\mathcal{P}_V(x) := \frac{m_x \dim V_x}{\dim V} = (\dim V_x)^2 \cdot \langle \chi_V, \chi_x \rangle \qquad \text{for } x \in \hat{G}. \tag{4.3.1}$$

The *trivial representation* will be denoted by triv. If H is a subgroup of G then we denote by $\rho\downarrow_H^G$ the *restriction of a representation ρ to H* (if G is fixed we just write $\rho\downarrow_H$).

For $\lambda \in \mathbb{Y}_n$ we denote by $\rho_\lambda \colon \mathfrak{S}_n \to \operatorname{End} V_\lambda$ *the irreducible representation of the symmetric group $\mathfrak{S}_n$ corresponding to the Young diagram λ* and by χ_λ its *normalized character*.

4.3.3 Asymptotics of characters and the approximate factorization property

We will use two results concerning asymptotics of characters. The first one, due to Feráy and the second named author, gives an upper bound on the irreducible characters.

Fact 4.3.1 ([FŚ11, Theorem 1]). *There exists a constant $a > 0$ such that for any Young diagram λ and any permutation $\pi \in \mathfrak{S}_{|\lambda|}$*

$$|\chi_\lambda(\pi)| \leqslant \left[a \max\left(\frac{r(\lambda)}{|\lambda|}, \frac{c(\lambda)}{|\lambda|}, \frac{|\pi|}{|\lambda|} \right) \right]^{|\pi|} \tag{4.3.2}$$

where $r(\lambda)$ and $c(\lambda)$ stand, accordingly, for the number of rows and the number of columns of λ.

The second result, due to Biane (and its generalization due to the second-named author), shows that the character calculated on the product of two fixed permutations with disjoint supports approximately factorizes.

Fact 4.3.2 ([Bia98, Corollary 1.3], [Bia01, Section 0], [Śni06, Theorem 1]). *Let $C \geqslant 1$ and $m \in \mathbb{N}$. There exists a constant $K > 0$ such that for each C-balanced Young diagram λ and all permutations $\sigma, \tau \in \mathfrak{S}_{|\lambda|}$ with disjoint supports and satisfying $|\sigma|, |\tau| \leqslant m$ we have*

$$\left|\chi_\lambda(\sigma\tau) - \chi_\lambda(\sigma)\chi_\lambda(\tau)\right| \leqslant \frac{K}{\left(\sqrt{|\lambda|}\right)^{|\sigma|+|\tau|+2}}.$$

4.3.4 Jucys–Murphy elements

In the applications of Fact 4.3.1 and Fact 4.3.2 we will encounter the expressions in the left-hand-side of (4.3.4). The lemma below gives an upper bound for their values.

Its proof uses *Jucys–Murphy elements* which often appear in the modern approach to the representation theory of the symmetric groups (see [CSST10]) and are defined as the following elements of the symmetric group algebra $\mathbb{C}\mathfrak{S}_n$

$$J_k := \sum_{1 \leqslant i < k} (i,k) = (1,k) + \cdots + (k-1,k) \in \mathbb{C}\mathfrak{S}_n \quad \text{for } 1 \leqslant k \leqslant n. \tag{4.3.3}$$

The elements $J_1, \ldots, J_n \in \mathbb{C}\mathfrak{S}_n$ form a commuting family in the symmetric group algebra. We will use them intensively in Section 4.6.

Lemma 4.3.3. *For any $c > 0$ and $n \in \mathbb{N}$*

$$\sum_{\pi \in \mathfrak{S}_n} c^{|\pi|} < \exp\left(\frac{n^2 c}{2}\right). \tag{4.3.4}$$

Proof. For any $c \in \mathbb{C}$ the following simple identity in the symmetric group algebra holds true

$$\sum_{\pi \in \mathfrak{S}_n} c^{|\pi|} \pi = (1 + cJ_1)(1 + cJ_2) \cdots (1 + cJ_n).$$

By applying the trivial representation to both sides of the above equality we get that for $c > 0$

$$\sum_{\pi \in \mathfrak{S}_n} c^{|\pi|} = (1+c)(1+2c) \cdots \big(1 + (n-1)c\big) < e^c e^{2c} \cdots e^{(n-1)c} < \exp\left(\frac{n^2 c}{2}\right). \square$$

4.4 The longitude and surfing

Our strategy towards the proof of Theorem 4.2.3 is to pass to the geographic coordinates of the point $X_t = X_t(T_N)$ from the scaled evacuation trajectory (4.2.5). Having the choice between the latitude and the longitude, we start with the more challenging problem of understanding how the longitude $\psi(X_t)$ changes over time t.

Instead of considering the longitude $\psi(X_t)$ directly, it will be more convenient to study the following random variable which we call *the theoretical longitude*:

$$\Psi_N^{\mathrm{th}}(t) := F_{\nu_{1-t}}\big(u(X_t)\big), \tag{4.4.1}$$

where $u(X_t)$ denotes the u-coordinate of $X_t = X_t(T_N)$, and $F_{\nu_{1-t}}$ is the cumulative distribution function of the limit measure ν_{1-t} which was defined in Section 4.2.3. Notice that

if in time t the box with the biggest number is positioned *exactly* on the circle of latitude $\alpha = 1 - t$, that is, $\alpha(X_t) = 1 - t$, then the theoretical longitude coincides with the longitude, i.e., $\Psi_N^{\mathrm{th}}(t) = \psi(X_t)$. Heuristically one would expect that $\Psi_N^{\mathrm{th}}(t) \approx \psi(X_t)$ for $N \to \infty$.

Roughly speaking, the following result states that (away from the polar regions which correspond to $t = 0$ and $t = 1$) the theoretical longitude of X_t does not change too much over time.

Theorem 4.4.1. *Assume that* $0 < t_1 < t_2 < 1$. *Then for each* $\varepsilon > 0$

$$\lim_{N\to\infty} \mathbb{P}_N\left\{T_N \in \mathcal{T}_{\square_N} : \left|\Psi_N^{\mathrm{th}}(t_2) - \Psi_N^{\mathrm{th}}(t_1)\right| > \varepsilon\right\} = 0.$$

In other words, the difference $\Psi_N^{\mathrm{th}}(t_2) - \Psi_N^{\mathrm{th}}(t_1)$ *converges in probability to* 0 *when* $N \to \infty$, *that is shortly,*

$$\Psi_N^{\mathrm{th}}(t_2) - \Psi_N^{\mathrm{th}}(t_1) \xrightarrow[N\to\infty]{P} 0.$$

The proof is quite involved; Sections 4.4 to 4.7.2 are a preparation while the proof of Theorem 4.4.1 itself will be given in Sections 4.7.3 and 4.7.4. The remaining part of the current section is devoted to a rough sketch of the proof.

Clearly, Theorem 4.4.1 is equivalent to the conjunction of the following two statements for $\varepsilon > 0$:

$$\lim_{N\to\infty} \mathbb{P}_N\left\{T_N \in \mathcal{T}_{\square_N} : \Psi_N^{\mathrm{th}}(t_2) - \Psi_N^{\mathrm{th}}(t_1) > \varepsilon\right\} = 0, \tag{4.4.2}$$

$$\lim_{N\to\infty} \mathbb{P}_N\left\{T_N \in \mathcal{T}_{\square_N} : \Psi_N^{\mathrm{th}}(t_2) - \Psi_N^{\mathrm{th}}(t_1) < -\varepsilon\right\} = 0. \tag{4.4.3}$$

We start with the proof of the upper bound (4.4.2). Then we will use the symmetry of the problem in order to prove the lower bound (4.4.3).

4.4.1 The single surfer scenario

We would like to present the problem of the evacuation path in a different, more vivid light. We will speak about a *square pool of side* N (=the square Young diagram $\square_N$) filled with $N^2 - 1$ *particles of water* (=the Young tableau T_N with the largest entry removed), a passive *surfer* (=the box with the biggest entry N^2) and its trajectory (or behavior) when the pool is being drained (=iteratively applying jeu de taquin). Our goal in Theorem 4.2.3 is to show that, when the pool is big enough, the surfer has some typical paths along which he/she moves as the pool is being drained.

In our proof of Theorem 4.4.1 we start our analysis at time t_1 when jeu de taquin was already applied

$$m_1 := \lfloor t_1 N^2 \rfloor \tag{4.4.4}$$

times. Our starting point is therefore the standard tableau

$$T'_N := \partial^{*m_1}(T_N)\big|_{\leqslant N^2 - m_1} \tag{4.4.5}$$

with $N^2 - m_1$ boxes (compare with (4.1.9)). We denote

$$w_1 = N^2 - m_1 - 1. \tag{4.4.6}$$

In this way the boxes with numbers $1, \ldots, w_1$ correspond to the *water* and the box with the maximal number $w_1 + 1$ to the *surfer*. The position of the latter box will be called *the initial*

position of the surfer and we will refer to the tableau T'_N as *the initial surfer configuration*. By removing the box with the surfer

$$W'_N := T'_N \backslash \{w_1 + 1\} \tag{4.4.7}$$

we get a standard Young tableau which encodes *the initial configuration of the water*.

As time goes by, at the time t_2 the jeu de taquin was already applied

$$m_2 := \lfloor t_2 N^2 \rfloor$$

times and we investigate the tableau

$$T''_N = \partial^{*m_2}(T_N)\big|_{\leqslant N^2 - m_2} = \partial^{*m_2 - m_1}(T'_N)\big|_{\leqslant N^2 - m_2}$$

with $w_2 + 1$ boxes, where

$$w_2 = N^2 - m_2 - 1. \tag{4.4.8}$$

The boxes with the numbers $1, \ldots, w_2$ correspond to the remaining particles of water and the box with the maximal number $w_2 + 1$ corresponds to the surfer; the position of the latter box will be called *the final position of the surfer*.

Our aim is to relate the final position of the surfer at the time t_2 to its initial position at the time t_1, preferably in the language of the theoretical longitude. As a point of reference we will introduce an additional *multisurfer story* which happens in a parallel universe in which we pay attention to k surfers.

4.4.2 Pieri tableaux

We consider the partial order on the plane $\mathbb{R}^2$ defined by:

$$(x_1, y_1) \preceq (x_2, y_2) \iff \big(x_1 \leqslant x_2 \ \wedge \ y_1 \geqslant y_2\big)\,.$$

Let k be a fixed natural number and M be a tableau in which the k largest entries are numbered by consecutive integers $l + 1, \ldots, l + k$. We say that the tableau M is a *k-Pieri tableau* if these k largest boxes are placed in *the increasing order* with respect to $\preceq$ (i.e., they are placed from north-west to south-east) or, equivalently, their u-coordinates are ordered increasingly, that is:

$$u^M_{l+1} < \cdots < u^M_{l+k}.$$

If the value of the number k is clear from the context, we will shortly say that M is *Pieri*.

It is easy to check that if M has at least $k + 1$ boxes then M is a k-Pieri tableau if and only if $j(M)$ is a k-Pieri tableau.

For standard Young tableaux we will consider the following more general notion. For a (skew) standard Young tableau T with n boxes and positive integers w and k such that $w + k \leqslant n$ we say that T is a $(w + 1, w + k)$*-Pieri tableau* if

$$u^T_{w+1} < \cdots < u^T_{w+k}. \tag{4.4.9}$$

The set of $(w + 1, w + k)$-Pieri standard tableaux of (skew) shape λ will be denoted by $\widetilde{\mathcal{T}}^{(w+1,w+k)}_\lambda$.

4.4.3 The multisurfer scenario

For *the multisurfer scenario* let $k = k(N)$ be a sequence of positive integers such that

$$\lim_{N\to\infty} k = \infty \quad \text{and} \quad \lim_{N\to\infty} \frac{k^2}{N} = 0. \tag{4.4.10}$$

For a fixed value of N we consider the $N \times N$ square pool filled with $N^2 - k$ *particles of water* on which k surfers (=k boxes with the biggest entries) are positioned in the increasing order. Formally speaking, by

$$\widetilde{\mathcal{T}}_{\square_N} = \widetilde{\mathcal{T}}_{\square_N}^{(N^2-k+1,N^2)}$$

we denote the set of standard Young tableaux of the square shape $\square_N$ which are k-Pieri, and by $\widetilde{\mathbb{P}}_N$ the uniform distribution on the set $\widetilde{\mathcal{T}}_{\square_N}$. We assume that M_N is a random tableau sampled with the uniform probability distribution $\widetilde{\mathbb{P}}_N$ on the set $\widetilde{\mathcal{T}}_{\square_N}$ In this scenario, in order to refer to the k surfers, we will use the name *multisurfers*.

We start our analysis when jeu de taquin was already applied $m_1 + 1 - k$ times with m_1 given again by (4.4.4) (notice that $m_1 + 1 - k \geqslant 0$ for N big enough). Our starting point is therefore the tableau

$$M'_N := \partial^{*m_1+1-k}(M_N)\big|_{\leqslant N^2-m_1-1+k} \tag{4.4.11}$$

with $N^2 - m_1 - 1 + k = w_1 + k$ boxes. We will refer to this tableau as *the initial multisurfer configuration*. In this way, just as in the single surfer scenario, the boxes with the numbers $1, \ldots, w_1$ correspond to the *water* (in particular, there is the same number of water particles as in the single surfer scenario). On the other hand, the boxes with the numbers $w_1 + 1, \ldots, w_1 + k$ correspond to the *multisurfers*. By removing the multisurfers

$$\widetilde{W}'_N := M'_N \backslash \{w_1 + 1, \ldots, w_1 + k\} \tag{4.4.12}$$

we get a standard Young tableau which encodes the initial configuration of the water.

As time goes by, at the time t_2 the jeu de taquin was already applied $m_2 + 1 - k$ times and we investigate the tableau

$$M''_N = \partial^{*m_2+1-k}(M_N)\big|_{\leqslant w_2+k} = \partial^{*m_2-m_1}(M'_N)\big|_{\leqslant w_2+k} \tag{4.4.13}$$

which consists of $w_2 + k$ boxes which correspond to w_2 particles of water and k multisurfers; we will refer to this tableau as *the final multisurfer configuration*.

4.4.4 Sketch of the proof of the upper bound (4.4.2)

4.4.4.1 The collective behavior of the multisurfers is not very random

Since the number of the multisurfers is small in comparison to the number of the rows/columns, as a first-order approximation we may treat the set of positions of k multisurfers at any fixed time as a collection of k independent copies of the position of a single surfer. We can expect therefore that the law of large numbers is applicable and, as $k \to \infty$, *the multisurfer empirical measure* (which is a random measure which encodes the scaled down u-coordinates of the multisurfers) converges in probability to the probability distribution of the position of the single surfer. In other words: *the collective behavior of the multisurfers is much less random than the behaviour of the single surfer*. This phenomenon is beneficial and will allow us to use the multisurfers as a moving frame of reference for tracing the position of the single surfer over time.

The above naive first-order approximation clearly cannot be true if $k = k(N)$ grows too fast with the size N of the square. Nevertheless, in Theorem 4.6.2 we will show that if

$k = k(N)$ grows at the right speed then a version of the law of large numbers indeed holds true. The proof of Theorem 4.6.2 is quite technically involved and the whole Section 4.6 is devoted to its proof.

4.4.4.2 The multisurfers provide information about the surfer

Let us fix some common initial configuration of the water for both the surfer and the multisurfers. In another first-order approximation let us assume for a moment that the density of the multisurfers is small enough that during the time interval $[t_1, t_2]$ all neighboring pairs of multisurfers are separated so that the multisurfers do not touch each other. If this is indeed the case and there are no interferences between the multisurfers then the time evolution of each multisurfer clearly coincides with the time evolution of the single surfer who would have the same initial position; by reversing the optics this means that we have a very direct information about some specific single surfer trajectories (namely, the ones which start from the positions of the multisurfers) in terms of the dynamics of the multisurfers, which we understand pretty well thanks to the aforementioned Theorem 4.6.2.

It is very convenient that *for a fixed initial configuration of the water, the trajectory of the single surfer depends in a monotonic way on the initial position of the surfer*. For this reason it is possible to get some partial information also about the single surfer trajectories starting from the points *between* the initial positions of two multisurfers. If the number $k = k(N)$ of the multisurfers tends to infinity as $N \to \infty$ such neighboring multisurfers should not be too far (in comparison to the size N of the square) which is enough to prove Theorem 4.4.1.

4.4.4.3 The single surfer and the multisurfer scenario on the same water configuration

Above we used the idea of considering the single surfer scenario *and* the multisurfer scenario on the same configuration of water. This idea sounds self-contradictory because each of these two scenarios gives rise to a *different* probability distribution on the set of configurations of the water. In Section 4.5 we shall explain how to overcome this difficulty and to (asymptotically) couple the surfer and the multisurfers on a single probability space. The resulting object can be visualized as water on which in two parallel universes there is (i) a single surfer, and (ii) k multisurfers. The single surfer and the multisurfers are like ghosts to one another and do not interact. Furthermore, *as long as the multisurfers do not touch each other, the relative position (with respect to the partial order $\prec$ on the plane) of the surfer and the ghosts of the multisurfers does not change over time: overtaking of the surfer by the multisurfers is not allowed*.

4.4.4.4 Overtaking is allowed in one direction only

The above discussion was based on a simplistic assumption that the multisurfers do not touch each other. Regretfully, in the real world this is not the case; multisurfers might influence each other and hence the multisurfer trajectories might differ from the single surfer trajectories on the same configuration of the water.

On the bright side, the assumption that the multisurfers are ordered as in the definition of the Pieri tableaux implies that the movement of each multisurfer depends only on (1) the configuration of the water, and (2) on these multisurfers which are to the north-west; the other multisurfers which are south-east have no influence on its dynamics. Furthermore, the impact of the multisurfers is unidirectional: the presence of the north-west multisurfer-neighbor can only push the multisurfer in the south-east direction. For the 'coupling' of the stories of the single surfer and the multisurfers on the common water this means that the ghosts of the multisurfers *are* allowed to overtake the surfer, but only in one direction. More precisely, the

number of the multisurfers which are north-west to the single surfer can only decrease over time (see Lemma 4.7.1 for the formal description of the above heuristics).

4.4.4.5 The order in which the proof of the upper bound (4.4.2) will be conducted

The rigorous proof of (4.4.2) will be conducted in the following order. First in Section 4.5 we will develop the content of Section 4.4.4.3. Then in Section 4.6 we will deal with the collective behavior of the multisurfers described in Section 4.4.4.1. In Section 4.7.1 we will work out the dynamics contained in Section 4.4.4.4. Finally, in the rest of Section 4.7 we will formally justify the heuristics from Section 4.4.4.2 and complete the proof.

4.5 Single surfer versus the multisurfer scenario

In Sections 4.4.1 and 4.4.3 we considered two random tableaux: T'_N and M'_N defined on two different probability spaces (which correspond to the single surfer and the multisurfer scenario respectively). In order to proceed with the ideas sketched in Section 4.4.4.3 we need to define some random tableaux $\mathbf{T}'_N$ and $\mathbf{M}'_N$ on a *common* probability space with (almost) the same distributions as T'_N and M'_N and such that the corresponding configurations of water coincide. A solution to this problem is provided by Proposition 4.5.1 below which is also the main result of the current section. We will compare the distributions with respect to *the total variation distance*.

Suppose that X and Y are random variables (possibly defined on different probability spaces) taking values in some finite set S with probability distributions $\mathbb{P}_X$ and $\mathbb{P}_Y$ respectively. We define the *total variation distance* between the random variables X and Y [Dur10, Section 3.6.1] (or, alternatively, between the probability distributions $\mathbb{P}_X$ and $\mathbb{P}_Y$) as

$$\delta(X,Y) = \delta(\mathbb{P}_X,\mathbb{P}_Y) := \frac{1}{2}\sum_{s\in S}\left|\mathbb{P}_X(s)-\mathbb{P}_Y(s)\right| = \max_{Z\subset S}\left|\mathbb{P}_X(Z)-\mathbb{P}_Y(Z)\right|. \tag{4.5.1}$$

Sometimes we will also denote this quantity by $\delta(X,\mathbb{P}_Y)$, etc.

Proposition 4.5.1. *For each $C \geqslant 1$ and $\Delta \in (0,1)$ there exists a constant $d > 0$ with the following property.*

Let λ be a C-balanced Young diagram and let k, w, a be positive integers such that $w < (1-\Delta)\,|\lambda|$ and $w \leqslant a \leqslant |\lambda| - k$.

Then there exists a pair of random tableaux $\mathbf{T}$ and $\mathbf{M}$ which are defined on the same probability space with the following properties:

(a) $\mathbf{T}$ *is a uniformly random element of $\mathcal{T}_\lambda$;*

(b) $\mathbf{M}$ *is a random element of $\widetilde{\mathcal{T}}_\lambda^{(a+1,a+k)}$;*

(c) the total variation distance between the distribution of $\mathbf{M}$ *and the uniform distribution on $\widetilde{\mathcal{T}}_\lambda^{(a+1,a+k)}$ fulfills the bound*

$$\delta\left(\mathbf{M},\mathbb{P}_{\widetilde{\mathcal{T}}_\lambda^{(a+1,a+k)}}\right) < d\frac{k^2}{\sqrt{|\lambda|-w}}; \tag{4.5.2}$$

(d) $\mathbf{T}\big|_{\leqslant w} = \mathbf{M}\big|_{\leqslant w}$ *holds true almost surely.*

The proof is postponed to Section 4.5.3. In the next two subsections we prepare to it by proving general lemmas on the probabilities of some particular events in the multisurfers

scenario (Section 4.5.1) and comparing the distributions of water beneath surfer(s) in both scenarios (Section 4.5.2). It turns out that these distributions are similar in terms of the total variation distance which asymptotically converges to 0, see Lemma 4.5.4.

4.5.1 Probability that a random tableau is Pieri

Lemma 4.5.2. *Let λ/μ be a skew Young diagram with n boxes and let $1 \leqslant k \leqslant n$. Then the cardinality of the set*

$$\widetilde{\mathcal{T}}_{\lambda/\mu}^{(w+1,w+k)} \qquad \text{for } w \in \{0,\dots,n-k\} \tag{4.5.3}$$

does not depend on the choice of w.

Proof. There is a simple bijection between the set $\widetilde{\mathcal{T}}_{\lambda/\mu}^{(w+1,w+k)}$ and the set of semistandard skew tableaux of shape λ/μ and of weight $(1^w, k, 1^{n-w-k})$ which is defined as follows. For a tableau $T \in \widetilde{\mathcal{T}}_{\lambda/\mu}^{(w+1,w+k)}$ we replace each entry from the set $\{w+1,\dots,w+k\}$ by the same number $w+1$, and we replace each entry $i \in \{w+k+1,\dots,n\}$ by $i+1-k$. It follows therefore that the cardinality of (4.5.3) is equal to the coefficient

$$\left[x_1 \cdots x_w x_{w+1}^k x_{w+2} \cdots x_{n+1-k}\right] s_{\lambda/\mu}$$

in the expansion of the skew Schur function in the basis of monomials. Since the skew Schur function is a symmetric polynomial, the proof is completed. □

Some notions defined for ordinary Young diagrams have their natural counterparts in the skew setup, given as follows. For $C \geqslant 1$ we say that a skew Young diagram λ/μ is *C-balanced* if λ/μ has at most $C\sqrt{|\lambda/\mu|}$ rows and at most $C\sqrt{|\lambda/\mu|}$ columns. Moreover we denote by $\mathbb{P}_{\lambda/\mu}$ the uniform measure on the set of standard Young tableaux of skew shape λ/μ.

We calculate now the probability of choosing a Pieri tableau from the set of standard Young tableaux of a specified skew shape.

Lemma 4.5.3. *For each $C \geqslant 1$ there exists a constant $c > 0$ with the following property. Let λ/μ be a C-balanced skew Young diagram with n boxes. Let k and w be integers such that $1 \leqslant k < \sqrt[4]{n}$ and $0 \leqslant w \leqslant n-k$. Then*

$$\left| k!\, \mathbb{P}_{\lambda/\mu}\left(\widetilde{\mathcal{T}}_{\lambda/\mu}^{(w+1,w+k)}\right) - 1 \right| < c\frac{k^2}{\sqrt{n}}. \tag{4.5.4}$$

Proof. Let T be a uniformly random standard tableau of skew shape λ/μ. It is easy to check that T is $(w+1, w+k)$-Pieri if and only if the rectified tableau $\operatorname{rect} T$ is $(w+1, w+k)$-Pieri (see Section 4.4.2 for the definition of Pieri tableaux). In the following we will describe the probability distribution of $\operatorname{rect} T$.

Recall that the plactic skew Schur polynomial $S_{\lambda/\mu}$ is the formal sum of the elements in the plactic monoid which correspond to all semistandard tableaux of shape λ/μ. The relations in the plactic monoid [Ful97, Section 2, Corollary 1] allow us to identify a skew tableau with its rectification and to express the skew plactic Schur polynomial as a linear combination of (non-skew) plactic Schur polynomials [Ful97, Section 5.1, Corollary 4]:

$$\frac{S_{\lambda/\mu}}{d_{\lambda/\mu}} = \sum_{\nu} \frac{c_{\mu\nu}^{\lambda} d_\nu}{d_{\lambda/\mu}} \cdot \frac{S_\nu}{d_\nu}, \tag{4.5.5}$$

where $c_{\mu\nu}^{\lambda}$ is the Littlewood–Richardson coefficient. If we restrict our attention only to the summands which correspond to (skew) *standard* tableaux, the left-hand side can be identified

with the probability distribution of rect T. The right-hand can be interpreted as a linear combination (over some Young diagrams ν) of the uniform measure on the set $\mathcal{T}_\nu$.

In this way we proved that a random tableau with the same distribution as rect T can be generated by the following two step procedure. Firstly, we select a random Young diagram ν with the probability distribution

$$\mathbb{P}(\nu) = \frac{c^\lambda_{\mu\nu} d_\nu}{d_{\lambda/\mu}}.$$

Secondly, we select a uniformly random standard tableau with the shape ν.

In particular, the probability that rect T is a $(w+1, w+k)$-Pieri tableau is a weighted arithmetic mean (over certain diagrams ν) of the probability that a uniformly random element of $\mathcal{T}_\nu$ is a $(w+1, w+k)$-Pieri tableau. It follows that it is enough to prove a version of the inequality (4.5.4) in which the skew diagram λ/μ is replaced by any diagram ν which contributes to (4.5.5); we will do it in the following.

We start with an observation that in the process of rectification the number of rows and the number of columns of a tableau cannot increase. Since λ/μ is C-balanced, it follows that any Young diagram ν which contributes to (4.5.5) is also C-balanced.

By Lemma 4.5.2 it is enough to consider the case $w = 0$. Let T be a uniformly random standard tableau of shape ν and let $\xi = \operatorname{sh} T|_{\leqslant k}$ be the positions of the first k boxes of T. The tableau T is $(1,k)$-Pieri if and only if $\xi = (k)$ is the one-row diagram. The remaining difficulty is therefore to identify the probability distribution of ξ.

The link between the combinatorics of standard Young tableaux and the irreducible representations of the symmetric groups (in particular, the branching rule) implies that the probability distribution of ξ coincides with the measure $\mathcal{P}_{V_\nu\downarrow_{\mathfrak{S}_k}}$ on the irreducible components of $V_\nu\downarrow_{\mathfrak{S}_k}$ which was defined in (4.3.1). Equation (4.3.1) gives therefore an exact formula

$$k!\,\mathbb{P}\left(T \in \widetilde{\mathcal{T}}_\nu^{(1,k)}\right) = k!\,\mathcal{P}_{V_\nu\downarrow_{\mathfrak{S}_k}}(\mathrm{triv}) = k!\left\langle \chi_\nu\downarrow_{\mathfrak{S}_k}, \chi_{\mathrm{triv}}\right\rangle = \sum_{\pi\in\mathfrak{S}_k} \chi_\nu(\pi)\,\overline{\chi_{\mathrm{triv}}(\pi)} = 1 + \sum_{\substack{\pi\in\mathfrak{S}_k\\ \pi\neq\mathrm{id}}} \chi_\nu(\pi). \quad (4.5.6)$$

In the following we will find an asymptotic bound for the second summand on the right-hand side.

By Fact 4.3.1 there exists a universal constant $a > 0$ (which depends only on C) such that for any $\pi \in \mathfrak{S}_k$

$$|\chi_\nu(\pi)| \leqslant \left(\frac{a}{\sqrt{n}}\right)^{|\pi|}. \quad (4.5.7)$$

It follows that the second summand on the right-hand side of (4.5.6) is bounded by

$$\left|\sum_{\substack{\pi\in\mathfrak{S}_k\\ \pi\neq\mathrm{id}}} \chi_\nu(\pi)\right| \leqslant \sum_{\pi\in\mathfrak{S}_k} \left(\frac{a}{\sqrt{n}}\right)^{|\pi|} - 1 \leqslant e^{\frac{ak^2}{\sqrt{n}}} - 1 = O\left(\frac{k^2}{\sqrt{n}}\right),$$

where we used Lemma 4.3.3 and the assumption that $\frac{k^2}{\sqrt{n}} = O(1)$. □

4.5.2 Comparison of distributions of water beneath surfer(s) in both scenarios

The following lemma shows that in the asymptotic setting the probability distributions of water beneath surfer(s) in the single surfer and the multisurfer scenarios are nearly equal.

Lemma 4.5.4. *For each $C \geqslant 1$ and $\Delta \in (0,1)$ there exists a constant $d > 0$ with the following property.*

Let λ be a C-balanced Young diagram and k, w and a be positive integers such that $w < (1-\Delta)\,|\lambda|$ and $w \leqslant a \leqslant |\lambda| - k$. Denote by T a uniformly random element of $\mathcal{T}_\lambda$ and by M a uniformly random element of $\widetilde{\mathcal{T}}_\lambda^{(a+1,a+k)}$. The total variation distance between the distributions of the restricted tableaux $T|_{\leqslant w}$ and $M|_{\leqslant w}$ fulfills the bound

$$\delta\left(T|_{\leqslant w}, M|_{\leqslant w}\right) < d\frac{k^2}{\sqrt{|\lambda| - w}}. \tag{4.5.8}$$

Proof. We start with an observation that the total variation distance is trivially bounded from above by 1. It follows that (provided $d \geqslant 1$) it is enough to consider the case when $k^4 \leqslant |\lambda| - w$.

Notice that the probability distribution $\mathbb{P}_{\widetilde{\mathcal{T}}_\lambda^{(a+1,a+k)}}(\cdot)$ coincides with the conditional probability $\mathbb{P}_{\mathcal{T}_\lambda}\left(\cdot \,\middle|\, \widetilde{\mathcal{T}}_\lambda^{(a+1,a+k)}\right)$. Therefore, for any $\mu \in \mathbb{Y}_w$ such that $\mu \subseteq \lambda$ and any $S \in \mathcal{T}_\mu$ we have, by the Bayes rule, that

$$\mathbb{P}_{\widetilde{\mathcal{T}}_\lambda^{(a+1,a+k)}}\left(M|_{\leqslant w} = S\right) = \frac{\mathbb{P}_{\mathcal{T}_\lambda}\left(M \in \widetilde{\mathcal{T}}_\lambda^{(a+1,a+k)} \;\middle|\; M|_{\leqslant w} = S\right)}{\mathbb{P}_{\mathcal{T}_\lambda}\left(\widetilde{\mathcal{T}}_\lambda^{(a+1,a+k)}\right)} \cdot \mathbb{P}_{\mathcal{T}_\lambda}\left(M|_{\leqslant w} = S\right).$$

By elementary algebra this equality can be rewritten as

$$\begin{aligned}
&\mathbb{P}_{\widetilde{\mathcal{T}}_\lambda^{(a+1,a+k)}}\left(M|_{\leqslant w} = S\right) - \mathbb{P}_{\mathcal{T}_\lambda}\left(M|_{\leqslant w} = S\right) = \\
&= \mathbb{P}_{\widetilde{\mathcal{T}}_\lambda^{(a+1,a+k)}}\left(M|_{\leqslant w} = S\right)\left[1 - k!\,\mathbb{P}_{\mathcal{T}_\lambda}\left(\widetilde{\mathcal{T}}_\lambda^{(a+1,a+k)}\right)\right] + \\
&\qquad + \mathbb{P}_{\mathcal{T}_\lambda}\left(M|_{\leqslant w} = S\right)\left[k!\,\mathbb{P}_{\mathcal{T}_\lambda}\left(M \in \widetilde{\mathcal{T}}_\lambda^{(a+1,a+k)} \;\middle|\; M|_{\leqslant w} = S\right) - 1\right].
\end{aligned} \tag{4.5.9}$$

Our strategy is to find an upper bound for the absolute value of the right-hand side.

The conditional probability in the second summand on the right-hand side, i.e.,

$$\mathbb{P}_{\mathcal{T}_\lambda}\left(M \in \widetilde{\mathcal{T}}_\lambda^{(a+1,a+k)} \;\middle|\; M|_{\leqslant w} = S\right), \tag{4.5.10}$$

is equal to the conditional probability that the restricted tableau $M|_{>w}$ is an $(a+1, a+k)$-Pieri tableau. In order to calculate this conditional probability we notice that the conditional probability distribution of the restricted tableau $M|_{>w}$ (under the condition $M|_{\leqslant w} = S$) is the uniform measure on the set of tableaux of shape λ/μ such that their entries form the multiset $(w+1, \ldots, n)$. In other words, the probability distribution of the random tableau $\left(M|_{>w}\right) - w$ (which is obtained by decreasing each entry of $M|_{>w}$ by w) is given by $\mathbb{P}_{\mathcal{T}_{\lambda/\mu}}$. In this way we proved that (4.5.10) is equal to

$$\mathbb{P}_{\mathcal{T}_{\lambda/\mu}}\left(\widetilde{\mathcal{T}}_{\lambda/\mu}^{(a+1-w,a+k-w)}\right). \tag{4.5.11}$$

By comparing the number of rows and columns, as well as the number of boxes of the skew diagram λ/μ with their counterparts for λ it follows that λ/μ is C'-balanced with

$$C' = C\sqrt{\frac{|\lambda|}{|\lambda| - w}} < \frac{C}{\sqrt{\Delta}}.$$

A fortiori λ and λ/μ are C''-balanced, where C'' is the right-hand side of the above inequality.

We apply Lemma 4.5.3 twice: for both expressions in the square brackets on the right-hand side of (4.5.9). It follows that there exists a universal constant $c > 0$ (which depends only on C'') such that

$$\left|\mathbb{P}_{\widetilde{\mathcal{T}}_\lambda^{(a+1,a+k)}}\left(M|_{\leqslant w} = S\right) - \mathbb{P}_{\mathcal{T}_\lambda}\left(M|_{\leqslant w} = S\right)\right| \leqslant$$
$$\leqslant \mathbb{P}_{\widetilde{\mathcal{T}}_\lambda^{(a+1,a+k)}}\left(M|_{\leqslant w} = S\right)\frac{ck^2}{\sqrt{|\lambda|}} + \mathbb{P}_{\mathcal{T}_\lambda}\left(M|_{\leqslant w} = S\right)\frac{ck^2}{\sqrt{|\lambda| - w}}.$$

By summing over all choices of S we get (4.5.8) for $d := \max(1, 2c)$, as required. □

4.5.3 Proof of Proposition 4.5.1

Proof of Proposition 4.5.1. We will sample the random tableaux $\mathbf{T}$ and $\mathbf{M}$ by the following two-step procedure. Firstly, we sample $\mathbf{T}$ with the uniform probability measure on $\mathcal{T}_\lambda$, that is $\mathbb{P}(\mathbf{T} = T) := \mathbb{P}_{\mathcal{T}_\lambda}(T)$ for any $T \in \mathcal{T}_\lambda$. After the tableau $\mathbf{T}$ was selected, we sample the tableau $\mathbf{M}$ with the conditional probability

$$\mathbb{P}\left(\cdot \mid \mathbf{T} = T\right) := \mathbb{P}_{\widetilde{\mathcal{T}}_\lambda^{(a+1,a+k)}}\left(\cdot \mid \left\{M \in \widetilde{\mathcal{T}}_\lambda^{(a+1,a+k)} : M|_{\leqslant w} = \mathbf{T}|_{\leqslant w}\right\}\right).$$

In this way the condition (d) is fulfilled trivially.

Therefore the probability distribution of $\mathbf{M}$ is given by

$$\mathbb{P}\left(\mathbf{M} = M\right) = \mathbb{P}_{\mathcal{T}_\lambda}\left\{T \in \mathcal{T}_\lambda : T|_{\leqslant w} = M|_{\leqslant w}\right\} \times$$
$$\mathbb{P}_{\widetilde{\mathcal{T}}_\lambda^{(a+1,a+k)}}\left(M \mid \left\{T \in \widetilde{\mathcal{T}}_\lambda^{(a+1,a+k)} : T|_{\leqslant w} = M|_{\leqslant w}\right\}\right). \quad (4.5.12)$$

The probability measure $\mathbb{P}_{\widetilde{\mathcal{T}}_\lambda^{(a+1,a+k)}}$ can be written in an analogous way as

$$\mathbb{P}_{\widetilde{\mathcal{T}}_\lambda^{(a+1,a+k)}}\left(M\right) = \mathbb{P}_{\widetilde{\mathcal{T}}_\lambda^{(a+1,a+k)}}\left\{T \in \widetilde{\mathcal{T}}_\lambda^{(a+1,a+k)} : T|_{\leqslant w} = M|_{\leqslant w}\right\} \times$$
$$\mathbb{P}_{\widetilde{\mathcal{T}}_\lambda^{(a+1,a+k)}}\left(M \mid \left\{T \in \widetilde{\mathcal{T}}_\lambda^{(a+1,a+k)} : T|_{\leqslant w} = M|_{\leqslant w}\right\}\right). \quad (4.5.13)$$

It follows that the process of sampling $\mathbf{M}$ as well as the process of sampling the uniformly random element of $\widetilde{\mathcal{T}}_\lambda^{(a+1,a+k)}$ can be viewed as a two-step procedure: we first sample the positions of the boxes $1, \ldots, w$ and in the second step the remaining boxes. Notice that in both sampling procedures in the second step we sample the remaining boxes with the same conditional distribution. It follows that the total variation distance between the measures (4.5.12) and (4.5.13) is bounded from above by the total variation distance (4.5.8) from Lemma 4.5.4 which completes the proof. □

4.6 The distribution of the u-coordinates of the multisurfers

Our main result in this section is Theorem 4.6.2 which shows that the multisurfer empirical measure (i.e., the distribution of the u-coordinates of the multisurfers) after draining a $(1-\alpha)$-fraction of the water converges to the limit measure ν_α (the limit distribution of the u-coordinate of the single surfer on the level curve g_α, cf. Section 4.2.3). Also Proposition 4.6.5 might be interesting from the viewpoint of algebraic combinatorics as it provides a direct

link between the statistical properties of uniformly random (a,b)-Pieri tableaux of some fixed shape and the celebrated Jucys–Murphy elements.

The following assumption on the 'amount of water' and the number of multisurfers will be central in the forthcoming results (Theorem 4.6.2 and Propositions 4.7.2 and 4.6.3).

Assumption 4.6.1. *Let $c > 0$ be the constant in Lemma 4.5.3 obtained for $C = 1$ for which (4.5.4) holds. We assume that $k = k(N)$ and $w = w(N)$ are sequences of positive integers which fulfill*

$$\lim_{N\to\infty} k(N) = \infty \quad \text{and} \quad k < \sqrt{\frac{N}{2c}} \quad \text{and} \quad w + k < N^2.$$

4.6.1 Counting multisurfers gives the longitude

Let $w = w(N)$ and $k = k(N)$ be sequences of nonnegative integers such that $0 < w + k < N^2$. Let M_N be a uniformly random tableau from $\widetilde{\mathcal{T}}_{\square_N}^{(w+1,w+k)}$. We use a shorthand notation $u_n := u_n^{M_N}$ for the u-coordinate of the box with the number n in the tableau M_N. For $u \in \mathbb{R}$ we define the random variable $G_N(u)$ to be the fraction of the multisurfers which have their scaled u-coordinate smaller than u, that is

$$G_N(u) := \frac{1}{k} \max\left\{ p \in \{1,\dots,k\} : \frac{1}{N} u_{w+p} \leqslant u \right\}. \tag{4.6.1}$$

Clearly, G_N is the cumulative distribution function of the random measure m_N on $\mathbb{R}$

$$m_N := \frac{1}{k} \sum_{1\leqslant p\leqslant k} \delta_{N^{-1}u_{w+p}}$$

where δ_x denotes the *delta measure concentrated at x*.

Theorem 4.6.2. *Let $\alpha \in (0,1)$. Let $w = w(N)$ and $k = k(N)$ fulfill Assumption 4.6.1 and*

$$\lim_{N\to\infty} \frac{w}{N^2} = \alpha.$$

Then for each $\varepsilon > 0$

$$\mathbb{P}_{\widetilde{\mathcal{T}}_{\square_N}^{(w+1,w+k)}}\left\{ M_N : \sup_{u\in\mathbb{R}} \left|F_{\nu_\alpha}(x) - G_N(x)\right| > \varepsilon \right\} = O\left(\frac{1}{k} + \frac{k^2}{N}\right)$$

with the constant in the O-notation depending only on α and ε.

In particular, if $k(N) \to \infty$ and $k(N) = o(\sqrt{N})$, i.e., (4.4.10) is satisfied, then the random sequence of cumulative distribution functions G_N with respect to the supremum norm converges in probability to the cumulative distribution function F_{ν_α} when $N \to \infty$, that is shortly,

$$\sup_{x\in\mathbb{R}} \left|F_{\nu_\alpha}(x) - G_N(x)\right| \xrightarrow{P} 0.$$

In order to prove this result we will compare the (random) moments of the empirical measure m_N and the moments of the measure ν_α which gives the asymptotics of the u-coordinate of a single box, cf. Section 4.2.3. In Proposition 4.6.3 below we shall calculate the moments of the empirical measure m_N. In Section 4.6.8 we will complete the proof of Theorem 4.6.2.

4.6.2 Moments of the empirical measure G_N

For each $\beta \in \mathbb{N}$ we define the *β-th moment of the random measure m_N* as

$$M_\beta := M_\beta(w,k) := \int_{\mathbb{R}} z^\beta \, \mathrm{d}m_N(z) = \frac{1}{k} N^{-\beta} \sum_{1 \leqslant p \leqslant k} u_{w+p}^\beta.$$

Notice that M_β is also a random variable. The following result expresses the first two moments of the random variable $M_\beta(w,k)$ (which is related to the problem of multisurfers) in terms of the first moment of the random variable $M_\beta(w,1)$ (which is related to the much simpler problem of a single surfer). This proposition is crucial to the proof of Theorem 4.6.2.

Proposition 4.6.3. *Let $w = w(N)$ and $k = k(N)$ fulfill Assumption 4.6.1. For each $\beta \in \mathbb{N}$, we have*

$$\mathbb{E}_{\widetilde{\mathbb{P}}_N} M_\beta(w,k) = \mathbb{E}_{\mathbb{P}_N} M_\beta(w,1) + O\left(\frac{k^2}{N}\right); \tag{4.6.2}$$

$$\mathrm{Var}_{\widetilde{\mathbb{P}}_N} M_\beta(w,k) = O\left(\frac{1}{k} + \frac{k^2}{N}\right) \tag{4.6.3}$$

with the constants in the O-notation depending only on β.

Remark 4.6.4. The counterpart of the above proposition in the paper of Romik and the second named author is [Rom15, Theorem 4.6]. There the error terms for the expected value and variance are much smaller, accordingly, $O\left(\frac{k}{N}\right)$ and $O\left(\frac{1}{k} + \frac{k}{N}\right)$. There are two reasons for which our error terms are much bigger, of the form, accordingly, $O\left(\frac{k^2}{N}\right)$ and $O\left(\frac{1}{k} + \frac{k^2}{N}\right)$.

- In the proof of Proposition 4.6.5 we will view the probability distribution of the multisurfers as a *conditional distribution* of the boxes with certain numbers in a uniformly random standard skew tableau with a specified shape *under the condition* that these boxes are suitably ordered (i.e., the tableau is Pieri). Unfortunately, the probability of the latter event depends heavily on the shape of the diagram and we do not have a very good control over the error term, see Lemma 4.5.3.

  Using our terminology in their context, the placement of the multisurfers by Romik and the second named author can also be seen as a conditional process: one first adds k boxes to a given Young diagram λ by k independent steps of the Plancherel growth process, and then *conditions* that these boxes are suitably ordered. In this case, however, the conditioning does not create additional difficulties because the probability of the event that the newly created boxes are Pieri is equal to $\frac{1}{k!}$ and does not depend on the shape of λ.

- The error $O\left(\frac{k^2}{N}\right)$ also appears during the application of Proposition 4.6.9. Romik and the second named author make use of [Rom15, Theorem 4.4] which is a counterpart of ours Proposition 4.6.5. They deal with the character of the left-regular representation which obviously is not troublesome and need not be estimated.

The proof of Proposition 4.6.3 is quite long. In Sections 4.6.3 to 4.6.5 we gather some tools helpful in proving Proposition 4.6.3. In particular, the goal of Section 4.6.3 is to provide a connection between the statistical properties of the multisurfers and the representation theory (see Proposition 4.6.5). Section 4.6.4 gives background for calculating the character $\chi_{\square_N}$ of the cosets appearing in (4.6.4). Section 4.6.5 is devoted mostly to an analysis of the permutations arising from the powers of Jucys–Murphy elements. Eventually, in Section 4.6.6

we give the proof of (4.6.2) and in Section 4.6.7 the proof of (4.6.3) which completes the proof of Proposition 4.6.3.

4.6.3 Multisurfers and the representation theory

The following result, Proposition 4.6.5, provides a link between the statistical properties of the multisurfers and the representation theory of the symmetric groups.

Let w, k, n be positive integers such that $w + k \leqslant n$. With a small abuse of notation we denote by $\mathfrak{S}_w$ the group of permutations of the set $\{1, \dots, w\}$ and by $\mathfrak{S}_k$ the group of permutations of the set $\{w+1, \dots, w+k\}$. In this way $\mathfrak{S}_w$ and $\mathfrak{S}_k$ are commuting subgroups of $\mathfrak{S}_w + k \subset \mathfrak{S}_n$. We define the element of the symmetric group algebra

$$p_{\mathfrak{S}_k} = \frac{1}{k!} \sum_{\sigma \in \mathfrak{S}_k} \sigma \in \mathbb{C}\mathfrak{S}_n.$$

Recall from Section 4.3.4 that the Jucys–Murphy elements $J_1, \dots, J_n$ form a commuting family in the symmetric group algebra $\mathbb{C}\mathfrak{S}_n$ and are given by

$$J_k := \sum_{1 \leqslant i < k} (i, k) = (1, k) + \dots + (k-1, k) \in \mathbb{C}\mathfrak{S}_n \quad \text{for } 1 \leqslant k \leqslant n.$$

Proposition 4.6.5. *Let w, k, n be positive integers such that $w + k \leqslant n$. Let $W(x_1, \dots, x_k)$ be a symmetric polynomial in k variables. Let $\lambda \in \mathbb{Y}_n$ be a Young diagram and T be a random element (sampled with the uniform distribution) of the set $\widetilde{\mathcal{T}}_\lambda^{(w+1, w+k)}$ of $(w+1, w+k)$-Pieri tableaux of shape λ. Then*

$$\begin{aligned} \mathbb{E}\, W\left(u_{w+1}^T, \dots, u_{w+k}^T\right) &= \frac{\chi_\lambda\left(W(J_{w+1}, \dots, J_{w+k}) \cdot p_{\mathfrak{S}_k}\right)}{\chi_\lambda\left(p_{\mathfrak{S}_k}\right)} \\ &= \frac{\chi_\lambda\left(W(J_{w+1}, \dots, J_{w+k}) \cdot p_{\mathfrak{S}_k}\right)}{\mathbb{P}_{\mathcal{T}_\lambda}\left(\widetilde{\mathcal{T}}_\lambda^{(w+1, w+k)}\right)}. \end{aligned} \tag{4.6.4}$$

The proof is postponed until the end of the current section until we gather the necessary tools.

We start with the following fundamental property of Jucys–Murphy elements.

Fact 4.6.6 ([Juc74])**.** *Let $\lambda \in \mathbb{Y}_n$ be a Young diagram, and let $u_1, \dots, u_n$ be the u-coordinates of its boxes (listed in an arbitrary order). Let $W(x_1, \dots, x_n)$ be a symmetric polynomial in n variables. Then:*

- *$W(J_1, \dots, J_n) \in \mathbb{C}\mathfrak{S}_n$ belongs to the center of the group algebra.*
- *The operator $\rho_\lambda\big(W(J_1, \dots, J_n)\big)$ is a multiple of the identity operator, so it can be identified with a complex number. The value of this number is equal to*

$$\chi_\lambda\Big(W(J_1, \dots, J_n)\Big) = W(u_1, \dots, u_n). \tag{4.6.5}$$

Lemma 4.6.7. *Let $\mu \in \mathbb{Y}_{w+k}$ be a Young diagram and let $W(x_1, \dots, x_k)$ be a symmetric polynomial in k variables. Then the operator*

$$\rho_\mu\big(W(J_{w+1}, \dots, J_{w+k})\big)$$

acts on each irreducible component V_ν of the restriction $V_\mu \downarrow_{\mathfrak{S}_w}^{\mathfrak{S}_{w+k}}$ as a multiple of the identity operator and can be identified with the complex number

$$W\left(u_{w+1}^{\mu/\nu}, \ldots, u_{w+k}^{\mu/\nu}\right). \tag{4.6.6}$$

Above, for a diagram ν with w boxes such that $\nu \subset \mu$ we denote by $u_{w+1}^{\mu/\nu}, \ldots, u_{w+k}^{\mu/\nu}$ the u-coordinates of the boxes of the skew diagram μ/ν (listed in an arbitrary order).

Proof. We will show that the lemma holds in the particular case when W is the *power-sum symmetric function*, that is

$$W(x_1, \ldots, x_k) := p_\beta(x_1, \ldots, x_k) := \sum_{1 \leqslant i \leqslant k} x_i^\beta$$

for some $\beta \in \mathbb{N}_0$. Since the power-sum symmetric functions generate the algebra of the symmetric polynomials and the representation ρ_μ is an algebra homomorphism, in this way we will prove that the lemma holds true in general.

Clearly,

$$\begin{aligned} W\left(J_{w+1}, \ldots, J_{w+k}\right) &= p_\beta\left(J_{w+1}, \ldots, J_{w+k}\right) = \\ &= p_\beta\left(J_1, \ldots, J_{w+k}\right) - p_\beta\left(J_1, \ldots, J_w\right). \end{aligned}$$

By Fact 4.6.6, the operator $p_\beta\left(J_1, \ldots, J_{w+k}\right)$ acts on the component V_μ as multiplication by the factor

$$p_\beta\left(u_1^\mu, \ldots, u_{w+k}^\mu\right) = \sum_{1 \leqslant i \leqslant w+k} \left(u_i^\mu\right)^\beta. \tag{4.6.7}$$

Again by Fact 4.6.6, for any $\nu \in \mathbb{Y}_w$, the operator $p_\beta\left(J_1, \ldots, J_w\right)$ acts on the component V_ν as multiplication by the factor

$$p_\beta\left(u_1^\nu, \ldots, u_w^\nu\right) = \sum_{1 \leqslant i \leqslant w} \left(u_i^\nu\right)^\beta. \tag{4.6.8}$$

Let $\nu \subset \mu$. The multiset of the u-coordinates of the boxes of μ is the union of (i) the multiset of the u-coordinates of the boxes of ν, and (ii) the multiset of the u-coordinates of the boxes of μ/ν. Therefore, by subtracting (4.6.8) from (4.6.7), we get that the operator $p_\beta\left(J_{w+1}, \ldots, J_{w+k}\right)$ acts on the component V_ν of the restriction $V_\mu \downarrow_{\mathfrak{S}_w}^{\mathfrak{S}_{w+k}}$ as multiplication by the scalar

$$p_\beta\left(u_{w+1}^{\mu/\nu}, \ldots, u_{w+k}^{\mu/\nu}\right) = \sum_{1 \leqslant i \leqslant k} \left(u_{w+i}^{\mu/\mu}\right)^\beta,$$

as required. □

Proof of Proposition 4.6.5. Observe that any tableau $T \in \widetilde{\mathcal{T}}_\lambda^{(w+1, w+k)}$ can be split into the following three parts: (i) a standard tableau P with entries from $\{1, \ldots, w\}$; we denote its shape by ν, (ii) a skew tableau Q which is k-Pieri with entries in $\{w+1, \ldots, w+k\}$; we denote its shape by μ/ν, and (iii) a skew tableau R with the entries $> w+k$ with shape λ/μ.

For fixed partitions μ and ν it is easy to count the number of tableaux P which contribute to (i) and the number of tableaux R which contribute to (iii): their cardinalities are by definition given by d_ν and $d_{\lambda/\mu}$ respectively. The number of k-Pieri tableaux Q which contribute to (ii) is slightly more challenging: it is equal to 1 if μ/ν has at most one box in each column and is equal to zero otherwise. A combinatorial interpretation of the Littlewood–Richardson coefficient $c_{\nu,(k)}^\mu$ for a single-row partition (k) (or, nomen omen, the Pieri rule) implies that

this coefficient coincides with the latter cardinality.

In this way we proved that the left-hand side of (4.6.4) is given by

$$\begin{aligned}\mathbb{E}\, W\Big(u^T_{w+1},\, \dots,\, u^T_{w+k}\Big) = \\ \frac{1}{\left|\widetilde{\mathcal{T}}^{(w+1,w+k)}_\lambda\right|} \sum_{T\in\widetilde{\mathcal{T}}^{(w+1,w+k)}_\lambda} W\Big(u^T_{w+1},\, \dots,\, u^T_{w+k}\Big) = \\ \frac{1}{\left|\widetilde{\mathcal{T}}^{(w+1,w+k)}_\lambda\right|} \sum_{\substack{\mu\in\mathbb{Y}_{w+k}\\ \mu\subset\lambda}} \sum_{\substack{\nu\in\mathbb{Y}_w\\ \nu\subset\mu}} d_{\lambda/\mu}\, d_\nu\, c^\mu_{\nu,(k)}\, W\Big(u^{\mu/\nu}_{w+1},\dots,u^{\mu/\nu}_{w+k}\Big). \quad (4.6.9)\end{aligned}$$

We will now investigate the numerator on the right hand side of (4.6.4). Each multiplicity $d_{\lambda/\mu}$ in the decomposition of the restriction of V_λ into irreducible components

$$V_\lambda\downarrow^{\mathfrak{S}^2_N}_{\mathfrak{S}_w+k} = \bigoplus_{\substack{\mu\in\mathbb{Y}_w\\ \mu\subset\lambda}} d_{\lambda/\mu} V_\mu$$

is equal to the number of skew standard Young tableaux of shape λ/μ. Since $W\big(J_{w+1},\, \dots,\, J_{w+k}\big)\cdot p_{\mathfrak{S}_k} \in \mathbb{C}\mathfrak{S}_w + k$, we get that

$$\begin{aligned}C_\lambda := \chi_\lambda\Big(W\left(J_{w+1},\, \dots,\, J_{w+k}\right)\cdot p_{\mathfrak{S}_k}\Big) = \\ = \frac{1}{\dim V_\lambda}\operatorname{Tr}_{V_\lambda}\rho_\lambda\Big(W\left(J_{w+1},\dots,J_{w+k}\right)\cdot p_{\mathfrak{S}_k}\Big) = \\ = \frac{1}{d_\lambda}\sum_{\substack{\mu\in\mathbb{Y}_{w+k}\\ \mu\subset\lambda}} d_{\lambda/\mu}\operatorname{Tr}_{V_\mu}\rho_\lambda\Big(W\left(J_{w+1},\dots,J_{w+k}\right)\cdot p_{\mathfrak{S}_k}\Big). \quad (4.6.10)\end{aligned}$$

The multiplicities in the decomposition of the restricted representation into irreducible components

$$V_\mu\downarrow^{\mathfrak{S}_w+k}_{\mathfrak{S}_w\times\mathfrak{S}_k} = \bigoplus_{\substack{\nu\in\mathbb{Y}_w\\ \xi\in\mathbb{Y}_k}} c^\mu_{\nu,\xi} V_\nu\otimes V_\xi$$

are given by Littlewood–Richardson coefficients. Therefore, since $p_{\mathfrak{S}_k}$ is a projection to the trivial representation, its image is given by

$$p_{\mathfrak{S}_k}\Big(V_\mu\Big) = p_{\mathfrak{S}_k}\Big(V_\mu\downarrow^{\mathfrak{S}_w+k}_{\mathfrak{S}_w\times\mathfrak{S}_k}\Big) = \bigoplus_{\nu\in\mathbb{Y}_w} c^\mu_{\nu,(k)} V_\nu\otimes V_{(k)} = \bigoplus_{\nu\in\mathbb{Y}_w} c^\mu_{\nu,(k)} V_\nu. \quad (4.6.11)$$

By combining (4.6.10), (4.6.11), and Lemma 4.6.7 we get the following closed formula for the numerator on the right-hand side of (4.6.4)

$$C_\lambda = \frac{1}{d_\lambda}\sum_{\substack{\mu\in\mathbb{Y}_{w+k}\\ \mu\subset\lambda}}\sum_{\nu\in\mathbb{Y}_w} d_{\lambda/\mu}\, c^\mu_{\nu,(k)}\, d_\nu\, W\Big(u^{\mu/\nu}_{w+1},\dots,u^{\mu/\nu}_{w+k}\Big). \quad (4.6.12)$$

On the other hand, by (4.6.12) evaluated for the constant polynomial $W\equiv 1$, we get the

following formula for the denominator on the right-hand side of (4.6.4)

$$\chi_\lambda\left(p_{\mathfrak{S}_k}\right) = \frac{1}{d_\lambda} \sum_{\substack{\mu\in\mathbb{Y}_{w+k}\\ \mu\subset\lambda}} \sum_{\nu\in\mathbb{Y}_w} d_{\lambda/\mu} c^{\mu}_{\nu,(k)} d_\nu = \frac{1}{d_\lambda}\cdot\left|\widetilde{\mathcal{T}}_\lambda^{(w+1,w+k)}\right| \tag{4.6.13}$$

where the last equality comes from (4.6.9) evaluated for $W \equiv 1$. Observe also that

$$\mathbb{P}_{\mathcal{T}_\lambda}\left(\widetilde{\mathcal{T}}_\lambda^{(w+1,w+k)}\right) = \frac{d_\lambda}{\left|\widetilde{\mathcal{T}}_\lambda^{(w+1,w+k)}\right|}. \tag{4.6.14}$$

Equations (4.6.9), (4.6.12), (4.6.13) and (4.6.14) complete the proof of (4.6.4). □

4.6.4 Character on a coset

Let us call *small* the elements of the set $\{1,\dots,w\}$ and *big* the elements of the set $\{w+1,\dots,w+k\}$. As before, we view the symmetric group $\mathfrak{S}_k$ as the subgroup of $\mathfrak{S}_w + k$ which consists of the permutations which can permute only the big elements.

For a Young diagram $\lambda \in \mathbb{Y}_n$ and a permutation $\pi \in \mathfrak{S}_w + k$ we define *the value of the character χ_λ on a left coset $\pi\mathfrak{S}_k \in \mathfrak{S}_w + k/\mathfrak{S}_k$* as an appropriate sum over the coset, that is

$$\chi_\lambda(\pi\mathfrak{S}_k) := \sum_{\sigma\in\pi\mathfrak{S}_k} \chi_\lambda(\sigma).$$

This definition is motivated by Proposition 4.6.5 because expressions of a similar flavor (up to the factor $\frac{1}{k!}$) appear on the right-hand side of (4.6.4). Our goal in this section is to understand the asymptotics of such characters on cosets.

For a left coset $\pi\mathfrak{S}_k \in \mathfrak{S}_w + k/\mathfrak{S}_k$ we define its *length* as

$$\|\pi\mathfrak{S}_k\| := w - \#(\text{cycles of } \pi \text{ which consist of only small elements}). \tag{4.6.15}$$

It is easy to check that if $\pi_1\mathfrak{S}_k = \pi_2\mathfrak{S}_k$ then the cycles of π_1 which consist of only small elements coincide with the analogous cycles of π_2; it follows that the above definition does not depend on the choice of the representative π of the coset.

Remind that for a permutation π we denote by $|\pi|$ *the length of* π, i.e., the minimal number of transpositions required to write π as their product.

Lemma 4.6.8. *For each left coset $\pi\mathfrak{S}_k$*

$$\|\pi\mathfrak{S}_k\| = \min\left\{|\sigma| : \sigma \in \pi\mathfrak{S}_k\right\}. \tag{4.6.16}$$

There exists a unique *permutation $\pi_0 \in \pi\mathfrak{S}_k$ for which the minimum on the right-hand side is achieved; the permutation $\pi_0 = \pi_0(\pi\mathfrak{S}_k)$ with this property will be called* minimal *for the coset $\pi\mathfrak{S}_k$.*

This minimal permutation has the following additional properties:

(a) for each $\sigma \in \mathfrak{S}_k$,

$$|\pi_0\sigma| = \|\pi\mathfrak{S}_k\| + |\sigma|. \tag{4.6.17}$$

(b) If π is such that each of its cycles permutes at most one big element, then $\pi = \pi_0$ is the minimal element.

Proof. We begin with the proof of the first assertion of the lemma. The permutation π can be written as a product of disjoint cycles $\pi = \pi_1\cdots\pi_\ell\pi_{\ell+1}\cdots\pi_L$, where $\pi_1,\dots,\pi_\ell$ are

the cycles which permute at least one big element, and $\pi_{\ell+1}, \dots, \pi_L$ permute only small elements.

Fix $i \in \{1, \dots, \ell\}$. Then π_i is a cycle of the form

$$\pi_i = \big(p_{1,1}, \dots, p_{1,r_1}, q_1, \quad p_{2,1}, \dots, p_{2,r_2}, q_2, \quad \dots, \quad p_{n,1}, \dots, p_{n,r_n}, q_n\big)\,,$$

for some $n \in \mathbb{N}$ and $r_1, \dots, r_n \in \mathbb{N}_0$, some big numbers $q_1, \dots, q_n$ and some small numbers $p_{r,s}$. Define

$$\tau_i := \big(q_n, q_{n-1}, \dots, q_1\big) \in \mathfrak{S}_k$$

as the cycle permuting (in the reverse direction) the big elements of the cycle π_i. Clearly,

$$\pi_i \tau_i = \big(p_{1,1}, \dots, p_{1,r_1}, q_1\big) \cdots \big(p_{n,1}, \dots, p_{n,r_n}, q_n\big)$$

gives a product of disjoint cycles, each permuting exactly one big element.

Then

$$\pi_0 := (\pi_1 \tau_1) \cdots (\pi_\ell \tau_\ell)\, \pi_{\ell+1} \cdots \pi_L \in \pi \mathfrak{S}_k \tag{4.6.18}$$

provides a decomposition into disjoint cycles which has the property that each cycle permutes at most one big element. Hence for any $\sigma \in \mathfrak{S}_k$ which permutes only big elements, the decomposition into disjoint cycles of the product $\pi_0 \sigma \in \pi \mathfrak{S}_k$ is obtained by merging appropriate cycles of π_0, it follows therefore that

$$|\pi_0 \sigma| = |\pi_0| + |\sigma|\,. \tag{4.6.19}$$

As a consequence, the minimum on the right-hand side of (4.6.16) is achieved on π_0 and it is the unique permutation with this property, as required.

We shall now show that the equality (4.6.16) holds true. It is enough to prove it in the special case when as the coset representative we take π_0 given by (4.6.18). In this special case (4.6.16) is equivalent to

$$\|\pi_0 \mathfrak{S}_k\| = |\pi_0|\,. \tag{4.6.20}$$

The explicit decomposition into disjoint cycles (4.6.18) implies that the left-hand side is equal to

$$w - (L - \ell).$$

On the other hand, (4.6.18) implies that π_0 has exactly $L - \ell$ cycles which permute only small elements and k additional cycles, one for each big element. It follows that the right-hand side of (4.6.20) is equal to

$$|\pi_0| = (w + k) - \big(L - \ell + k\big) = w - (L - \ell)$$

which concludes the proof of (4.6.16).

Property (a) is now a direct consequence of (4.6.19) and (4.6.20).

For the proof of property (b), if π is such that each of its cycles permutes at most one big element then our construction gives $\pi = \pi_0$ so π is the minimal representative of the coset. □

The next proposition gives an insight to the irreducible characters corresponding to square diagrams evaluated on left cosets.

Proposition 4.6.9. *For each positive integer L there exists a constant C_L with the following property.*

Let positive integers w and k be arbitrary and let $\pi_0 \in \pi\mathfrak{S}_k$ be the minimal representative of a left coset $\pi\mathfrak{S}_k \in \mathfrak{S}_w + k/\mathfrak{S}_k$. If $\|\pi\mathfrak{S}_k\| \leqslant L$ and $N^2 \geqslant w + k$ and $N > k^2$ then

$$\left|\chi_{\square_N}(\pi\mathfrak{S}_k) - \chi_{\square_N}(\pi_0)\right| < \frac{C_L k^2}{N^{\|\pi\mathfrak{S}_k\|+1}}, \tag{4.6.21}$$

$$\left|\chi_{\square_N}(\pi\mathfrak{S}_k)\right| < \frac{2C_L}{N^{\|\pi\mathfrak{S}_k\|}}. \tag{4.6.22}$$

Proof. Let $d = d(L) \geqslant 1$ be a constant (which depends only on L) big enough so that it guarantees that

$$L + k \leqslant dN.$$

By Fact 4.3.1, Lemma 4.6.8(a) and Lemma 4.3.3 we have

$$\left|\chi_{\square_N}(\pi\mathfrak{S}_k) - \chi_{\square_N}(\pi_0)\right| \leqslant \sum_{\substack{\sigma\in\mathfrak{S}_k\\ \sigma\neq\mathrm{id}}} \left|\chi_{\square_N}(\pi_0\sigma)\right| \leqslant \sum_{\substack{\sigma\in\mathfrak{S}_k\\ \sigma\neq\mathrm{id}}} \left(\frac{ad}{N}\right)^{|\pi_0\sigma|} \leqslant$$

$$\left(\frac{ad}{N}\right)^{\|\pi\mathfrak{S}_k\|}\left[\exp\left(\frac{adk^2}{2N}\right) - 1\right] = \frac{(ad)^{\|\pi\mathfrak{S}_k\|+1}}{2}\frac{k^2}{N^{\|\pi\mathfrak{S}_k\|+1}}\frac{\exp\left(\frac{adk^2}{2N}\right)-1}{\frac{adk^2}{2N}}.$$

Since $\frac{e^x-1}{x}$ is a bounded function on the interval $\left(0, \frac{ad}{2}\right]$, we get (4.6.21) as required.

By (4.6.21) and Fact 4.3.1 we get

$$\left|\chi_{\square_N}(\pi\mathfrak{S}_k)\right| < \frac{C_L k^2}{N^{\|\pi\mathfrak{S}_k\|+1}} + \left(\frac{ad}{N}\right)^{|\pi_0|} = \frac{1}{N^{\|\pi\mathfrak{S}_k\|}}\left(C_L\frac{k^2}{N} + (ad)^{\|\pi\mathfrak{S}_k\|}\right).$$

It follows that we can increase the value of the constant C_L in such a way that both (4.6.21) and (4.6.22) are fulfilled. □

4.6.5 Products of Jucys–Murphy elements

4.6.5.1 Set partitions

For calculations of the moments (4.6.2) and (4.6.3) we will need to better understand the sum of products $\sum_{p=1}^{k} J_{w+p}^{\beta}$. We will use similar concepts and notions to the ones from [Rom15, Section 4.9]. Notice that

$$J_{w+p}^{\beta} = \sum_{1\leqslant j_1,\ldots,j_\beta\leqslant w+p-1} (j_1, w+p)\cdots(j_\beta, w+p). \tag{4.6.23}$$

We denote the summands contributing to the right-hand side of (4.6.23) in the following way. For any p and a sequence $j = (j_1, \ldots, j_\beta) \in [w+p-1]^\beta$ define

$$\sigma_{p,j} := (j_1, w+p)\cdots(j_\beta, w+p). \tag{4.6.24}$$

We also denote

$$Z_\Sigma(j) := \{r \in \{1,\ldots,\beta\} : j_r \leqslant w\};$$
$$Z_\Pi(j) := \{r \in \{1,\ldots,\beta\} : j_r > w\}.$$

The sets $Z_\Sigma(j)$ and $Z_\Pi(j)$ indicate which elements of the sequence j are, respectively, *small* and *big*. Notice that $Z_\Sigma \cup Z_\Pi = \{1,\dots,\beta\}$ and, since $Z_\Sigma(j)$ and $Z_\Pi(j)$ are disjoint,

$$\left|Z_\Sigma(j)\right| + \left|Z_\Pi(j)\right| = \beta.$$

We consider the equivalence relation $\sim$ on $Z_\Sigma(j)$ (respectively, on $Z_\Pi(j)$) given by

$$m \sim n \iff j_m = j_n.$$

We denote by $\Sigma(j)$ and $\Pi(j)$ the sets of the equivalence classes of the relation $\sim$ on, respectively, $Z_\Sigma(j)$ and $Z_\Pi(j)$. Then the numbers of the equivalence classes

$$\begin{aligned}\left|\Sigma(j)\right| &= \left|\{j_1,\dots,j_\beta\} \cap \{1,\dots,w\}\right|,\\ \left|\Pi(j)\right| &= \left|\{j_1,\dots,j_\beta\} \cap \{w+1,\dots,w+k\}\right|\end{aligned}$$

indicate how many different small / big elements appear in the sequence j.

We say that A is a set *a set-partition of* X, and denote it by $A \in \mathrm{SPar}(X)$, if A is a collection of disjoint non-empty subsets of X such that $\bigcup A = X$.

We call (A,B) *a pair of complementary set-partitions of* X if $A \cup B$ is a set-partition of X such that

$$\left(\bigcup A\right) \cap \left(\bigcup B\right) = \varnothing.$$

This terminology may be a bit misleading since neither A nor B need to be a set-partition of X. Note also that we allow the situations when $A = \varnothing$ or $B = \varnothing$. For example, consider a sequence $j \in [w+p-1]^\beta$, then the pair $\big(\Sigma(j),\Pi(j)\big)$ is a pair of complementary set-partitions of $[\beta]$.

For a pair (Σ,Π) of complementary set-partitions of $[\beta]$ we will say that *the sequence* $j \in [w+p-1]^\beta$ *is of type* (Σ,Π) if $\Sigma = \Sigma(j)$ and $\Pi = \Pi(j)$. If this is the case, we will use a shorthand notation $j \in (\Sigma,\Pi)$.

Lemma 4.6.10. *Let* $p_1,p_2 \in \{1,\dots,k\}$ *and* $s \in [w+p_1-1]^\beta$, *and* $t \in [w+p_2-1]^\beta$. *Suppose that* s *and* t *are of the same type. Denote* $\sigma_1 := \sigma_{p_1,s}$ *and* $\sigma_2 := \sigma_{p_2,t}$. *Then*

(a) There exists a permutation $g \in \mathfrak{S}_w \times \mathfrak{S}_k$ *such that* $g(w+p_1) = w+p_2$ *and* $g(s_m) = t_m$ *for* $m \in \{1,\dots,\beta\}$;

(b) Permutations σ_1 *and* σ_2 *are conjugate by* g, *that is* $\sigma_1 = g^{-1}\sigma_2 g$;

(c) $\|\sigma_1\mathfrak{S}_k\| = \|\sigma_2\mathfrak{S}_k\|$.

Proof. Denote

$$\begin{aligned}A_{\leqslant w} &:= [w]\backslash\{s_m : m = 1,\dots,\beta\};\\ B_{\leqslant w} &:= [w]\backslash\{t_m : m = 1,\dots,\beta\}.\end{aligned}$$

Since $\Sigma(s) = \Sigma(t)$, we have $|A_{\leqslant w}| = |B_{\leqslant w}|$, so there exists a bijection $\delta_1 \colon A_{\leqslant w} \to B_{\leqslant w}$. For the same reason, there exists a bijection $\delta_2 \colon A_{>w} \to B_{>w}$ between analogously defined sets

$$\begin{aligned}A_{>w} &:= \{w+1,\dots,w+k\}\backslash\left(\{s_m : m = 1,\dots,\beta\} \cup \{w+p_1\}\right);\\ B_{>w} &:= \{w+1,\dots,w+k\}\backslash\left(\{t_m : m = 1,\dots,\beta\} \cup \{w+p_2\}\right).\end{aligned}$$

Then $g\colon \mathfrak{S}_w + k \to \mathfrak{S}_w + k$ given by

$$g(x) := \begin{cases} w + p_2 & \text{if } x = w + p_1, \\ t_m & \text{if } x = s_m \text{ for some } m \in \{1, \dots, \beta\}, \\ \delta_1(x) & \text{if } x \in A_{\leqslant w}, \\ \delta_2(x) & \text{if } x \in A_{>w}. \end{cases}$$

clearly fulfills the properties required in (a) and it is easy to check that (b) indeed holds true.

In order to prove (c) it is enough to notice that (b) implies that σ_1 and σ_2 have the same number of cycles permuting only small elements. □

4.6.5.2 Inequalities concerning the character of J^{β}_{w+p}

In the proof of Proposition 4.6.3 we will deal with the numbers of the form $O(N^x)$ where the exponent is given by the right-hand-side of (4.6.25). Our next aim is to show that these exponents are always nonpositive and only in some special cases are equal to 0.

Lemma 4.6.11. *Let $x_1, x_2, \dots \in \{1, \dots, w + k\}$ and $y_1, y_2, \dots \in \{w + 1, \dots, w + k\}$ be infinite sequences. Define a function $f : \mathbb{N}_0 \to \mathbb{Z}$ by*

$$f(\ell) := 2\#\big(\{x_1, \dots, x_\ell\} \cap \{1, \dots, w\}\big) + \#\big(\{x_1, \dots, x_\ell\} \cap \{w + 1, \dots, w + k\}\big) - \|(x_1, y_1) \cdots (x_\ell, y_\ell)\mathfrak{S}_k\| - \ell. \quad (4.6.25)$$

Then $f \leqslant 0$ and f is weakly decreasing.

Moreover, suppose that $\ell \in \mathbb{N}$ is such that $x_{\ell+1} \in \{x_1, \dots, x_\ell\}$ and $x_{\ell+1}$ and $y_{\ell+1}$ belong to different cycles in the cycle decomposition of the product $(x_1, y_1) \cdots (x_\ell, y_\ell)$. Then $f(\ell + 1) < f(\ell)$ and, in particular, $f(n) < 0$ for all $n \geqslant \ell + 1$.

Proof. Let ℓ be a non-negative integer; we will show that $f(\ell + 1) \leqslant f(\ell)$.

Consider first the case $x_{\ell+1} > w$. Then

$$(x_1, y_1) \cdots (x_{\ell+1}, y_{\ell+1})\mathfrak{S}_k = (x_1, y_1) \cdots (x_\ell, y_\ell)\mathfrak{S}_k$$

so

$$f(\ell + 1) = \begin{cases} f(\ell) - 1 & \text{if } x_{\ell+1} \in \{x_i : i \leqslant \ell\}, \\ f(\ell) & \text{otherwise,} \end{cases} \quad (4.6.26)$$

thus $f(\ell + 1) \leqslant f(\ell)$, as required.

Assume now that $x_{\ell+1} \leqslant w$. Our strategy is to compare the cycle decomposition of the products

$$(x_1, y_1) \cdots (x_\ell, y_\ell) \quad \text{and} \quad (x_1, y_1) \cdots (x_{\ell+1}, y_{\ell+1}) \quad (4.6.27)$$

and to deduce in this way (via the definition (4.6.15)) the relationship between the coset lengths

$$\|(x_1, y_1) \cdots (x_{\ell+1}, y_{\ell+1})\mathfrak{S}_k\| \quad \text{and} \quad \|(x_1, y_1) \cdots (x_\ell, y_\ell)\mathfrak{S}_k\|.$$

Consider the following two cases.

- Suppose $x_{\ell+1} \notin \{x_i : i \leqslant \ell\}$. Then the cycle decomposition of the permutation on the right-hand side of (4.6.27) arises from its counterpart on the left-hand side by merging the fixpoint $x_{\ell+1}$ with the cycle which contains $y_{\ell+1}$. It follows that

$$\|(x_1, y_1) \cdots (x_{\ell+1}, y_{\ell+1})\mathfrak{S}_k\| = \|(x_1, y_1) \cdots (x_\ell, y_\ell)\mathfrak{S}_k\| + 1$$

hence $f(\ell+1) = f(\ell)$, as required.

- Suppose $x_{\ell+1} \in \{x_i : i \leqslant \ell\}$. The cycle decomposition of the right-hand side of (4.6.27) is obtained from its counterpart on the left-hand side either by merging two cycles or by splitting one cycle into two cycles. Each of these two operations can change the number of cycles which permute only small elements by at most 1. It follows that

$$\|(x_1,y_1)\cdots(x_{\ell+1},y_{\ell+1})\mathfrak{S}_k\| \geqslant \|(x_1,y_1)\cdots(x_\ell,y_\ell)\mathfrak{S}_k\| - 1$$

so $f(\ell+1) \leqslant f(\ell)$, as required.

This completes the proof that f is weakly decreasing.

Since $f(0) = 0$ it follows that $f \leqslant 0$ and the proof of the first part of the lemma is complete.

We will prove the second part of the lemma by revisiting the above proof.

If $x_{\ell+1} > w$ then by (4.6.26), $f(\ell) = f(\ell-1) - 1$, as required.

On the other hand, when $x_{\ell+1} \leqslant w$ the cycle decomposition of the right-hand side of (4.6.27) is obtained from its counterpart on the left-hand side by merging two cycles: the one containing $x_{\ell+1}$ with the one containing $y_{\ell+1}$. Therefore the number of cycles which consist of only small elements at the right-hand side of (4.6.27) is bounded from above by its counterpart for the left-hand side of (4.6.27). Hence

$$\|(x_1,y_1)\cdots(x_{\ell+1},y_{\ell+1})\mathfrak{S}_k\| \geqslant \|(x_1,y_1)\cdots(x_\ell,y_\ell)\mathfrak{S}_k\|$$

and so $f(\ell+1) \leqslant f(\ell) - 1$, as required. □

Corollary 4.6.12. *Let $x_1,\ldots,x_\ell \in \{1,\ldots,w+k\}$ and $y_1,\ldots,y_\ell \in \{w+1,\ldots,w+k\}$. Denote*

$$\begin{aligned} |\Sigma| &:= \#\left(\{x_1,\ldots,x_\ell\} \cap \{1,\ldots,w\}\right); \\ |\Pi| &:= \#\left(\{x_1,\ldots,x_\ell\} \cap \{w+1,\ldots,w+k\}\right); \\ \|\sigma S_k\| &:= \|(x_1,y_1)\cdots(x_\ell,y_\ell)S_k\|. \end{aligned}$$

Then for $N \geqslant 1$

$$N^{2|\Sigma|}\, k^{|\Pi|}\, N^{-\|\sigma S_k\|-\ell} \leqslant \left(\frac{k}{N}\right)^{|\Pi|}.$$

4.6.6 The mean value of M_β – the proof of (4.6.2)

Proof of (4.6.2). Our goal is to calculate the expected value of the moment $M_\beta(w,k)$ (recall Section 4.6.2). By Proposition 4.6.5,

$$\begin{aligned} \mathbb{E}_{\tilde{\mathbb{P}}_N} M_\beta(w,k) &= \frac{1}{\mathbb{P}_N\left(\widetilde{\mathcal{T}}_{\square_N}^{(w+1,w+k)}\right)} \cdot \frac{1}{k} N^{-\beta} \chi_{\square_N}\left(\mathcal{J} p_{\mathfrak{S}_k}\right) = \\ &= \frac{1}{k!\,\mathbb{P}_N\left(\widetilde{\mathcal{T}}_{\square_N}^{(w+1,w+k)}\right)} \cdot \frac{1}{k} N^{-\beta} \chi_{\square_N}(\mathcal{J}\mathfrak{S}_k) \end{aligned} \tag{4.6.28}$$

where (recall the definition (4.6.24) of $\sigma_{p,j}$)

$$\mathcal{J} := \sum_{p=1}^{k} J_{w+p}^{\beta} = \sum_{p=1}^{k} \sum_{j \in [w+p-1]^\beta} \sigma_{p,j} \in \mathbb{C}\mathfrak{S}_w + k.$$

Since $\square_N$ is C-balanced with $C = 1$, by Lemma 4.5.3 the denominator on the right-hand side of (4.6.28) fulfills

$$k!\,\mathbb{P}_N\left(\widetilde{\mathcal{T}}_{\square_N}^{(w+1,w+k)}\right) = 1 + O\left(\frac{k^2}{N}\right)$$

with the constant in the O-notation equal to c from Lemma 4.5.3. By Assumption 4.6.1 the right hand side is separated from 0 and therefore

$$\frac{1}{k!\,\mathbb{P}_N\left(\widetilde{\mathcal{T}}_{\square_N}^{(w+1,w+k)}\right)} = 1 + O\left(\frac{k^2}{N}\right). \tag{4.6.29}$$

Equation (4.6.32) from Proposition 4.6.13 below provides the necessary asymptotics of the numerator and completes the proof of (4.6.2). □

We consider an analogue of $\mathcal{J}$ in which each summand is replaced by the minimal element of the appropriate coset

$$\mathcal{J}_0 := \pi_0(\mathcal{J}) = \sum_{p=1}^{k} \sum_{j\in[w+p-1]^\beta} \pi_0(\sigma_{p,j}) \in \mathbb{C}\mathfrak{S}_w + k.$$

The following proposition provides the missing element of the above proof of (4.6.2).

Proposition 4.6.13. *Let $\beta \in \mathbb{N}$ be fixed. Let $k, N \in \mathbb{N}$ be such that $N^2 > w + k$ and $k^2 < N$. Then*

$$\chi_{\square_N}(\mathcal{J}_0) = kN^\beta\left[\mathbb{E}_{\mathbb{P}_N} M_\beta(w,1) + O\left(\frac{k}{N}\right)\right]; \tag{4.6.30}$$

$$\chi_{\square_N}(\mathcal{J}\mathfrak{S}_k) = \chi_{\square_N}(\mathcal{J}_0) + O\left(kN^\beta\frac{k^2}{N}\right); \tag{4.6.31}$$

$$\chi_{\square_N}(\mathcal{J}\mathfrak{S}_k) = kN^\beta\left[\mathbb{E}_{\mathbb{P}_N} M_\beta(w,1) + O\left(\frac{k^2}{N}\right)\right] \tag{4.6.32}$$

with the constants in the O-notation depending only on β.

The remaining part of this section is devoted to its proof.

4.6.1 Decomposition of $\chi_{\square_N}(\mathcal{J}_0)$

Denote

$$A := \sum_{p=1}^{k} \sum_{j\in[w]^\beta} \chi_{\square_N}\left(\pi_0\left(\sigma_{p,j}\right)\right);$$

and for a pair of complementary set-partitions (Σ, Π) of $[\beta]$ let us also denote

$$B^{(\Sigma,\Pi)} := \sum_{p=1}^{k} \sum_{j\in(\Sigma,\Pi)} \chi_{\square_N}\left(\pi_0\left(\sigma_{p,j}\right)\right). \tag{4.6.33}$$

With these notations

$$\chi_{\square_N}(\mathcal{J}_0) = A + \sum_{\substack{(\Sigma,\Pi)\\ \Pi\neq\varnothing}} B^{(\Sigma,\Pi)}. \tag{4.6.34}$$

Notice that the number of summands is finite, depends only on β and does not depend on N or k. Therefore, it is enough to find the asymptotics for each individual summand on the right-hand side.

4.6.6.2 Asymptotics of A

By Lemma 4.6.8(b), $\pi_0\left(\sigma_{p,j}\right) = \sigma_{p,j}$ for all $j \in [w]^\beta$. Since the character is constant on each conjugacy class, the contribution of the summands in A to the character is the same for each value of p and

$$A = \sum_{p=1}^{k} \chi_{\square_N}\left(\sum_{j\in[w]^\beta} \sigma_{p,j}\right) = k\cdot\chi_{\square_N}\left(J^\beta_{w+1}\right).$$

We apply Proposition 4.6.5 for $k=1$; in this special case $p_{\mathfrak{S}_1} = \mathrm{id}$ and $\chi_{\square_N}(p_{\mathfrak{S}_1}) = 1$, thus

$$A = k\,\mathbb{E}_{\mathbb{P}_N} u^\beta_{w+1} = kN^\beta\,\mathbb{E}_{\mathbb{P}_N} M_\beta(w,1). \tag{4.6.35}$$

4.6.6.3 Asymptotics of $B^{(\Sigma,\Pi)}$

Let $j \in [w+p-1]^\beta$. By Lemma 4.6.8 the coset length

$$\|\sigma_{p,j}\mathfrak{S}_k\| \leqslant \|\sigma_{p,j}\| \leqslant \beta$$

is uniformly bounded from above by the number of factors in (4.6.24). By Fact 4.3.1 and Lemma 4.6.8 it follows that there exists a universal constant C_β such that

$$\left|\chi_{\square_N}\left(\pi_0\left(\sigma_{p,j}\right)\right)\right| \leqslant C_\beta N^{-\|\sigma_{p,j}\mathfrak{S}_k\|}$$

holds true for each $j \in [w+p-1]^\beta$.

Let us fix a pair (Σ,Π) of complementary set-partitions of $[\beta]$. The number of the summands on the right-hand side of (4.6.33) is equal to the following sum of falling factorials

$$\sum_{p=1}^{k} (w)_{|\Sigma|}\cdot(p)_{|\Pi|} \leqslant N^{2|\Sigma|}\,k^{|\Pi|+1}.$$

By combining these observations with Corollary 4.6.12 we conclude that

$$\left|B^{(\Sigma,\Pi)}\right| \leqslant C_\beta N^{-\|\sigma_{p,j}\mathfrak{S}_k\|}\cdot N^{2|\Sigma|}\,k^{|\Pi|+1} \leqslant C_\beta\,kN^\beta\left(\frac{k}{N}\right)^{|\Pi|}. \tag{4.6.36}$$

The last two arguments imply also that for any $p \in \{1,\dots,k\}$

$$\sum_{j\in(\Sigma,\Pi)} \frac{k^2}{N^{\|\sigma_{p,j}\mathfrak{S}_k\|+1}} \leqslant \frac{k^2}{N}\,N^\beta\left(\frac{k}{N}\right)^{|\Pi|}. \tag{4.6.37}$$

4.6.6.4 Proof of Proposition 4.6.13

Proof of Proposition 4.6.13. The asymptotics of the summands which contribute to the right-hand side of (4.6.34) is provided by the equality (4.6.35) and the estimate (4.6.36) (for pairs (Σ, Π) of complementary set-partitions of $[\beta]$ with $\Pi \neq \varnothing$). In this way the proof of (4.6.30) is complete.

By Proposition 4.6.9 there exists $H_\beta > 0$ such that

$$\left|\chi_{\square_N}(\mathcal{J}\mathfrak{S}_k) - \chi_{\square_N}(\mathcal{J}_0)\right| \leqslant H_\beta \sum_{p=1}^{k} \sum_{j \in [w+p-1]^\beta} \frac{k^2}{N^{\|\sigma_{p,j}\mathfrak{S}_k\|+1}}. \tag{4.6.38}$$

The summands on the right-hand side can be grouped according to the type (Σ, Π) of the sequence j. For a fixed value of β there are only finitely many possible types, and the total contribution of the sequences j of a specific type (Σ, Π) is bounded from above by (4.6.37) which completes the proof of (4.6.31).

Equation (4.6.32) is a direct consequence of (4.6.30) and (4.6.31). □

4.6.7 The variance of M_β – the proof of (4.6.3)

We will mimic the concepts from Section 4.6.6, however, the calculations will be more involved.

Proof of (4.6.3). We first calculate the second moment of M_β. By Proposition 4.6.5 and then (4.6.29)

$$\begin{aligned}\mathbb{E}_{\tilde{\mathbb{P}}_N} M_\beta(w,k)^2 &= \frac{1}{k!\,\mathbb{P}_N\left(\widetilde{\mathcal{T}}^{(w+1,w+k)}_{\square_N}\right)} \cdot \frac{1}{k^2} N^{-2\beta} \chi_{\square_N}\left(\mathcal{J}^2\mathfrak{S}_k\right) \\ &= \left(1 + O\left(\frac{k^2}{N}\right)\right) \frac{1}{k^2} N^{-2\beta} \chi_{\square_N}\left(\mathcal{J}^2\mathfrak{S}_k\right) \end{aligned} \tag{4.6.39}$$

where (recall the definition (4.6.24) of $\sigma_{p,j}$)

$$\mathcal{J}^2 := \left(\sum_{p=1}^{k} J^\beta_{w+p}\right)^2 = \sum_{p_1,p_2=1}^{k} \sum_{\substack{s \in [w+p_1-1]^\beta \\ t \in [w+p_2-1]^\beta}} \sigma_{p_1,s}\sigma_{p_2,t} \in \mathbb{C}\mathfrak{S}_w + k.$$

Equation (4.6.42) from Proposition 4.6.14 below provides the necessary asymptotics of the numerator in (4.6.39) and gives us

$$\mathbb{E}_{\tilde{\mathbb{P}}_N} M_\beta(w,k)^2 = \frac{1}{k}\mathbb{E}_{\mathbb{P}_N} M_{2\beta}(w,1) + \left(1 - \frac{1}{k}\right)\left(\mathbb{E}_{\mathbb{P}_N} M_\beta(w,1)\right)^2 + O\left(\frac{k^2}{N}\right)$$

with the constant in the O-notation depending only on β. By (4.6.2) we finally get

$$\begin{aligned}\mathrm{Var}_{\tilde{\mathbb{P}}_N} M_\beta(w,k) &= \mathbb{E}_{\tilde{\mathbb{P}}_N} M_\beta(w,k)^2 - \left(\mathbb{E}_{\tilde{\mathbb{P}}_N} M_\beta(w,k)\right)^2 = \\ &\frac{1}{k}\left[\mathbb{E}_{\mathbb{P}_N} M_{2\beta}(w,1) - \left(\mathbb{E}_{\mathbb{P}_N} M_\beta(w,1)\right)^2\right] + O\left(\frac{k^2}{N}\right) = O\left(\frac{1}{k} + \frac{k^2}{N}\right)\end{aligned}$$

with the constant in the O-notation depending only on β. This completes the proof of (4.6.3) (and Proposition 4.6.3). □

We consider an analogue of $\mathcal{J}^2$ in which each summand is replaced by the minimal element of the appropriate coset

$$\mathcal{J}^2_* := \pi_0\left(\mathcal{J}^2\right) = \sum_{p_1,p_2=1}^{k} \sum_{\substack{s\in[w+p_1-1]^\beta \\ t\in[w+p_2-1]^\beta}} \pi_0\left(\sigma_{p_1,s}\sigma_{p_2,t}\right) \in \mathbb{C}\mathfrak{S}_w + k.$$

The following proposition provides the missing component of the above proof of (4.6.3).

Proposition 4.6.14. *Let $\beta \in \mathbb{N}$ and $k, N \in \mathbb{N}$ be such that $N^2 \geqslant w + k$ and $k^2 < N$. Then*

$$\chi_{\square_N}\left(\mathcal{J}^2_*\right) = k^2N^{2\beta}\left[\frac{1}{k}\mathbb{E}_{\mathbb{P}_N}M_{2\beta}\left(w,1\right) + \left(1-\frac{1}{k}\right)\left(\mathbb{E}_{\mathbb{P}_N}M_\beta(w,1)\right)^2 + O\left(\frac{k}{N}\right)\right]; \quad (4.6.40)$$

$$\chi_{\square_N}\left(\mathcal{J}^2\mathfrak{S}_k\right) = \chi_{\square_N}\left(\mathcal{J}^2_*\right) + O\left(k^2N^{2\beta}\frac{k^2}{N}\right); \quad (4.6.41)$$

$$\chi_{\square_N}\left(\mathcal{J}^2\mathfrak{S}_k\right) = k^2N^{2\beta}\left[\frac{1}{k}\mathbb{E}_{\mathbb{P}_N}M_{2\beta}\left(w,1\right) + \left(1-\frac{1}{k}\right)\left(\mathbb{E}_{\mathbb{P}_N}M_\beta(w,1)\right)^2 + O\left(\frac{k^2}{N}\right)\right] \quad (4.6.42)$$

with the constants in the O-notation depending only on β.

The remaining part of this section is devoted to its proof.

4.6.7.1 Decomposition of $\chi_{\square_N}\left(\mathcal{J}^2_*\right)$

For any $p_1, p_2 \in \{1,\dots,k\}$ denote

$$P_{p_1,p_2}(\beta) := [w+p_1-1]^\beta \times [w+p_2-1]^\beta$$

and let

$$A := \sum_{p=1}^{k} \sum_{s,t\in[w]^\beta} \chi_{\square_N}\left(\pi_0\left(\sigma_{p,s}\sigma_{p,t}\right)\right);$$

Let us define *the concatenation of sequences $a = (a_1,\dots,a_x)$ and $b = (b_1,\dots,b_y)$* as the sequence $a \sqcup b := (a_1,\dots,a_x,b_1,\dots,b_y)$. For any pair of complementary set-partitions (Σ,Π) of the set $[2\beta]$ let us denote

$$B^{(\Sigma,\Pi)} := \sum_{p_1,p_2=1}^{k} \sum_{\substack{(s,t)\in P_{p_1,p_2}(\beta), \\ s\sqcup t\in(\Sigma,\Pi)}} \chi_{\square_N}\left(\pi_0\left(\sigma_{p_1,s}\sigma_{p_2,t}\right)\right) \quad (4.6.43)$$

and if Σ is a set-partition of $[2\beta]$ denote

$$C^{\Sigma} := \sum_{\substack{p_1,p_2\in\{1,\dots,k\},\\ p_1\neq p_2}} \sum_{\substack{s,t\in[w]^{\beta},\\ s\sqcup t\in(\Sigma,\varnothing)}} \chi_{\square_N}\left(\pi_0\left(\sigma_{p_1,s}\sigma_{p_2,t}\right)\right). \tag{4.6.44}$$

With these notations

$$\chi_{\square_N}\left(\mathcal{J}_*^2\right) = A + \sum_{\substack{(\Sigma,\Pi)\\ \Pi\neq\varnothing}} B^{(\Sigma,\Pi)} + \sum_{\Sigma} C^{\Sigma}. \tag{4.6.45}$$

Notice that the number of summands on the right hand side of (4.6.45) is finite, depends only on β and does not depend on N or k. Therefore, it is enough to find the asymptotics for each individual summand on the right-hand side.

4.6.7.2 Asymptotics of A

We proceed in the same way as in Section 4.6.6.2 to get an exact formula

$$A = kN^{2\beta}\,\mathbb{E}_{\mathbb{P}_N} M_{2\beta}(w,1). \tag{4.6.46}$$

4.6.7.3 Asymptotics of $B^{(\Sigma,\Pi)}$

We follow the lines from Section 4.6.6.3.

Let us fix some pair (Σ,Π) of complementary set-partitions of $[2\beta]$. By Fact 4.3.1 and Lemma 4.6.8 there exists $C_\beta > 0$ such that each summand corresponding to $(s,t)\in P_{p_1,p_2}(\beta)$ such that $s\sqcup t\in(\Sigma,\Pi)$ fulfills the asymptotic bound

$$\left|\chi_{\square_N}\left(\pi_0\left(\sigma_{p_1,s}\sigma_{p_2,t}\right)\right)\right| \leqslant C_\beta N^{-\|\sigma_{p_1,s}\sigma_{p_2,t}\mathfrak{S}_k\|}.$$

On the other hand, the number of the summands on the right-hand side of (4.6.43) is bounded from above by

$$\sum_{p_1,p_2=1}^{k} w_{|\Sigma|}\cdot\max\{p_1,p_2\}_{|\Pi|} \leqslant N^{2|\Sigma|}\,k^{|\Pi|+2}.$$

By combining these observations with Corollary 4.6.12 used for the concatenated sequence $s\sqcup t$ we conclude that

$$\left|B^{(\Sigma,\Pi)}\right| \leqslant C_\beta\,k^2N^{2\beta}\left(\frac{k}{N}\right)^{|\Pi|}. \tag{4.6.47}$$

The last two arguments imply also that

$$\sum_{p_1,p_2=1}^{k}\ \sum_{\substack{(s,t)\in P_{p_1,p_2}(\beta),\\ s\sqcup t\,\in\,(\Sigma,\Pi)}} \frac{k^2}{N^{\|\sigma_{p_1,s}\sigma_{p_2,t}\mathfrak{S}_k\|+1}} \leqslant \frac{k^2}{N}\cdot k^2N^{2\beta}\left(\frac{k}{N}\right)^{|\Pi|}. \tag{4.6.48}$$

These estimations show that if a pair (Σ,Π) of complementary set-partitions of $[2\beta]$ is such that $\Pi\neq\varnothing$ then the contribution of $B^{(\Sigma,\Pi)}$ to (4.6.45) is of relatively small order.

4.6.7.4 Asymptotics of C^{Σ}. Connected set-partitions of $[2\beta]$

We will need to be much more subtle in calculating (and estimating) the summand C^{Σ}. We will treat the summand C^{Σ} in two different ways depending on the structure of Σ.

Let Σ be a set-partition of $[2\beta]$. We say that Σ *is connected* if there exists a block $\pi \in \Sigma$ which contains simultaneously some element of the set $\{1,\dots,\beta\}$ and some element of the set $\{\beta+1,\dots,2\beta\}$, that is formally, $\pi \cap [\beta] \neq \varnothing$ and $\pi \cap \{\beta+1,\dots,2\beta\} \neq \varnothing$. Each such a block $\pi \in \Sigma$ will be called *a link*. If Σ does not have any links then we say that Σ *is disconnected*.

4.6.7.5 Asymptotics of C^Σ for connected Σ

Let us fix a connected set-partition Σ of $[2\beta]$. We set

$$n_\Sigma := \min\left\{i \in \{\beta+1,\dots,2\beta\} : \exists_{\pi\in\Sigma}\ \ (i \in \pi \text{ and } \pi \text{ is a link in } \Sigma)\right\}.$$

In other words, n_Σ indicates the least number $i > \beta$ belonging to some link π of Σ.

Notice that for distinct p_1, p_2 and a pair of sequences (s,t) such that $s \sqcup t \in (\Sigma, \varnothing)$ the assumptions of the second part of Lemma 4.6.11 are fulfilled for the sequences $(x_i) = s \sqcup t$ and $(y_i) = (p_1,\dots,p_1,p_2,\dots,p_2)$, and $\ell := \beta + n_\Sigma - 1$. Therefore an inequality

$$2\,|\Sigma| - \|\sigma_{p_1,s}\sigma_{p_2,t}\mathfrak{S}_k\| - 2\beta \leqslant -1$$

holds for any (s,t) such that $s \sqcup t \in (\Sigma,\varnothing)$ with Σ connected.

We now follow the lines in Section 4.6.7.3 to get the upper bound

$$\left|C^\Sigma\right| \leqslant C_\beta\,(k^2-k)N^{2\beta-1} \tag{4.6.49}$$

which holds for each connected set-partition Σ of the set $[2\beta]$. This shows that the contribution of C^Σ with connected Σ to (4.6.45) is of relatively small order.

4.6.7.6 Asymptotics of C^Σ for disconnected Σ

We will show that

$$\sum_{\substack{\Sigma:\\ \Sigma \text{ is disconnected}}} C^\Sigma = (k^2-k)N^{2\beta}\left(\left(\mathbb{E}_{\mathbb{P}_N} M_\beta(w,1)\right)^2 + O\left(N^{-2}\right)\right) \tag{4.6.50}$$

with the constant in the O-notation depending only on β.

Recall that the C^Σ, defined in (4.6.44), is the sum of characters $\chi_{\square_N}$ evaluated on the minimal permutations $\pi_0\left(\sigma_{p_1,s}\sigma_{p_2,t}\right)$. When Σ is disconnected and $p_1 \neq p_2$, in the permutation $\sigma_{p_1,s}\sigma_{p_2,t}$ each cycle permutes at most one big element, so by Lemma 4.6.8(b) $\sigma_{p_1,s}\sigma_{p_2,t}$ is the minimal permutation. Hence whenever Σ is disconnected

$$C^\Sigma = \sum_{\substack{p_1,p_2\in\{1,\dots,k\},\\ p_1\neq p_2}} \sum_{\substack{s,t\in[w]^\beta,\\ s\sqcup t\in(\Sigma,\varnothing)}} \chi_{\square_N}\left(\sigma_{p_1,s}\sigma_{p_2,t}\right).$$

For any set partition Σ of $[2\beta]$ let us define

$$\widetilde{C}^\Sigma := \sum_{\substack{p_1,p_2\in\{1,\dots,k\},\\ p_1\neq p_2}} \sum_{\substack{s,t\in[w]^\beta,\\ s\sqcup t\in(\Sigma,\varnothing)}} \chi_{\square_N}\left(\sigma_{p_1,s}\right)\chi_{\square_N}\left(\sigma_{p_2,t}\right).$$

Then by Proposition 4.6.5 applied twice for $k = 1$

$$\sum_{\Sigma} \widetilde{C}^{\Sigma} = \sum_{\substack{p_1,p_2\in\{1,\dots,k\},\\ p_1\neq p_2}} \left(\sum_{s\in[w]^\beta} \chi_{\square_N}\left(\sigma_{p_1,s}\right) \right) \left(\sum_{t\in[w]^\beta} \chi_{\square_N}\left(\sigma_{p_2,t}\right) \right) = (k^2-k)N^{2\beta}\left(\mathbb{E}_{\mathbb{P}_N} M_\beta(w,1)\right)^2. \quad (4.6.51)$$

Our aim is to show that (4.6.51) is a good approximation for the left-hand-side of (4.6.50).

By Fact 4.3.2 there exists a constant $K_\beta > 0$ which depends only on β (in particular it does not depend on N or k) such that for any distinct p_1, p_2 and a pair of sequences (s,t) such that $s \sqcup t \in (\Sigma, \varnothing)$ with Σ disconnected

$$\left| \chi_{\square_N}\left(\sigma_{p_1,s}\sigma_{p_2,t}\right) - \chi_{\square_N}\left(\sigma_{p_1,s}\right)\chi_{\square_N}\left(\sigma_{p_2,t}\right) \right| \leqslant K_\beta \left(N^{-|\sigma_{p_1,s}|-|\sigma_{p_2,t}|-2} \right).$$

Let us denote for any set-partition Σ of $[2\beta]$

$$R^{\Sigma} := \sum_{\substack{p_1,p_2\in\{1,\dots,k\},\\ p_1\neq p_2}} \sum_{\substack{s,t\in[w]^\beta,\\ s\sqcup t\in(\Sigma,\varnothing)}} N^{-|\sigma_{p_1,s}|-|\sigma_{p_2,t}|-2}.$$

With the introduced notation the following inequality holds

$$\left| \sum_{\Sigma} \widetilde{C}^{\Sigma} - \sum_{\substack{\Sigma:\\ \Sigma \text{ is disconnected}}} C^{\Sigma} \right| \leqslant \sum_{\substack{\Sigma:\\ \Sigma \text{ is disconnected}}} K_\beta R^{\Sigma} + \sum_{\substack{\Sigma:\\ \Sigma \text{ is connected}}} \left| \widetilde{C}^{\Sigma} \right|. \quad (4.6.52)$$

We now investigate the asymptotics of the sums on the right-hand-side of (4.6.52).

4.6.7.7 Asymptotics of the right-hand-side of (4.6.52)

Observe that if Σ is connected and (s,t) is a pair of sequence such that $s \sqcup t \in (\Sigma, \varnothing)$ then

$$|\Sigma| = |\Sigma(s \sqcup t)| \leqslant |\Sigma(s)| + |\Sigma(t)| - 1.$$

We follow the lines from Section 4.6.6.3 to get the upper bound

$$\left| \widetilde{C}^{\Sigma} \right| \leqslant C_\beta^2 \, (k^2-k) N^{2\beta-2} \quad (4.6.53)$$

for any connected Σ with universal constant $C_\beta > 0$ depending only on β.

On the other hand, by Lemma 4.6.8(b) and (4.6.37) for any set-partition Σ of $[2\beta]$

$$R^{\Sigma} \leqslant (k^2-k) \left[\sum_{s\in[w]^\beta} N^{-|\sigma_{p_1,s}|-1} \right]^2 \leqslant (k^2-k) N^{2\beta-2}. \quad (4.6.54)$$

Inserting approximations (4.6.53) for connected Σ and (4.6.54) for disconnected Σ into (4.6.52) and taking into account (4.6.51) proves (4.6.50).

4.6.7.8 Asymptotics of the sum $\sum_{\Sigma} C^{\Sigma}$

By (4.6.49) and (4.6.50) we get

$$\sum_{\Sigma} C^{\Sigma} = (k^2-k)N^{2\beta}\left(\left(\mathbb{E}_{\mathbb{P}_N} M_\beta(w,1)\right)^2 + O\left(N^{-1}\right)\right). \tag{4.6.55}$$

4.6.7.9 Finishing the proof of Proposition 4.6.14

Proof of Proposition 4.6.14. Inserting the equality (4.6.46) and approximations (4.6.47) (for complementary set-partitions (Σ,Π) with $\Pi \neq \varnothing$) and (4.6.55) into (4.6.45) we conclude that (4.6.40) holds true.

By Proposition 4.6.9 there exists $C_\beta > 0$ such that

$$\left|\chi_{\square_N}\left(\mathcal{J}^2\mathfrak{S}_k\right) - \chi_{\square_N}\left(\mathcal{J}_*^2\right)\right| \leqslant C_\beta \sum_{p_1,p_2=1}^{k} \sum_{(s,t)\in P_{p_1,p_2}(\beta)} \frac{k^2}{N^{\|\sigma_{p_1,s}\sigma_{p_2,t}\mathfrak{S}_k\|+1}}. \tag{4.6.56}$$

The summands on the right-hand side can be grouped according to the types (Σ,Π) of the sequences $s \sqcup t$. By (4.6.48) the right-hand side of (4.6.56) estimates by $\frac{k^2}{N}k^2N^{2\beta}$ which ends the proof of (4.6.41).

Equation (4.6.42) is a direct consequence of (4.6.40) and (4.6.41). □

This finishes the proof of Proposition 4.6.3

4.6.8 Proof of Theorem 4.6.2

The proof is based on [Rom15, Section 4.10]. We start with a general fact.

Lemma 4.6.15. *Let $\varepsilon > 0$ and μ be a compactly supported probability measure on $\mathbb{R}$. Let $x \in \mathbb{R}$ be a continuity point of the cumulative distribution function F_μ of μ. Then there exist $\delta > 0$ and an integer $A > 0$ with the following property:*
if m is a probability measure on $\mathbb{R}$ such that its moments (up to order A) are δ-close to the moments of μ then

$$\left|F_\mu(x) - F_m(x)\right| \leqslant \varepsilon$$

where F_m is the cumulative distribution function of m.

Proof. If this would not be the case, there would exist a sequence of probability measures which converges to μ in moments, but would not converge to μ in the weak topology of probability measures. This is not possible, since μ is compactly supported and therefore uniquely determined by its moments [Dur10, Section 3.3.5]. □

We now prove Theorem 4.6.2.

Proof of Theorem 4.6.2. We mimic the proof of [Rom15, Theorem 4.1]. Pittel and Romik [PR07, Theorem 2] found explicitly the limit distribution ν_α which describes the u-coordinate of the (scaled) position of the box with the entry $\lfloor \alpha N^2 \rfloor$ in a uniformly random tableau $T_N \in \mathcal{T}_{\square_N}$ as the semicircle distribution (4.2.4) (recall Section 4.2.3). In our setting this result describes the u-coordinate of the surfer after draining $1-\alpha$ fraction of water. Since 'the amount of remaining water w' is such that $\frac{w}{N^2} \to \alpha$, the β-th moment γ_β of the distribution ν_α equals

$$\gamma_\beta := \int x^\beta \, \mathrm{d}\nu_\alpha(x) = \lim_{N\to\infty} \mathbb{E}_{\mathbb{P}_N} M_\beta(w,1).$$

By Proposition 4.6.3 we get using Chebyshev's inequality that for any $\varepsilon > 0$ and $\beta \in \mathbb{N}$

$$\mathbb{P}_{\widetilde{\mathcal{T}}^{(w+1,w+k)}_{\square_N}}\left(\left|M_\beta(w,k) - \gamma_\beta\right| > \varepsilon\right) = O\left(\frac{1}{k} + \frac{k^2}{N}\right).$$

The cumulative distribution function F_{ν_α} of the semicircle measure ν_α is continuous and therefore any $x \in \mathbb{R}$ is its continuity point. Let $x \in \mathbb{R}$ and let A and δ be the constants given by Lemma 4.6.15. Then by the union bound

$$\mathbb{P}_{\widetilde{\mathcal{T}}^{(w+1,w+k)}_{\square_N}}\left\{\left|F_{\nu_\alpha}(x) - G_N(x)\right| > \varepsilon\right\} \leqslant \sum_{\beta=1}^{A} \mathbb{P}_{\widetilde{\mathcal{T}}^{(w+1,w+k)}_{\square_N}}\left(\left|M_\beta(w,k) - \gamma_\beta\right| > \delta\right) = O\left(\frac{1}{k} + \frac{k^2}{N}\right) \quad (4.6.57)$$

with the constant in the O-notation depending only on ε.

For the proof of Theorem 4.6.2 we need to obtain the uniform version of (4.6.57) in which the event on the left hand side is taken with supremum over $u \in \mathbb{R}$. This can be easily done by choosing a finite set $X \subseteq \mathbb{R}$ with the property that its image F_{ν_α} is an ϵ-net for the interval $[0,1]$; such a set exists because F_{ν_α} is continuous. The pointwise result (4.6.57) implies that the following estimate for the supremum over the finite set X holds true:

$$\mathbb{P}_{\widetilde{\mathcal{T}}^{(w+1,w+k)}_{\square_N}}\left\{M_N : \sup_{x\in X}\left|F_{\nu_\alpha}(x) - G_N(x)\right| > \varepsilon\right\} = O\left(\frac{1}{k} + \frac{k^2}{N}\right). \quad (4.6.58)$$

Let $x_1 < \cdots < x_\ell$ be the elements of X. The assumption about the set X implies that

$$F_{\nu_\alpha}(x_1) < \epsilon, \qquad F_{\nu_\alpha}(x_{i+1}) < F_{\nu_\alpha}(x_i) + 2\epsilon, \qquad F_{\nu_\alpha}(x_\ell) > 1 - \epsilon. \quad (4.6.59)$$

The elements of X divide the real line into $\ell + 1$ intervals:

$$(-\infty, x_1],\ [x_1, x_2],\ \ldots,\ [x_{\ell-1}, x_\ell],\ [x_\ell, \infty).$$

By considering each interval separately, using monotonicity of the cumulative distribution function F_{ν_α} and the monotonicity of G_N, as well as (4.6.59) it follows that

$$\sup_{x\in\mathbb{R}}\left|F_{\nu_\alpha}(x) - G_N(x)\right| < 2\epsilon + \sup_{x\in X}\left|F_{\nu_\alpha}(x) - G_N(x)\right|.$$

In this way (4.6.58) completes the proof. □

4.7 Proof of Theorem 4.4.1

The current section is devoted to the proof of Theorem 4.4.1.

4.7.1 Overtaking only in one direction

We start with a precise statement of the heuristic ideas from Section 4.4.4.4.

Lemma 4.7.1. *Fix $k, n \in \mathbb{N}$. Let tableaux $T \in \mathcal{T}_\mu$ of shape μ with $n+1$ boxes and $M \in \widetilde{\mathcal{T}}^{(n+1,n+k)}_\nu$ of shape ν with $n+k$ boxes be such that*

$$T|_{\leqslant n} = M|_{\leqslant n}.$$

If $1 \leqslant p \leqslant k$ *is such that*

$$\mathrm{pos}_T(n+1) \preceq \mathrm{pos}_M(n+p) \preceq \cdots \preceq \mathrm{pos}_M(n+k)$$

then jeu de taquin preserves the latter relations, that is

$$\mathrm{pos}_{j(T)}(n+1) \preceq \mathrm{pos}_{j(M)}(n+p) \preceq \cdots \preceq \mathrm{pos}_{j(M)}(n+k).$$

Proof. Clearly, $j(T)\big|_{\leqslant n} = j(M)\big|_{\leqslant n}$. Notice also that the boxes in jeu de taquin paths for tableaux T and M match at least to the boxes $\leqslant n$. As mentioned in Section 4.4.2, $j(M)$ is a k-Pieri tableau, so

$$\mathrm{pos}_{j(M)}(n+p) \preceq \cdots \preceq \mathrm{pos}_{j(M)}(n+k)$$

and therefore it remains to prove that

$$\mathrm{pos}_{j(T)}(n+1) \preceq \mathrm{pos}_{j(M)}(n+p). \tag{4.7.1}$$

We consider the following two cases:

1. The box $n+1$ in T slid during jeu de taquin, i.e., $\mathrm{pos}_T(n+1) \neq \mathrm{pos}_{j(T)}(n+1)$. Consider two subcases:

   1a) The box $n+1$ in T slid to the left; in this case it does not matter how (and if) the box $n+p$ in M slid and (4.7.1) holds.

   1b) The box $n+1$ in T slid to the bottom. Then we use the assumption that M is k-Pieri to show that if $\mathrm{pos}_M(n+p) = \mathrm{pos}_T(n+1)$ then $n+p$ in M also slid to the bottom and (4.7.1) holds. On the other hand if $\mathrm{pos}_T(n+1) \prec \mathrm{pos}_M(n+p)$ then the box $n+p$ in M must be strictly to the right of $n+1$ in T and it does not matter if it slides or not, so (4.7.1) also holds.

2. The box $n+1$ in T did not slide, i.e., $\mathrm{pos}_T(n+1) = \mathrm{pos}_{j(T)}(n+1)$. In this case, the JDT path in T ends on some box $\leqslant n$ which is strictly left-top or strictly right-bottom to the $\mathrm{pos}_T(n+1)$. Hence, if $\mathrm{pos}_T(n+1) = \mathrm{pos}_M(n+p)$ then the box $n+p$ in M does not slide. Otherwise, (by the initial relation) it must be strictly to the right (and weakly to the bottom) of $\mathrm{pos}_T(n+1)$ and it does not matter if it slides or not. All in all, (4.7.1) holds. □

4.7.2 Relative position of the surfer

We recommend the reader to recall the notions in Section 4.4 and heuristics for the proof of Theorem 4.4.1 in Section 4.4.4.

Let $0 < t_1 < t_2 < 1$ and denote

$$w := \lceil (1-t_1)N^2 \rceil - 1.$$

Let k be a positive integer such that $w + k \leqslant N^2$. By Proposition 4.5.1 used for $C = 1$, $\Delta = t_1$, $a = w$ and $\lambda = \square_N$ there exists a pair of random tableaux $\mathbf{T}$, $\mathbf{M}$ defined on the same probability space with the following properties:

(A1) $\mathbf{T}$ is a uniformly random element of $\mathcal{T}_{\square_N}$;

(A2) $\mathbf{M}$ is a random element of $\widetilde{\mathcal{T}}_{\square_N}^{(w+1,w+k)}$ sampled according to the distribution which fulfills the following total variation distance bound

$$\delta\left(\mathbf{M}, \mathbb{P}_{\widetilde{\mathcal{T}}_{\square_N}^{(w+1,w+k)}}\right) \leqslant d\frac{k^2}{\sqrt{N^2-w}}$$

for some universal constant $d > 0$ which depends only on t_1;

(A3) $\mathbf{T}\big|_{\leqslant w} = \mathbf{M}\big|_{\leqslant w}$ holds true almost surely.

Since the dual promotion ∂^* is a bijection, by (A1) the tableau $\mathbf{T}\big|_{\leqslant w+1}$ has the same distribution as the initial configuration of the single surfer T'_N (see (4.4.5)) and by (A2) the tableau $\mathbf{M}\big|_{\leqslant w+k}$ has approximately the same distribution (up to the total variation distance in (A2)) as the initial configuration of the multisurfers M'_N (see (4.4.11)). Moreover, by (A3) the initial configurations of water are the same for both stories. Therefore we will refer to the box $w+1$ in $\mathbf{T}$ as the *surfer* and to the boxes $w+1,\dots,w+k$ in $\mathbf{M}$ as the *multisurfers*.

Recall that the definition (4.6.1) of the random variable $G_N(u)$ depends implicitly on the choice of the tableau M_N. For an integer $0 \leqslant q \leqslant w$ we denote by $G_N^q(u)$ this random variable obtained by substituting M_N with $j^q(\mathbf{M})$. We underline here that M_N and $j^q(\mathbf{M})$ need not have the same distribution. We also define $\widetilde{G}_N^q$ to be the fraction of the multisurfers which are to the left of the surfer, more precisely

$$\widetilde{G}_N^q := G_N^q\left(\frac{1}{N}u_{w+1}^{j^q(\mathbf{T})}\right) = \frac{1}{k}\max\left\{p \in \{1,\dots,k\} : u_{w+p}^{j^q(\mathbf{M})} \leqslant u_{w+1}^{j^q(\mathbf{T})}\right\}. \tag{4.7.2}$$

The following proposition gives a relation between $\widetilde{G}_N^q$ and the theoretical longitude of the surfer on the common probability space of the surfer and multisurfers defined in the beginning of this section.

Proposition 4.7.2. *Let $s \geqslant 0$ and $t > 0$ be such that $s + t < 1$. Let $w(N) = \lceil (1-t)N^2 \rceil - 1$ for $N \in \mathbb{N}$ and let $k = k(N)$ fulfill Assumption 4.6.1. Let $q = q(N)$ be a sequence of non-negative integers such that*

$$0 \leqslant q(N) \leqslant \lfloor (1-t)N^2 \rfloor \quad \text{and} \quad \lim_{N\to\infty} \frac{q}{N^2} = s.$$

Then for any $\varepsilon > 0$

$$\mathbb{P}\left((\mathbf{T},\mathbf{M}) : \left|\widetilde{G}_N^q - F_{\nu_{1-t-s}}\left(\frac{1}{N}u_{w+1}^{j^q(\mathbf{T})}\right)\right| > \varepsilon\right) = O\left(\frac{1}{k} + \frac{k^2}{N}\right)$$

and the constant in the O-notation depends only on s, $t+s$ and ε.

Proof. By the discussion below Equation (4.7.2)

$$\mathbb{P}\left((\mathbf{T},\mathbf{M}) : \left|\widetilde{G}_N^q - F_{\nu_{1-t-s}}\left(\frac{1}{N}u_{w+1}^{j^q(\mathbf{T})}\right)\right| > \varepsilon\right) = \mathbb{P}\left((\mathbf{T},\mathbf{M}) : \left|G_N^q\left(\frac{1}{N}u_{w+1}^{j^q(\mathbf{T})}\right) - F_{\nu_{1-t-s}}\left(\frac{1}{N}u_{w+1}^{j^q(\mathbf{T})}\right)\right| > \varepsilon\right).$$

The latter is bounded from above by

$$\mathbb{P}\left((\mathbf{T},\mathbf{M}) : \sup_{x\in\mathbb{R}}\left|G_N^q(x) - F_{\nu_{1-t-s}}(x)\right| > \varepsilon\right). \tag{4.7.3}$$

The random event in (4.7.3) is expressed purely in terms of the random tableau $j^q(\mathbf{M})$ and does not involve the random tableau $\mathbf{T}$. For this reason the probability in (4.7.3), due to the

condition (A2) on page 133 and the bijectivity of the dual promotion ∂^*, is equal to

$$\mathbb{P}_{\widetilde{\mathcal{T}}_{\square_N}^{(w-q+1,w-q+k)}}\left(M_N : \sup_{x\in\mathbb{R}}\left|G_N(x) - F_{\nu_{1-t-s}}(x)\right| > \varepsilon\right) + O\left(\frac{k^2}{N}\right)$$

with the constant in the O-notation depending only on t. Since $\lim \frac{w-q}{N^2} = 1-t-s > 0$ we can apply Theorem 4.6.2 which completes the proof. □

4.7.3 Proof of the upper bound (4.4.2) in Theorem 4.4.1

Let $k = k(N)$ be such that $k(N) \to \infty$ and $k(N) = o(\sqrt{N})$, i.e., (4.4.10) is satisfied. We will use the results from Section 4.7.2 to prove the upper bound (4.4.2). Let $q := \lfloor t_2 N^2 \rfloor - \lfloor t_1 N^2 \rfloor$. Recall that $w = \lceil (1-t_1)N^2 \rceil - 1$ (cf. Section 4.7.2).

By (A1) from Section 4.7.2 we can translate the probability on the left-hand-side of (4.4.2) into the setting of $\mathbf{T}$ in the following way

$$\mathbb{P}_N\Big(T \in \mathcal{T}_{\square_N} : \Psi_N^{\mathrm{th}}(t_2) - \Psi_N^{\mathrm{th}}(t_1) > \varepsilon\Big) = \mathbb{P}\left((\mathbf{T},\mathbf{M}) : F_{\nu_{1-t_2}}\left(\frac{1}{N}u_{w+1}^{j^q(\mathbf{T})}\right) - F_{\nu_{1-t_1}}\left(\frac{1}{N}u_{w+1}^{\mathbf{T}}\right) > \varepsilon\right);$$

note that the event on the right-hand side *does not* involve the tableau $\mathbf{M}$. The latter probability can be estimated from above via the union bound by the sum of probabilities of the following three events:

- the fraction of the multisurfers in the final position (i.e., in time t_2) which are to the left of the surfer is 'unusually small', that is

$$A := \left\{(\mathbf{T},\mathbf{M}) : F_{\nu_{1-t_2}}\left(\frac{1}{N}u_{w+1}^{j^q(\mathbf{T})}\right) - \widetilde{G}_N^q > \frac{\varepsilon}{2}\right\};$$

- the number of the multisurfers which are to the left of the surfer increases over time, more precisely

$$B := \left\{(\mathbf{T},\mathbf{M}) : \widetilde{G}_N^q - \widetilde{G}_N^0 > 0\right\};$$

- the fraction of the multisurfers in the initial position (i.e, in time t_1) which are to the left of the surfer is 'unusually big', that is

$$C := \left\{(\mathbf{T},\mathbf{M}) : \widetilde{G}_N^0 - F_{\nu_{1-t_1}}\left(\frac{1}{N}u_{w+1}^{\mathbf{T}}\right) > \frac{\varepsilon}{2}\right\}.$$

By Proposition 4.7.2 the probabilities of the events A and C are of order $O\left(\frac{1}{k} + \frac{k^2}{N}\right)$. By Lemma 4.7.1 the event $B = \varnothing$ is impossible. The choice of the sequence k as in the beginning of this subsection implies that the upper bound (4.4.2) holds.

4.7.4 Proof of the lower bound (4.4.3) in Theorem 4.4.1

For any Young diagram λ and tableau $T \in \mathcal{T}_\lambda$ we will denote by λ^{tr} and T^{tr}, respectively, the diagram and the tableau obtained by a *transposition* of the diagram λ and the tableau T.

The transposition of tableaux gives a natural bijection between the sets $\mathcal{T}_\lambda$ and $\mathcal{T}_{\lambda^{\mathrm{tr}}}$ of standard tableaux, respectively, of shape λ and its transpose λ^{tr}. Moreover, under the

transposition the u-coordinate of the given box in a standard tableau T changes its sign, namely for any $n \in \{1, \dots, |T|\}$

$$u_n^T = -u_n^{T^{\mathrm{tr}}}. \tag{4.7.4}$$

In particular, the u-coordinate of the surfer $u(X_t)$ changes its sign under the transposition, i.e., $u(X_t) = -u(X_t^{\mathrm{tr}})$ where X_t^{tr} denotes the position of the surfer in the transposed tableau T^{tr}.

Recall that for any $\alpha \in (0,1)$ by ν_α we denote the limit measure found by Pittel and Romik on the circle of latitude α, see Section 4.2.3. The pushforward of the measure ν_α under the involution $\mathbb{R} \ni z \mapsto -z$ is a measure $\tilde{\nu}_\alpha$ which fulfills the following equality

$$\tilde{\nu}_\alpha\big((-\infty, u]\big) = \nu_\alpha\big([-u, \infty)\big) \qquad \text{for all } u \in \mathbb{R}. \tag{4.7.5}$$

Notice that by (4.7.4) the measure $\tilde{\nu}_\alpha$ is the limit measure on the circle of latitude α for the transposed sequence of Young diagrams $(\square_N^{\mathrm{tr}})$.

Let us denote the position of the surfer in the transposed tableau by X_t^*, cf. (4.2.5), and the theoretical longitude of the surfer in the transposed tableau by η, i.e.,

$$\eta(t) := F_{\tilde{\nu}_{1-t}}\big(u(X_t^*)\big) \quad \text{for } t \in [0,1].$$

Observe that by (4.7.5) and the continuity of $F_{\nu_{1-t}}$

$$\eta(t) = 1 - F_{\nu_{1-t}}\big(-u(X_t^*)\big). \tag{4.7.6}$$

Equation (4.4.2) applied to the transposed tableaux gives

$$\lim_{N\to\infty} \mathbb{P}_N\left\{T \in \mathcal{T}_{\square_N^{\mathrm{tr}}} : \eta(t_2) - \eta(t_1) > \varepsilon\right\} = 0.$$

On the other hand by (4.7.6) and then (4.7.4) we get

$$\eta(t_2) - \eta(t_1) = \big[1 - F_{\nu_{1-t_2}}\big(-u(X_{t_2}^*)\big)\big] - \big[1 - F_{\nu_{1-t_1}}\big(-u(X_{t_1}^*)\big)\big] =$$
$$F_{\nu_{1-t_1}}\Big(u\big((X_{t_1}^*)^{\mathrm{tr}}\big)\Big) - F_{\nu_{1-t_2}}\Big(u\big((X_{t_2}^*)^{\mathrm{tr}}\big)\Big).$$

Since $(X_t^*)^{\mathrm{tr}}$ reflects the position of the surfer in the original (not-transposed) tableau we have

$$\eta(t_2) - \eta(t_1) = \Psi_N^{\mathrm{th}}(t_1) - \Psi_N^{\mathrm{th}}(t_2).$$

Since we consider the uniform distribution on the set of tableaux, this ends the proof of the lower bound (4.4.3) and completes the proof of Theorem 4.4.1.

4.8 Proof of Theorem 4.2.3

4.8.1 Plan for the proof of Theorem 4.2.3

We will make the following steps in the proof of Theorem 4.2.3:

(S1) Pick a candidate for the random variable $\Psi_N \colon \mathcal{T}_{\square_N} \to [0,1]$.

(S2) Prove a *pointwise version of Theorem 4.2.3:* with the help of Lemma 4.8.1 and Theorem 4.4.1 we will show that the chosen candidate gives a good approximation of surfer's position for an arbitrary $t \in (0,1)$, i.e.,

$$\forall_{t\in(0,1)} \lim_{N\to\infty} \mathbb{P}_N\left(T_N \in \mathcal{T}_{\square_N} : \left|X_t(T_N) - P_{1-t,\Psi_N(T_N)}\right| > \varepsilon\right) = 0. \tag{4.8.1}$$

The proof will be given in Section 4.8.5.

(S3) Prove *the full (i.e., the original) version of Theorem 4.2.3*, i.e.,

$$\lim_{N\to\infty} \mathbb{P}_N\left(T_N \in \mathcal{T}_{\square_N} : \sup_{t\in[0,1]} \left| X_t(T_N) - P_{1-t,\Psi_N(T_N)} \right| > \varepsilon \right) = 0.$$

We will start with a finite ε-net of the family of level curves $\{h_\alpha : \alpha \in [0,1]\}$ parameterized by $0 = \alpha_0 < \alpha_1 < \cdots < \alpha_p < \alpha_{p+1} = 1$. By the previous point, (4.8.1) holds uniformly for $t \in \{\alpha_0, \ldots, \alpha_{p+1}\}$ in a finite set. Then for the intermediate moments of time $\alpha_i < t < \alpha_{i+1}$ we will use the monotonicity of the sliding path and in this way justify that (4.8.1) holds *uniformly* over $t \in (0,1)$. This proof will be given in Section 4.8.6.

In the very end, in Section 4.8.7, we will show that the probability distribution of the random variable Ψ_N converges to the uniform distribution on the unit interval $[0,1]$.

4.8.2 Auxiliary notation

In the proof we will switch between the position of the surfer in the XY and the UV coordinate systems as well as in the geographic coordinates. For any $t \in (0,1)$ let us introduce the notation for the true and the theoretical $u-$ and $v-$coordinate; namely we define the following functions $\mathcal{T}_{\square_N} \to \mathbb{R}$ by

$$\begin{aligned} u_t &:= u(X_t)\,, \\ v_t &:= v(X_t) \end{aligned} \qquad \text{and} \qquad \begin{aligned} u_t^{\mathrm{th}} &:= \left(F_{\nu_{1-t}}\right)^{-1}\left(\Psi_N^{\mathrm{th}}(t)\right), \\ v_t^{\mathrm{th}} &:= h_{1-t}\left(u_t^{\mathrm{th}}\right) \end{aligned}$$

(recall that $\Psi_N^{\mathrm{th}}(t) = F_{\nu_{1-t}}(u_t)$, cf. (4.4.1), and see Section 4.2.2 for the definition of h_t). Denote additionally for any $t \in [0,1]$

$$\left(x_t, y_t\right) := X_t \quad \text{and} \quad \left(x_t^{\mathrm{th}}, y_t^{\mathrm{th}}\right) := \left(\frac{v_t^{\mathrm{th}} - u_t^{\mathrm{th}}}{2}, \frac{u_t^{\mathrm{th}} + v_t^{\mathrm{th}}}{2}\right).$$

4.8.3 The surfer's position can be asymptotically recovered from the theoretical longitude

We start with the result which shows that, in principle, it is possible to recover the the true position of the surfer X_t in the time $t \in (0,1)$ from its theoretical longitude $\Psi_N^{\mathrm{th}}(t)$.

Lemma 4.8.1. *Let* $0 < t < 1$. *For any* $\varepsilon > 0$

$$\lim_{N\to\infty} \mathbb{P}_N\Big(T_N \in \mathcal{T}_{\square_N} : \; u_t(T_N) \neq u_t^{\mathrm{th}}(T_N)\Big) = 0 \tag{4.8.2}$$

and

$$\lim_{N\to\infty} \mathbb{P}_N\Big(T_N \in \mathcal{T}_{\square_N} : \; \left|v_t(T_N) - v_t^{\mathrm{th}}(T_N)\right| > \varepsilon\Big) = 0. \tag{4.8.3}$$

Proof. Let $0 < t < 1$ and $\varepsilon > 0$. We start with the proof of (4.8.2). Recall that the position of the surfer X_t corresponds to the position of the box with the number $\lceil (1-t)N^2 \rceil$ in the tableau

$(\partial^*)^{\lfloor tN^2 \rfloor}(T_N)$, cf. (4.2.5), and so by [PR07, Theorem 2] the random variable u_t converges in distribution to the measure ν_{1-t} which has no atoms and has a compact connected support

$$\operatorname{supp}(\nu_{1-t}) = \left[-2\sqrt{t(1-t)},\, 2\sqrt{t(1-t)}\right].$$

Observe that since ν_{1-t} has no atoms, whenever $u_t \in \operatorname{supp}(\nu_{1-t})$ then by the definition

$$u_t^{\mathrm{th}} = F^{-1}_{\nu_{1-t}}\left(\Psi_N^{\mathrm{th}}(t)\right) = u_t. \tag{4.8.4}$$

On the other hand

$$\mathbb{P}_N\big(T_N \in \mathcal{T}_{\square_N} :\ u_t(T_N) \notin \operatorname{supp}(\nu_{1-t})\big) \xrightarrow{N\to\infty} 0. \tag{4.8.5}$$

Indeed, for any $\varepsilon > 0$ consider the function $f_\varepsilon : \mathbb{R} \to \mathbb{R}$ given by

$$f_\varepsilon(x) := 1 - \min\left\{1, \frac{1}{\varepsilon}\operatorname{dist}\big(x, \mathbb{R}\setminus \operatorname{supp}(\nu_{1-t})\big)\right\}, \quad x \in \mathbb{R},$$

where $\operatorname{dist}(x, A) := \inf\{d(x,y) : y \in A\}$ is the Hausdorff distance of the point x from a set A. Clearly f_ε is continuous and bounded.

The distribution of the random variable u_t is a pushforward of the measure $\mathbb{P}_N$ under the mapping $T_N \mapsto u_t(T_N)$. Therefore by the convergence in distribution of the random variable u_t to the distribution given by the measure ν_{1-t} we get for any $\varepsilon > 0$

$$\mathbb{P}_N\big(T_N \in \mathcal{T}_{\square_N} :\ u_t(T_N) \notin \operatorname{supp}(\nu_{1-t})\big) \leqslant \int_{\mathcal{T}_{\square_N}} f_\varepsilon(u_t)\, \mathrm{d}\mathbb{P}_N \xrightarrow{N\to\infty} \int_{\mathbb{R}} f_\varepsilon \,\mathrm{d}\nu_{1-t}. \tag{4.8.6}$$

Clearly, f_ε converges pointwise as $\varepsilon \to 0$ to the indicator function $\mathbb{1}_{\overline{\mathbb{R}\setminus \operatorname{supp}(\nu_{1-t})}}$, therefore by the Lebesgue dominated convergence theorem

$$\lim_{\varepsilon\to 0}\int_{\mathbb{R}} f_\varepsilon \,\mathrm{d}\nu_{1-t} = \nu_{1-t}\left(\overline{\mathbb{R}\setminus \operatorname{supp}(\nu_{1-t})}\right) = \nu_{1-t}\Big(\partial\big(\operatorname{supp}(\nu_{1-t})\big)\Big) = 0.$$

This together with (4.8.6) implies (4.8.5).

A conjunction of (4.8.4) and (4.8.5) proves (4.8.2).

Equation (4.8.3) follows from the result of Biane [Bia98, Theorem 1.5.1]. We will shortly describe it here, but the more developed discussion and precise statements formulated using our notation are placed in Section 4.10.

The boundary of a Young diagram λ seen in the (u, v)-coordinate system can be viewed as a non-negative 1-Lipschitz function ω_λ, see Figure 4.14. The function ω_λ is initially defined on the interval I given by the range of the u-coordinates of λ, but it can be extended to a function defined on the real line $\mathbb{R}$ by gluing $\omega_\lambda|_I$ with the modulus function $x \mapsto |x|$. This extended function $\omega_\lambda : \mathbb{R} \to \mathbb{R}_+$ is called *the profile of* λ, cf. Section 4.10.1.

The restriction $T|_{\leqslant\lfloor(1-t)N^2\rfloor}$ of the random tableau T has a (random) shape

$$\lambda_{1-t} := \operatorname{sh} T|_{\leqslant\lfloor(1-t)N^2\rfloor}$$

whose (random) profile $\omega_{\lambda_{1-t}}$ is such that the following equality in terms of the u- and v-coordinates of the surfer (in time t) holds true:

$$v_t(T_N) = \omega_{\lambda_{1-t}}\big(u_t(T_N)\big)\,.$$

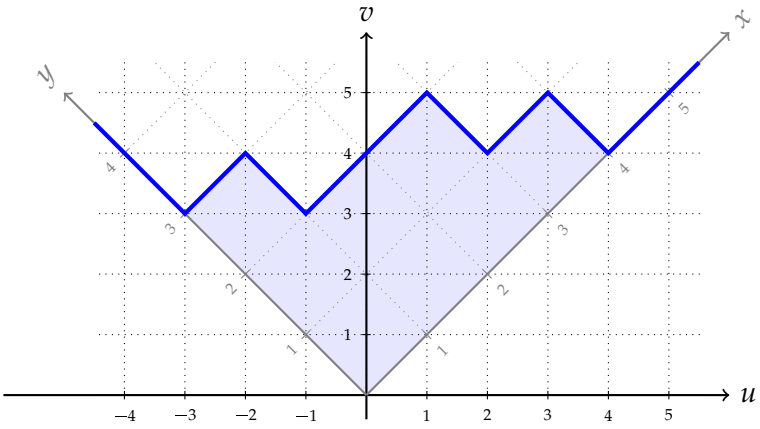

Figure 4.14: A Young diagram $\lambda = (4,3,1)$ shown in the Russian convention. The blue solid line represents its profile ω_λ. The (u,v)-coordinate system corresponding to the Russian convention and the XY- coordinate system corresponding to the French convention are shown.

On the other hand if $u_t(T_N) = u_t^{\text{th}}(T_N)$ then

$$v_t^{\text{th}}(T_N) = h_{1-t}(u_t^{\text{th}}(T_N)) = h_{1-t}(u_t(T_N)).$$

We proved in (4.8.2) that the set of tableaux $T_N \in \mathcal{T}_{\square_N}$ for which $u_t(T_N) = u_t^{\text{th}}(T_N)$ has asymptotically full probability. Therefore with asymptotically full probability the following inequality holds

$$\left|v_t(T_N) - v_t^{\text{th}}(T_N)\right| \leqslant \sup_{x\in\mathbb{R}} \left|\omega_{\lambda_{1-t}}(x) - h_{1-t}(x)\right|. \tag{4.8.7}$$

By the aforementioned result [Bia98, Theorem 1.5.1] (see Proposition 4.10.1 for the precise general statement) the right-hand-side of (4.8.7) converges in probability to 0. This completes the proof of (4.8.3) and Lemma 4.8.1.

□

4.8.4 A candidate for the random variable $\Psi_N(T_N)$, development of (S1)

Pick any $t_0 \in (0,1)$ and define for $T_N \in \mathcal{T}_{\square_N}$

$$\Psi_N(T_N) := \Psi_N^{\text{th}}(t_0)(T_N).$$

We will show that the random variable Ψ_N has the desired properties from Theorem 4.2.3.

For any $t \in [0,1]$ we define the *approximated u- and v-coordinate* of the surfer as

$$u_t^\Psi := \left(F_{v_{1-t}}\right)^{-1}(\Psi_N),$$
$$v_t^\Psi := h_{1-t}\left(u_t^\Psi\right).$$

These definitions were chosen in such a way that that the *approximated position of the surfer* in the XY coordinate system

$$\left(x_t^\Psi, y_t^\Psi\right) := \left(\frac{v_t^\Psi - u_t^\Psi}{2}, \frac{u_t^\Psi + v_t^\Psi}{2}\right) = P_{1-t,\Psi_N(T_N)}$$

is the point which appears in the statement of Theorem 4.2.3 and Eq. (4.8.1).

With this notation the expression in the modulus in the event in (4.8.1) takes the form

$$\left|X_t(T_N) - P_{1-t,\Psi_N(T_N)}\right| = \frac{1}{\sqrt{2}}\left|(u_t, v_t) - \left(u_t^{\Psi}, v_t^{\Psi}\right)\right|.$$

4.8.5 The proof of (S2) – the pointwise version of Theorem 4.2.3

Let $\varepsilon > 0$ and $t \in (0,1)$. By the triangle inequality,

$$\left|u_t(T_N) - u_t^{\Psi}(T_N)\right| \leqslant \left|u_t(T_N) - u_t^{\mathrm{th}}(T_N)\right| + \left|u_t^{\mathrm{th}}(T_N) - u_t^{\Psi}(T_N)\right| \tag{4.8.8}$$

and

$$\left|v_t(T_N) - v_t^{\mathrm{th}}(T_N)\right| \leqslant \left|v_t(T_N) - v_t^{\mathrm{th}}(T_N)\right| + \left|v_t^{\mathrm{th}}(T_N) - v_t^{\Psi}(T_N)\right|. \tag{4.8.9}$$

By Lemma 4.8.1, in each of the above two inequalities the first summand on the right-hand side converges in probability to 0, that is,

$$\left|u_t(T_N) - u_t^{\mathrm{th}}(T_N)\right| \xrightarrow{P} 0 \quad \text{and} \quad \left|v_t(T_N) - v_t^{\mathrm{th}}(T_N)\right| \xrightarrow{P} 0.$$

The second summands on the right hand side of (4.8.8) and (4.8.9) are the distances between the values of uniformly continuous functions, respectively, $\psi \mapsto u_t^{\psi}$ and the composition $\psi \mapsto h_{1-t}(u_t^{\psi})$ evaluated at the arguments

$$\Psi_N^{\mathrm{th}}(t) \quad \text{and} \quad \Psi_N^{\mathrm{th}}(t_0) = \Psi_N.$$

By Theorem 4.4.1 with $t_1 = \min(t, t_0)$ and $t_2 = \max(t, t_0)$ the distance between these two arguments converges in probability to 0, i.e.,

$$\Psi_N^{\mathrm{th}}(t) - \Psi_N \xrightarrow{P} 0.$$

Therefore we get

$$\left|u_t^{\mathrm{th}}(T_N) - u_t^{\Psi}(T_N)\right| \xrightarrow{P} 0 \quad \text{and} \quad \left|v_t^{\mathrm{th}}(T_N) - v_t^{\Psi}(T_N)\right| \xrightarrow{P} 0.$$

As the result

$$\left|u_t(T_N) - u_t^{\Psi}(T_N)\right| \xrightarrow{P} 0 \quad \text{and} \quad \left|v_t(T_N) - v_t^{\Psi}(T_N)\right| \xrightarrow{P} 0$$

which completes the proof (4.8.1) which is the pointwise version of Theorem 4.2.3.

4.8.6 The proof of (S3) – the full version of Theorem 4.2.3

4.8.6.1 Uniform continuity of the geographic coordinate system

We start with showing that the geographic coordinate system on the square (recall Section 4.2.4) is uniformly continuous.

Lemma 4.8.2. *The function*

$$[0,1] \times [0,1] \ni (\alpha, \psi) \mapsto P_{\alpha,\psi} = \left(x_\alpha^{\psi}, y_\alpha^{\psi}\right)$$

is uniformly continuous.

Proof. Since the mapping $\left(x_\alpha^\psi, y_\alpha^\psi\right) \mapsto \frac{1}{\sqrt{2}}\left(u_\alpha^\psi, v_\alpha^\psi\right)$ is an isometry (as a rotation in $\mathbb{R}^2$) it is enough to show that each coordinate of the function

$$[0,1]\times[0,1] \ni (\alpha,\psi) \mapsto \left(u_\alpha^\psi, v_\alpha^\psi\right) = \left(u_\alpha^\psi, h_{1-\alpha}\left(u_\alpha^\psi\right)\right)$$

is uniformly continuous.

Recall that the limit distribution ν_α has density (4.2.4). It is easy to show that for any $\alpha \in (0,1)$ the cumulative distribution function F_{ν_α} of ν_α fulfills the equation

$$F_{\nu_\alpha}(u) = F_{\mathrm{SC}}\left(\frac{u}{2\sqrt{\alpha(1-\alpha)}}\right) \quad \text{for all } |u| \leqslant 2\sqrt{\alpha(1-\alpha)}$$

where F_{SC} denotes the cumulative distribution function of the standard semicircle distribution with the density (4.1.3). This implies that for any $\psi \in [0,1]$ and $\alpha \in (0,1)$ we get

$$\psi = F_{\nu_{1-\alpha}}\left(u_\alpha^\psi\right) = F_{\mathrm{SC}}\left(\frac{u_\alpha^\psi}{2\sqrt{\alpha(1-\alpha)}}\right),$$

which after applying F_{SC}^{-1} gives

$$u_\alpha^\psi = 2\sqrt{\alpha(1-\alpha)}\cdot F_{\mathrm{SC}}^{-1}(\psi). \tag{4.8.10}$$

Moreover, by the definition $P_{0,\psi} = (0,0) \in \mathbb{R}^2$ and $P_{1,\psi} = (1,1) \in \mathbb{R}^2$ (cf. Section 4.2.4), hence (4.8.10) holds for all $\psi \in [0,1]$ and $\alpha \in [0,1]$.

Therefore the mapping $(\alpha,\psi) \mapsto u_\alpha^\psi$ is uniformly continuous since $\psi \mapsto F_{\mathrm{SC}}^{-1}(\psi)$ is uniformly continuous. Indeed, F_{SC}^{-1} is the inverse function of F_{SC} which is injective on $\left[-2\sqrt{\alpha(1-\alpha)}, 2\sqrt{\alpha(1-\alpha)}\right]$, continuous and has compact domain and range.

The function $(\alpha,u) \mapsto h_\alpha(u)$ is uniformly continuous on the domain

$$\Diamond := \left\{(\alpha,u) : \alpha \in [0,1] \text{ and } |u| \leqslant 2\sqrt{\alpha(1-\alpha)}\right\}$$

(as a continuous mapping on the compact set $\Diamond$). Hence the function $(\alpha,\psi) \mapsto v_\alpha^\psi$ is uniformly continuous as the composition of two uniformly continuous functions:

$$\Diamond \ni (\alpha,u) \mapsto h_\alpha(u) \quad \text{and} \quad (\alpha,\psi) \mapsto (1-\alpha, u_\alpha^\psi) \in \Diamond. \qquad \square$$

4.8.6.2 The proof of (S3) – the full version of Theorem 4.2.3

Let $\varepsilon > 0$. By Lemma 4.8.2 the function

$$[0,1]\times[0,1] \ni (\alpha,\psi) \mapsto P_{\alpha,\psi}$$

is uniformly continuous, so there exists $\delta > 0$ such that

$$\forall_{s,t\in[0,1]}\ |s-t| < \delta \implies \forall_{\psi\in[0,1]}\ \left|P_{s,\psi} - P_{t,\psi}\right| < \varepsilon. \tag{4.8.11}$$

Let us take a finite δ-net $0 = \alpha_1 < \cdots < \alpha_n = 1$ of the interval $[0,1]$. By the pointwise version (S2) of Theorem 4.2.3, which we proved in Section 4.8.5,

$$\left|X_{\alpha_i}(T_N) - P_{1-\alpha_i, \Psi_N(T_N)}\right| \xrightarrow{P} 0 \quad \text{for} \quad i \in \{1,\ldots,n\} \tag{4.8.12}$$

(the latter holds for $i = 1$ and $i = n$ by the definition of $P_{\alpha,\psi}$, cf. Section 4.2.4). Therefore there exists a subset $\mathcal{T}_N^* \subseteq \mathcal{T}_{\square_N}$ of asymptotically full measure which consists of tableaux T_N with the property that for each $i \in \{1, \dots, n\}$

$$\left|x_{\alpha_i}(T_N) - x^{\Psi}_{\alpha_i}(T_N)\right| < \varepsilon \quad \text{and} \quad \left|y_{\alpha_i}(T_N) - y^{\Psi}_{\alpha_i}(T_N)\right| < \varepsilon. \tag{4.8.13}$$

By the monotonicity of the sliding path for any $i \in \{1, \dots, n-1\}$ and $t \in [\alpha_i, \alpha_{i+1}]$

$$x_{\alpha_{i+1}} \leqslant x_t \leqslant x_{\alpha_i} \quad \text{and} \quad y_{\alpha_{i+1}} \leqslant y_t \leqslant y_{\alpha_i}. \tag{4.8.14}$$

By (4.8.13) and (4.8.14) for any $T_N \in \mathcal{T}_N^*$ and any $i \in \{1, \dots, n-1\}$ and $t \in [\alpha_i, \alpha_{i+1}]$ the following system of inequalities is satisfied:

$$\begin{cases} -\varepsilon + \left(x^{\Psi}_{\alpha_{i+1}} - x^{\Psi}_t\right) \leqslant x_t - x^{\Psi}_t \leqslant \left(x^{\Psi}_{\alpha_i} - x^{\Psi}_t\right) + \varepsilon; \\ -\varepsilon + \left(y^{\Psi}_{\alpha_{i+1}} - y^{\Psi}_t\right) \leqslant y_t - y^{\Psi}_t \leqslant \left(y^{\Psi}_{\alpha_i} - y^{\Psi}_t\right) + \varepsilon. \end{cases}$$

Since for any $t \in [0, 1]$

$$X_t = (x_t, y_t) \quad \text{and} \quad P_{1-t,\Psi_N(T_N)} = \left(x^{\Psi}_t, y^{\Psi}_t\right)$$

and by (4.8.11) for any $i \in \{1, \dots, n-1\}$ and $t \in [\alpha_i, \alpha_{i+1}]$

$$\max\left\{\left|x^{\Psi}_{\alpha_i} - x^{\Psi}_t\right|, \left|x^{\Psi}_{\alpha_{i+1}} - x^{\Psi}_t\right|, \left|y^{\Psi}_{\alpha_i} - y^{\Psi}_t\right|, \left|y^{\Psi}_{\alpha_{i+1}} - y^{\Psi}_t\right|\right\} < \varepsilon$$

we infer that for $T_N \in \mathcal{T}_N^*$

$$\sup_{t\in[0,1]} \left|X_t(T_N) - P_{1-t,\Psi_N(T_N)}\right| < 2\varepsilon.$$

This completes the proof of (S3) since $\mathcal{T}_N^*$ has asymptotically full probability.

4.8.7 Limit distribution of the random variable Ψ_N

We will show the second component of Theorem 4.2.3, namely that the random variable Ψ_N converges in distribution to the uniform distribution on the unit interval $[0, 1]$.

Let G_N denote the cumulative distribution function of the random variable $\Psi_N : \mathcal{T}_{\square_N} \to [0, 1]$. For any $z \in [0, 1]$ we have (recall (4.4.1))

$$G_N(z) = \mathbb{P}_N\left(T_N : \ F_{\nu_{1-t_0}}\left(u_{t_0}(T_N)\right) \leqslant z\right) = \mathbb{P}_N\left(T_N \in \mathcal{T}_{\square_N} : \ u_{t_0}(T_N) \leqslant \left(F_{\nu_{1-t_0}}\right)^{-1}(z)\right). \tag{4.8.15}$$

By [PR07, Theorem 2], the distribution of the random variable u_{t_0} converges weakly (as $N \to \infty$) to the measure ν_{1-t_0} which has no atoms, so the right-hand side of (4.8.15) converges to

$$F_{\nu_{1-t_0}}\left(F^{-1}_{\nu_{1-t_0}}(z)\right) = z$$

which is the cumulative distribution function of the uniform measure $U(0, 1)$. This completes the proof of the second component of Theorem 4.2.3, and hence the proof of Theorem 4.2.3.

4.9 The correspondence between evacuation and sliding paths

The results which we consider in this section hold for general, not necessarily square tableaux. For a tableau $T \in \mathcal{T}_\lambda$ with $n = |\lambda|$ boxes we denote by

$$\operatorname{revevac}(T) = \Big(\operatorname{pos}_n\big(j^{n-1}(T)\big),\ \ldots,\ \operatorname{pos}_n\big(j^1(T)\big),\ \operatorname{pos}_n(T) \Big)$$

the evacuation path (4.1.8) written in the reverse order.

The following result shows an intimate relationship between the sliding paths and the evacuation paths and, in particular, implies equivalence of Theorems 4.2.3 and 4.2.4 (see Section 4.9.2 for the proof).

Proposition 4.9.1. *Let λ be a fixed Young diagram and let $T \in \mathcal{T}_\lambda$ be a random standard Young tableau sampled according to the uniform measure on $\mathcal{T}_\lambda$. Then the probability distributions of the lazy sliding path $\mathbf{q}(T)$ and the evacuation path $\operatorname{revevac}(T)$ coincide.*

Proof. We will construct a certain bijection $\varepsilon^* \colon \mathcal{T}_\lambda \to \mathcal{T}_\lambda$ on the set of tableaux of shape λ. Clearly, the random tableaux T and $\varepsilon^*(T)$ have the same distribution. An application of Proposition 4.9.3 below completes the proof. □

In the remaining part of this section we will present the details of the map ε^* and we will prove that Proposition 4.9.3 indeed holds true.

4.9.1 Dual evacuation

The dual evacuation has a beautiful algorithmic description in terms of the manipulations of the boxes of T, cf. [PW11, Definition 2.10], however we will not make use of it. For our purposes it is more convenient to define the dual evacuation ε^* implicitly by Robinson–Schensted–Knuth correspondence as follows. For a permutation $\sigma = (\sigma_1, \ldots, \sigma_n) \in \mathfrak{S}_n$ we denote

$$\sigma^\sharp := (n+1-\sigma_n, \ldots, n+1-\sigma_1) \in \mathfrak{S}_n.$$

If σ corresponds to a pair (P, Q) under RSK, then $\sigma^\sharp$ corresponds to $\big(\varepsilon^*(P), \varepsilon^*(Q)\big)$ under RSK, see [Sta99, A1.2.10].

We will use the following fact (see [Sag01, Proposition 3.9.3] for the proof).

Fact 4.9.2 ([Sch63])**.** *For any $\sigma \in \mathfrak{S}_n$, the following identity holds up to renumbering of the boxes on the left-hand side, so that the resulting tableau becomes standard*

$$\big(j \circ Q\big)(\sigma) = (Q \circ s)(\sigma) \qquad \text{for } \sigma = (\sigma_1, \ldots, \sigma_n) \in \mathfrak{S}_n \tag{4.9.1}$$

where $s(\sigma) = s(\sigma_1, \sigma_2, \ldots, \sigma_n) := (\sigma_2, \ldots, \sigma_n)$ is a shift.

Proposition 4.9.3.

$$\mathbf{q}(T) = \operatorname{revevac}\big(\varepsilon^*(T)\big).$$

Proof. For any tableaux R, S we will use a shorthand notation

$$R/S = \operatorname{sh} R/\operatorname{sh} S$$

for the skew diagram obtained by subtracting their shapes. In all examples below this skew diagram $R/S = \{\square\}$ consists of a single box; we will write shortly $\square = R/S$.

Let $T = Q(\sigma)$ be a recording tableau of some permutation σ; with these notations $\varepsilon^*(T) = Q\left(\sigma^\sharp\right)$.

By (4.9.1), the lazy sliding path fulfills for $i \in [n]$

$$\mathbf{q}_i(T) \;=\; Q\left(\sigma_1,\dots,\sigma_i\right)/j\big(Q\left(\sigma_1,\dots,\sigma_i\right)\big) \;=\; Q\left(\sigma_1,\sigma_2,\dots,\sigma_i\right)/Q\left(\sigma_2,\dots,\sigma_i\right). \quad (4.9.2)$$

On the other hand, by (4.9.1), applying jeu de taquin $n-i$ times to $\varepsilon^*(T) = Q\left(\sigma^\sharp\right)$, leads to the tableau (up to renumbering boxes on the left-hand side so that the tableau becomes standard)

$$j^{n-i}\left(\varepsilon^*(T)\right) = Q\left(n+1-\sigma_i,\dots,n+1-\sigma_2,n+1-\sigma_1\right).$$

The position of the box with the maximal entry in a recording tableau can be found by comparing this tableau to the recording tableau of a truncated sequence; it follows that

$$\mathrm{pos}_n\, j^{n-i}\left(\varepsilon^*(T)\right) = Q\left(n+1-\sigma_i,\dots,n+1-\sigma_2,n+1-\sigma_1\right)/ Q\left(n+1-\sigma_i,\dots,n+1-\sigma_2\right). \quad (4.9.3)$$

By the result of Schensted [Sch61, Lemma 7] and Greene theorem [Gre74, Theorem 3.1] the shapes of the tableaux which contribute to the right-hand sides of (4.9.2) and (4.9.3) are equal which concludes the proof. □

4.9.2 Proof of Theorem 4.2.4

Proof of Theorem 4.2.4. Let $N \in \mathbb{N}$. Let $\Psi_N \colon \mathcal{T}_{\square_N} \to [0,1]$ be the random variable which is given by Theorem 4.2.3. We define the random variable $\widetilde{\Psi}_N \colon \mathcal{T}_{\square_N} \to [0,1]$ by

$$\widetilde{\Psi}_N(T_N) := \Psi_N(\varepsilon^*(T_N)).$$

Since ε^* is a bijection,

$$\begin{aligned}
\mathbb{P}_N\Big\{T_N \in \mathcal{T}_{\square_N} : \sup_{t\in[0,1)} \Big|X_t(T_N) - P_{1-t,\Psi_N(T_N)}\Big| > \varepsilon\Big\} = \\
\mathbb{P}_N\Big\{T_N \in \mathcal{T}_{\square_N} : \sup_{t\in[0,1)} \Big|X_t(\varepsilon^*(T_N)) - P_{1-t,\Psi_N(\varepsilon^*(T_N))}\Big| > \varepsilon\Big\} = \\
\mathbb{P}_N\Big\{T_N \in \mathcal{T}_{\square_N} : \sup_{t\in[0,1)} \Big|\frac{1}{N}\mathbf{q}_{\lceil(1-t)N^2\rceil}(T_N) - P_{1-t,\widetilde{\Psi}_N(T_N)}\Big| > \varepsilon\Big\} = \\
\mathbb{P}_N\Big\{T_N \in \mathcal{T}_{\square_N} : \sup_{t\in(0,1]} \Big|\frac{1}{N}\mathbf{q}_{\lfloor tN^2\rfloor}(T_N) - P_{t,\Psi_N(T_N)}\Big| > \varepsilon\Big\},
\end{aligned}$$

where the second equality is a consequence of Proposition 4.9.3. By Theorem 4.2.3 the left-hand side converges to 0 in the limit $N \to \infty$; on the other hand the right-hand side is the probability which appears in Theorem 4.2.4. □

4.10 Generalizations of the main results for non-square tableaux

4.10.1 Continuous diagrams

We call a function $\omega : \mathbb{R} \to \mathbb{R}$ a *continuous diagram* [Ker93a; Ker98] if

- ω is a 1-Lipschitz function, i.e.,

$$|\omega(u_1) - \omega(u_2)| \leqslant |u_1 - u_2| \qquad \text{for all } u_1, u_2 \in \mathbb{R};$$

- $\omega(u) = |u|$ for sufficiently large $|u|$.

We will denote the set of continuous diagrams by $\mathcal{CY}$; we endow this set with the L^∞-metric. (Our definition is more specific than the one of Kerov [Ker93a] who allows to additionally translate our *centered* continuous diagrams along the real line.)

Any (usual) Young diagram λ seen in the (u,v)-coordinate system is a 1-Lipschitz function defined on some interval (given by the range of the u-coordinates of λ) and has slopes equal to ± 1. It can be extended outside its initial domain by a modulus function $x \mapsto |x|$. In this way we obtain a continuous diagram ω_λ to which we will refer as *the profile of* λ, see Figure 4.14.

Let $s > 0$. For a continuous diagram ω we define *the scaling of* ω *by* s as the following continuous diagram denoted by $s\omega$

$$s\omega\colon\ \mathbb{R} \ni u \mapsto s \cdot \omega\left(s^{-1}u\right).$$

Let (λ_N) be a sequence of Young diagrams with the property that the sequence of the corresponding rescaled profiles

$$\left(\frac{1}{\sqrt{|\lambda_N|}}\omega_{\lambda_N}\right)$$

converges to a continuous diagram Λ in the L^∞-metric, that is,

$$\sup_{u\in\mathbb{R}}\left|\frac{1}{\sqrt{|\lambda_N|}}\,\omega_{\lambda_N}\left(\sqrt{|\lambda_N|}\,u\right) - \Lambda(u)\right| \xrightarrow{N\to\infty} 0.$$

We will call Λ *the limit shape* for the sequence of Young diagrams (λ_N) and denote such convergence by $\frac{1}{\sqrt{|\lambda_N|}}\lambda_N \to \Lambda$.

4.10.2 The asymptotic setup

Let $C \geqslant 1$ be a fixed constant. For each integer $N \geqslant 1$ let λ_N be a C-balanced Young diagram. We assume that

$$\lim_{N\to\infty} |\lambda_N| = \infty$$

and that there exists a limit shape $\Lambda \in \mathcal{CY}$ for the sequence (λ_N), i.e., that $\frac{1}{\sqrt{|\lambda_N|}}\lambda_N \to \Lambda$.

Our goal in Section 4.10 is to find counterparts of Theorems 4.2.3 and 4.2.4 in which the sequence $(\square_N)$ of square diagrams is replaced by the sequence (λ_N) of C-balanced Young diagrams.

4.10.3 The limit curves

The result of Pittel and Romik concerning the existence of the level curves [PR07, Theorem 1(i)], cf. Section 4.2.2, is a special case of a more general phenomenon. Using the results of Biane [Bia98, Theorem 1.2 and Theorem 1.5.1] one can show that under the assumptions from Section 4.10.2 there exists a family of level curves for a uniformly random Young tableau of the shape λ_N (in the limit as $N \to \infty$). The following proposition describes precisely this result.

Proposition 4.10.1. *Let (λ_N) be a sequence of C-balanced Young diagrams such that $|\lambda_N| \to \infty$ and $\frac{1}{\sqrt{|\lambda_N|}}\lambda_N \to \Lambda$ for some continuous diagram $\Lambda \in \mathcal{CY}$ (i.e., (λ_N) fulfills the assumptions in Section 4.10.2). For any $\alpha \in [0,1]$ there exists a continuous diagram*

$\Lambda_\alpha \in \mathcal{CY}$ such that

$$\frac{1}{\sqrt{|\lambda_N|}} \operatorname{sh}\Big(T_N\big|_{\leqslant \lfloor \alpha \cdot |\lambda_N| \rfloor}\Big) \xrightarrow{P} \Lambda_\alpha$$

where T_N is a uniformly random element of $\mathcal{T}_{\lambda_N}$.

We will say that Λ_α is *the α-level curve* for the sequence (λ_N) or, shortly, the α-level curve for the diagram Λ. Note that Λ_0 is the empty diagram and $\Lambda_1 = \Lambda$.

For example, in the case when $\lambda_N = \square_N$ is a square Young diagram, the α-level curve for (λ_N) is the curve h_α, cf. Section 4.2.2.

Remark 4.10.2. Biane proved his results [Bia98, Theorem 1.2 and Theorem 1.5.1] with the tools of the free probability theory [MS17], but Proposition 4.10.1 can be also showed using the beam models [Sun18] or by solving a gradient variational problem [KP21].

4.10.4 The limit measures on the level curves

The second result of Pittel and Romik which gives explicitly the limit measure on the α-level curve for the square diagram [PR07, Theorem 2], cf. Section 4.2.3, is a special case of another general result. It turns out that to every continuous diagram we can associate two natural measures – the *transition measure* and the *cotransition measure* – which have very natural interpretations in the case of the usual Young diagrams.

4.10.4.1 Transition measure of a continuous diagram

To any continuous diagram $\omega \in \mathcal{CY}$, one can associate a probability measure μ_ω, called *the transition measure of ω* [Ker93b; Bia98], as the unique compactly supported measure on $\mathbb{R}$ such that its Cauchy transform

$$G_{\mu_\omega}(z) := \int_{\mathbb{R}} \frac{1}{z-x}\, \mathrm{d}\mu_\omega(x)$$

is given by the equation

$$G_{\mu_\omega}(z) = \frac{1}{z} \exp \int_{\mathbb{R}} \frac{1}{x-z} \sigma'(x)\, \mathrm{d}x = \frac{1}{z} \exp \int_{\mathbb{R}} \frac{1}{(x-z)^2} \sigma(x)\, \mathrm{d}x$$

where $\sigma(u) := (\omega(u) - |u|)/2$.

The motivations for this notion are related to random walks on the set of Young diagrams: the atoms of the transition measure μ_{ω_λ} of a usual Young diagram λ correspond to the Markov's transition probabilities in the Plancherel growth process starting in λ [Ker93b, Section 3.2].

The mapping which to a continuous diagram ω assigns the transition measure μ_ω is a *homeomorphism* [Ker93b, Section 2.3]. Moreover, a continuous diagram is uniquely determined by its transition measure.

4.10.4.2 Cotransition measure of a continuous diagram

For a continuous diagram $\omega \in \mathcal{CY}$ we define its *area* as the area of the region between the profile and the x- and the y-axis:

$$A(\omega) = \int_{\mathbb{R}} \big(\omega(x) - |x|\big)\, \mathrm{d}x.$$

The cotransition measure ν_ω of ω is defined as the unique probability measure with the Cauchy transform G_{ν_ω} given by the following equation [Rom04, Equation (8)]:

$$\frac{A(\omega)}{2} G_{\nu_\omega}(x) = x - \frac{1}{G_{\mu_\omega}(x)}. \tag{4.10.1}$$

By convention, the cotransition measure of the empty diagram $\nu_{\omega_\varnothing} = \delta_0$ is defined to be the measure concentrated in 0.

The cotransition measure ν_{ω_λ} of a usual Young diagram λ is the distribution of the u-coordinate of the box with the maximal entry $|\lambda|$ in a uniformly random standard tableau of shape λ, cf. [Rom04, page 628 and the comment below Eq. (6)]. In particular, the measure ν_α introduced in Section 4.2.3 to which we referred as *the limit measure* is the cotransition measure corresponding to the continuous diagram h_α (more precisely, to the proper extension of the function h_α given by (4.2.2) by $x \mapsto |x|$ and $x \mapsto 2 - |x|$).

Be advised that diagrams of different shape may have the same cotransition measure. For example, the square Young diagram $\square_N$ has the same cotransition measure $\nu_{\omega_{\square_N}} = \delta_0$ concentrated at the point $u = 0$, no matter which size of the square $N \in \mathbb{N}$ we choose. However, if we restrict our considerations to the set of (centered) continuous diagrams of fixed positive area, then any diagram is uniquely determined by its cotransition measure and this correspondence is a homeomorphism, [Rom04, Theorem 6].

4.10.4.3 The limit measures on the level curves of continuous diagram

We will refer to the cotransition measure ν_{Λ_α} corresponding to the α-level curve Λ_α for a continuous diagram Λ as *the limit* (or *cotransition*) *measure* on the level curve Λ_α.

The cumulative distribution function of the limit measure ν_{Λ_α} will be denoted by F_{Λ_α}, i.e.,

$$F_{\Lambda_\alpha}(u) := \nu_{\Lambda_\alpha}\big((-\infty, u]\big) \text{ for each } u \in \mathbb{R}.$$

The density of the limit measure ν_{Λ_α} will be denoted by f_{Λ_α}, whenever this density exists.

4.10.5 The geographic coordinate system

We will endow a continuous diagram Λ with the system of geographic coordinates, cf. Section 4.2.4. For this purpose we view the shape Λ as the following compact subset of the (x, y)-Cartesian plane

$$\Lambda^{\mathrm{Cart}} := \overline{\big\{(x,y) \in \mathbb{R}^2 : \ |x-y| < x+y < \Lambda(x-y)\big\}} = \\ \overline{\big\{(x,y) \in [0,\infty)^2 : \ x+y < \Lambda(x-y)\big\}}.$$

(Recall that $u = x - y$ and $v = x + y$ are the (u, v) coordinates, cf. Section 4.2.2.)

For any $\alpha \in [0, 1]$ we define *the quantile function* for the limit measure ν_{Λ_α} by the formula

$$Q_{\Lambda_\alpha}(\psi) := \inf\big\{u \in \operatorname{supp}(\nu_{\Lambda_\alpha}) : \ F_{\Lambda_\alpha}(u) \geqslant \psi\big\} \quad \text{for } \psi \in [0,1] \tag{4.10.2}$$

where $\operatorname{supp}(\mu)$ denotes *the support* of the measure μ. In particular, $Q_{\Lambda_0} \equiv 0$.

For given $\alpha \in [0, 1]$ and $\psi \in [0, 1]$ there is exactly one point $p = (x, y) \in \Lambda^{\mathrm{Cart}}$ such that

- p lies on the level curve Λ_α seen in the XY-coordinates system, i.e.,

$$x + y = \Lambda_\alpha(x - y);$$

- the u-coordinate of p is given by the quantile function:

$$u(p) = x - y = Q_{\Lambda_\alpha}(\psi).$$

We will denote this point by $P_{\alpha,\psi} := (x_\alpha^\psi, y_\alpha^\psi) \in \Lambda^{\mathrm{Cart}}$. In particular, by the definition of $\nu_{\Lambda_0} = \delta_0$ we have $P_{0,\psi} = (0,0) \in \mathbb{R}^2$ for any $\psi \in [0,1]$. Additionally we denote by

$$u_\alpha^\psi := x_\alpha^\psi - y_\alpha^\psi \quad \text{and} \quad v_\alpha^\psi := x_\alpha^\psi + y_\alpha^\psi$$

the u- and v-coordinate of the point $P_{\alpha,\psi}$.

We will refer to the mapping $[0,1]^2 \ni (\alpha,\psi) \mapsto P_{\alpha,\psi} \in \Lambda^{\mathrm{Cart}}$ as to *the geographic coordinates system*.

Remark 4.10.3. There may be some problem with defining the counterparts of the longitude and the latitude (the geographic coordinates) of the point $p \in \Lambda^{\mathrm{Cart}}$ like we did in Section 4.2.4. We defined *the latitude* as *the unique* $\alpha \in [0,1]$ for which p lies on the level curve h_α (more precisely, on the restriction of the level curve h_α to the support of the corresponding cotransition measure ν_α). We are not sure if such uniqueness holds in a general case when Λ is an arbitrary continuous diagram. To make things worse, the definition of *the longitude* depends on the limit measure $\nu_{\Lambda_{\alpha(p)}}$ corresponding to the $\alpha(p)$-level curve (circle of latitude with the latitude $\alpha(p)$, cf. Sections 4.2.2 and 4.2.4). In the worst scenario, not only we shall pick some latitude $\alpha(p)$, but also the limit measure $\nu_{\Lambda_{\alpha(p)}}$ may have atoms. In particular, an attempt of using these direct counterparts of the definitions from Section 4.2.4 in the more general context may lead to the situation in which several points have the same geographic coordinates or some geographic coordinates (α,ψ) are not used. The case of the L-shape diagram, see Figure 4.10, is an example of the first problem.

Problem 4.10.4. Let Λ be a continuous diagram. Show that for any point

$$p \in \Lambda^{\mathrm{UV}} := \overline{\left\{(u,v) : \ u \in \mathbb{R} \ \text{ and } \ |u| < v < \Lambda(u)\right\}}$$

there is a unique $\alpha \in [0,1]$ with the property that

$$p \in \left\{(u, \Lambda_\alpha(u)) : \ u \in \mathrm{supp}(\nu_{\Lambda_\alpha})\right\}.$$

In other words, show that for any point $p \in \Lambda^{\mathrm{UV}}$ there exists a unique level curve Λ_α (for some $\alpha \in [0,1]$) which restricted to the support of the corresponding cotransition measure ν_{Λ_α} contains p.

4.10.6 Extension of the main results

Theorem 4.10.5. *Let (λ_N) fulfill the assumptions in Section 4.10.2) and assume that*

(⋆) the geographic coordinates system is continuous, i.e., the map $[0,1]^2 \ni (\alpha,\psi) \mapsto P_{\alpha,\psi}$, is continuous.

Then the analogues of Theorems 4.2.3 and 4.2.4 hold true, i.e., if T_N is a uniformly random element of $\mathcal{T}_{\lambda_N}$ then:

- *there exists a family of random variables $\Psi_N : \mathcal{T}_{\lambda_N} \to [0,1]$ indexed by $N \in \mathbb{N}$ such that*

$$\sup_{t\in[0,1]} \left| X_t(T_N) - P_{1-t,\Psi_N(T_N)} \right| \xrightarrow{P} 0, \tag{4.10.3}$$

- *there exists a family of random variables* $\widetilde{\Psi}_N : \mathcal{T}_{\lambda_N} \to [0,1]$ *indexed by* $N \in \mathbb{N}$ *such that*

$$\sup_{t\in[0,1]} \left| \frac{1}{N} \mathbf{q}_{\lfloor t|\lambda_N|\rfloor}(T_N) - P_{t,\widetilde{\Psi}_N(T_N)} \right| \xrightarrow{P} 0.$$

The probability distribution of the random variable Ψ_N *(respectively,* $\widetilde{\Psi}_N$*) converges, as* $N \to \infty$*, to the uniform distribution on the unit interval* $[0,1]$.

Proof. The proof of Theorem 4.2.3 is applicable in this more general case – one shall replace all occurrences of the $\square_N$ by λ_N and change the references to the limit measures. We enumerate the properties of square Young diagrams which played the crucial role in the proof of Theorem 4.2.3.

- $\square_N$ is a 1-balanced Young diagram (we used this property in Proposition 4.5.1 and Theorem 4.6.2);
- the cotransition measure ν_α corresponding to the level curve h_α has no atoms and has a connected support (we used this property in Theorem 4.4.1 and Proposition 4.5.1);
- the distribution of u_α – the u-coordinate of the surfer in time α – converges to the cotransition measure $\nu_{1-\alpha}$ (we used this property in Lemma 4.8.1);
- the uniform continuity of the geographic coordinates system, i.e., the uniform continuity of the mapping $(\alpha, \psi) \mapsto P_{\alpha,\psi}$, cf. Lemma 4.8.2.

Notice that the counterparts of all these properties are present in our new setting. In particular, the distribution of the u-coordinate of the surfer converges to the proper limit measure since the correspondence between the (centered) continuous diagrams of fixed positive area and the cotransition measures is a homeomorphism, cf. Section 4.10.4.2. Moreover, the assumption $(\star)$ on the continuity of the geographic coordinates system assures that for any $\alpha \in [0,1]$ the support of the limit measure ν_{Λ_α} is connected. □

4.10.7 Example: random rectangular tableaux

For any real numbers $a, b > 0$ let $\square_{a\times b}$ denote the rectangle with the left bottom corner positioned in $(0,0) \in \mathbb{R}^2$ and with sides a and b (on X and Y axis, respectively, when seen in the (x,y)-coordinates system).

Let (M_i) and (N_i) be two sequences of positive integers which fulfill the conditions from Section 4.1.1.3, i.e., $M_i \to \infty$ and $N_i \to \infty$, and there is some (shape parameter) $\theta > 0$ such that

$$\lim_{i\to\infty} \frac{M_i}{N_i} = \theta.$$

We define for $i \in \mathbb{N}$

$$\lambda_i := \square_{M_i \times N_i}$$

to be the rectangular Young diagram which has M_i rows and N_i columns.

The following theorem generalizes Theorem 4.2.4 (which is a special case for $M_i = N_i = i$).

Corollary 4.10.6. *For* $i \in \mathbb{N}$ *let* T_i *be a uniformly random tableau of the shape* $\square_{M_i\times N_i}$*. Then the rescaled lazy sliding path* $\frac{1}{\sqrt{M_i N_i}} \mathbf{q}(T_i)$ *with respect to the supremum norm converges in probability to the random function*

$$t \mapsto \Xi_S(t) = 2\sqrt{t(1-t)}\, S + \frac{\theta - 1}{\sqrt{\theta}}\, t \tag{4.10.4}$$

where S *denotes the random variable with the standard semicircular distribution, cf.* (4.1.3).

Proof. We will check that the assumptions of Theorem 4.10.5 are fulfilled and find the explicit formula for the geographic coordinates system.

Clearly, the sequence $\left(\frac{1}{\sqrt{M_iN_i}}\square_{M_i\times N_i}\right)$ converge to the limit shape $\Lambda = \square_{\sqrt{\theta}\times 1/\sqrt{\theta}}$. We apply Lemma 4.10.7 below with $a := 1/\sqrt{\theta}$ and $b := \sqrt{\theta}$ to see that

- the geographic coordinates system on $\square_{\sqrt{\theta}\times 1/\sqrt{\theta}}$ is continuous,
- for any $\psi \in [0,1]$ and $\alpha \in [0,1]$ the ψ-th quantile u_ψ of the cotransition measure ν_{Λ_α} is given by
$$u_\psi = 2\sqrt{\alpha(1-\alpha)}F_{\mathrm{SC}}^{-1}(\psi) + \frac{\theta-1}{\sqrt{\theta}}\alpha$$
where F_{SC} denotes the cumulative distribution function of the standard semicircle distribution, cf. (4.1.3).

Notice that if U is a random variable with the uniform $U(0,1)$ distribution then $F_{\mathrm{SC}}^{-1}(U)$ has the standard semicircle distribution.

By Theorem 4.10.5 (its second and third part) the (rescaled) lazy sliding path $\frac{1}{\sqrt{M_iN_i}}\mathbf{q}(T_i)$ with respect to the supremum norm converges in probability to the random function (4.10.4). □

Lemma 4.10.7. *Let $a, b > 0$ and $\Lambda := \omega_{\square_{a\times b}}$ be the profile of $\square_{a\times b}$. Then for any $\alpha \in (0,1)$ the cotransition measure ν_{Λ_α} corresponding to the α-level curve Λ_α has the density*

$$f_{\nu_{\Lambda_\alpha}}(x) = \frac{1}{2\sqrt{ab\cdot\alpha(1-\alpha)}}\, f_{\mathrm{SC}}\left(\frac{x+\alpha(a-b)}{2\sqrt{ab\cdot\alpha(1-\alpha)}}\right) \tag{4.10.5}$$

where f_{SC} is the density of the standard semicircular distribution, cf. (4.1.3).

Proof. The following calculations use (4.10.1) and some relations between the R-transform and the Cauchy transform of the appropriate transition measures, see [MS17, Section 3] for the theory.

The Cauchy transform of the transition measure μ_Λ of the rectangular diagram is given by [Rom04, Equation (2)]

$$G(z) := G_{\mu_\Lambda}(z) = \frac{z-(b-a)}{(z+a)(z-b)}. \tag{4.10.6}$$

It is an analytic function and in some neighborhood of ∞ it is invertible [MS17, Section 3, Theorem 17(i)]. Moreover, there exists a neighborhood $U \subset \mathbb{C}$ of 0 for which $G|_{G^{-1}(U)}$ is invertible [MS17, Section 3, Theorem 17(ii)] and we can calculate the R-transform of the measure μ_Λ with the formula [MS17, Section 3, Theorem 17(iii)]

$$R(z) := R_{\mu_\Lambda}(z) = G^{-1}(z) - \frac{1}{z} \quad \text{for } z \in U\backslash\{0\}.$$

Substituting in the latter z with $G(z')$ (for some $z' \in G^{-1}(U\backslash\{0\})$) we get the relation

$$z = R\big(G(z)\big) + \frac{1}{G(z)} \quad \text{for } z \in G^{-1}(U\backslash\{0\}). \tag{4.10.7}$$

We use this equality in order to substitute each occurrence of the variable z on the right-hand side of (4.10.6); by clearing of the denominator we obtain

$$R(G) + \frac{1}{G} - (b-a) = G\cdot\left(R(G)+\frac{1}{G}+a\right)\left(R(G)+\frac{1}{G}-b\right), \tag{4.10.8}$$

where we used the shorthand notation $G = G(z)$. By the choice of U as the neighborhood of 0 we get that (4.10.8) is fulfilled with G replaced by any complex number $z \in U\backslash\{0\}$, i.e., the R-transform fulfills the following quadratic equation for any $z \in U\backslash\{0\}$

$$R(z) + \frac{1}{z} - (b-a) = z \cdot \left(R(z) + \frac{1}{z} + a\right)\left(R(z) + \frac{1}{z} - b\right). \tag{4.10.9}$$

Now, we will calculate the Cauchy transform of the transition measure μ_{Λ_α} on the level curve Λ_α. Denote by R_α and G_α, respectively, the R-transform and the G-transform of μ_{Λ_α}. The R-transforms of the transition measures μ_Λ and μ_{Λ_α} are related by the following correspondence [Bia98, Theorem 1.2]

$$R_\alpha(z) := R_{\mu_{\Lambda_\alpha}}(z) = R(\alpha \cdot z) \quad \text{for } z \in U\backslash\{0\}.$$

Let us put $\alpha \cdot z$ instead of z in (4.10.9) (this substitution is legal since the neighborhood U can be taken to be a convex set). Equation (4.10.9) implies therefore that $R_\alpha(z)$ is a solution to the following quadratic equation

$$R_\alpha(z) + \frac{1}{\alpha z} - (b-a) = \alpha z \left(R_\alpha(z) + \frac{1}{\alpha z} + a\right)\left(R_\alpha(z) + \frac{1}{\alpha z} - b\right) \tag{4.10.10}$$

for any $z \in U\backslash\{0\}$.

In (4.10.10) we substitute each occurrence of the variable z by $G_\alpha(z)$; this substitution is valid as long as $|z|$ is big enough so that $G_\alpha(z) \in U\backslash\{0\}$. Let us denote additionally $H_\alpha = \frac{1}{G_\alpha}$; then we use the relation (4.10.7) and substitute each occurrence of $R_\alpha\big(G_\alpha(z)\big)$ by $z - H_\alpha(z)$. Then (4.10.10) takes the form

$$H_\alpha(z)\left(z - (b-a) + \left(\frac{1}{\alpha} - 1\right) H_\alpha(z)\right) = \alpha\left(z + a + \left(\frac{1}{\alpha} - 1\right) H_\alpha(z)\right)\left(z - b + \left(\frac{1}{\alpha} - 1\right) H_\alpha(z)\right) \tag{4.10.11}$$

which holds if $|z|$ is big enough. For any z big enough, the latter is a quadratic equation in $H_\alpha(z)$ which has two solutions given by explicit (but complicated, so we omit writing them here) formulas. These solutions come from two branches of the complex square root. The function H_α must be analytic in some neighborhood of ∞ and therefore can be given by only one (family) of these solutions. Moreover, H_α must have a proper asymptotics, more precisely [MS17, Section 3.1, Lemma 3]

$$\lim_{y\to\infty} \frac{H_\alpha(iy)}{y} = i,$$

which allows us to choose the proper solution.

The formula for H_α gives also an explicit formula for the Cauchy transform of the cotransition measure ν_{Λ_α} on the level curve Λ_α as (cf. (4.10.1))

$$G_{\nu_{\Lambda_\alpha}}(z) = \frac{1}{\alpha a b}\big(z - H_\alpha(z)\big).$$

The function $G_{\nu_{\Lambda_\alpha}}$ is analytic (since H_α is analytic); we will use its analytic continuation to the upper halfplane $\mathbb{C}^+$.

With this (complicated) formula for $G_{\nu_{\Lambda_\alpha}}$ we can now recover the density of the cotransition measure ν_{Λ_α} using the Stieltjes inversion formula [MS17, Section 3, Theorem 6]. One

can easily show that this density is the properly rescaled and translated standard semicircle distribution, cf. (4.1.3). □

4.10.8 What if the geographic coordinates system is not uniformly continuous?

The situation when the geographic coordinates system $(\alpha, \psi) \mapsto P_{\alpha,\psi} \in \Lambda^{\mathrm{Cart}}$ (recall Section 4.10.5) is not uniformly continuous is not rare. One among many examples is the limit shape Λ which is the L-shape, cf. Figure 4.10. In this case there are some α-level curves (for α big enough) for which the corresponding cotransition measure is supported on two disjoint intervals. This forces the function $\psi \mapsto P_{\alpha,\psi}$ to have a discontinuity related to the hole between the intervals. Therefore in such situation Theorem 4.10.5 does not apply since the assumption (⋆) is not fulfilled.

Problem 4.10.8. Find a counterpart of the assumption (⋆) for which the conclusion of Theorem 4.10.5 holds true.

4.11 The correspondence between Young tableaux and particle systems. Proof of Theorem 4.1.1

We will first describe a bijection which links a recording tableau with a unique history of a particular Totally Asymmetric Simple Exclusion Process, recall Section 4.1.1. We will base on the articles of Rost [Ros81], as well as Romik and the second named author [Rom15, Section 7]. Then, in Section 4.11.3 we will prove Theorem 4.1.1.

4.11.1 The correspondence between a Young diagram with a distinguished corner and a configuration of particles – Rost's mapping

Let λ be a non-empty Young diagram and $\square$ be one of its inner corners, i.e., $\square$ is a cell of λ such that the shape $\lambda \backslash \square$ is still a Young diagram, see Figure 4.15. Following [Rom15, Section 7.1], we will present the two-step algorithm in which to the pair $(\lambda, \square)$ we assign a configuration of holes and particles with exactly one second class particle. To our best knowledge the foundations for this mapping were first laid in [Ros81, Remark 1], and therefore we will call it *Rost's mapping*.

In the first step of the Rost's mapping, given a Young diagram λ we draw its profile ω_λ in the Russian coordinates system (see Figure 4.14 and Section 4.10.1 for the definition of the profile). To the profile ω_λ there corresponds a unique configuration of holes and (first class) particles on $\mathbb{Z}' := \mathbb{Z} + \frac{1}{2}$ which appears in the following way. For each $m \in \mathbb{Z}$ exactly one of the following two cases holds true:

- in the case when the slope of the profile ω_λ on the interval $[m, m+1]$ is equal to -1 then we put a (first class) particle at the site $m + \frac{1}{2}$ of the lattice $\mathbb{Z}' := \mathbb{Z} + \frac{1}{2}$;
- in the case when the slope of the profile ω_λ on the interval $[m, m+1]$ is equal to $+1$ then we put a hole at the site $m + \frac{1}{2}$ (in other words, the site $m + \frac{1}{2}$ is vacant).

The distinguished inner corner $\square$ corresponds in the above particle system to a *hole–particle pair*. We outline this hole–particle pair with a red rectangle, see the top and the middle part of Figure 4.15.

In the second step of Rost's mapping we define a particle configuration on $\mathbb{Z}$. We start with merging the hole–particle pair outlined in the red rectangle into the single particle which we will call *the second class particle*. We put it in the middle of the initial interval containing the hole-particle pair. Then we translate all holes and particles which are placed to the left

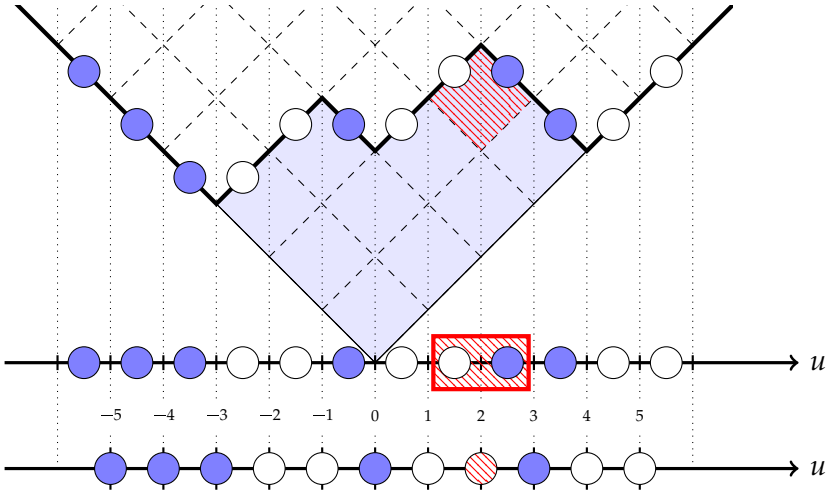

Figure 4.15: Above: the Young diagram $(4,4,2)$ and its marked inner corner in the second row. In the middle: the corresponding configuration of particles on the shifted lattice $\mathbb{Z}'$ via Rost's mapping. The marked inner corner corresponds to the pair of nodes in the rectangle. Below: the corresponding configuration of particles (including the second class particle) on the lattice $\mathbb{Z}$.

of the second class particle by $+\frac{1}{2}$ and we translate all holes and particles which are placed to the right of the second class particle by $-\frac{1}{2}$. These steps are illustrated in the middle and bottom part of Figure 4.15. In this way we end up with the configuration of particles on $\mathbb{Z}$ with a single second class particle.

4.11.2 The correspondence between the standard tableaux and the histories of TASEP

Recall that for a standard tableau T and a positive integer $p \leqslant |T|$ we define the restricted tableau $T|_{\leqslant p}$ to be the tableau which consists of only these boxes of T which have entries $\leqslant p$.

For a standard tableau T with $n \geqslant 1$ boxes and any $p \in \{1,\dots,n\}$ let us define

$$\lambda^{(p)} := \lambda^{(p)}(T) := \mathrm{sh}\Big(T|_{\leqslant p}\Big),$$
$$\square^{(p)} := \square^{(p)}(T) := \mathbf{q}_p(T),$$

that is, $\big(\lambda^{(p)}, \square^{(p)}\big)$ is the pair which consists of the Young diagram $\lambda^{(p)}(T)$ which is the shape of the restricted tableau $T|_{\leqslant p}$ and the last box along the sliding path in T which contains a number $\leqslant p$, cf. Section 4.2.6.

Let T be a standard tableau with $n \geqslant 1$ boxes. For any $t \in \{1,\dots,n\}$ let us consider the system of particles $P_t := P_t(T)$ which corresponds to the pair $(\lambda^{(t)}, \square^{(t)})$ via Rost's mapping defined in Section 4.11.1. Notice that the initial configuration P_1 is such that the second class particle is located at the site $u = 0$, all negative nodes are occupied by the first class particles and all positive nodes are occupied by holes. Such configuration is called *the Dirac sea*. Observe that for any $t \in \{1,\dots,n-1\}$ the neighboring states P_t and P_{t+1} differ by one of the three transitions described in Section 4.1.1.1 (cf. Figure 4.2, see [Rom15, Sections 7.2 and 7.3] for a step-by-step proof). Therefore the family $(P_t)_{t\in\{1,\dots,n\}}$ is a history of the particle system starting from the Dirac sea.

Given the above observation, it is easy to see that the mapping which to the standard tableau T with n boxes associates the history $\big(P_t(T)\big)_{t\in\{1,\dots,n\}}$ of the particle system is *a*

bijection between the set of standard tableaux with n boxes and the possible n-step histories of particle systems starting from the Dirac sea. Moreover, for a tableau T and any $t \in \{1, \dots, |T|\}$ the u-coordinate of the box $\mathbf{q}_t(T)$ in the lazy sliding path is the position of the second class particle in time t in the corresponding TASEP, see [Rom15, Proposition 7.1].

4.11.3 Proof of Theorem 4.1.1

Proof of Theorem 4.1.1. Let us denote by $\mathcal{T}_{M\times N}$ the set of standard tableaux of $M \times N$ rectangular shape (where M is a number of rows and N is a number of columns).

In the following we discard the particles and holes which do not occupy the nodes (4.1.1). In this way the correspondence defined in Section 4.11.2 gives a bijection between $\mathcal{T}_{M_i\times N_i}$ and the set of histories of the particle system considered in Section 4.1.1.1. In this correspondence for any $t \in \{1, \dots, M_iN_i\}$ the position of the second class particle in time t in the TASEP corresponds to the u-coordinate of the box $\mathbf{q}_t(T)$ in the lazy sliding path. In the special case $M_i = N_i = i$ when $M_i \times N_i = \square_i$ an application of Theorem 4.2.4 completes the proof. In the general case we apply Corollary 4.10.6 instead. □

Bibliography

[AD95] D. Aldous and P. Diaconis. “Hammersley’s interacting particle process and longest increasing subsequences”. In: *Probab. Theory Related Fields* 103.2 (1995), pp. 199–213. DOI: 10.1007/BF01204214.

[Ang+07] Omer Angel et al. “Random sorting networks”. In: *Adv. Math.* 215.2 (2007), pp. 839–868. DOI: 10.1016/j.aim.2007.05.019.

[AO20] I. Azangulov and G. Ovechkin. “Estimation of the time of Bernoulli scheme coordinates reach the first column of Young tableau”. In: *Funktsional. Anal. i Prilozhen.* 54.2 (2020), pp. 78–84. DOI: 10.4213/faa3773.

[Aza20] Iskander Azangulov. “Distribution of fluctuations of Bernoulli system P-tableaux under RSK mapping”. In Russian. Private communication. Bachelor’s Thesis. Saint Petersburg State University, 2020.

[BDJ00] J. Baik, P. Deift, and K. Johansson. “On the distribution of the length of the second row of a Young diagram under Plancherel measure”. In: *Geom. Funct. Anal.* 10.4 (2000), pp. 702–731. DOI: 10.1007/PL00001635.

[BDJ99] Jinho Baik, Percy Deift, and Kurt Johansson. “On the distribution of the length of the longest increasing subsequence of random permutations”. In: *J. Amer. Math. Soc.* 12.4 (1999), pp. 1119–1178. DOI: 10.1090/S0894-0347-99-00307-0.

[BF87] Albert Benassi and Jean-Pierre Fouque. “Hydrodynamical limit for the asymmetric simple exclusion process”. In: *Ann. Probab.* 15.2 (1987), pp. 546–560. URL: http://links.jstor.org/sici?sici=0091-1798(198704)15:2<546:HLFTAS>2.0.CO;2-1&origin=MSN.

[Bia01] Philippe Biane. “Approximate factorization and concentration for characters of symmetric groups”. In: *Internat. Math. Res. Notices* 4 (2001), pp. 179–192. DOI: 10.1155/S1073792801000113.

[Bia02] P. Biane. “Free probability and combinatorics”. In: *Proceedings of the International Congress of Mathematicians, Vol. II (Beijing, 2002)*. Higher Ed. Press, Beijing, 2002, pp. 765–774.

[Bia98] Philippe Biane. “Processes with free increments”. In: *Math. Z.* 227.1 (1998), pp. 143–174. DOI: 10.1007/PL00004363.

[BOO00] Alexei Borodin, Andrei Okounkov, and Grigori Olshanski. “Asymptotics of Plancherel measures for symmetric groups”. In: *J. Amer. Math. Soc.* 13.3 (2000), pp. 481–515. DOI: 10.1090/S0894-0347-00-00337-4.

[Bur48] J. M. Burgers. “A mathematical model illustrating the theory of turbulence”. In: *Advances in Applied Mechanics*. edited by Richard von Mises and Theodore von Kármán, Academic Press, Inc., New York, 1948, pp. 171–199.

[CG05] Eric Cator and Piet Groeneboom. “Hammersley’s process with sources and sinks”. In: *Ann. Probab.* 33.3 (2005), pp. 879–903. DOI: 10.1214/009117905000000053.

[CŚ09] Benoît Collins and Piotr Śniady. "Representations of Lie groups and random matrices". In: *Trans. Amer. Math. Soc.* 361.6 (2009), pp. 3269–3287. DOI: 10.1090/S0002-9947-09-04624-8.

[CSST10] Tullio Ceccherini-Silberstein, Fabio Scarabotti, and Filippo Tolli. *Representation theory of the symmetric groups*. Vol. 121. Cambridge Studies in Advanced Mathematics. The Okounkov-Vershik approach, character formulas, and partition algebras. Cambridge: Cambridge University Press, 2010, pp. xvi+412.

[Dur10] Rick Durrett. *Probability: theory and examples*. Fourth. Cambridge Series in Statistical and Probabilistic Mathematics. Cambridge: Cambridge University Press, 2010, pp. x+428.

[Duz19] Vasilii S. Duzhin. "Investigation of insertion tableau evolution in the Robinson–Schensted–Knuth correspondence". In: *Discrete and Continuous Models and Applied Computational Science* 27.4 (2019), pp. 316–324. URL: http://journals.rudn.ru/miph/article/view/22914.

[DV20] Duncan Dauvergne and Bálint Virág. "Circular support in random sorting networks". In: *Trans. Amer. Math. Soc.* 373.3 (2020), pp. 1529–1553. DOI: 10.1090/tran/7819.

[DVJ08] D. J. Daley and D. Vere-Jones. *An introduction to the theory of point processes. Vol. II*. Second. Probability and its Applications (New York). General theory and structure. Springer, New York, 2008, pp. xviii+573. DOI: 10.1007/978-0-387-49835-5.

[DZ99] Jean-Dominique Deuschel and Ofer Zeitouni. "On increasing subsequences of I.I.D. samples". In: *Combin. Probab. Comput.* 8.3 (1999), pp. 247–263. DOI: 10.1017/S0963548399003776.

[Fer92] Pablo A. Ferrari. "Shock fluctuations in asymmetric simple exclusion". In: *Probab. Theory Related Fields* 91.1 (1992), pp. 81–101. DOI: 10.1007/BF01194491.

[FF94] P. A. Ferrari and L. R. G. Fontes. "Current fluctuations for the asymmetric simple exclusion process". In: *Ann. Probab.* 22.2 (1994), pp. 820–832. URL: http://links.jstor.org/sici?sici=0091-1798(199404)22:2<820:CFFTAS>2.0.CO;2-4&origin=MSN.

[FK95] P. A. Ferrari and C. Kipnis. "Second class particles in the rarefaction fan". In: *Ann. Inst. H. Poincaré Probab. Statist.* 31.1 (1995), pp. 143–154. URL: http://www.numdam.org/item?id=AIHPB_1995__31_1_143_0.

[FM09] Pablo A. Ferrari and James B. Martin. "Multiclass Hammersley-Aldous-Diaconis process and multiclass-customer queues". In: *Ann. Inst. Henri Poincaré Probab. Stat.* 45.1 (2009), pp. 250–265. DOI: 10.1214/08-AIHP168.

[FŚ11] Valentin Féray and Piotr Śniady. "Asymptotics of characters of symmetric groups related to Stanley character formula". In: *Ann. of Math. (2)* 173.2 (2011), pp. 887–906. DOI: 10.4007/annals.2011.173.2.6.

[FS20] Wai-Tong Louis Fan and Timo Seppäläinen. "Joint distribution of Busemann functions in the exactly solvable corner growth model". In: *Prob. Math. Phys.* 1.1 (2020), pp. 55–100. DOI: 10.2140/pmp.2020.1.55.

[Ful97] William Fulton. *Young tableaux*. Vol. 35. London Mathematical Society Student Texts. With applications to representation theory and geometry. Cambridge University Press, Cambridge, 1997, pp. x+260.

[Gre74] Curtis Greene. "An extension of Schensted's theorem". In: *Advances in Math.* 14 (1974), pp. 254–265. DOI: 10.1016/0001-8708(74)90031-0.

[GS17] Vadim Gorin and Mykhaylo Shkolnikov. "Interacting particle systems at the edge of multilevel Dyson Brownian motions". In: *Adv. Math.* 304 (2017), pp. 90–130. DOI: 10.1016/j.aim.2016.08.034.

[Ham72] J. M. Hammersley. "A few seedlings of research". In: *Proceedings of the Sixth Berkeley Symposium on Mathematical Statistics and Probability (Univ. California, Berkeley, Calif., 1970/1971), Vol. I: Theory of statistics*. 1972, pp. 345–394.

[Joh01] Kurt Johansson. "Discrete orthogonal polynomial ensembles and the Plancherel measure". In: *Ann. of Math. (2)* 153.1 (2001), pp. 259–296. DOI: 10.2307/2661375.

[JS98] Philippe Jacquet and Wojciech Szpankowski. "Analytical de-Poissonization and its applications". In: *Theoret. Comput. Sci.* 201.1-2 (1998), pp. 1–62. DOI: 10.1016/S0304-3975(97)00167-9.

[Juc74] A.-A. A. Jucys. "Symmetric polynomials and the center of the symmetric group ring". In: *Rep. Mathematical Phys.* 5.1 (1974), pp. 107–112.

[Ker00] S. V. Kerov. "Anisotropic Young diagrams and symmetric Jack functions". In: *Funktsional. Anal. i Prilozhen.* 34.1 (2000), pp. 51–64, 96. DOI: 10.1007/BF02467066.

[Ker93a] S. V. Kerov. "Asymptotics of the separation of roots of orthogonal polynomials". In: *Algebra i Analiz* 5.5 (1993), pp. 68–86.

[Ker93b] S. V. Kerov. "Transition probabilities of continual Young diagrams and the Markov moment problem". In: *Funktsional. Anal. i Prilozhen.* 27.2 (1993), pp. 32–49, 96. DOI: 10.1007/BF01085981.

[Ker98] Sergei Kerov. "Interlacing measures". In: *Kirillov's seminar on representation theory*. Vol. 181. Amer. Math. Soc. Transl. Ser. 2. Amer. Math. Soc., Providence, RI, 1998, pp. 35–83. DOI: 10.1090/trans2/181/02.

[Ker99] S. Kerov. "A differential model for the growth of Young diagrams". In: *Proceedings of the St. Petersburg Mathematical Society, Vol. IV*. Vol. 188. Amer. Math. Soc. Transl. Ser. 2. Amer. Math. Soc., Providence, RI, 1999, pp. 111–130. DOI: 10.1090/trans2/188/06.

[Kin93] J. F. C. Kingman. *Poisson processes*. Vol. 3. Oxford Studies in Probability. Oxford Science Publications. The Clarendon Press, Oxford University Press, New York, 1993, pp. viii+104.

[KP21] Richard Kenyon and István Prause. *Gradient variational problems in* $\mathbb{R}^2$. 2021. arXiv: 2006.01219 [math.AP].

[Kup02] Greg Kuperberg. "Random words, quantum statistics, central limits, random matrices". In: *Methods Appl. Anal.* 9.1 (2002), pp. 99–118. DOI: 10.4310/MAA.2002.v9.n1.a3.

[Lig99] Thomas M. Liggett. *Stochastic interacting systems: contact, voter and exclusion processes*. Vol. 324. Grundlehren der Mathematischen Wissenschaften [Fundamental Principles of Mathematical Sciences]. Springer-Verlag, Berlin, 1999, pp. xii+332. DOI: 10.1007/978-3-662-03990-8.

[LS77] B. F. Logan and L. A. Shepp. "A variational problem for random Young tableaux". In: *Advances in Math.* 26.2 (1977), pp. 206–222. DOI: 10.1016/0001-8708(77)90030-5.

[Mar21] Mikołaj Marciniak. "Hydrodynamic limit of the Robinson–Schensted–Knuth algorithm". In: *Random Structures & Algorithms* (2021). DOI: https://doi.org/10.1002/rsa.21016. eprint: https://onlinelibrary.wiley.com/doi/pdf/10.1002/rsa.21016.

[Mél11] Pierre-Loïc Méliot. "Kerov's central limit theorem for Schur–Weyl and Gelfand measures (extended abstract)". In: *Discrete Mathematics & Theoretical Computer Science* DMTCS Proceedings vol. AO, 23rd International Conference on Formal Power Series and Algebraic Combinatorics (FPSAC 2011) (Jan. 2011). URL: https://dmtcs.episciences.org/2943.

[MG05] Thomas Mountford and Hervé Guiol. "The motion of a second class particle for the TASEP starting from a decreasing shock profile". In: *Ann. Appl. Probab.* 15.2 (2005), pp. 1227–1259. DOI: 10.1214/105051605000000151.

[MMŚ21a] Mikołaj Marciniak, Łukasz Maślanka, and Piotr Śniady. "Poisson limit of bumping routes in the Robinson–Schensted correspondence". In: *Probab. Theory Related Fields* 181.4 (2021), pp. 1053–1103. DOI: 10.1007/s00440-021-01084-y.

[MMŚ21b] Łukasz Maślanka, Mikołaj Marciniak, and Piotr Śniady. *Poisson limit theorems for the Robinson–Schensted correspondence and for the multi-line Hammersley process*. 2021. arXiv: 2005.13824v2 [math.PR]. URL: https://arxiv.org/abs/2005.13824v2.

[MS17] James A. Mingo and Roland Speicher. *Free probability and random matrices*. Vol. 35. Fields Institute Monographs. Springer, New York; Fields Institute for Research in Mathematical Sciences, Toronto, ON, 2017, pp. xiv+336. DOI: 10.1007/978-1-4939-6942-5.

[MŚ20a] Łukasz Maślanka and Piotr Śniady. "Limit shapes of evacuation and jeu de taquin paths in random square tableaux". In: *Sém. Lothar. Combin.* 84B (2020), Art. 8, 12.

[MŚ20b] Sho Matsumoto and Piotr Śniady. "Random strict partitions and random shifted tableaux". In: *Selecta Math. (N.S.)* 26.1 (2020), Paper No. 10, 59. DOI: 10.1007/s00029-020-0535-2.

[MŚ22] Łukasz Maślanka and Piotr Śniady. "Second class particles and limit shapes of evacuation and sliding paths for random tableaux". In: *arXiv* (2022). DOI: arXiv:1911.08143v3.

[Oko00] Andrei Okounkov. "Random matrices and random permutations". In: *Internat. Math. Res. Notices* 20 (2000), pp. 1043–1095. DOI: 10.1155/S1073792800000532.

[Oko06] Andrei Okounkov. "Random partitions and instanton counting". In: *International Congress of Mathematicians. Vol. III*. Eur. Math. Soc., Zürich, 2006, pp. 687–711.

[pik15] pikachuchameleon. *Total variation distance of two random vectors whose components are independent*. Question on Stack Exchange forum Mathematics. 2015. eprint: https://math.stackexchange.com/q/1558845.

[PR07] Boris Pittel and Dan Romik. "Limit shapes for random square Young tableaux". In: *Adv. in Appl. Math.* 38.2 (2007), pp. 164–209. DOI: 10.1016/j.aam.2005.12.005.

[PW11] Steven Pon and Qiang Wang. "Promotion and evacuation on standard Young tableaux of rectangle and staircase shape". In: *Electron. J. Combin.* 18.1 (2011), Paper 18, 18.

[Rez95] Fraydoun Rezakhanlou. "Microscopic structure of shocks in one conservation laws". In: *Ann. Inst. H. Poincaré Anal. Non Linéaire* 12.2 (1995), pp. 119–153. DOI: 10.1016/S0294-1449(16)30161-5.

[Rom04] Dan Romik. "Explicit formulas for hook walks on continual Young diagrams". In: *Adv. in Appl. Math.* 32.4 (2004), pp. 625–654. DOI: 10.1016/S0196-8858(03)00096-4.

[Rom06] Dan Romik. "Permutations with short monotone subsequences". In: *Adv. in Appl. Math.* 37.4 (2006), pp. 501–510. DOI: 10.1016/j.aam.2005.08.008.

[Rom12] Dan Romik. "Arctic circles, domino tilings and square Young tableaux". In: *Ann. Probab.* 40.2 (2012), pp. 611–647. DOI: 10.1214/10-AOP628.

[Rom15] Dan Romik. *The surprising mathematics of longest increasing subsequences*. Vol. 4. Institute of Mathematical Statistics Textbooks. Cambridge University Press, New York, 2015, pp. xi+353.

[Ros81] H. Rost. "Nonequilibrium behaviour of a many particle process: density profile and local equilibria". In: *Z. Wahrsch. Verw. Gebiete* 58.1 (1981), pp. 41–53. DOI: 10.1007/BF00536194.

[RŚ15] Dan Romik and Piotr Śniady. "Jeu de taquin dynamics on infinite Young tableaux and second class particles". In: *Ann. Probab.* 43.2 (2015), pp. 682–737. DOI: 10.1214/13-AOP873.

[RŚ16] Dan Romik and Piotr Śniady. "Limit shapes of bumping routes in the Robinson-Schensted correspondence". In: *Random Structures Algorithms* 48.1 (2016), pp. 171–182. DOI: 10.1002/rsa.20570.

[Ś13] Piotr Śniady. "Combinatorics of asymptotic representation theory". In: *European Congress of Mathematics*. Eur. Math. Soc., Zürich, 2013, pp. 531–545.

[Sag01] Bruce E. Sagan. *The Symmetric Group: Representations, combinatorial algorithms, and symmetric functions*. Second. Vol. 203. Graduate Texts in Mathematics. Representations, combinatorial algorithms, and symmetric functions. New York: Springer-Verlag, 2001, pp. xvi+238. DOI: 10.1007/978-1-4757-6804-6.

[Sch61] C. Schensted. "Longest increasing and decreasing subsequences". In: *Canadian J. Math.* 13 (1961), pp. 179–191. DOI: 10.4153/CJM-1961-015-3.

[Sch63] M. P. Schützenberger. "Quelques remarques sur une construction de Schensted". In: *Math. Scand.* 12 (1963), pp. 117–128.

[Sep01] Timo Seppäläinen. "Second class particles as microscopic characteristics in totally asymmetric nearest-neighbor K-exclusion processes". In: *Trans. Amer. Math. Soc.* 353.12 (2001), pp. 4801–4829. DOI: 10.1090/S0002-9947-01-02872-0.

[Sep98] Timo Seppäläinen. "Large deviations for increasing sequences on the plane". In: *Probab. Theory Related Fields* 112.2 (1998), pp. 221–244. DOI: 10.1007/s004400050188.

[Śni06] Piotr Śniady. "Gaussian fluctuations of characters of symmetric groups and of Young diagrams". In: *Probab. Theory Related Fields* 136.2 (2006), pp. 263–297. DOI: 10.1007/s00440-005-0483-y.

[Śni14] Piotr Śniady. "Robinson-Schensted-Knuth algorithm, jeu de taquin, and Kerov-Vershik measures on infinite tableaux". In: *SIAM J. Discrete Math.* 28.2 (2014), pp. 598–630. DOI: 10.1137/130930169.

[Spi70] Frank Spitzer. "Interaction of Markov processes". In: *Advances in Math.* 5 (1970), 246–290 (1970).

[Sta07] Richard P. Stanley. "Increasing and decreasing subsequences and their variants". In: *International Congress of Mathematicians. Vol. I*. Eur. Math. Soc., Zürich, 2007, pp. 545–579. DOI: 10.4171/022-1/21.

[Sta99] Richard P. Stanley. *Enumerative combinatorics. Vol. 2*. Vol. 62. Cambridge Studies in Advanced Mathematics. With a foreword by Gian-Carlo Rota and appendix 1 by Sergey Fomin. Cambridge: Cambridge University Press, 1999, pp. xii+581. DOI: 10.1017/CBO9780511609589.

[Sun18] Wangru Sun. *Dimer model, bead model and standard Young tableaux: finite cases and limit shapes*. 2018. arXiv: 1804.03414 [math.PR].

[Tho00] Hermann Thorisson. *Coupling, stationarity, and regeneration*. Probability and its Applications (New York). Springer-Verlag, New York, 2000, pp. xiv+517. DOI: 10.1007/978-1-4612-1236-2.

[Ula61] Stanislaw M. Ulam. "Monte Carlo calculations in problems of mathematical physics". In: *Modern mathematics for the engineer: Second series*. McGraw-Hill, New York, 1961, pp. 261–281.

[Ver20] A. M. Vershik. "Combinatorial coding of Bernoulli schemes and asymptotics of Young tables". In: *Funktsional. Anal. i Prilozhen.* 43.2 (2020), pp. 3–24. DOI: 10.4213/faa3740.

[Ver95] Anatoly M. Vershik. "Asymptotic combinatorics and algebraic analysis". In: *Proceedings of the International Congress of Mathematicians, Vol. 1, 2 (Zürich, 1994)*. Birkhäuser, Basel, 1995, pp. 1384–1394.

[VK77] A. M. Veršik and S. V. Kerov. "Asymptotic behavior of the Plancherel measure of the symmetric group and the limit form of Young tableaux". In: *Dokl. Akad. Nauk SSSR* 233.6 (1977), pp. 1024–1027.

[VK85a] A. M. Vershik and S. V. Kerov. "Asymptotic behavior of the maximum and generic dimensions of irreducible representations of the symmetric group". In: *Funktsional. Anal. i Prilozhen.* 19.1 (1985), pp. 25–36, 96.

[VK85b] A. M. Vershik and S. V. Kerov. "Asymptotic of the largest and the typical dimensions of irreducible representations of a symmetric group". In: *Functional Analysis and Its Applications* 19.1 (1985), pp. 21–31. DOI: 10.1007/BF01086021.